**UNIVERSITA' DEGLI STUDI "G. d'Annunzio"**

**Chieti-Pescara**

---

**SCUOLA SUPERIORE "G. d'Annunzio"**

DOTTORATO DI RICERCA IN NEUROSCIENZE E IMAGING

CICLO XXXVIII

# *The respiratory modulation of interoceptive and exteroceptive perception: heartbeat-related and attentional neural dynamics*

*La modulazione respiratoria della percezione enterocettiva ed esterocettiva: dinamiche neurali legate al battito cardiaco e all'attenzione*

**Dipartimento di Neuroscienze, Imaging e Scienze Cliniche**

**Settore Scientifico Disciplinare PSIC-01A/PSIC-01B**

*Dottoranda*

*Francesca della Penna*

*Coordinatore*

*Prof. Carlo Sestieri*

*Tutor*

*Prof. Marcello Costantini*

Anni Accademici 2022/2025

# Abstract

Converging evidence suggests that respiration shapes interoceptive processing at both neural and behavioral levels. The heartbeat-evoked potential (HEP), an EEG fluctuation associated with the cortical processing of cardiac signals, is higher during exhalation compared to inhalation, reflecting heightened interoceptive accuracy in the same respiratory phase. Moreover, recent research indicates that humans continuously and automatically modulate their breathing to temporally align exteroceptive stimuli with specific phases of the respiratory cycle. This process has been interpreted as a form of active sensing and is associated with faster responses and improved perceptual accuracy. However, it remains unclear whether individuals actively adjust their breathing to optimize interoceptive performance in a similar way.

The present thesis aimed to investigate how respiration shapes interoceptive and exteroceptive perception and whether breathing is actively regulated to optimize the processing of internal bodily signals. Across three studies, we examined behavioral and physiological markers of perception using two independent datasets and different interoceptive and exteroceptive tasks. The results consistently showed that perceptual accuracy was higher during exhalation than inhalation. Converging physiological evidence further supported this behavioral effect, including enhanced heartbeat-evoked potentials (HEP), phase-locking of respiration to the expected stimulus, and increased heartbeat-related cortical oscillations in the alpha and theta frequency bands during exhalation. In addition, a fourth ongoing study extends this research by investigating interoceptive processes in contexts of transient and chronic fatigue. Together, these findings support the view that respiration may act as a physiological mechanism shaping interoceptive perception, extending the concept of respiratory active sensing to the interoceptive domain.

# Acknowledgments

This thesis exists thanks to an unstable and explosive combination of coffee, stubbornness, swearing, passion, and people who deserve far more than a simple acknowledgment. Among them, several truly deserve to be mentioned by name.

A special thank-you goes to my Supervisors, Prof. Marcello Costantini and Prof. Francesca Ferri, for guiding me with patience, trust, and the right balance of freedom and direction.

My deepest gratitude goes to Dr. Andrea Zaccaro, who taught me everything I am now proud of and who accompanied me through this path with dedication, clarity, and constant support.

Many thanks also to Prof. Mauro Gianni Perrucci for his availability and assistance.

Beyond these individual contributions, I am equally grateful for the community that surrounded me throughout this journey. My sincere thanks go to the entire TEAM Lab, past and present, for the discussions, the shared struggles, and the sense of belonging that made even the longest days feel lighter.

I am deeply grateful to my friends, for “willingly” taking part in my experiments and making far more possible than they realize.

To those who believed in me long before I could believe in myself: thank you. Your trust carried me further than any certainty of mine ever could.

And finally, my heartfelt thanks go to my life partner, Francesco - without whom I would struggle to get out of bed, let alone write a thesis. His support, constancy, and ability to keep me grounded have been the quiet foundation beneath every page of this work.

# Table of Contents

**Abstract** ..... 2
**Acknowledgments** ..... 3
**Table of Contents** ..... 4
**Chapter 1 Introduction** ..... 5
**1.1 Interoception** ..... 6
**1.2 Interoceptive accuracy, sensibility, and awareness** ..... 7
**1.3 Methods for assessing interoceptive accuracy** ..... 9
**1.4 Afferent interoceptive pathways** ..... 12
**1.5 Cardiac interoception** ..... 14
**1.6 Respiratory interoception** ..... 16
**1.7 EEG correlates of interoception** ..... 19
**1.8 Heartbeat-modulated cortical oscillations** ..... 22
**1.9 Interoception and fatigue** ..... 24
**1.10 General aim** ..... 27
**Chapter 2 Empirical studies** ..... 29
**Study 1 Breathing strategies to influence perception: Evidence for interoceptive and exteroceptive active sensing** ..... 30
**Study 2 Attention to cardiac sensations enhances the heartbeat-evoked potential during exhalation** ..... 62
**Study 3 Cardio-respiratory interactions in interoceptive perception: The role of heartbeat-modulated cortical oscillations** ..... 92
**Study 4 Interoception and fatigue: preliminary data from an ongoing study** ..... 128
**Chapter 3 General Discussion and Conclusions** ..... 145
**References** ..... 151
**Appendix A Supplementary Material for Study 1** ..... 181
**Appendix B Published version of Study 2** ..... 202
**Appendix C Published version of Study 3** ..... 222

# Chapter 1

# Introduction

# Introduction

## 1.1 Interoception

Information from the internal and external environment of the body reaches the central nervous system through specialized pathways, with the aim of maintaining homeostasis and modulating behavior to appropriately react to stimuli. To detect and discriminate incoming information, the central nervous system relies on sensory receptors, which can be represented by sensory neurons, as in the case of thermoception, or by specialized cells that transmit the signal to the primary afferent neuron, as in the case of more complex senses such as vision. Perception of information arising from the stimulation of tactile, auditory, visual receptors, and more generally all receptors that are activated by events occurring outside the body, is called *exteroception*; stimulation of aortic baroreceptors, visceral receptors and, more generally, of all receptors that collect information from within the body, is instead referred to as *interoception*. Sherrington was the first to introduce, in 1906, the term *interoception*, referring to the senses that convey information about the internal state of the body to the central nervous system, including, for example, taste (Berntson & Khalsa, 2021). However, the term interoception has been revised over the years. According to Vaitl, interoception includes two different forms of perception: proprioception, which conveys signals originating from skeletal muscles, joints, and tendons, and viscероception, which conveys information from internal organs (Vaitl, 1996). Based on more recent neuroanatomical research (Craig, 2002), however, interoception has been redefined as the sense of the physiological condition of the body (Ceunen et al., 2016), including hunger, thirst, cardiac and respiratory signals (Murphy et al., 2017). Interoception is therefore considered to be much more than simple viscероception and to include the cognitive and emotional processing of the internal state of the body (Cameron, 2001; Verdejo-Garcia et al., 2012). Atypical interoceptive processing has been linked to psychiatric disorders such as anxiety and depression (Pollatos et al., 2009), schizophrenia (Ardizzi et al., 2016), eating disorders and Autism

Spectrum Disorders (Murphy et al., 2018), and to emotional regulation and obesity (Robinson et al., 2021; Willem et al., 2019).

For a stimulus to be perceived, it must reach the threshold of consciousness; in this case it is defined as *conscious perception*. According to Molle and Coste, two elements are involved in conscious perception: the intensity of the stimulus and the degree of attention allocated to its perception (Molle & Coste, 2022). Attention is a neural process that allows one to orient interest towards specific perceptual aspects, both internal and external. A crucial aspect of attention is therefore the disengagement from stimuli and/or sensations that are considered irrelevant in that moment, allowing only some information to access later processing stages. However, attention not only acts as a filter for information, but also affects the degree to which information is processed: with regard to salient information, Farb and colleagues note that "paying attention to a particular sensory stimulus selectively enhances domain-specific cortical representations" (Farb et al., 2013).

More recent studies have allowed this characteristic to be evaluated also for endogenous stimuli: directing attention to an internal bodily stimulus should increase and enhance the neural representation of that stimulus itself (H. Feldman & Friston, 2010). However, assessing and analyzing the perception of endogenous stimuli is not straightforward; therefore, many studies have focused on a particularly salient interoceptive stimulus: the heartbeat.

### 1.2 Interoceptive accuracy, sensibility, and awareness

Interoception is the perception of signals arising from within the body. *Interoceptive accuracy* is therefore a value assigned to performance in detecting endogenous signals.

The most easily measurable interoceptive signal, and the one traditionally used to measure and assess interoception, is the heartbeat. Interoceptive accuracy is thus defined as performance on behavioral tests of heartbeat perception (Garfinkel et al., 2015), and is calculated by relating perceived heartbeats to actual heartbeats. The calculation of accuracy varies depending on the type of interoceptive task administered to the participant.

Interoceptive accuracy is distinct from *interoceptive sensibility*, which reflects an individual's perception of their own performance, assessed via self-report questionnaires. Questionnaires ask participants to rate their awareness of a series of bodily sensations, including signals arising from the cardiovascular, digestive, and excretory systems (Critchley & Harrison, 2013).

The most commonly used questionnaire to assess interoceptive sensibility is the Body Perception Questionnaire (BPQ), developed by Porges and colleagues in 1993. Designed to quantify the degree of body awareness and the reactivity of the autonomic nervous system, it includes items on bodily and visceral states, responses to stress, and clinical history. Initially composed of 122 items, it was reformulated into two versions: the Body Perception Questionnaire - Short Form (BPQ-SF), consisting of 46 items, and the Body Perception Questionnaire - Very Short Form (BPQ-VSF), consisting of 22 items. The BPQ and BPQ-SF allow the assessment of body awareness and supradiaphragmatic and subdiaphragmatic reactivity: the evaluation of autonomic reactivity of organs above the diaphragm provides a measure of supradiaphragmatic reactivity, which appears to reflect sympathetic "fight or flight" responses, whereas the evaluation of autonomic reactivity of organs below the diaphragm allows the quantification of subdiaphragmatic reactivity, which reflects vagal reactivity as well as the activity of the sympathetic and enteric nervous systems (Cabrera et al., 2018).

Another widely used questionnaire is the Multidimensional Assessment of Interoceptive Awareness (MAIA), developed by Mehling and colleagues, and initially tested primarily in individuals already familiar with the concept of body awareness, such as meditators and yoga practitioners (Mehling et al., 2012). It is a 32-item self-report questionnaire designed to measure key aspects of the mind-body relationship, divided into eight scales that assess different modalities of interoceptive attention: awareness of comfortable, uncomfortable, or neutral bodily sensations; tendency to ignore or not ignore sensations of pain or discomfort; tendency not to worry; ability to sustain and control attention to bodily sensations; awareness of the connection between bodily sensations and emotional states; ability to regulate psychological distress through attention to bodily sensations; active listening to the body; and experiences of the body as safe and trustworthy (Mehling et al., 2012).

*Interoceptive awareness* refers to the conscious perception of endogenous sensations that form a physiological brain representation of the body (Mehling et al., 2012), such as heartbeat, breathing, satiety, hunger, and intestinal peristalsis. It arises from the relationship between confidence and interoceptive accuracy and is calculated by assessing the correspondence between interoceptive accuracy measured with a specific task and confidence ratings about one's performance during the task (Garfinkel et al., 2015).

The terms interoceptive accuracy and interoceptive awareness are often used interchangeably; however, they are distinct concepts. Evidence for this comes from Khalsa and colleagues' 2008 study, in which both interoceptive accuracy and sensibility were evaluated in a sample of meditators with at least fifteen years of experience and in non-meditators. No significant differences in interoceptive accuracy on a heartbeat perception task were found between meditators and non-meditators; however, meditators rated their interoceptive performance as superior and reported finding the task easy (Khalsa et al., 2008). Thus, although high interoceptive awareness may be accompanied by high accuracy on detection tasks, the two dimensions are not necessarily directly linked (Ceunen et al., 2013).

### 1.3 Methods for assessing interoceptive accuracy

Paradigms used to determine interoceptive accuracy are designed to objectively quantify differences in behavioral performance. One of the most commonly used approaches involves Heartbeat Detection tasks, since heartbeats are discrete, frequent events that can be easily measured (Garfinkel et al., 2015). Tasks designed to assess heartbeat perception vary and include simple heartbeat counting tasks as well as more complex paradigms requiring participants to judge whether particular external stimuli are presented in phase with their own heartbeat.

The task traditionally used is the Schandry task, or *Heartbeat Counting Task* (HCT): participants are asked, during short intervals of variable duration (25 s, 35 s, 45 s, 100 s), to silently count their perceived or estimated heartbeats without palpating the pulse or making any physiological changes

that could facilitate heartbeat perception (Schandry, 1981). The control condition usually involves counting auditory stimuli during the same time intervals. Interoceptive accuracy is then computed by considering both the actual and the reported heartbeats (Garfinkel et al., 2015). Perfect heartbeat detection yields a perception score of 1, whereas overestimates or underestimates produce a perception score lower than 1 (Brener & Ring, 2016).

Although the Schandry paradigm is the classic method for assessing interoceptive accuracy, it is not free from criticism. In Brener and Ring's 1996 study, which used the Schandry task under different conditions, reported heart rates were found to be more similar to self-estimated heart rates prior to the task than to actual heart rates (Ring & Brener, 1996). Participants first completed a questionnaire in which they estimated their heart rate in various positions and conditions - rest or exercise - and then performed the Schandry task while sitting upright, standing, lying supine, or recovering from physical exercise. Results showed that counted heartbeats were on average lower than the previously estimated heartbeats, which in turn were lower than the actual heartbeats. These findings suggest that the Schandry task may not be able to distinguish between individuals who can accurately detect heartbeats and those with accurate beliefs about their heart rate (Phillips et al., 1999).

Other tasks used to assess interoceptive accuracy are the Heartbeat Discrimination Task and the Heartbeat Detection Task.

In the *Heartbeat Discrimination Task* (HDT), participants must determine whether a visual or auditory stimulus is synchronous or asynchronous with their own heartbeat. In the classic paradigm developed by Whitehead and colleagues, the external stimulus is a visual stimulus presented a few milliseconds after the R-peak, specifically 128 ms (synchronous condition) or 384 ms (asynchronous condition), and participants must decide whether the stimulus was presented immediately after their heartbeat or with a delay (Whitehead et al., 1977). However, subsequent studies have consistently shown that the conscious perception of heartbeat sensations typically occurs later in the cardiac cycle, approximately between 100 and 300 ms after the R-peak, with a mean peak temporal perception around ~250 ms (Betka et al., 2021; Brener & Kluvitse, 1988; Yates et al., 1985). Since the only

difference between the two trial types is the latency between the participant's R-peaks and the visual feedback, mere knowledge of one's heart rate would not help in performing the task, making this paradigm more reliable and less prone to errors and misclassification (Phillips et al., 1999); however, HDT is not a purely interoceptive task, as it relies on multisensory integration of an exteroceptive and an interoceptive stimulus (Hickman et al., 2020). In the HDT, correctly identified synchronous trials are considered *hits*, asynchronous trials incorrectly judged as synchronous are *false alarms*, synchronous trials incorrectly judged as asynchronous are *misses*, while asynchronous trials correctly identified as asynchronous are *correct rejections*. Interoceptive accuracy is calculated by subtracting the false alarm rate from the hit rate, as quantified by the d' parameter derived from Signal Detection Theory (Schulz et al., 2013).

Another commonly used method is the *Heartbeat Detection Task* (HBD), in which participants must press a button every time they perceive their heartbeat. Tapping accuracy (TA) is calculated by comparing participants' button presses with the timing of their actual heartbeats as measured by the ECG. To assess accuracy, each tapped response is time-locked to the participant's ECG signal, and its temporal relation to the preceding R-peak is examined. A response is classified as accurate if it occurs within a predefined temporal window following the R-peak. Crucially, this window is not fixed but is adjusted on a trial-by-trial basis according to the participant's instantaneous heart rate, such that slower heart rates are associated with longer response windows and faster heart rates with shorter ones (Melloni et al., 2013). This procedure allows controlling for ongoing heart rate fluctuations, including those related to respiratory sinus arrhythmia, and to minimize confounds due to individual or state-dependent differences in cardiac physiology. Interoceptive accuracy is then quantified using a normalized index that reflects the proportion of correctly detected heartbeats relative to the total number of recorded heartbeats, with higher values indicating better detection performance (Yoris et al., 2017).

As the HCT, this task can be criticized since individuals, regardless of their true cardioperceptive sensibility, may be able to generate accurate scores by estimating their heart rate. However, in the

detection task this problem can be addressed by examining the latency between heartbeats and taps: for example, if a participant presses the button more frequently around R + 250 ms than at other latencies, this would indicate that they used heartbeat sensations as a cue for tapping (Brener & Ring, 2016). Nonetheless, this is not always easy to demonstrate. In a 1988 study by Flynn and Clemens, participants performed the HBD and a control task in which they pressed a button in synchrony with an auditory stimulus. Each tap was assigned to a 100 ms bin according to its latency from the R-peak. Results showed that cardiac taps were evenly distributed across bins, whereas taps in the control task were clustered, indicating that participants were unable to perceive their heartbeat (Flynn & Clemens, 1988). There thus appears to be competition between the motor demand of pressing the button and heartbeat detection, which interferes with cardioception (Brener & Ring, 2016).

The *Heartbeat Attention Task* consists of alternating 20-second blocks in which participants either focus their attention on their own heartbeat or, in a control condition, on external stimuli of various kinds, such as visual or auditory stimuli (Petzschner et al., 2019), without palpating the pulse and concentrating on the heart and heartbeat sensations. While this task does not provide a numerical measure of accuracy, it allows the identification of cortical regions associated with interoceptive attention, while excluding potential confounds related to other task demands, such as muscle artifacts resulting from movement in tapping tasks (Khalsa & Lapidus, 2016).

### 1.4 Afferent interoceptive pathways

Visceral sensitivity is mediated by receptors located within the body that detect changes occurring in visceral organs. Such receptors include chemoreceptors, mechanoreceptors, osmoreceptors, glucoreceptors, and humoral receptors, as well as free nerve endings that convey sensations of pain and temperature (Berntson & Khalsa, 2021). As described by Chen and colleagues (2021): “Interoceptors are molecular sensors or neuronal receptors that directly detect various interoceptive signals and transduce them into electrical, hormonal, or other non-neural signals that must be integrated and interpreted by the brain” (Chen et al., 2021). Interoceptive signals are therefore

heterogeneous in nature: examples of non-neural signals include those propagated along hypothalamic-pituitary axes, whereas neural interoceptive signals comprise thermal and nociceptive sensitivity, whose receptors are expressed in peripheral nerve terminals (Chen et al., 2021).

Visceral afferents, which include vagal, glossopharyngeal, and facial afferents, enter the spinal cord through dorsal root ganglia and reach the brain via the nucleus of the solitary tract (NTS), the parabrachial nucleus (PBN) in the brainstem, and the basal ventromedial thalamic nucleus (VMb), eventually projecting to the anterior cingulate cortex (ACC) and the insular cortex, where signals can reach the threshold of consciousness (Craig, 2002). Interoceptive signals are mainly processed at subcortical levels and only rarely reach conscious awareness, as in cases where bodily homeostasis is disrupted (e.g., rapid breathing, tachycardia, full bladder; Berntson & Khalsa, 2021). Lamina I fibers project to the NTS, the parabrachial nucleus, the periaqueductal gray, and other autonomic output nuclei in the brainstem (Critchley & Harrison, 2013), as well as to two distinct thalamic regions: the ventroposterior medial nucleus (VMpo), which receives sympathetic afferents, and the basal ventromedial nucleus (VMb), which receives primarily parasympathetic afferents. Together, these nuclei receive all homeostatic afferents from the body (Craig, 2002). However, VMpo is the main viscerosensory relay along the spinothalamic tract (Critchley & Harrison, 2013).

Anatomofunctional studies in animals have revealed a distributed cortical representation of visceral organs. These areas include primary and secondary somatosensory cortices, the insula, the ventromedial prefrontal cortex (vmPFC), and motor regions of the cingulate cortex (Azzalini et al., 2019). Evidence supporting a central role of the insula in the processing of interoceptive signals also comes from the fMRI study by Critchley and colleagues (2004). After completing the BPQ, participants performed the HDT, in which they decided whether their heartbeat was in phase with a sequence of ten tones triggered by the subject's own heartbeat. Functional MRI results showed greater bilateral activation in somatosensory cortices, the anterior insula, and the inferior frontal cortex. Insular activation correlated most strongly with interoceptive accuracy, and gray matter volume in

the right anterior insula was positively associated with objective measures of interoceptive performance and with participants' subjective ratings of their performance (Critchley et al., 2004).

In a more recent work, Craig analyzed results from several functional MRI studies to identify the role of the anterior insular cortex in interoceptive awareness and proposed a model that may explain how AIC fulfills this role. According to the author, interoceptive information is processed within the insular cortex along a posterior-anterior gradient: homeostatic information is first sent to the posterior insular cortex, then integrated in the mid-insula, where it is associated with emotionally salient environmental stimuli, and finally projected to the anterior insular cortex, where the representation of the "sentient self" is constructed (Craig, 2009).

### 1.5 Cardiac interoception

The heart beats autonomously thanks to the activity of its natural pacemakers, the sinoatrial node and the atrioventricular node; however, heart rate is controlled by the nervous system. The activity of baroreceptors, mechanoreceptors that respond to changes in blood pressure, and chemoreceptors, which respond to changes in the partial pressure of oxygen and carbon dioxide and to pH variations, triggers reflex mechanisms controlled by both branches of the autonomic nervous system. Afferents from baroreceptors and chemoreceptors reach the nucleus of the solitary tract, which sends excitatory projections to bulbar nuclei housing parasympathetic vagal motoneurons and inhibitory projections to pontine nuclei of origin for sympathetic motoneurons, ultimately altering heart rate (Andresen & Kunze, 1994). Activation of atrial baroreceptors, which reaches its maximum intensity about 300 ms after the R-peak, produces cardiovascular arousal.

Cardiovascular arousal influences several cognitive processes, including visual perception of fearful stimuli (Garfinkel et al., 2014; Garfinkel & Critchley, 2016), memory (Critchley & Garfinkel, 2016; Mather et al., 2016), pain (Edwards et al., 2001; Ozturk et al., 2025), and intentional inhibition (Makowski et al., 2020; Rae et al., 2020). In a 2020 Go/NoGo experiment, Rae and colleagues showed that individual differences in interoceptive ability were related to rates of intentional inhibition and

decision speed: participants with higher interoceptive awareness tended to withhold movements and respond more slowly than participants with lower interoceptive awareness (Rae et al., 2020). This is due to the fact that, during states of cardiovascular arousal, baroreceptor activity increases, strengthening connections with the nucleus of the solitary tract, thalamus, and insular cortex, which is responsible for updating the representation of the body's physiological state (Garfinkel & Critchley, 2016).

The cardiovascular system is the most extensively studied source of interoceptive signals. As Khalsa and Lapidus point out: "Cardiac interoception can be defined as the process of detecting, encoding, and representing information about the state of the cardiovascular system" (Khalsa & Lapidus, 2016). Cardioception, or cardiac interoception, is therefore assessed by measuring individuals' ability to perceive their own heartbeat, quantified objectively through heartbeat detection and/or discrimination tasks that yield a value - interoceptive accuracy - allowing one to distinguish "good" from "poor" heartbeat perceivers.

The involvement of the insular cortex in interoceptive accuracy has been demonstrated by several studies (Caseras et al., 2013; Critchley et al., 2004; Pollatos et al., 2007). In these studies, correlations between interoceptive accuracy and brain activity were calculated at the group level, revealing brain markers of good heartbeat perceivers, thereby supporting the notion that interoceptive accuracy is a stable individual trait (Baltazar et al., 2021).

Emotionally significant events are often associated with physiological changes, particularly in cardiovascular activity, such as an increase in heart rate in anxiety-inducing situations. However, tasks used to quantify cardiac accuracy are typically performed under resting-state conditions and may therefore not capture interoceptive intensity (Khalsa & Lapidus, 2016). Indeed, when measured at rest, interoceptive accuracy is generally low: only about 30% of individuals are typically classified as good perceivers (Brener & Ring, 2016).

Moreover, the ability to perceive one's cardiac activity appears to be influenced by factors such as body mass index (BMI), age and gender (Fittipaldi et al., 2020). In a 2009 study by Khalsa and

colleagues, a negative correlation between interoceptive ability and age was found, indicating that interoceptive accuracy declines with age, whereas no correlation was found with sex or BMI (Khalsa, Rudrauf, & Tranel, 2009). In contrast, Grabauskaitė's 2017 study found a direct relationship between sex and interoceptive accuracy: male participants performed better on interoceptive accuracy measures derived from the HCT, whereas self-report questionnaire results showed that women tended to notice bodily sensations more frequently and better understand the relationship between physical sensations and emotions (Grabauskaitė et al., 2017).

Regarding the relationship between BMI and interoceptive accuracy, a 2021 meta-analysis by Robinson and colleagues, examining associations between interoception and BMI in adults and children, found a clear positive association between body weight and interoceptive deficits; however, it remains unclear whether interoceptive deficits are a cause or a consequence of weight gain and obesity (Robinson et al., 2021).

Cardiac interoception is thus related to several mental functions and processes. Interoceptive dysfunction is increasingly recognized as an important component in various mental health conditions, including anxiety disorders, mood disorders, eating disorders, and substance use disorders (Khalsa et al., 2018).

### 1.6 Respiratory interoception

Breathing is a vital rhythmic process that emerges from the joint activity of respiratory muscles and brainstem circuits. The respiratory cycle consists of two main phases: inhalation and exhalation. Inhalation is driven by contraction of inspiratory muscles (J. L. Feldman, 1986), such as diaphragm and external intercostal muscles; during inhalation, lung volume increases caused by the downward displacement of the diaphragm towards the abdomen. Exhalation is normally a passive process resulting from lung recoil following relaxation of the inspiratory muscles (Del Negro et al., 2018). However, during hyperventilation, exhalation can be actively initiated by contracting expiratory muscles, including internal intercostal muscles and anterior abdominal wall muscles, causing

increased intra-abdominal pressure that facilitates the upward movement of the diaphragm. Ventilation proceeds autonomously thanks to specific neuronal populations located in the brainstem. Rhythm generation occurs in the medulla within pacemaker inspiratory neurons of the pre-Bötzinger complex, while rhythm modulation is carried out by pontine neurons in the apneustic and pneumotaxic centers, which regulate depth and frequency of breathing, respectively (Dhingra et al., 2024; J. C. Smith et al., 1991). Beyond motor control, breathing generates a continuous stream of interoceptive information arising from pulmonary and airway mechanoreceptors sensitive to lung inflation and deflation. These include slowly adapting pulmonary stretch receptors (SARs) and rapidly adapting pulmonary receptors (RARs), which encode dynamic changes in lung volume, airway pressure, and airflow (Chan et al., 2024; Yu, 2021). Afferent signals from these mechanoreceptors are conveyed predominantly via the vagus nerve to the caudal nucleus of the solitary tract (NTS) in the medulla (Neuhuber & Berthoud, 2022; R. Smith et al., 2017; Zoccal et al., 2014), a key integrative hub for visceral sensory information. Notably, RARs are primarily activated by lung stretch during inhalation (Chan et al., 2024; Yu, 2021), while remaining relatively silent during exhalation (Del Negro et al., 2018; Krohn et al., 2023; Kubin et al., 2006; Noble & Hochman, 2019). As a consequence, respiratory afferent signaling is markedly phase-dependent, with inhalation characterized by strong mechanosensory input to brainstem circuits and exhalation by a relative attenuation of respiratory afferent drive (Noble & Hochman, 2019). This marked asymmetry in respiratory afferent signaling across the breathing cycle has been proposed to translate into phase-specific modulations of cortical excitability and information processing, thereby shaping cognitive and perceptual functions in a respiration-dependent manner.

Besides its primary function, breathing is involved in different physiologically relevant functions, such as regulation of body fluid pH (Palmer & Clegg, 2023) and volume (Serikov & Fleming, 2001), heat dissipation (Haut et al., 2021) and articulated sound production and speech (Huber et al., 2005; Tong & Sataloff, 2022); breathing can therefore enter conscious awareness and be voluntarily controlled, as in meditation (Karunarathne et al., 2023; Zaccaro et al., 2018), physical exercise

(Bernasconi & Kohl, 1993), particular emotional states such as anxiety (Paulus, 2013; Tan et al., 2019) and fear (Van Diest et al., 2009), or in the case of airway obstruction (Barnes et al., 2019). For this reason, Farb and colleagues have described breathing as a "unique interoceptive source" (Farb et al., 2013). Indeed, through voluntary modulation of breathing, it is possible to alter interoceptive representations in the insular cortex (Weng et al., 2021).

Accumulating evidence indicates that the respiratory cycle does not merely reflect a background physiological rhythm, but actively modulates perceptual, cognitive and neural processes across multiple sensory domains (Arshamian et al., 2018; Brændholt et al., 2025; Flexman et al., 1974; Gallego et al., 1991; Grund et al., 2022; Kluger et al., 2021; Mizuhara & Nittono, 2023; Perl et al., 2019; Zelano et al., 2016). Respiratory phase-dependent effects have been reported for cardiac interoception, with variations in heartbeat detection performance and heartbeat-evoked potentials across inhalation and exhalation phases (Zaccaro et al., 2022), suggesting changes in the processing and cortical representation of visceral signals. Beyond interoception, breathing phase has also been shown to influence nociceptive processing (Arsenault et al., 2013), visual (Flexman et al., 1974) and somatosensory (Grund et al., 2022) perception. These effects point to a broad impact of respiration on sensory gain and signal integration, extending from brainstem circuits to cortical networks. Theoretical frameworks such as predictive coding propose that respiration may act as a cyclical modulator of sensory precision, dynamically adjusting the balance between top-down predictions and bottom-up sensory evidence (Barrett & Simmons, 2015; Seth, 2013; Seth & Friston, 2016). Within this view, inhalation and exhalation may be associated with differential gain control mechanisms, whereby inspiratory phases enhance the weighting of incoming sensory information, while expiratory phases favor internal integration and reduced sensory interference (J. L. Feldman & Del Negro, 2006; Muñoz-Ortiz et al., 2019). Together, these findings support the notion that respiration constitutes a fundamental organizing rhythm for perceptual processing, shaping both interoceptive and exteroceptive experience through phase-dependent modulation of neural excitability and sensory gain. Several studies have demonstrated that respiration can become temporally coupled with task

structure, showing high respiratory phase coherence across trials. This phenomenon suggests that participants tend to adjust their breathing rhythm in anticipation of upcoming stimuli (Grund et al., 2022; Harting et al., 2025; Huijbers et al., 2014; Johannknecht & Kayser, 2022; Stetza et al., 2025). In the somatosensory domain, Grund et al. (2022) showed that individuals spontaneously synchronize their respiratory cycle with the expected timing of tactile events, a strategy that was associated with enhanced perceptual sensitivity during the expiratory phase. Such respiration-stimulus alignment is thought to influence sensory processing by optimizing neural responsiveness, leading to faster responses and improved accuracy. These findings are consistent with the active sensing framework, which conceptualizes perception as an active, goal-directed process shaped by rhythmic bodily signals (Allen et al., 2023; Boyadzhieva & Kayhan, 2021; Corcoran et al., 2018; Schroeder et al., 2010). Within this view, breathing can be actively modulated to support the sampling and processing of sensory information.

### 1.7 EEG correlates of interoception

The cortical response to the heartbeat is called the Heartbeat-Evoked Potential (HEP), an event-related potential arising from the brain's processing of interoceptive signals associated with systole. It is recorded over frontal, central, and parietal regions of the cerebral cortex from 200 to 650 ms after the R-peak, regardless of whether the heartbeat is consciously perceived or not (Ainley et al., 2016), and is sensitive to several factors, including attention (Petzschner et al., 2019), motivation (Weitkunat & Schandry, 1990), and pain (Schulz et al., 2013).

One of the pioneering studies that identified HEP amplitude and topography was carried out by Schandry and Montoya in 1993. EEG activity was recorded in healthy participants during HCT and an exteroceptive control task in which participants counted auditory stimuli over specific time intervals, and the role of attention in modulating the HEP was assessed. The authors found that the amplitude of the cortical response evoked by the heartbeat depended not only on attentional focus but also on participants' ability to perceive their own heartbeats: the effect was stronger in "poor" than in

“good” perceivers. This was probably due to the greater novelty of heartbeat sensations in the attention condition for poor perceivers compared with good perceivers, who appeared to show a permanent tendency to monitor their own heartbeats. Topographical analysis of HEPs showed that the main effects occurred between 350 and 550 ms after the R-peak, with larger responses in frontal than in central and parietal regions (Montoya et al., 1993).

In a more recent study by Pollatos and Schandry, participants underwent EEG and ECG recording during a heartbeat perception task to examine HEP changes. After dividing the sample into “good” and “poor” perceivers based on interoceptive accuracy, the authors found, contrary to previous findings, that mean HEP amplitudes were markedly greater in good perceivers within a 250-350 ms window after the R-peak at central and frontocentral electrodes compared with poor perceivers (Pollatos & Schandry, 2004).

Interoceptive accuracy is therefore a very useful parameter that correlates positively with HEP amplitude in interoceptive tasks: in individuals with higher interoceptive accuracy, HEP amplitude is greater than in individuals with lower interoceptive accuracy (Pollatos & Schandry, 2004).

Consistent with this result, Mai and colleagues (2018) found a relationship between HEP amplitude and interoceptive accuracy in adolescents: during a heartbeat attention condition, HEPs were larger over frontocentral regions in participants with higher interoceptive accuracy - good vs. poor perceivers - whereas no relationship was observed between interoceptive accuracy and HEP amplitude in the resting-state condition, suggesting that HEP is a neural marker of interoception (Mai et al., 2018).

In a study by Schulz and colleagues (2015), HEP was examined under normal food intake and food deprivation conditions. HEP amplitude was higher in the fasting condition over frontal and central channels, in a window from 455 to 595 ms post R-peak, showing that short-term food deprivation can alter the neural representation of afferent signals from the cardiovascular system. The authors also found greater HEP amplitude in the right than in the left hemisphere, suggesting that HEP may be

generated by multiple sources probably involving the insula and anterior cingulate cortex (Schulz et al., 2015).

A stronger modulation of HEP in the right hemisphere compared with the left was also reported by Pollatos and Schandry (2004): during a heartbeat attention task, HEPs were larger in participants with greater interoceptive accuracy, particularly in the right hemisphere. Stimulation of a body region elicits greater activity in contralateral somatosensory and insular cortices (Hari et al., 1993), which may explain this difference. Although the heart is located in the center of the chest, it is not oriented parallel to the body's vertical axis: the apex of the left ventricle points towards the left side of the body, providing greater stimulation to the left side of the chest and resulting in a larger cortical representation in the right hemisphere (Pollatos & Schandry, 2004).

In the study by Petzschner and colleagues, the interaction between attentional focus and cortical processing of single heartbeats was assessed, demonstrating that attention modulates the amplitude of the heartbeat-evoked potential. Specifically, participants underwent EEG recording while performing a heartbeat attention task consisting of alternating 20-second blocks in which they focused their attention either on their heartbeat (interoceptive condition) or on an auditory stimulus (exteroceptive condition). The results showed that HEPs were significantly larger during the interoceptive condition in a time window between 524 and 620 ms after the R-peak over right central channels (Petzschner et al., 2019).

Attentional modulation of HEP has also been proposed in relation to somatosensory perception and the cardiac cycle. EEG studies by Al and colleagues (2020, 2021) showed that HEP amplitude is negatively correlated with the ability to detect and localize near-threshold tactile stimuli, and that the perception of such stimuli is more likely during diastole than during systole. They also found that HEP amplitude is larger in systole than in diastole. The authors suggested that rhythmic bodily fluctuations, such as heartbeats, are treated as predictable events, and that the resulting physiological changes are not consciously perceived, allowing the brain to minimize the noise of internal signals (Al et al., 2020, 2021).

The effects of the cardiac cycle on the processing of internal signals were also examined by Ambrosini and colleagues in 2019. In two self-face recognition studies, in which participants had to recognize their own face morphed with either unfamiliar or familiar faces at increasing proportions, discrimination was more accurate and faster in systole than in diastole, suggesting that atrial baroreceptor activity speeds up processing of signals involved in self-face recognition (Ambrosini et al., 2019).

Variability in HEP topography and latency relative to the R-peak may be due to differences in the tasks used across experiments, which recruit different cortical areas depending on task demands.

Moreover, given the wide variety of studies examining HEP changes under different conditions - such as attention (Petzschner et al., 2019), somatosensory perception (Al et al., 2020), motivation (Weitkunat & Schandry, 1990), and pain (Schulz et al., 2013) - the observed topographical and temporal differences may indicate that HEP is involved not only in the neural processing of systole, but also, and perhaps more importantly, in the processing of signals related to the self, as opposed to signals arising from outside the body.

### 1.8 Heartbeat-modulated cortical oscillations

Beyond event-related neural responses (event-related potentials, ERPs), the central nervous system dynamically shapes sensory and interoceptive information through ongoing rhythmic fluctuations of neural activity, commonly referred to as neural oscillations. These oscillations reflect coordinated changes in neuronal excitability across distributed networks and provide a temporal framework for integrating information over multiple time scales. Neural oscillations are increasingly recognized as a fundamental mechanism for shaping perceptual, motor and cognitive processes (Calderone et al., 2014; Thut et al., 2012; Thut & Miniussi, 2009). In the context of interoception, oscillatory activity offers a particularly informative window into how internal bodily signals are dynamically processed, weighted and integrated with ongoing cognitive demands. Crucially, interoceptive signals differ from most exteroceptive inputs as they are not discrete events but continuous bodily rhythms (Lopez-

Martin et al., 2026). Cardiac and respiratory activity unfold as ongoing oscillatory processes, producing afferent inputs whose influence on neural processing varies as a function of their phase within the cardiac and respiratory cycles (Allen et al., 2022; Zaccaro et al., 2022). From this perspective, interoceptive processing is intrinsically linked to the timing of bodily rhythms: the central nervous system must continuously sample, weight, and integrate bodily signals that fluctuate across multiple physiological time scales. Within this framework, neural oscillations provide a natural mechanism for aligning internal bodily rhythms with neural excitability (Engelen et al., 2025; Kluger et al., 2021), enabling the selective amplification or attenuation of interoceptive inputs depending on their timing within ongoing cortical dynamics. Accordingly, oscillatory measures in the time-frequency domain have increasingly been proposed as sensitive markers of cardiac and respiratory signal processing (Park et al., 2018), complementing traditional event-related approaches such as heartbeat-evoked potentials (HEPs). Consistent with this view, intracranial EEG (iEEG) studies have shown that heartbeats are accompanied by systematic modulations of cortical oscillatory activity, including changes in spectral power (Park et al., 2018; I. Treves, 2020) and phase consistency (Park et al., 2018) across low-frequency bands in regions implicated in interoceptive processing, such as the insula and somatosensory cortex. These heartbeat-locked oscillatory dynamics have been observed across resting-state conditions (Kim & Jeong, 2019), altered states of consciousness (Liuzzi et al., 2024), emotional contexts (Kato et al., 2020; Kim et al., 2019), and interoceptive-exteroceptive processing (Fló et al., 2024; García-Cordero et al., 2017; Pultsina et al., 2025), suggesting that time-frequency measures capture fundamental aspects of how cardiac signals are represented in the brain. Importantly, since cardiac and respiratory rhythms are physiologically coupled (respiratory sinus arrhythmia, RSA; Brecher & Hubay, 1955; Larsson et al., 2021), heartbeat-related neural oscillations are themselves embedded within the respiratory cycle. This opens the possibility that respiratory phase further modulates the cortical processing of cardiac signals, dynamically reshaping interoceptive representations through cross-frequency and cross-system interactions between brain, heart, and lungs (Allen et al., 2022).

### 1.9 Interoception and fatigue

Fatigue is a clinically relevant symptom across a wide range of immunological, endocrine, neuroinflammatory, oncological, and psychiatric disorders (Chaudhuri & Behan, 2004; Dantzer et al., 2014; Wessely et al., 1996), and it represents a dominant symptom reported by individuals affected by Long COVID (Sandler et al., 2021). SARS-CoV-2 infection has recently been identified as a potential trigger for post-infectious fatigue syndromes (Wilson, 2020). At the same time, fatigue is not limited to pathological conditions. Healthy individuals regularly experience transient fatigue in daily life, typically as a consequence of physical or cognitive exertion. This form of fatigue is generally reversible and disappears once the stressor is removed, and it has been extensively investigated in the context of sport science during both isometric (Berchicci et al., 2013) and dynamic (Tamburro et al., 2020) tasks. However, the susceptibility to and severity of transient fatigue varies across individuals. In some cases, even routine daily activities can elicit disproportionate and persistent fatigue, with negative effects for quality of life and work ability (Wanigatunga et al., 2018). Despite its impact on economy, society and quality of life, the mechanisms underlying both pathological and transient fatigue remain poorly understood. Even less is known about how biological, physiological, neural, and psychological factors interact to give rise to the subjective experience of fatigue and to its large interindividual variability. Recently, however, a unifying theoretical framework has been proposed, according to which both pathological and transient fatigue arise from inference processes grounded in interoception (Greenhouse-Tucknott et al., 2022). In interoceptive predictive models of fatigue, the brain continuously generates predictions about the internal state of the body and compares them with incoming viscerosensory input. When persistent mismatches between predicted and actual bodily states occur (interoceptive prediction errors), this results in a state of dyshomeostasis, characterized by chronically enhanced “interoceptive surprise”. Such chronic dyshomeostasis undermines the individual’s perceived control over bodily states (self-efficacy) and is phenomenologically experienced as fatigue (Stephan et al., 2016). Importantly, this mechanism can be driven by peripheral dysfunctions in the body, by structural lesions affecting

afferent or efferent interoceptive pathways (e.g., demyelination in multiple sclerosis), or by functional impairments such as inflammation in chronic fatigue syndrome. Thus, fatigue can emerge from disturbances at multiple levels of the interoceptive circuitry, including the transmission and cortical representation of visceral signals. Similarly, interoceptive predictive models of fatigue suggest that also subjective symptoms of transient fatigue are associated with increasing interoceptive prediction error leading to a decrease of self-efficacy (Greenhouse-Tucknott et al., 2022). During prolonged physical or cognitive exertion, increasing metabolic demands and physiological instability lead to progressively larger interoceptive prediction errors, which in turn reduce confidence in control over bodily states and give rise to the subjective experience of fatigue (Greenhouse-Tucknott et al., 2022). In this sense, pathological and transient fatigue share a common computational and physiological foundation, despite their distinct origins.

In pathological fatigue, converging evidence further supports the relevance of interoception. Patients with multiple sclerosis who report fatigue symptoms show reduced interoceptive accuracy, typically assessed using heartbeat counting tasks (Ardizzi et al., 2016; Ardizzi & Ferri, 2018; Gonzalez Campo et al., 2020; Schandry, 1981; Tsakiris et al., 2011). Thus, impaired ability to detect and attend to bodily signals is associated with pathological fatigue. Notably, interoceptive accuracy varies widely also in healthy individuals (Ardizzi et al., 2016; Ardizzi & Ferri, 2018; Tsakiris et al., 2011), suggesting that vulnerability to fatigue may be partly rooted in individual differences in interoceptive processing.

Emerging evidence indicates that vulnerability to fatigue is also shaped by epigenetic mechanisms. DNA methylation regulates gene expression without altering the DNA sequence and enables cells to adapt to physiological and pathological conditions. Altered methylation patterns have been observed in several disorders characterized by fatigue, including myalgic encephalomyelitis/chronic fatigue syndrome (Helliwell et al., 2020), multiple sclerosis (Celarain & Tomas-Roig, 2020), fibromyalgia (Ciampi de Andrade et al., 2017), chronic widespread musculoskeletal pain (Burri et al., 2016), and SARS-CoV-2 infection (Balnis et al., 2021; Castro de Moura et al., 2021; Corley et al., 2021). These changes affect genes involved in neural plasticity, immune regulation, and metabolism. For example,

altered methylation of NR3C1, a glucocorticoid receptor gene, is linked to inflammatory processes in chronic fatigue syndrome (Vangeel et al., 2018), while hypomethylation of the BDNF gene is associated with abnormal myelination in multiple sclerosis (Nociti et al., 2019).

Although direct evidence linking NR3C1 and BDNF methylation to interoceptive dimensions is still limited, converging findings suggest that epigenetic regulation of genes involved in neural plasticity and stress-response systems may modulate the processing and the cortical representation of bodily signals. For example, peripheral levels of BDNF have been shown to be specifically associated with interoceptive awareness, suggesting that BDNF-related mechanisms may contribute to the processing and evaluation of visceral bodily signals (Mercader et al., 2010).

This evidence indicates that fatigue is closely related to the processing of interoceptive signals and to the mechanisms through which visceral information is integrated, predicted, and evaluated in the brain. Particularly, cardiac and respiratory afferents, their cortical representations, and their modulation by attention and physiological regulation appear to play a relevant role in shaping both the subjective experience of fatigue and its interindividual variability across health and disease.

### 1.10 General aim

Building on this theoretical background, the present thesis comprises three empirical studies and a fourth ongoing study, which together address the general aim of investigating 1) how respiration shapes interoceptive and exteroceptive perception through attentional and cardiorespiratory brain mechanisms, 2) whether breathing is actively regulated to optimize the processing of internal and external bodily signals and 3) how interoceptive processing is regulated under conditions of fatigue.

The first study aimed to test whether humans actively adjust their breathing to optimize the perception of anticipated interoceptive and exteroceptive stimuli, thereby extending the concept of active sensing from the exteroceptive to the interoceptive domain. We developed an experimental approach that allowed us to examine breathing modulations in a trial-by-trial manner, enabling us to 1) investigate phase-locking behavior to the expected stimulation onsets and to 2) determine whether participants modulated respiratory phase and amplitude differently across tasks.

The second study investigated how HEPs and respiratory phase-related HEP modulations (ΔHEP) change across different interoceptive and exteroceptive attention tasks, and determined whether these changes are specifically driven by cardiac interoceptive attention and by specific respiratory phases; in particular we developed an experimental approach to 1) distinguish the impact of respiratory phases on HEP during tasks involving cardiac and respiratory interoceptive attention as well as their exteroceptive counterparts, 2) test whether HEP amplitude is higher during cardiac interoceptive attention compared to exteroceptive and non-cardiac interoceptive tasks and 3) examine whether HEP changes are specific for a respiratory phase, with the prediction that exhalation would contribute more strongly to HEP increases.

The third study aimed to determine how respiratory phase shapes heartbeat-modulated cortical oscillations during cardiac interoceptive attention, and to clarify whether these time-frequency neural markers provide mechanistic insight into cardio-respiratory interactions underlying interoceptive perception. Specifically, we reanalyzed a previously collected dataset (Zaccaro et al., 2024) in the time-frequency domain to characterize heartbeat-modulated power, inter-trial coherence (ITC), and

functional connectivity across respiratory phases during 1) rest, 2) a cardiac interoceptive task (heartbeat counting task, HCT) and 3) an exteroceptive control task (cardiac-tone counting task, C-TCT).

The fourth ongoing study aims to investigate whether respiratory modulation of cardiac interoceptive processing is preserved and functionally relevant under conditions of fatigue, and to determine how cardio-respiratory and brain interactions contribute to individual differences in perceived fatigability. This study is currently ongoing; analyses are still in progress, and the results reported here are preliminary and have not yet been fully interpreted.

# Chapter 2

# Empirical studies

# Study 1

## Breathing strategies to influence perception: Evidence for interoceptive and exteroceptive active sensing

This study is currently under review. A preprint version is available online:

della Penna F., Zaccaro A., Bayram B., Bubbico F., Perrucci M.G., Costantini M., Ferri F. (2025). Breathing strategies to influence perception: Evidence for interoceptive and exteroceptive active sensing. Preprint available at: https://doi.org/10.1101/2025.05.15.654033

It should be noted that the version included in this thesis corresponds to the most recent revised manuscript and differs substantially from the preprint version. For this reason, the preprint is not included as an appendix. Instead, only the supplementary materials are provided in the appendix, as they have been extensively updated during the revision process and are not available in their current form online.

## 1. Introduction

The respiratory cycle exerts a systematic influence on perceptual and cognitive functions, modulating sensory processing across multiple domains. Several studies have shown phase-dependent enhancements in detection or response speed across specific sensory modalities (Flexman et al., 1974; Gallego et al., 1991; Grund et al., 2022; Kluger et al., 2021; Park et al., 2020, 2022; Perl et al., 2019), as well as task-related phase locking between respiration and expected stimulus timing (Harting et al., 2025; Huijbers et al., 2014; Johannknecht & Kayser, 2022; Stetza et al., 2025). Recent work has extended these effects to interoceptive processing, showing that the amplitude of the heartbeat-evoked potential (HEP) increases during exhalation and correlates with higher interoceptive accuracy (Zaccaro et al., 2022). These findings suggest that respiration modulates cardiac interoception in a way that mirrors its influence on exteroceptive perception. However, it remains unclear whether individuals actively adjust their breathing to enhance interoceptive processing, as has been observed for exteroceptive stimuli.

Given converging findings of respiration as an active sensing mechanism, it is plausible that similar strategic adjustments may also occur in the interoceptive domain. Building on this evidence, we hypothesized that participants would modulate their breathing during both exteroceptive and interoceptive tasks, aligning their respiratory cycle with trial onset to optimize perceptual accuracy. We further predicted that greater respiratory phase coherence across trials would be associated with higher perceptual accuracy, particularly during exhalation. In this study, we investigated the relationship between respiration and the perception of anticipated (i.e., cued) interoceptive and exteroceptive stimuli using two tasks: a heartbeat discrimination task (HDT; Betka et al., 2021) and a tactile detection task (TDT; Grund et al., 2022). Specifically, we aimed to characterize respiratory modulation of 1) interoceptive and 2) exteroceptive performances, and 3) directly compare these effects.

## 2. Materials and methods

### 2.1 Ethics statement

The study was approved by the Ethics Committee of the Department of Psychology, "G. d'Annunzio" University of Chieti-Pescara (Protocol Number 23014). The study was conducted in accordance with the guidelines of the Italian Association of Psychology and the Declaration of Helsinki and its later amendments. Participants were unaware of the specific aims of the experiment. After reading the consent form, all participants provided written informed consent.

### 2.2 Participants

Forty-one healthy volunteers (25 females; 3 left-handed; mean age: 24 ± 4.74 years [mean ± SD]) participated in the study. Eligibility was determined based on self-reported criteria, including: (1) no personal or family history of psychiatric, neurological, or somatic disorders; (2) no chronic or acute respiratory conditions; and (3) no use of medications affecting pulmonary or cardiovascular function. All participants had a body mass index (BMI) within the normal range (24.07 ± 5.36) and normal or corrected-to-normal vision. For the exteroceptive task (TDT), inclusion required an accuracy range of 0.25 to 0.75 and a d' index greater than 0 (Grund et al., 2022). For the interoceptive task (HDT), participants were included if their accuracy exceeded 0.55 and their d' index was greater than 0 (Sokol-Hessner et al., 2015; Whitehead et al., 1977). In the two-alternative-forced-choice (2AFC) heartbeat discrimination task, chance accuracy is 0.5 (Kleckner et al., 2015), but scores around this level provide limited evidence that a participant is genuinely able to discriminate heartbeat timing rather than responding at random. A recent study (Tsuchimochi, 2024) applied a stricter exclusion threshold of 0.6. We here adopted a slightly more tolerant but still conservative threshold of 0.55, to ensure that included participants demonstrated performance above chance, while minimizing unnecessary participant exclusion. Further details are provided in section *3.1. Participant selection*.

### 2.3 Apparatus and stimuli

The experiment was conducted at the Institute of Advanced Biomedical Technologies (ITAB) of the "G. d'Annunzio" University of Chieti-Pescara. Participants were recruited via flyers and social media advertisements. Electrophysiological data were recorded using a BIOPAC system (MP160, BIOPAC Systems Inc., Goleta, CA, USA) and AcqKnowledge software. Electrocardiogram (ECG) data were acquired using three Ag/AgCl pre-gelled electrodes positioned over the left and right clavicles and the right costal margin (ground electrode). Respiration was recorded via a chest-placed respiratory transducer (TSD201, BIOPAC Systems Inc., Goleta, CA, USA). Near-threshold tactile stimuli consisted of square-wave electrical pulses (0.2 ms duration) delivered through a constant current stimulator (Digitimer DS7A, Hertfordshire, UK) via electrodes attached to the left index finger (anode: medial phalanx; cathode: proximal phalanx). Stimulation intensity remained constant throughout the experiment, as determined during the initial threshold assessment (mean: 1.38 mA; range: 0.8-2.4 mA). Auditory stimuli consisted of three consecutive pure tones (1000 Hz, 30 ms duration, 60 dB) presented via a buzzer, synchronized in real-time with participants' heartbeats as detected by the ECG. R-peaks were detected online using a DTU100 Digital Trigger Unit (BIOPAC Systems Inc., Goleta, CA, USA), which monitors the ECG signal and generates a square-wave pulse each time the ECG signal exceeds a threshold set close to the R-peak. This trigger was sent simultaneously to the data-acquisition computer and to the experimental computer to control the timing of sound delivery. For the heartbeat discrimination task (HDT), trials were classified as S+ (synchronous; auditory tones delivered 250 ms after the R-peak) and S- (asynchronous; tones delivered 550 ms after the R-peak), depending on the temporal delay between the R-peak and auditory stimulus onset (see Section 2.4.2 for details). To assess the temporal precision of the system, we computed the delay between R-peak detection and actual sound onset for each trial. The mean latency was 0.252 ± 0.004 s (mean ± SD) for S+ trials and 0.552 ± 0.004 s for S- trials, confirming that auditory stimuli were delivered at the intended delays with minimal jitter. To rule out the possibility that respiratory phase modulated latency jitter, we compared jitter values between inhalation and

exhalation. A paired-sample t-test showed no significant difference ($t_{27}$ = -0.43, p = 0.67). A linear mixed-effects model including respiratory phase, trial type (S+/S-), and their interaction as fixed factors, and subject as a random intercept, likewise revealed no significant effects (respiratory phase: p = 0.65; trial type: p = 0.46; interaction: p = 0.81). These results confirm that the temporal precision of stimulus delivery was not influenced by the respiratory cycle. All tasks were administered using E-Prime 3.0 (Psychology Software Tools, Pittsburgh, PA, USA).

### 2.4 Experimental design

The experimental session included a cardiac interoceptive task (HDT) and a somatosensory exteroceptive task (TDT), administered within-subjects. The order of task administration was counterbalanced across participants, and all participants completed both tasks in a single session on the same day. The HDT was preceded by an audiovisual (AV) familiarization task (Betka et al., 2021), and the TDT was preceded by an individual somatosensory threshold assessment. The entire session lasted approximately 1.5 hours. Experimental procedures are depicted in Figure 1.

#### 2.4.1 AV familiarization task

In the AV familiarization task (Betka et al., 2021), participants judged the simultaneity of a flashing dot and a sequence of three auditory tones. The task comprised two conditions: simultaneous (S+) and non-simultaneous (S-). In the S+ condition, the dot and tones were presented without delay (0 ms); in the S- condition the tones were delayed by 550 ms. The task included 30 trials (15 S+, 15 S-) in random order. After each trial, participants indicated whether the stimuli were simultaneous and rated their confidence on a 4-point Likert scale (1 = very unconfident; 4 = very confident).

#### 2.4.2 Heartbeat discrimination task

In the HDT, participants focused on their heartbeat and judged whether it was simultaneous with three auditory tones (Betka et al., 2021; Garfinkel et al., 2015; Katkin et al., 1982; Schulz et al., 2013). Two

conditions were included: S+ (tone onset delayed by 250 ms after the R-peak) and S- (tone onset delayed by 550 ms after the R-peak) (Betka et al., 2021; Garfinkel et al., 2015, 2016; Koreki et al., 2022). The task comprised 200 trials (100 S+, 100 S-), divided into four blocks of 50 trials (25 S+, 25 S- in random order). After each trial, participants provided a simultaneity judgment and rated confidence from 1 (very unconfident) to 4 (very confident). Each trial began with a white fixation cross, presented for a variable duration between 1 and 2 seconds, followed by a visual cue (fixation cross turning red). The red cross remained on the screen throughout the auditory stimulation period. Unbeknownst to the participant, cue duration varied by condition (S+: 800 ms; S-: 500 ms) to prevent participants from inferring the condition based on the shorter trial duration associated with the S+ condition. In both S+ and S- trials, the interval between cue onset (fixation cross turning red) and the onset of the first tone was kept constant (1050 ms), with the red cross displayed throughout this period. In S+ trials, the red cue lasted 800 ms, followed by a tone at R + 250 ms; in S- trials, the red cue lasted 500 ms, followed by a tone at R + 550 ms (S+: 800 + 250 = 1050 ms; S-: 500 + 550 = 1050 ms). This procedure ensured identical cue-tone timing across conditions, aside from the unavoidable variability introduced by individual heart rate and the cardiac phase at trial onset. Mean trial duration for the S+ condition was 3.18 ± 0.26 s (mean ± SD); mean trial duration for the S- condition was 3.18 ± 0.21 s. A two-tailed t-test revealed no significant difference in trial duration between conditions ($t_{27}$ = 0.03, p = 0.97). Following tone presentation, simultaneity and confidence ratings were collected (1.5 seconds per response; Fig. 1A). Participants were instructed not to manually check their heartbeat. Before beginning, they confirmed that the respiratory belt did not interfere with heartbeat perception. Participants were also instructed to breathe spontaneously and not to hold their breath. Breaks were allowed between blocks to prevent fatigue.

The HDT was adapted from Betka et al. (2021), which used five consecutive auditory stimuli. However, five consecutive heartbeats are likely distributed across more than one respiratory phase, making it difficult to assign the trial exclusively to either inhalation or exhalation. To address this issue, we first conducted a pilot study in which HDT was presented in three different variations: 3

consecutive tones, 2 consecutive tones, and 1 single tone (see Supplemental material, Text S1: pilot study). The goal of the pilot study was to identify the shortest possible HDT variant that would maintain the desired accuracy above 0.5. The implementation of these shorter trials would allow for a precise trial-by-trial determination of respiratory phases.

### 2.4.3 Tactile detection task

In the TDT (Grund et al., 2022), participants reported whether they perceived a near-threshold tactile stimulus on the left index finger. Two conditions were included: S+ (electrical pulse delivered) and S- (catch trials, no stimulation). The task consisted of 300 trials (200 S+, 100 S-), divided into four blocks of 75 trials (50 S+, 25 S- in random order). After each trial, participants reported whether they perceived the stimulus and rated confidence from 1 (very unconfident) to 4 (very confident). Each trial began with a white fixation cross, presented for a variable duration between 1 and 2 seconds, followed by a visual cue (fixation cross turning red) for 500 ms before the tactile stimulus. The red cross remained on the screen throughout the stimulation period. Trial duration was fixed at 620 ms. Response screens for detection and confidence lasted 1.5 seconds each (Fig. 1B). Prior to the TDT, participants underwent a tactile threshold assessment using an up-and-down method (Mylius et al., 2023): starting with a suprathreshold intensity, an initial rough estimation of the threshold was obtained by 1) decreasing the electrical intensity by 50% when the participant detected the stimulus, and 2) increasing the intensity by 50% when the participant did not detect the stimulus. A test block of 15 trials (10 stimulated, 5 catch) confirmed the threshold, defined as detection in 4-6 of 10 stimulated trials (0.5 accuracy). This procedure was repeated twice before the experiment and between each block to maintain accuracy around 0.5 (never below 0.25 and never above 0.75) throughout the task (Grund et al., 2022).

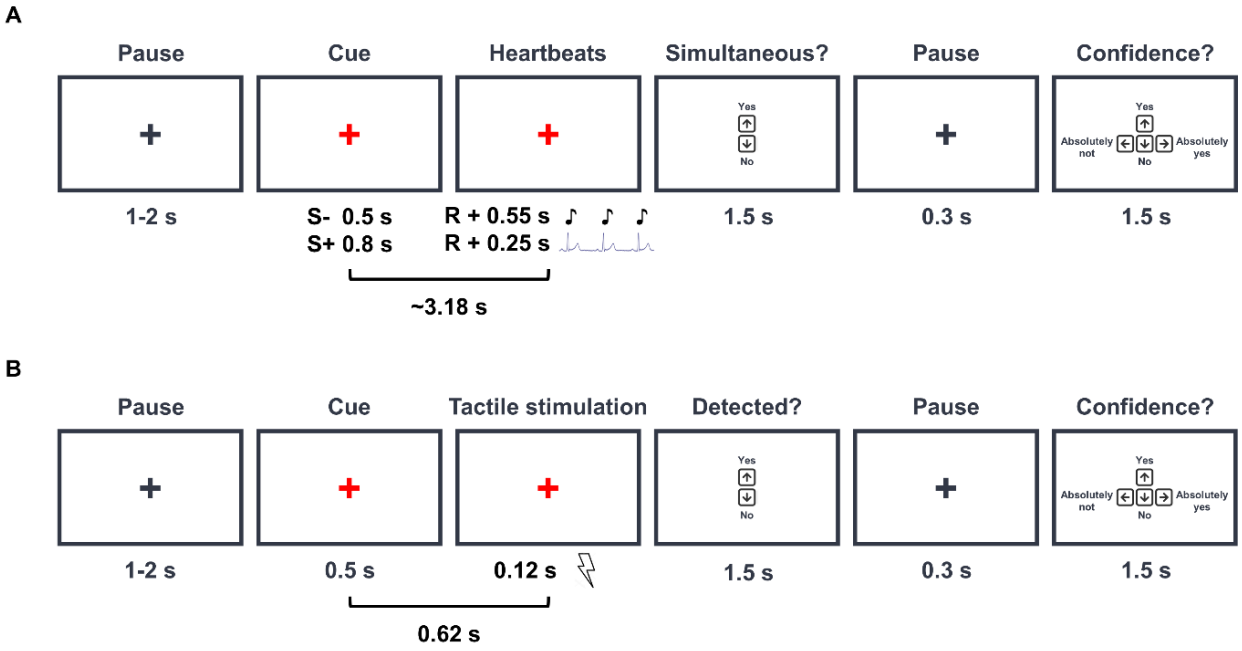



**Figure 1. Experimental procedures**. **A)** Heartbeat discrimination task: each trial began with a neutral fixation cross (1-2 s), followed by a cue (0.5 or 0.8 s) during which the cross turned red and the three tones were presented. The average trial duration (3.18 ± 0.22 s) is indicated beneath the line connecting the "Cue" and "Heartbeats" boxes. After the stimulation, a simultaneity question appeared (1.5 s), with no delay between the last sound and the onset of the question, followed by a fixation cross (0.3 s) and a confidence rating (1.5 s). In both S+ and S- trials, the interval between cue onset (fixation cross turning red) and the onset of the first tone was kept constant (1050 ms), with the red cross displayed throughout this period. In S+ trials, the red cue lasted 800 ms, followed by a tone at R + 250 ms; in S- trials, the red cue lasted 500 ms, followed by a tone at R + 550 ms (S+: 800 + 250 = 1050 ms; S-: 500 + 550 = 1050 ms). This procedure ensured identical cue-tone timing across conditions, aside from the unavoidable variability introduced by individual heart rate and the cardiac phase at trial onset. Consequently, participants could not infer trial type from visual timing cues. Mean trial duration was 3.18 s ± 0.22 s. **B)** Tactile detection task: each trial began with a neutral fixation cross (1-2 s), followed by a cue (0.5) after which the electrical pulse was delivered (in a time window lasting 0.12 s). The fixed trial duration (0.62 s) is indicated beneath the line connecting the "Cue" and "Tactile stimulation" boxes. After the stimulation, a detection question appeared (1.5 s), with no delay between the electrical pulse and the onset of the question, followed by a fixation cross (0.3 s) and a confidence rating (1.5 s).

### 2.5 Cardio-respiratory data acquisition and pre-processing

Cardio-respiratory signals were recorded at a sampling rate of 2 kHz. A band-pass filter (0.1-50 Hz) and a 50-Hz notch filter were applied. The signals were then downsampled to 256 Hz. Data analysis was conducted using custom MATLAB scripts (R2023b, MathWorks Inc.). R-peaks were detected using the Pan-Tompkins algorithm (Pan & Tompkins, 1985). Respiratory phases (inhalation and exhalation) were identified using the *findpeaks* function. Inhalation onsets were marked at local

minima (troughs), whereas exhalation onsets were marked at local maxima (peaks). A complete respiratory cycle was defined as the interval between two consecutive troughs. Outliers, defined as values exceeding three scaled median absolute deviations from the local median within a moving 1-second window, were linearly interpolated using neighboring values. The data were subsequently smoothed with a 1-second window filter (Savitzky & Golay, 1964) and z-scored.

### 2.6 Heart rate variability analyses

As a control analysis, heart rate variability (HRV) was computed to assess potential differences in autonomic cardiac regulation between the two tasks. The time series of intervals between consecutive R-peaks (tachogram) was computed from the ECG signal. The tachogram was pre-processed and analyzed using Kubios software (Kubios HRV Standard, version 3.5, Tarvainen et al., 2014) to extract both time- and frequency-domain HRV indices. The following parameters were calculated: mean RR interval (ms; average latency between consecutive R-peaks), SDNN (ms; standard deviation of normal-to-normal intervals), mean HR (bpm; mean heart rate), STD HR (bpm; standard deviation of heart rate), RMSSD (ms; root mean square of successive differences), VLF power ($ms^2$; very low frequency band), LF power ($ms^2$; low frequency band), HF power ($ms^2$; high frequency band), and the LF/HF ratio (balance between sympathetic and parasympathetic activity). HRV parameters were statistically compared between the two tasks using paired-sample t-tests on the subset of participants included in both task analyses (n = 22), to verify that the observed behavioral and respiratory differences were not confounded by changes in autonomic activity.

### 2.7 Task accuracy assessment

Task performance in HDT and TDT was evaluated using signal detection theory (Green & Swets, 1966), which describes the ability to distinguish weak stimuli from background noise (Wickens, 2001). Within this framework, response outcomes included hits (correctly detecting the stimulus), misses (failing to detect the stimulus), correct rejections (correctly identifying the absence of a

stimulus), and false alarms (incorrectly identifying the presence of a stimulus). In this study, a hit corresponded to an S+ trial accurately identified as S+, a miss was an S+ trial incorrectly marked as S-, a correct rejection was an S- trial accurately identified as S-, and a false alarm was an S- trial incorrectly marked as S+ (Forkmann et al., 2016; Katkin et al., 1982; Rominger et al., 2021; Schulz et al., 2013, 2021; Sokol-Hessner et al., 2015; Whitehead et al., 1977). This method enabled the assessment of task accuracy, sensitivity (d'), and response criterion (c).

Task accuracy was defined as the proportion of correct responses relative to the total number of trials (Garfinkel et al., 2016; Kleckner et al., 2015):

$$\text{Task accuracy} = \frac{\text{Hits} + \text{Correct rejections}}{\text{Hits} + \text{Misses} + \text{Correct rejections} + \text{False alarms}}$$

Sensitivity (d') reflects a participant's ability to distinguish between signal and noise (i.e., the absence of a signal). Higher d' values indicate greater sensitivity. It is calculated using the following formula (Michal et al., 2014; Rominger et al., 2021; Schulz et al., 2021; Sokol-Hessner et al., 2015):

Sensitivity (d') = z (Hit rate) - z (False alarm rate)

where the hit rate is the proportion of hits relative to the total number of S+ trials, the false alarm rate is the proportion of false alarms relative to the total number of S- trials, and z denotes the normal inverse cumulative distribution function.

The response criterion (c) represents a participant's decision threshold for determining whether a signal is present. A lower criterion indicates a tendency to report the presence of a signal, leading to more hits but also more false alarms. Conversely, a higher criterion indicates a tendency to report the absence of a signal, resulting in more misses but also more correct rejections. If c equals zero, the participant is unbiased. The criterion is computed as follows (Mylius et al., 2023):

$$\text{Criterion (c)} = -\frac{1}{2} \times [\text{ z (Hit rate)} + \text{z (False alarm rate)}]$$

where the hit rate and false alarm rate are defined as above, and z is the normal inverse cumulative distribution function. Accuracy, d', and c were computed separately for inhalation and exhalation.

Trial classification (inhalation or exhalation) was based on the timing of stimulus presentation, specifically the first heartbeat of the trial in the HDT and the tactile stimulation in the TDT.

### 2.8 Statistical analyses

#### 2.8.1 Overview

To investigate breathing behavior and its relationship with perceptual accuracy, we performed a series of analyses across interoceptive (HDT) and exteroceptive (TDT) tasks. First, we examined key respiratory parameters (i.e., breathing frequency, average inhalation duration, average exhalation duration) to assess differences in breathing patterns between tasks (Respiratory parameters analysis). To determine whether participants actively modulated their respiration around stimulus presentation, we computed the event-related respiratory signal (ERrS analysis). We then assessed inter-trial coherence to evaluate the consistency of respiratory phase alignment relative to stimulus onset (ITC analysis).

To determine whether participants' perceptual performance varied as a function of the respiratory phase at the time of stimulus presentation, we conducted paired-samples t-tests between inhalation and exhalation for accuracy, sensitivity (d'), and response criterion (c), separately for the HDT and the TDT (Behavioral analysis). To examine whether respiration predicted task performance, we used generalized linear mixed models (GLMM analysis). Additionally, to explore the directionality of the effect observed in the GLMM, we tested for uniformity the distribution of respiratory phase angles for both correct and incorrect trials across the respiratory cycle (Respiratory phase clustering analysis). Finally, we explored whether respiration-related modulation of performance was driven by phase alignment (ITC), amplitude modulation (ERrS), or both, by computing ERrS and ITC for correct and incorrect trials (ERrS and ITC analyses for correct and incorrect trials).

### 2.8.2 Respiratory parameters analyses

To investigate differences in breathing patterns across tasks, we calculated key respiratory parameters, including average inhalation duration, average exhalation duration, and breathing frequency, for both the HDT and TDT, using custom MATLAB scripts (R2023b, MathWorks Inc.). We assessed differences in these parameters between the interoceptive task (HDT) and the exteroceptive task (TDT) using paired-samples t-tests.

### 2.8.3 Event-related respiratory signal analyses

To examine whether participants actively modulated their breathing cycle and whether this modulation differed between tasks, we computed the event-related respiratory signal (ERrS) using FieldTrip (Oostenveld et al., 2011). Respiratory data were time-locked to cue onset (the white cross turning red) and segmented from -500 ms to 3000 ms. The ERrS was then calculated by averaging trials separately for the HDT and TDT. A baseline correction using the -500 to 0 ms pre-cue interval was applied to the averaged ERrS traces, to align the task-related signals to a common reference level. This procedure was used for visualization purposes and to enable statistical comparison of ERrS amplitude and dynamics between tasks, as well as for within-task contrasts between correct and incorrect trials. For finer-grained analysis, the 3-second active phase was divided into six 500 ms bins, and the ERrS from these bins was compared across tasks using a permutation-based t-test, with Benjamini and Yekutieli correction procedure (Benjamini & Yekutieli, 2001) applied for multiple comparisons.

### 2.8.4 Inter-trial coherence analyses

To assess the consistency of respiratory phase alignment across trials, reflecting participants' tendency to synchronize their breathing with trial onset, we conducted inter-trial coherence (ITC) analyses using FieldTrip (Oostenveld et al., 2011). In both tasks, the respiratory signal was epoched from -0.5 to 3 s relative to cue onset and band-pass filtered between 0.1 and 0.6 Hz. We applied the

Hilbert transform to the filtered respiratory signal, from which the instantaneous phase was extracted as the argument of the complex output. For each participant, phase values were first converted into unit-length complex vectors and ITC was calculated as the magnitude of their circular mean across trials: this yields a time-resolved measure ranging from 0 (random phase distribution) to 1 (perfect phase alignment across trials). This procedure is in line with previous studies (Eidelman-Rothman et al., 2019; Khadir et al., 2024; Noda et al., 2017; Sihn & Kim, 2022; Zareian et al., 2020). Additionally, ITC values were normalized to the -500 to 0 ms pre-cue interval to obtain relative ITC (rITC). This baseline normalization was used to facilitate statistical comparison of ITC amplitudes between tasks (HDT vs. TDT) and for within-task contrasts between correct and incorrect trials, by aligning ITC measures to a common reference level. Importantly, all analyses assessing respiratory phase alignment within each task (i.e., time windows showing significant ITC increases relative to baseline) were performed on non-normalized, absolute ITC values, ensuring that no transformation affected the underlying respiratory phase structure. ITC values were analyzed across two distinct phases: baseline (500 ms before cue onset) and active (up to 3 seconds following cue onset, corresponding to trial duration). For finer-grained analysis, the active phase was further divided into six consecutive 500 ms bins. To assess statistical significance, each of the six active-phase bins was compared to the baseline phase using a permutation-based t-test, with Benjamini and Yekutieli correction procedure (Benjamini & Yekutieli, 2001) applied for multiple comparisons.

### 2.8.5 Behavioral analyses

Based on the computed values of task accuracy, sensitivity (d'), and response criterion (c), we performed paired-sample t-tests to assess whether participants' performance differed between inhalation and exhalation. These analyses were conducted separately for each task (HDT and TDT).

### 2.8.6 Generalized linear mixed model

To examine whether respiration predicted task accuracy, respiratory phase angles were extracted for each trial at the time point corresponding to the maximum ITC value for each task. These phase angles were entered into the model as their sine and cosine components (Harting et al., 2025; Kluger et al., 2021, 2023; Saltafossi et al., 2025). The sine and cosine components of the respiratory phase angles were then used as predictors of accuracy values in generalized linear mixed models (GLMMs) implemented in MATLAB using the *fitglme* function. For each task (HDT and TDT), a first baseline model predicted accuracy from task condition (sync/async and stim/catch, respectively for HDT and TDT) with participant included as a random intercept. A second model additionally included respiratory phase, modelled via sine and cosine transformations. A third model was implemented including condition and instantaneous heart rate (iHR), estimated on a trial-by-trial basis. Specifically, iHR was derived from RR intervals between consecutive heartbeats occurring within each trial. In the HDT, where three heartbeats were typically present, two RR intervals were computed, converted into iHR values, and averaged to obtain a single iHR estimate. In the TDT, where only two heartbeats occurred, iHR was calculated from the RR interval between those beats. A fourth model included both respiratory phase (sine and cosine) and iHR. Finally, a fifth model additionally included interaction terms between iHR and the sine and cosine components of respiratory phase. Model fits were compared using likelihood ratio tests (LRTs). Specifically, LRTs were used to compare: Model 2 vs. Model 1 to test the contribution of respiratory phase; Model 3 vs. Model 1 to test the contribution of iHR; Model 4 vs. Model 2 to test whether iHR explains additional variance beyond respiration; Model 4 vs. Model 3 to assess whether respiratory phase or iHR provides the stronger contribution; Model 5 vs. Model 4 to test whether cardiac activity modulates (interacts with) respiratory effects. The model formulas are reported below:

Model 1: Accuracy ~ 1 + condition + (1 | ID)

Model 2: Accuracy ~ 1 + condition + resp sin + resp cos + (1 | ID)

Model 3: Accuracy ~ 1 + condition + iHR + (1 | ID)

Model 4: Accuracy ~ 1 + condition + resp sin + resp cos + iHR + (1 | ID)

Model 5: Accuracy ~ 1 + condition + resp sin * iHR + resp cos * iHR + (1 | ID)

To quantify the amplitude of respiratory influences on accuracy, the fixed-effect coefficients associated with the sine and cosine predictors were collapsed into a single vector norm (Saltafossi et al., 2025) defined as:

$$\nu = \sqrt{\beta_{cos}^2 + \beta_{sin}^2}$$

This metric was tested against a null distribution generated from randomized accuracy. For each of the 5000 permutations, accuracy values were randomly reassigned across trials within each participant and condition (S+ and S- trials), thereby eliminating the original coupling between accuracy and respiratory phase while preserving the proportion of correct responses for each participant and for each condition. The GLMM containing the sine and cosine terms was refitted to each permuted dataset, and the corresponding vector norm was recalculated, yielding a permutation-based null distribution of vector norms. The empirical vector norm was then compared against this distribution, and statistical significance was determined by assessing whether it exceeded the 95th percentile of the null distribution, corresponding to the proportion of null values greater than or equal to the observed value.

### 2.8.7 Respiratory phase clustering analyses

To assess whether changes in task accuracy were related to the respiratory phase, we tested for uniformity the distribution of respiratory phase angles for both correct and incorrect trials across the respiratory cycle using the Rayleigh test (Berens, 2009), separately for the HDT and TDT. Importantly, the same respiratory phase angles extracted for the GLMM analyses (see Section 2.8.6) were used here. Additionally, the Watson-Williams test (Berens, 2009) was applied to compare the mean phase directions of correct and incorrect trials within each task. To control for potential false positives, we implemented a non-parametric permutation procedure. Behavioral accuracy labels

(correct vs. incorrect) were randomly reassigned across trials within each participant, thereby preserving each participant's respiratory phase angle distribution and the number of correct and incorrect trials, while eliminating the original trial-wise correspondence between respiratory phase and behavioral outcome. For each permutation, respiratory phases associated with the permuted correct or incorrect trials condition were selected, and a subject-level circular mean phase was computed. These subject-level mean phases were subsequently entered into a second-order Rayleigh test to quantify group-level phase clustering. This procedure was repeated 5000 times, yielding a permutation-based null distribution of Rayleigh Z statistics. Statistical significance was defined a priori by comparing the observed Rayleigh Z statistic to the 95th percentile of the permutation-derived null distribution, corresponding to a one-sided significance threshold of $\alpha = 0.05$.

### 2.8.8 Event-related respiratory signal analyses for correct and incorrect trials

To assess whether changes in task accuracy were related to respiratory amplitude modulation, we analyzed the ERrS of correct and incorrect trials in both tasks. As described previously, the active-phase bins were compared between correct and incorrect trials within each task (HDT and TDT) using a cluster-based permutation test, with Benjamini and Yekutieli correction procedure (Benjamini & Yekutieli, 2001) applied for multiple comparisons.

### 2.8.9 Inter-trial coherence analyses for correct and incorrect trials

We further investigated whether task accuracy was related to respiratory phase consistency across trials by analyzing ITC separately for correct and incorrect trials in both tasks, segmented into baseline and active phases, as previously described. Correct trials included hits and correct rejections, while incorrect trials included misses and false alarms. To assess statistical significance, each of the six active-phase bins was compared with the baseline phase using a permutation-based t-test, conducted separately for correct and incorrect trials. To compare rITC values between correct and incorrect trials within each task, a permutation-based t-test was performed across the six active-phase

bins. This methodology was applied within HDT and TDT. The Benjamini and Yekutieli correction procedure (Benjamini & Yekutieli, 2001) for multiple comparisons was applied.

## 3. Results

### 3.1 Participant selection and behavioral performance

We evaluated 41 healthy volunteers who completed both an interoceptive and an exteroceptive task. The interoceptive task was the HDT (adapted from Betka et al., 2021), in which participants judged the simultaneity of their own heartbeat with a sequence of three acoustic signals. The choice of the three-sound condition was based on the results from the pilot study (see Supplemental material, Text S1: pilot study). The exteroceptive task was the TDT (adapted from Grund et al., 2022), where participants detected near-threshold tactile stimuli. Thirteen participants were excluded from the HDT: six due to task accuracy (defined as the proportion of correct responses - hits and correct rejections - relative to the total number of trials) below 0.55 (0.51 ± 0.01 [mean ± SD]) and seven because of a d' score below 0 (-0.06 ± 0.03). This resulted in an HDT sample size of N = 28 (16 females, 3 left-handed; age: 26 ± 5.1 years). Mean accuracy was 0.61 ± 0.08, mean d' was 0.68 ± 0.46, and mean criterion was -0.29 ± 0.42. Nine participants were excluded from the TDT: six due to task accuracy above 0.75 (0.8 ± 0.06) and three because of a d' score below 0 (-0.24 ± 0.03) (Grund, et al., 2022). This resulted in a TDT sample size of N = 32 (19 females, 3 left-handed; age: 25 ± 4.7 years). Mean accuracy was 0.56 ± 0.1, mean d' was 0.89 ± 0.63, and mean criterion was 0.66 ± 0.49. When considering only those who successfully completed both tasks, the sample used for joint analyses comprised 22 participants (12 females, 3 left-handed; age: 26.3 ± 5.01 years).

For all trial-by-trial analyses that involved separating trials by behavioral outcome (see Sections 3.8, 3.9 and 3.10), participants contributed on average 117 ± 17 correct and 83 ± 17 incorrect trials in the HDT, and 159 ± 30 correct and 140 ± 30 incorrect trials in the TDT.

### 3.2 Respiratory parameters analyses

To investigate breathing patterns across the two tasks, we computed the breathing frequency, average inhalation duration and average exhalation duration, for both HDT and TDT. We then conducted paired t-tests to assess task-related differences. A total of 22 participants met the inclusion criteria for both tasks and were included in this analysis. Breathing frequency was significantly lower during HDT compared to TDT ($t_{21}$ = -3.81, p = 0.001, d = -0.81, Fig. 2A). The average inhalation duration was significantly longer during HDT than TDT ($t_{21}$ = 4.24, p = 0.0004, d = 0.9, Fig. 2B) and the average exhalation duration showed a trend for an increase during HDT compared to TDT ($t_{21}$ = 1.87, p = 0.076, d = 0.4, Fig. 2C). To explore whether trial duration influenced participants' respiratory patterns, we correlated mean trial duration with mean respiratory cycle duration across participants. In the HDT, a significant positive correlation was observed (r = 0.39, p = 0.04), indicating that participants' breathing patterns adapted to the temporal structure of the task, with slower breathing associated with longer trial durations. This analysis could not be performed for the TDT because trial duration was fixed (0.62 s) and therefore did not vary across participants.

### 3.3 Event-related respiratory signal analyses

We computed the ERrS for both the HDT and TDT to investigate if participants synchronized their breathing differently depending on task timing. A significant difference in breathing patterns between HDT and TDT was observed in two distinct time windows: 0-0.5 seconds (t = 2.56, p = 0.004, $p_{FDR}$ = 0.022, d = 0.66) and 2-2.5 seconds after cue onset (t = -2.38, p = 0.007, $p_{FDR}$ = 0.022, d = -0.61, Fig. 2D). To ensure that the observed effects were not simply due to the presentation of three consecutive stimuli during HDT, as opposed to a single stimulus in the TDT, we examined ERrS in the 1-tone condition of the pilot study and compared it to ERrS measured during the TDT. This analysis confirmed that differences in ERrS between tasks were not due to the different number of stimuli presented (see Supplemental material, Text S1: pilot study, Fig. S1).

### 3.4 Inter-trial coherence analyses

To assess the consistency of respiratory phase alignment across trials, we conducted ITC analyses, which revealed significant modulation in both the HDT and TDT, indicating that participants synchronized their breathing with trial onset. Within-task comparisons were performed using non-normalized (absolute) ITC values. In the HDT, ITC values significantly increased compared to the baseline phase from 1.5 to 3 seconds after cue onset (all $p_{FDR}$ values < 0.02; statistics are reported for the least significant time window: t = 2.4, p = 0.009, $p_{FDR}$ values = 0.02, d = 0.45; see Supplemental Table S4). In the TDT, ITC values significantly increased from 1 to 3 seconds after cue onset (all $p_{FDR}$ values < 0.0003; statistics are reported for the least significant time window: t = 4.39, p = 0.0002, $p_{FDR}$ = 0.0003, d = 0.78; see Supplemental Table S5). Peak ITC values were observed 2.25 seconds after cue onset during the HDT and 1.95 seconds after cue onset during the TDT. The comparison of relative ITC (normalized) values between the HDT and TDT was not significant across all time windows (all ps > 0.1, Fig. 2E; see Supplemental Table S3), indicating that participants synchronized their breathing with trial onset similarly in both tasks (Fig. 2E). Finally, to assess whether respiratory coupling reflected a stable individual characteristic across tasks, we computed Spearman's rank-order correlations between the mean rITC values extracted from the task-specific significant time windows for the two tasks (HDT: 1.5-3 s after cue onset; TDT: 1-3 s after cue onset). The correlation between the two measures was not significant ($\rho$ = -0.22, p = 0.32), suggesting that respiratory coupling is not a stable individual trait across domains.

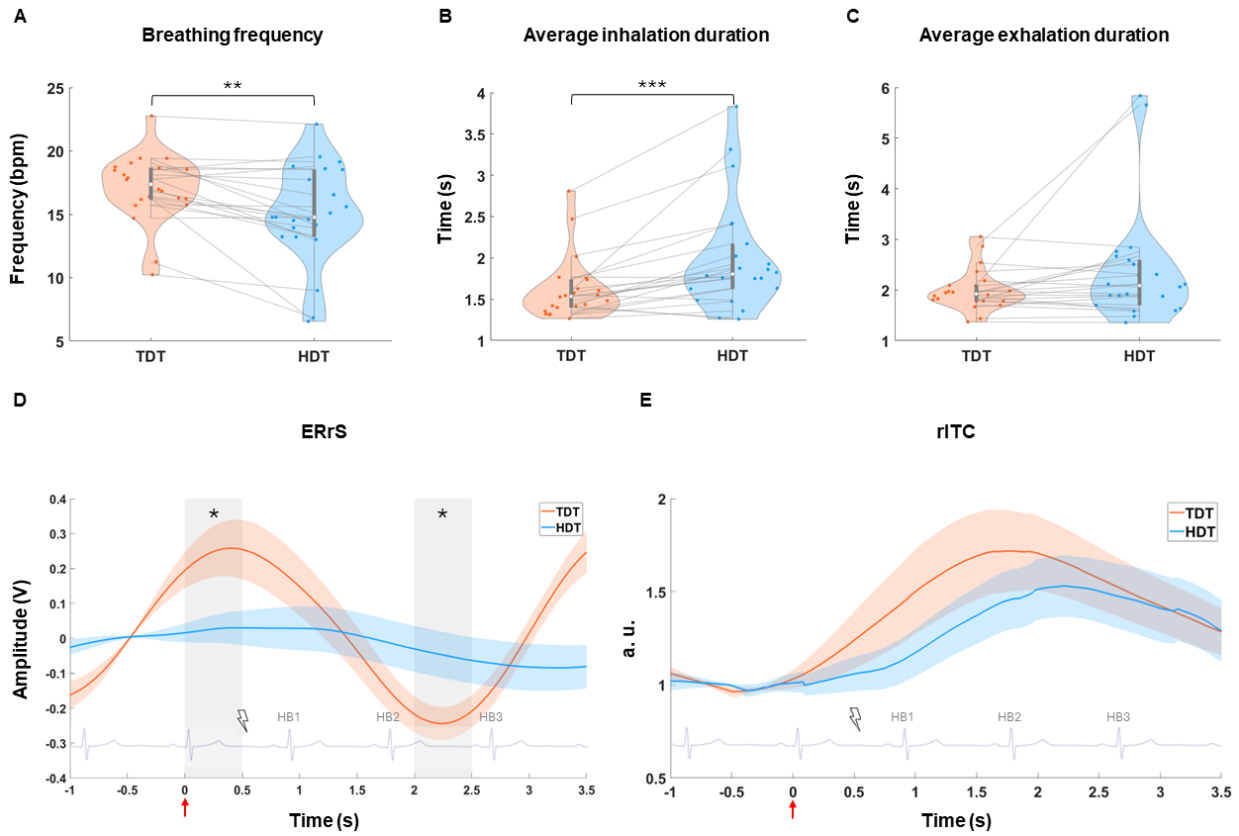



**Figure 2. Respiratory modulations across tasks. A)** Breathing frequency; **B)** Average inhalation duration; **C)** Average exhalation duration. **D)** ERrS. **E)** rITC. Gray areas represent the windows of statistical significance. Red arrows represent the cue onset in both conditions; lightning symbol represents the onset of the electrical stimulation in the TDT; the overlaid ECG signal represents an example of an S- trial, included to illustrate the temporal dynamics of the trial with the three target heartbeats highlighted. Abbreviations: HDT - heartbeat discrimination task; TDT - tactile discrimination task; ERrS - event-related respiratory signal; rITC - relative inter-trial coherence. * $p < 0.05$, ** $p < 0.01$, *** $p < 0.001$.

### 3.5 Heartbeat discrimination task: behavioral analysis

HDT accuracy was significantly higher for trials initiated during the exhalation phase compared to the inhalation phase ($t_{27} = 2.09$, $p = 0.046$, $d = 0.4$, Fig. 3A-left). While sensitivity (d') and criterion (c) did not show statistically significant differences between inhalation and exhalation, both measures exhibited a trend towards significance. Specifically, sensitivity tended to be higher during exhalation than inhalation ($t_{27} = 1.78$, $p = 0.086$, $d = 0.34$, Fig. 3A-right), whereas criterion tended to be lower during exhalation ($t_{27} = -1.86$, $p = 0.073$, $d = -0.35$, Fig. S3A). These trends appear to be driven by differences in the hit rate, which was significantly higher during exhalation compared to inhalation

($t_{27}$ = 2.54, p = 0.017, d = 0.48, Fig. S3B). In contrast, no significant difference was found in the false alarm rate ($t_{27}$ = -0.263, p = 0.8, d = -0.05, Fig. S3C).

### 3.6 Tactile detection task: behavioral analysis

TDT accuracy exhibited a trend towards significance, tending to be higher during exhalation than inhalation ($t_{31}$ = 1.95, p = 0.06, d = 0.35, Fig. 4A-left). This trend appears to be driven by a significantly higher false alarm rate during inhalation compared to exhalation ($t_{31}$ = 2.36, p = 0.025, d = 0.42, Fig. S3F), while no significant difference was found in the hit rate ($t_{31}$ = -1.69, p = 0.1, d = -0.3, Fig. S3E). Task sensitivity (d') was significantly higher during the exhalation phase compared to the inhalation phase ($t_{31}$ = 6.84, p = 1.17 × $10^{-7}$, d = 1.21, Fig. 4A-right), while no significant differences were observed for criterion (c) between inhalation and exhalation ($t_{31}$ = -0.43, p = 0.67, d = -0.08, Fig S3D).

### 3.7 Generalized linear mixed models analysis

A GLMM approach was employed to determine whether the trial-level phase angle of the respiratory signal could predict trial accuracy in both HDT and TDT. The trial-level instantaneous respiratory phase was extracted at the time points corresponding to maximum ITC values observed for each task (2.25 seconds after cue onset for HDT and 1.95 seconds for TDT). Phase angles (sine and cosine transformed) were then used as predictors of accuracy values. Compared to the baseline (Model 1), the inclusion of respiratory phase significantly enhanced model fit for both tasks (HDT: LRT-Stat = 8.12, p = 0.02; TDT: LRT-Stat = 7.89, p = 0.02). For HDT, respiratory phase had a significant impact on trial-level accuracy, showing a significant effect of the cosine component (β = -0.03, t = -2.81, p = 0.005). The model also indicated significant main effect of condition (β = -0.2, t = -15.9, p < 0.0001, Fig. S2A). For the TDT, respiratory phase significantly influenced trial-level accuracy, showing a significant effect of the cosine component (β = -0.02, t = -2.8, p = 0.005). The model also showed significant main effect of condition (β = 0.38, t = 38.6, p < 0.0001, Fig. S2B). To further test whether

trial-level accuracy was significantly modulated across the respiratory cycle, we assessed the overall amplitude of the phase-dependent effect by computing the vector norm, obtained by combining the GLMM beta weights of the sine and cosine coefficients ($\beta_{sin}$, $\beta_{cos}$), defined as:

$$\nu = \sqrt{\beta_{cos}^2 + \beta_{sin}^2}$$

This value was then compared against a permutation-based null distribution derived from 5000 iterations in which trial accuracies were randomly permuted across trials within each participant and condition. The empirical vector norm exceeded the 95th percentile of the permutation-derived null distribution in both HDT ($p = 0.021$, proportion of permuted vector norms ≥ empirical value: $p = 0.015$) and TDT (proportion of permuted vector norms ≥ empirical value: $p = 0.01$), indicating a significant modulation of behavioral accuracy across the respiratory cycle.

As a control analysis, we examined whether instantaneous heart rate (iHR) could account for the observed respiratory phase effects. We therefore fitted a GLMM in which respiration was replaced by trial-by-trial iHR (Model 3 - "iHR"). For the HDT, the inclusion of iHR did not improve model fit compared to the baseline model (iHR vs. baseline: LRT-Stat: 0.54, $p = 0.46$), while for the TDT the iHR-based model yielded an improvement in fit relative to the baseline model (iHR vs. baseline: LRT-Stat: 221.85, $p < 0.001$), indicating that iHR significantly predicted trial-level accuracy only in the TDT. We therefore fitted an alternative model including both respiratory phase (sine and cosine) and iHR as predictors (Model 4 - "resp + iHR"), and compared it to the respiration-based model (Model 2 - "resp") and the iHR-based model (Model 3 - "iHR"). For the HDT, the LRT comparing Model 4 and Model 2 showed no improvement in model fit (resp + iHR vs. resp: LRT-Stat: $9.4 \times 10^{-5}$, $p = 0.99$), while the comparison between Model 4 and Model 3 revealed a significant improvement in fit (resp + iHR vs. iHR: LRT-Stat: 7.58, $p = 0.023$), indicating that the respiratory phase significantly predicted trial-level accuracy, while iHR did not explain additional variance beyond respiratory information. For TDT, the comparison between Model 4 and Model 2 showed significant improvement (resp + iHR vs. resp: LRT-Stat: 26.8, $p < 0.001$), as well as for the comparison between

Model 4 and Model 3 (resp + iHR vs. iHR: LRT-Stat: 12.88, p = 0.002), indicating that both the respiratory phase and iHR provided unique and additive contributions to the prediction of trial-level accuracy. Additionally, to test for the interaction between respiratory components and iHR on predicting accuracy, we developed an additional model (Model 5 - "resp × iHR") and compared it with Model 4. The LRT revealed no improvement in fit for either HDT (resp × iHR vs. resp + iHR: LRT-Stat = 1.54, p = 0.46) or TDT (resp × iHR vs. resp + iHR: LRT-Stat = 1.71, p = 0.43), suggesting that respiratory and cardiac signals contributed independently to behavioral performance, without evidence for synergistic modulation. Full results are provided in Supplemental Table S14 (models fittings results) and S15 (LRT).

### 3.8 Respiratory phase clustering analyses

To assess the specific direction of the effect found with the GLMM, we tested the uniformity of the distribution of phase angles for both correct and incorrect trials across the respiratory cycle with the Rayleigh test. The clustering of all responses combined (regardless of accuracy) was significant for both HDT ($Z = 3.34$, $p = 0.03$, $V_{mean} = 2.69$) and TDT ($Z = 15.5$, $p = 2.14 \times 10^{-8}$, $V_{mean} = 2.82$) around the late phase of exhalation. In the HDT, the Rayleigh test indicated a significant clustering of correct trials during exhalation ($Z = 6.51$, $p = 0.001$, $V_{mean} = 2.60$; Fig. 3B-left), whereas the clustering of incorrect trials was not significant ($Z = 2.50$, $p = 0.08$, $V_{mean} = 2.72$; Fig. 3B-right). The Watson-Williams test for equal means between correct and incorrect trials was not significant ($F = 0.08$, $p = 0.78$). In the TDT, the Rayleigh test revealed significant clustering of both correct ($Z = 14.7$, $p = 6.23 \times 10^{-8}$, $V_{mean} = 2.89$; Fig. 4B-left) and incorrect trials ($Z = 14.34$, $p = 9.98 \times 10^{-8}$, $V_{mean} = 2.71$; Fig. 4B-right) during exhalation. However, the Watson-Williams test between correct and incorrect trials was not significant ($F = 0.59$, $p = 0.45$).

To further assess whether respiratory phase alignment was specifically linked to behavioral outcomes, behavioral accuracy labels were randomly reassigned across trials within each participant while preserving the original accuracy distribution. This procedure was repeated 5000 times to

generate a permutation-based null distribution of the group-level Rayleigh Z statistic, which was then compared with the observed statistic. For the HDT, the observed group-level Rayleigh Z statistic for correct trials exceeded the 95th percentile of the permutation-derived null distribution ($Z_{95th}$ = 5.47, $Z_{observed}$ = 6.51), indicating a robust and non-random association between respiratory phase and correct responses. In contrast, the observed Z statistic for incorrect HDT trials did not exceed the corresponding null threshold ($Z_{95th}$ = 5.75, $Z_{observed}$ = 2.50), confirming no evidence for an outcome-specific phase alignment in incorrect responses. For the TDT, as described above, both correct and incorrect trials exhibited strong respiratory phase clustering at the descriptive level. The observed Rayleigh Z statistics for both outcomes were below the 95th percentiles of their respective permutation-based null distributions (correct: $Z_{95th}$ = 16.6, $Z_{observed}$ = 14.7; incorrect: $Z_{95th}$ = 16.6, $Z_{observed}$ = 14.3). This pattern suggests that respiratory phase alignment in the TDT reflects a strong and global task-related property, but not a specific association with performance.

### 3.9 Event-related respiratory signal analyses for correct and incorrect trials

To assess whether the effect observed with the GLMM approach was driven by respiratory amplitude modulation, we computed the ERrS of correct and incorrect trials in both tasks. In the HDT, ERrS differed significantly between correct and incorrect trials 2.5-3 s after cue onset, with more negative values observed during correct trials (t = -2.8, p = 0.004, $p_{FDR}$ = 0.03, d = -0.53; Fig. 3C-left). No significant differences were observed between conditions in the earlier time windows from 0 to 2.5 s after cue onset (all $p_{FDR}$ values > 0.05; see Supplemental Table S6). In the TDT, no significant differences in breathing patterns between correct and incorrect trials were observed in any of the analyzed time windows (all ps > 0.1 in all time windows; Fig. 4C-left; see Supplemental Table S7).

### 3.10 Inter-trial coherence analyses for correct and incorrect trials

We further investigated whether the observed effect could be associated with respiratory phase consistency by analyzing ITC separately for correct and incorrect trials in both tasks. In HDT, ITC

values for correct trials significantly increased relative to baseline within a time window of 1 to 3 seconds after cue onset (all $p_{FDR}$ values < 0.02; statistics are reported for the least significant time window: t = 2.35, p = 0.013, $ps_{FDR}$ = 0.02, d = 0.44; see Supplemental Table S8). For incorrect trials, ITC values increased relative to baseline from 2 to 3 seconds after cue onset, though this effect did not survive correction for multiple comparisons (all $p_{FDR}$ values > 0.1; see Supplemental Table S9). The comparison between relative ITC values for correct and incorrect trials showed no significant differences in any of the analyzed time windows (all $p_{FDR}$ values > 0.08; Fig. 3C-right; see Supplemental table S10). In the TDT, for correct trials, ITC values significantly increased relative to baseline from 1 to 3 seconds after cue onset (all $p_{FDR}$ values < 0.0003; statistics are reported for the least significant time window: t = 4.64, p = $1.99 \times 10^{-4}$, $p_{FDR} = 2.99 \times 10^{-4}$, d = 0.82; see Supplemental Table S11). A similar effect was observed for incorrect trials, with ITC values increasing within the same time window (all $p_{FDR}$ values < 0.0006; statistics are reported for the least significant time window: t = 3.54, p = $3.99 \times 10^{-4}$, $p_{FDR} = 5.98 \times 10^{-4}$, d = 0.63; see Supplemental Table S12). The comparison between relative ITC for correct and incorrect trials was not significant (all ps > 0.25; Fig. 4C-right; see Supplemental Table S13).

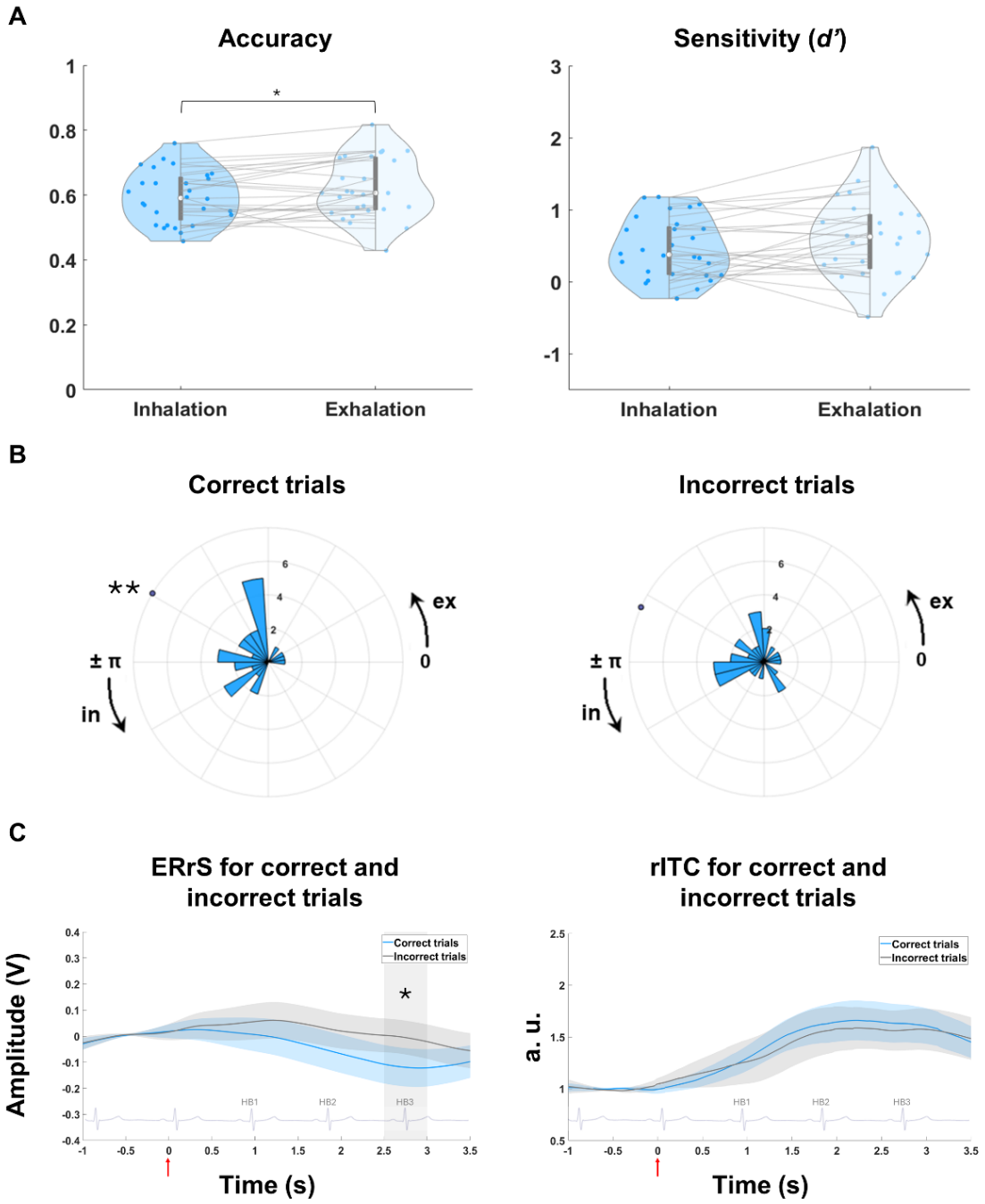



**Figure 3. Relationship between respiration and accuracy in the heartbeat discrimination task.** **A)** Accuracy (left) and sensitivity (d') (right) obtained by dividing the respiratory signal into inhalation and exhalation phases. **B)** Distribution of correct (left) and incorrect (right) trials across the respiratory cycle. Colored dots indicate circular means, while black arrows represent the direction of the respiratory cycle; 0 rad: exhalation onset; π rad: inhalation onset. The asterisk indicates statistical significance. **C)** ERrS (left) and rITC (right) assessed for correct and incorrect trials. The gray area represents the window of statistical significance. Red arrows represent the cue onset; the overlaid ECG signal represents an example of an S- trial, included to illustrate the temporal dynamics of the trial with the three target heartbeats highlighted. Abbreviations: ex - exhalation; in - inhalation; ERrS - event-related respiratory signal; rITC - relative inter-trial coherence. * $p < 0.05$, ** $p < 0.01$.

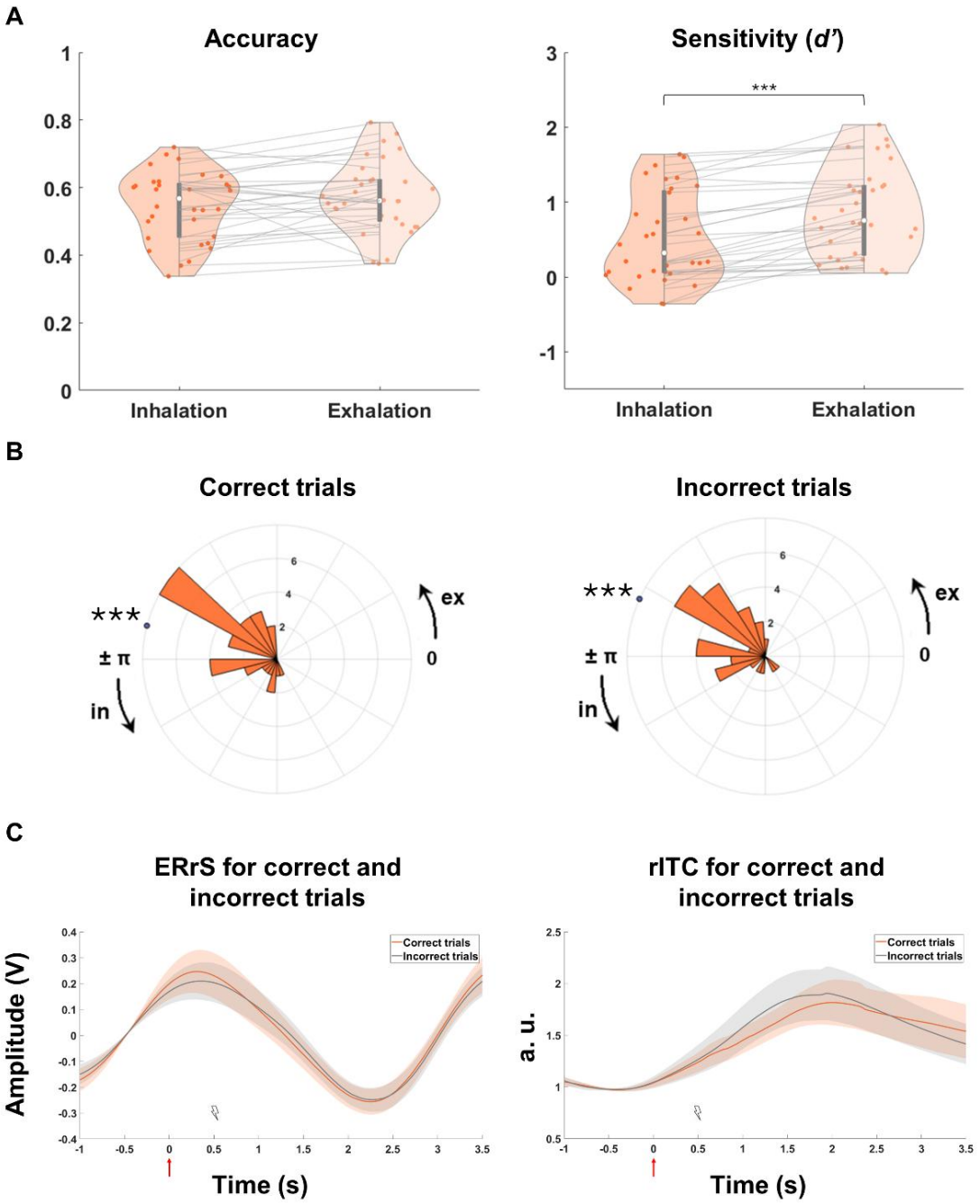



**Figure 4. Relationship between respiration and accuracy in the tactile detection task. A)** Accuracy (left) and sensitivity (d') (right) obtained by dividing the respiratory signal into inhalation and exhalation phases. * $p < 0.05$, *** $p < 0.001$. **B)** Distribution of correct (left) and incorrect (right) trials across the respiratory cycle. Colored dots indicate circular means, while black arrows represent the direction of the respiratory cycle; 0 rad: exhalation onset; π rad: inhalation onset. The asterisks indicate statistical significance. **C)** ERrS (left) and rITC (right) assessed for correct and incorrect trials. Gray areas represent the window of statistical significance. Red arrows represent the cue onset; lightning symbol represents the onset of the electrical stimulation. Abbreviations: ex - exhalation; in - inhalation; ERrS - event-related respiratory signal; rITC - relative inter-trial coherence. *** $p < 0.001$.

### 3.11 Heart rate variability analyses

To verify whether the observed differences between tasks were accompanied by changes in autonomic cardiac regulation, HRV parameters were compared between the two tasks using paired-sample t-tests. No significant differences emerged for any of the HRV indices (all ps > 0.1), indicating similar autonomic modulation across the two conditions. Table 1 reports the t-test results for each HRV parameter in the two tasks.

| | Mean ± SD HDT | Mean ± SD TDT | t value | p value | Effect size (Cohen's d) |
|---|---|---|---|---|---|
| Mean RR (ms) | 816.2 ± 92.2 | 841.2 ± 108.4 | -1.5428 | 0.138 | -0.3289 |
| SDNN (ms) | 51.6 ± 12.9 | 48.8 ± 19.9 | 0.6698 | 0.510 | 0.1428 |
| Mean HR (bpm) | 74.4 ± 8.6 | 72.4 ± 9.0 | 1.3889 | 0.179 | 0.2961 |
| STD HR (bpm) | 5.1 ± 1.5 | 4.4 ± 2.1 | 1.5923 | 0.126 | 0.3395 |
| Min HR (bpm) | 61.1 ± 6.5 | 61.1 ± 8.2 | -0.0065 | 0.995 | -0.0014 |
| Max HR (bpm) | 106.5 ± 22.4 | 101.9 ± 23.1 | 0.8713 | 0.393 | 0.1858 |
| RMSSD (ms) | 44.5 ± 16.2 | 48.2 ± 29.4 | -0.7644 | 0.453 | -0.1630 |
| VLF ($ms^2$) | 139.04 ± 68.9 | 151.8 ± 121.5 | -0.4659 | 0.646 | -0.0993 |
| LF ($ms^2$) | 1541.6 ± 838.2 | 1235.8 ± 815.2 | 1.3339 | 0.197 | 0.2844 |
| HF ($ms^2$) | 958.4 ± 750.8 | 1067.5 ± 1163.9 | -0.5105 | 0.615 | -0.1088 |
| LF/HF | 2.2 ± 1.6 | 1.7 ± 1.2 | 1.7148 | 0.101 | 0.3656 |

**Table 1. Cardiac parameters across the heartbeat discrimination task and the tactile detection task.** None of the comparisons reached statistical significance (all ps > 0.1). The table reports the test statistic (t), degrees of freedom (df), p-values, and effect sizes (Cohen's d) for each HRV index in the two tasks. Abbreviations: Mean RR - Mean R-R Interval; SDNN - Standard Deviation of Normal-to-Normal Intervals; Mean HR - Mean Heart Rate; STD HR - Standard Deviation of Heart Rate; Min HR - Minimum Heart Rate; Max HR - Maximum Heart Rate; RMSSD - Root Mean Square of Successive Differences; VLF - Very Low Frequency Power; LF - Low Frequency Power; HF - High Frequency Power; LF/HF: Low Frequency to High Frequency Ratio; HDT - heartbeat discrimination task; TDT - tactile detection task.

## 4. Discussion

We investigated whether individuals strategically adjust respiration to optimize the processing of anticipated interoceptive and exteroceptive stimuli. Results indicated that participants modulated their respiration across tasks, exhibiting phase synchronization and task-specific respiratory patterns time-locked to trial onset. In the HDT, task performance was enhanced during exhalation. In the exteroceptive domain, our results replicate those reported by Grund et al. (2022) using a similar tactile detection paradigm. Separate mixed-effects models for the HDT and TDT showed that including the respiratory phase angle as a predictor for accuracy significantly improved model fit. Importantly, the respiratory phase was sampled at the time of maximal ITC, which occurred after the behavioral response in the TDT. However, due to the pseudo-periodic nature of respiration and its slow timescale, phase alignment can extend across neighboring time points, such that phase values sampled after the response are not independent of earlier phases but reflect a sustained and temporally coherent respiratory state (Harting et al., 2025; Stetza et al., 2025). Including instantaneous heart rate significantly improved model fit only in the TDT, indicating that the probability of a correct response varied systematically with respiratory phase and instantaneous heart rate. We further examined the distribution of trial-level respiratory phase angles across the respiratory cycle separately for correct and incorrect trials. In the HDT, respiratory phase angles were selectively clustered only for correct responses, with alignment occurring around the late phase of exhalation. In contrast, in the TDT, both correct and incorrect trials exhibited phase clustering of respiratory phases around exhalation, indicating that respiratory phase alignment in the TDT reflects a global task-related effect. This selective pattern suggests that respiratory phase alignment does not simply reflect unspecific factors such as stimulus timing, motor responses or overall task structure, but rather emerges when interoceptive information is successfully accessed. When comparing trial-locked respiratory activity between correct and incorrect trials, significant differences emerged in the HDT, while no difference was observed in TDT. Finally, during the HDT, we found increased respiratory ITC relative to baseline specifically for correct trials, while during the TDT, ITC was higher relative to baseline for

both correct and incorrect trials. These findings underline a link between respiratory phase alignment and task performance in the interoceptive domain while suggesting that phase-locking in the exteroceptive domain is less strongly associated with perceptual accuracy.

Taken together, these results confirm that specific phases of the respiratory cycle facilitate the perception of near-threshold stimuli in both the interoceptive and exteroceptive domains. Moreover, they support the view that respiration is not merely a passive modulator but is actively regulated by individuals to optimize perceptual outcomes, consistent with the interoceptive predictive coding framework (Barrett & Simmons, 2015; Seth, 2013; Seth & Friston, 2016). Although this behavior has been previously demonstrated in the exteroceptive domain (Grund et al., 2022; Harting et al., 2025; Huijbers et al., 2014; Perl et al., 2019), our findings extend this mechanism to the cardiac interoceptive domain, providing support for the notion of a respiratory active inference strategy (Boyadzhieva & Kayhan, 2021; Corcoran et al., 2018): individuals appear to modulate their respiration to enhance the perception of internal bodily signals. We refer to this process as interoceptive respiratory active sensing.

We propose that, although the phase-locking of exhalation to sensory inputs appears behaviorally similar across tasks, it is driven by distinct underlying mechanisms shaped by specific task demands. In the HDT, respiratory-related afferents may induce interoceptive noise that masks cardiac signals when systoles occur during inhalation (Noble & Hochman, 2019; Streeter et al., 2012). This is consistent with findings showing improved interoceptive accuracy during breath-holding conditions, where respiratory interference is minimized (Lavalley et al., 2024; R. Smith et al., 2020, 2021). At higher cortical levels, exhalation is associated with reduced cortical excitability, which may facilitate interoceptive attention due to the suppression of task-irrelevant distractors. Consequently, individuals may initiate exhalation to actively increase the perceptual salience of heartbeat sensations (Ainley et al., 2016; Larsson et al., 2021).

Although prior studies have reported perceptual benefits during inhalation, whereas others, including the present study, report benefits during exhalation, these results are not necessarily

contradictory. Instead, they suggest that the optimal respiratory phase for perception depends on the computational demands of the task. In the auditory domain, enhanced sensory responses during exhalation have been attributed to a release of cognitive resources, since exhalation inherently demands less active engagement than inhalation (J. L. Feldman & Del Negro, 2006; Muñoz-Ortiz et al., 2019). These available resources may then be reallocated to facilitate the processing of weak or ambiguous sensory inputs (Mizuhara et al., 2024, 2025). An alternative explanation, grounded in the predictive coding framework, suggests that in tasks requiring precise somatosensory perception, such as the TDT, exhalation may be actively initiated to induce a parasympathetically mediated reduction in heart rate. This reduction may, in turn, attenuate baroreceptor-related afferent signalling, which has been shown to suppress somatosensory processing during cardiac systole (Saltafossi et al., 2023). Accordingly, if exhalation effectively reduces cardiac-related afferent input, it is plausible that fine somatosensory perception is facilitated during this respiratory phase. More generally, when cardiac signals are not informative for the task at hand, limiting their influence may help preserve the temporal and spatial precision required for accurate tactile processing. This account is supported by evidence showing that cardiac deceleration often precedes the presentation of salient exteroceptive stimuli, possibly serving as a preparatory mechanism to enhance sensory processing (Skora et al., 2022).-Within this framework, inhalation may preferentially support externally oriented, exploratory processing, whereas exhalation may facilitate precision-demanding tasks by reducing physiological and interoceptive noise.

Some limitations of this study warrant consideration. First, the two tasks inherently differed in trial duration. Although the pilot study using a single-stimulus HDT partially addressed potential effects of trial duration, the remaining discrepancy may still have contributed to the differences in respiratory dynamics observed across tasks. Therefore, direct between-task comparisons should be interpreted with caution, and primary emphasis should be placed on within-task effects. Second, the use of fixed time windows for S+ and S- trials may have reduced task sensitivity due to interindividual variability in cardiac signal perception (Lyyra & Parviainen, 2018; Wiens et al., 2000). Adopting a

modified version of the paradigm, such as the method of constant stimuli, could improve sensitivity and generalizability of results (Brener et al., 1994; Wiens & Palmer, 2001). Finally, as this study did not employ EEG, any interpretation of respiration in modulating the higher-order neural basis of cardiac and somatosensory perception remains speculative. Future EEG research could help clarify the neural mechanisms underlying respiratory-phase modulation of both interoceptive and exteroceptive accuracy.

In conclusion, the present findings suggest that respiration is a physiological process that is actively regulated to optimize both the perception of internal bodily sensations and external stimuli. From this perspective, respiration may continuously support the integration of bodily and sensory information by shifting the relative weighting of interoceptive and exteroceptive processing, depending on contextual demands. This interpretation aligns with recent evidence showing that cardiac interoceptive signals can modulate exteroceptive perception through specific competitive and facilitative mechanisms (Loescher et al., 2025). Based on this principle, future research should investigate whether voluntary respiratory control practices can modulate interoceptive, exteroceptive, and motor functioning (Sandoval et al., 2025). In addition, clarifying how breathing contributes to shape internal and external perception may provide a framework for developing respiratory-based intervention strategies. Such strategies may be particularly relevant for mental health conditions characterized by concurrent alterations in interoceptive and exteroceptive processing, including schizophrenia (Fan et al., 2025), schizotypy (Pasciucco et al., 2025), eating disorders (Lutz et al., 2019), social anxiety disorders (Judah et al., 2018), and major depression (Terhaar et al., 2012), as well as conditions involving broader sensory processing difficulties (Van Den Boogert et al., 2022) and age-related changes in perceptual and bodily signal processing (Pasciucco et al., 2026).

# Study 2

## Attention to cardiac sensations enhances the heartbeat-evoked potential during exhalation

This study has been published as:

Zaccaro A., della Penna F., Mussini E., Parrotta E., Perrucci M.G., Costantini M., Ferri F. (2024). Attention to cardiac sensations enhances the heartbeat-evoked potential during exhalation. *iScience*. https://doi.org/10.1016/j.isci.2024.109586

The version presented in this thesis has been adapted to fit the overall structure of the dissertation. The original published version is provided in Appendix B.

## 1. Introduction

Cardiac activity is widely intertwined with respiration, another fundamental interoceptive rhythm in the human body (Chen et al., 2021; Khalsa, Rudrauf, Feinstein, et al., 2009; Weng et al., 2021). Given the strong interactions between cardiac function and respiration at the physiological level (Brecher & Hubay, 1955), we recently investigated the effects of respiratory phases on cardiac interoception in healthy participants. We observed an increase in late HEP amplitude and cardiac interoceptive accuracy during exhalation compared to inhalation while performing the interoceptive condition of the Heartbeat Detection Task (HBD; Zaccaro et al., 2022). Our interpretation was grounded in the continuous reception of both cardiac and respiratory sensations by the brain through vagal pathways, with the latter predominantly conveyed during inhalation (Noble & Hochman, 2019; Streeter et al., 2012). Consequently, heartbeat sensations during inhalation may compete with concurrent respiratory sensations. This competition may decrease during exhalation, resulting in a reduction of respiratory interference. Therefore, during HBD, when cardiac sensations are heightened by attention, increased HEP and interoceptive accuracy may manifest during exhalation (Zaccaro et al., 2022).

Despite these findings, some ambiguities remained regarding the relationships between HEP, attention, and respiratory phases. Firstly, while previous studies have compared HEP amplitude between cardiac interoceptive tasks and exteroceptive tasks (Coll et al., 2021), there is a lack of research comparing HEP amplitude between cardiac interoceptive tasks and *non-cardiac* interoceptive tasks, which involve focusing on interoceptive sensations unrelated to the heart. As such, HEP augmentation has been associated not only with attention focused towards the heart, but also on the bodily self or the self in a broader sense (Babo-Rebelo, Buot, et al., 2016; Babo-Rebelo, Wolpert, et al., 2016; Park et al., 2016, 2018; Sel et al., 2016). Secondly, in our previous study (Zaccaro et al., 2022), confounding factors such as motor activity involved in HBD posed challenges for direct comparison of respiratory phase-related HEP effects between the interoceptive and exteroceptive condition.

Here, we have developed an experimental approach to distinguish the impact of respiratory phases on HEP during different types of interoceptive and exteroceptive attention. We used the Heartbeat Counting Task (HCT) to elicit cardiac interoception while avoiding potential movement-related issues present in HBD. In the first analysis, we compared HEP amplitude between tasks focused on cardiac interoception and exteroception, as well as tasks targeting *non-cardiac* interoception and exteroception, specifically focusing on respiration. Given the established links between HEP and cardiac interoceptive attention (Coll et al., 2021), we expected an increase in HEP amplitude during the cardiac interoceptive task (HCT) compared to exteroceptive task, with no HEP changes during the respiratory interoceptive task. In the second analysis, we explored how attention influenced HEP responses in interaction with respiration, aiming to determine whether putative changes in HEP amplitude during HCT were specific to a given respiratory phase. Given the connections between interoceptive sensibility, trait mindfulness, and HEP activity (Baranauskas et al., 2017; Billeci et al., 2021; Verdonk et al., 2021), we also investigated whether they were associated with HEPs recorded during exhalation and inhalation. Based on our previous findings that showed higher late HEPs during exhalation (Zaccaro et al., 2022), we predicted a stronger contribution of exhalation in driving the expected HEP amplitude increase during HCT and its associations with interoceptive sensibility and mindfulness. If confirmed, these findings would highlight a previously overlooked role of respiratory phases in modulating cardiac interoception. In addition, recognizing the role of each specific respiratory phase in shaping interoception may provide valuable insights for clinical populations that show altered interoceptive functions, such as major depression or anxiety disorders (Bonaz et al., 2021). For example, specific impairments of cardiac signal processing during exhalation may benefit from the development of respiratory-based interventions to fine-tune cardiac interoception. These findings could potentially refine therapeutic applications, such as mindfulness and slow breathing practices.

## 2. Materials and Methods

### 2.1 Ethics statement

The Institutional Review Board of Psychology of the Department of Psychological, Health and Territorial Sciences, "G. d'Annunzio" University of Chieti-Pescara, Italy, approved the study (Protocol Number 44_26_07_2021_21016). Participants were blind to the experimental aims. The study was conducted in conformity with the Italian Association of Psychology and the Declaration of Helsinki and its later amendments. All participants read and signed an informed consent.

### 2.2 Human participants

Thirty-four (19 females; 1 left-handed; age: 27.48 ± 4.28 years [mean ± SD]) white healthy volunteers were recruited. The eligibility of each volunteer was confirmed based on self-reported criteria: 1) absence of personal and/or family history of psychiatric, neurological, and somatic disorders; 2) no chronic and/or acute conditions involving the respiratory tracts; 3) no use of substances interacting with the central nervous system in the previous week; 4) no experience in mindfulness-based meditation and/or breath-control practices. All participants were of normal weight and had normal or corrected-to-normal vision. Sample size was estimated using G*Power 3.1 (v3.1.9.7; Faul et al., 2009). Considering a 2×2 factorial design, we estimated a medium effect size of partial eta squared ($\eta$p2) of 0.06, based on a recent meta-analysis on attentional effects on HEP (Coll et al., 2021), which corresponds to a Cohen's f of 0.25. Significance level was set to alpha = 0.05, and the power (1 - beta) at 0.85. The total estimated sample size was 26. We excluded 2 participants from the testing of HEPs, regardless of the respiratory phase, due to noisy EEG (N = 32, 17 females; 1 left-handed; age: 27.57 ± 4.33 years [mean ± SD]). Additionally, we excluded 4 participants from the testing of HEP changes among respiratory phases due to noisy respiratory data (N = 28, 13 females; 1 left-handed; age: 27.88 ± 4.46 years [mean ± SD]).

### 2.3 Experimental procedure

After a resting-state (baseline), participants performed two interoceptive tasks and two exteroceptive tasks, requiring them to focus their attention inside or outside the body, respectively (Attention Focus factor). During the interoceptive and exteroceptive tasks, participants had to process either cardiac or respiratory signals (System factor). Participants sat comfortably in front of a computer at an optimal distance (around 60 cm) for keyboard use and screen visibility. Room lighting and noise were minimized, and the temperature and humidity were maintained at a comfortable level. Participants received written instructions (see below) presented through E-Prime 3.0 software (Psychology Software Tools, Pittsburgh, PA, USA). Subsequently, the experimenter ensured participants understood the instructions, allowing them to ask questions if any doubts arose. Baseline was always performed first. Participants were seated for 10 minutes in a resting-state condition with eyes open, watching a fixation cross at the centre of a monitor, and letting their mind wander without focusing on anything in particular (Raichle et al., 2001). Participants were also asked to breathe spontaneously.

The cardiac interoceptive task was HCT (Pollatos & Schandry, 2004; Schandry et al., 1986). Participants were given the following instructions in line with Desmedt et al. (2018): "*In this task, direct your attention to your heart and the associated physical sensations. You are required to sustain your focus on your heart for various durations and count the number of heartbeats you perceive. Begin silently counting when the heart symbol appears on the screen. When the heart symbol disappears, report the number of heartbeats you are sure you felt. Only report the number of heartbeats you are sure about, without trying to estimate your heart rate. During each trial, keep your eyes open, gaze at the screen and avoid moving. Refrain from guiding your responses by checking your pulse in your wrists or neck. Breathe spontaneously and avoid changing your breathing frequency or holding your breath*". HCT consisted of three blocks, each one comprising four randomized trials of the following durations: 25, 35, 45, and 100 seconds (Ardizzi & Ferri, 2018; Di Lernia et al., 2018; Ueno et al., 2020), for a total of 12 trials. After each trial, participants reported the number of perceived heartbeats and rated their performance (HCT confidence) on a 10-points

Likert scale from 0 (very bad) to 9 (excellent). No feedback was provided about their performance. The respiratory interoceptive task was BCT (Herrero et al., 2018). Participants were given the following instructions: "*In this task, direct your attention to your breath and the associated physical sensations. You are required to sustain your focus on your breath for various durations and count the number of breaths you take. Begin silently counting your breaths when the lungs symbol appears on the screen. When the lungs symbol disappears, report the number of breaths you took. Refrain from changing the rhythm or depth of your breathing, simply stay aware of your breath without making any change*". BCT consisted of five trials of 120 seconds each. After each trial, participants reported the number of performed respiratory cycles, and rated their performance (BCT confidence). They were asked to rate the ease in performing the task without modifying the respiratory rate on a Likert scale from 0 (very difficult) to 9 (very easy). No feedback was provided about their performance. The order of tasks and blocks/trials within each task was randomized.

The exteroceptive tasks mirrored the interoceptive tasks. In C-TCT, participants were presented with digitally constructed heartbeat sounds and instructed to mentally count and report the number of heard heartbeats (Wiebking et al., 2015). C-TCT consisted of three blocks of four randomized trials of different durations (25, 35, 45, and 100 seconds). Heartbeats were presented at an irregular frequency at an average frequency of 60 bpm. After each trial, participants reported the number of heard heartbeats and rated their performance (C-TCT confidence). In B-TCT, participants were presented with audio samples of respiratory sounds (adapted from Herrero et al., 2018) comprising inhalation and exhalation sounds at irregular frequencies (mean: 18 breaths per minute). B-TCT consisted of five trials of 120 seconds each. After each trial, participants reported the number of heard respiratory cycles and rated their performance (B-TCT confidence), and the perceived ease in performing the task without modifying the respiratory rate. The order of tasks and blocks/trials within each task was randomized.

The interoceptive and exteroceptive tasks were presented in a counterbalanced order between participants. Before starting the experiment, participants had to perform a brief training session and

verbally confirm that they could not feel their heartbeat through the respiratory belt, in case the belt was mounted too tight (Zaccaro et al., 2022). To ensure a similar number of epochs, baseline and tasks lasted 10 minutes each. EEG, ECG, and respiratory signals were recorded throughout the entire experiment. The experimental design is depicted in Fig. S11. All tasks were administered using the E-Prime 3.0 software (Psychology Software Tools, Pittsburgh, PA, USA).

### 2.4 Electrophysiological recording

EEG signals were acquired using a 64-channel BrainAmp EEG system (BrainCap MR, BrainVision LLC, Garner, NC, USA). Electrodes were positioned on the scalp following the International 10-20 system. Electrode impedance was kept below 10 kΩ for all channels. ECG was recorded from three electrodes: two placed over the left costal margin and the right clavicle, and the ground located on the right costal margin (MP160, BIOPAC Systems Inc, Goleta, CA, USA). Three additional electrodes, serving as the backup, were integrated in the EEG recording system via an external Electrode Input Box (BrainProducts GmbH, BrainVision LLC, Gilching, Germany), and were placed over the left and right clavicles, with the ground located on the left costal margin. Breathing activity was recorded via a respiratory belt placed around the chest (respiratory transducer TSD201, BIOPAC Systems Inc, Goleta, CA, USA). The systems running the BrainAmp EEG, MP160, and TSD201 were connected with the system running the E-Prime 3.0 software and were synchronized with a TriggerStation™ (BRAINTRENDS LTD 2010, Italy). The sampling rate was 2.5 kHz for all signals. Band-pass filtering was applied from 0.016 to 250 Hz, along with 50-Hz notch filtering. Subsequently, all signals were down-sampled to 512 Hz.

### 2.5 ECG data analysis

ECG data were processed using custom MATLAB code (R2021a, MathWorks Inc, Natick, MA, USA). ECG signal was high-pass filtered at 0.1 Hz to remove baseline fluctuations (Saltafossi et al., 2023). R-peaks were detected with the Pan-Tompkins algorithm (Pan & Tompkins, 1985). To measure

Heart Rate Variability (HRV), the time series of the distance between consecutive R-peaks (tachogram) was computed and ectopic beats were corrected using a point process model (Citi et al., 2012). This procedure corrected very few heartbeats (baseline: range 0-4 heartbeats; HCT: 0-16; BCT: 0-9; C-TCT: 0-11; B-TCT: 0-9). Kubios software (Kubios HRV Standard, v3.5; Tarvainen et al., 2014) was used to pre-process the tachogram and extract average HR and frequency-domain HRV features of interest. ECG pre-processing was carried out using Kubios routines. Detrending involved removing the best straight-line fit linear trend from the ECG data. The ECG tachogram was interpolated at 4 Hz. Frequency-domain analysis utilized the Fast Fourier Transform (FFT)-based Welch's periodogram applied to the detrended RR series. In the Welch's periodogram method, the window width was set to 300 seconds, with a default overlap of 50% (Tarvainen et al., 2014). We calculated HR (bpm, the average number of heartbeats in one minute), High Frequency (HF: 0.15-.4 Hz) log power (log ms2/Hz, the log-transformed power of HF band; Lewis et al., 2012; Malik et al., 1996), HRV total power (ms2/Hz, the sum of power values in HF, Low Frequency-LF, and Very Low Frequency bands), and Low Frequency/High Frequency ratio (LF/HF).

**2.6 Respiratory data analysis**

Respiratory data were processed using custom MATLAB scripts (R2021a, MathWorks Inc, Natick, MA, USA). The respiratory signal was first high-pass filtered at 0.1 Hz to remove baseline wander. Respiratory phases were detected following a validated procedure (Grund et al., 2022; Power et al., 2020). Outliers (i.e., values exceeding three scaled median absolute deviations from the local median within a moving 1-second window) were linearly interpolated with their neighbouring values. The data were then smoothed with a 1-second-window filter (Savitzky & Golay, 1964) and z-scored. Inhalation and exhalation onsets were identified as the local minima (trough) and the local maxima (peaks). Peaks and troughs were required to be at least 2 seconds apart and the minimum prominence of the interquartile range of the z-scored data was multiplied by a value ranging from 0.3 to 0.8, depending on the participant's respiratory trace (Grund et al., 2022). A respiratory cycle was defined

as the interval from one inhalation onset (referred to as “trough”) to the subsequent trough. Respiratory cycles with outlier durations (i.e., different from two times the median) were excluded. Rejected respiratory cycles were 6 ± 5 [mean ± SD] for the baseline, 9 ± 6 for HCT, 4 ± 3 for BCT, 12 ± 6 for C-TCT, and 8 ± 7 for B-TCT. The number of retained artifact-free respiratory cycles in the entire sample was 3997 for the baseline (143 ± 37 [mean ± SD]), 3969 for HCT (142 ± 31), 4053 for BCT (145 ± 34), 4590 for C-TCT (164 ± 28), and 4440 for B-TCT (159 ± 27). Respiratory features of interest were the breathing rate (breaths/min), average inhalation duration (sec), average exhalation duration (sec), and the Inhalation/Exhalation ratio.

**2.7 EEG data analysis**

EEG data were pre-processed using the EEGLAB toolbox (v2022.1; Delorme & Makeig, 2004). EEG data were filtered using a Hamming windowed FIR filter from 0.5 to 45 Hz (Al et al., 2020, 2021). EEG segments with poor signal quality were manually rejected. Independent Component Analysis (ICA) was applied to remove heartbeat, ocular, and muscle artefacts (FastICA; Hyvarinen, 1999). ECG, respiratory channel, and excessively noisy channels were excluded from ICA decomposition. There were a few noisy channels (less than 5), always peripheral, known not to contribute to HEP generation (Coll et al., 2021). Independent Components (ICs) were rejected based on IC time series, scalp map, and power spectrum (Delorme & Makeig, 2004). Particular attention was given to the Cardiac Field Artifact (CFA), as it highly impacts HEP activity (Coll et al., 2021). ICs contaminated by CFA were identified by plotting R-peaks over IC time series. ICs with activations time-locked to ECG R-peak were removed (Fig. S12; Al et al., 2020, 2021; Zaccaro et al., 2022). To facilitate the visual inspection, the cross-correlation between each IC time course and ECG channel was calculated. Removed ICs ranged from 1 to 6 (3 ± 1 [mean ± SD]), while CFA-related ICs ranged from 0 to 3 (1 ± 1 [mean ± SD]). After ICA, previously identified noisy channels were interpolated using their neighbours (Junghöfer et al., 2000). Pruned EEG signals were then re-referenced to the average

reference (Zaccaro et al., 2022) as recommended (Candia-Rivera et al., 2021). A depiction of a 10-second comparison of EEG before and after ICA in the same participant is presented in Fig. S13.

HEPs were computed using ERPLAB toolbox (v9.00; Lopez-Calderon & Luck, 2014). R-peaks were identified with HEPLAB toolbox (Perakakis, 2019). Manual correction of mis-detected peaks was performed and EEG was epoched between -100 and 600 ms around each R-peak (Coll et al., 2021). To account for potential voltage drifts, a regression baseline correction was employed using the Reduction of Electroencephalographic Artifacts toolbox (RELAX v1.1.5; Bailey, Biabani, et al., 2023; Bailey, Hill, et al., 2023). The regression baseline correction method calculates the trial-based average amplitude within the baseline period and regresses out the influence of the baseline period from each time point in the HEP time window. This approach avoids introducing differences from the baseline into the HEP period of interest, contrasting with the subtraction baseline correction method (Alday, 2019). Epochs followed by an R-peak by less than 600 ms were excluded to avoid overlap between HEP epoch and the following R-peak (Babo-Rebelo, Buot, et al., 2016; Zaccaro et al., 2022). The number of epochs excluded was generally low (20 ± 60 [mean ± SD]). The high SD is attributed to two participants with elevated HR, resulting in a higher number of rejected epochs compared to the average. Epochs were excluded if they exceeded a peak-to-peak threshold of 100 $\mu$V (Blankenship et al., 2018; Villena-González et al., 2017; Zaccaro et al., 2022) within a moving window (size: 200 ms; overlap: 50%; Lopez-Calderon & Luck, 2014). The number of rejected epochs exceeding this threshold was very low (4 ± 10 [mean ± SD] epochs for the baseline, 4 ± 11 for HCT, 2 ± 6 for BCT, 3 ± 9 for C-TCT, and 3 ± 10 for B-TCT). Epochs were averaged within participants during each task, resulting in four HEP bins named as follows: HCT, C-TCT, BCT, and B-TCT. HEP epochs were then assigned to inhalation and exhalation based on the respiratory phase in which the respective R-peak occurred. This resulted in ten HEP bins named as follows: baseline inhalation and exhalation; HCT inhalation and exhalation; C-TCT inhalation and exhalation; BCT inhalation and exhalation; B-TCT inhalation and exhalation.

### 2.8 Task accuracy assessment

HCT accuracy was calculated following validated procedures (Candia-Rivera et al., 2022; Hart et al., 2013; Schandry, 1981) based on the number of counted heartbeats in relation to the heartbeats recorded with ECG. The formula was:

$$\text{HCT accuracy} = 1 - \frac{|(\text{Recorded heartbeats} - \text{Counted heartbeats})|}{\text{Recorded heartbeats}}$$

In the absence of excessive over-reporting, scores range from 0 to 1, where higher scores indicate better accuracy. The accuracy of each trial was then averaged over the 12 HCT trials (Candia-Rivera et al., 2022; Garfinkel et al., 2015; Hart et al., 2013). Similarly, C-TCT accuracy was calculated as follows:

$$\text{C} - \text{TCT accuracy} = 1 - \frac{|(\text{Presented heartbeats} - \text{Counted heartbeats})|}{\text{Presented heartbeats}}$$

Accuracy for BCT and B-TCT were calculated based on the number of counted respiratory cycles in relation to performed respiratory cycles and presented respiratory sounds, respectively. Within each task, self-reported performance (confidence) was averaged among the trials.

### 2.9 Psychometric questionnaires

FFMQ (Baer et al., 2006; Italian version by Giovannini et al., 2014) and MAIA (Mehling et al., 2012; Italian version by Calì et al., 2015) were administered via the Qualtrics online platform (Qualtrics, Provo, UT, USA). In FFMQ, participants were asked to answer to 39 statements on a 5-point Likert scale from 1 (never) to 5 (always). FFMQ measures trait mindfulness, i.e., the tendency to stay aware of perceptions, thoughts, emotions, and actions without distraction, non-judgment, and immediate reaction. We focused on FFMQ total score to correlate HEP amplitude with trait mindfulness (Verdonk et al., 2021). In MAIA, participants were asked to answer to 37 statements on a 6-point Likert scale from 0 (never) to 5 (always). It consists of eight scales assessing facets of interoceptive sensibility. Given previous association with HEP activity (Baranauskas et al., 2017; Billeci et al., 2021), we focused on the Trusting and Not-Worrying scales of MAIA. The Trusting scale assesses

the experience of the body as safe and trustworthy and the Not-Worrying scale assesses emotional distress for bodily sensations of pain and/or discomfort.

### 2.10 Statistical analysis

#### 2.10.1 Heartbeat Evoked Potential statistical analyses

HEP changes were assessed with the Mass Univariate ERP Toolbox (MUT; (Groppe et al., 2011a, 2011b). To test for interaction effects in factorial designs, we followed the procedure included in the Factorial Mass Univariate ERP Toolbox (FMUT; (Fields & Kuperberg, 2020). Cluster-based permutation tests were performed with HEP amplitude as dependent variable and System (cardiac vs. respiratory) and Attention Focus (interoceptive vs. exteroceptive) as within-participant factors. The cluster mass tested clusters instead of individual electrodes or time points. Firstly, spatially (neighbouring channels) and temporally (contiguous time points) adjacent points with a p-value below 0.05 were included into a cluster. A cluster statistic was calculated by summing t-values within each cluster. The null distribution was estimated through Monte Carlo permutations, in which condition labels were randomly shuffled 10000 times and the largest cluster-level statistic for each randomization was entered into the null distribution. Statistical significance was determined by comparing the experimentally observed cluster-level statistics with the randomly-generated null distribution. Clusters exceeding the 1 - alpha percentile of the distribution (two-tails) were significant (Fields & Kuperberg, 2020). The maximum distance for two electrodes to be included into a cluster was 5.44 cm (*chan_hood* = 0.61). To test for interaction effects, we used the permutation of residuals method (Anderson & Braak, 2003; Still & White, 1981; Winkler et al., 2014). For instance, to test the 2×2 interaction (System by Attention Focus) we calculated the difference between the two levels of Attention Focus for each level of System and conducted paired cluster-based permutation t-tests comparing difference values (HCT minus C-TCT vs. BCT minus B-TCT; Groppe et al., 2011b). Planned t-tests were conducted using paired cluster-based permutation t-tests implemented in MUT (Groppe et al., 2011a). Specifically, we planned to compare HCT vs. C-TCT, HCT vs. BCT, BCT vs.

B-TCT, and C-TCT vs. B-TCT (number of planned t-tests: 4). Based on previous research (Baranauskas et al., 2017; Gray et al., 2007; Kumral et al., 2022; Petzschner et al., 2019; Pollatos et al., 2016; Villena-González et al., 2017; Zaccaro et al., 2022), we tested HEP amplitude at each electrode and time point separately in an early (100-350 ms) and a late time window (350-600 ms) after the R-peak. We excluded external electrodes (F7, F8, FT7, FT8, T7, T8, TP7, TP8, P7, P8, PO7, PO8, O1, O2, Oz, TP9, and TP10) that are susceptible to noise contamination and contribute less to HEP modulations, in line with a recent meta-analysis (Coll et al., 2021). We then investigated HEP differences between inhalation and exhalation across tasks. We conducted a cluster-based permutation tests with HEP as dependent variable, and System (cardiac vs. respiratory), Attention Focus (interoceptive vs. exteroceptive), and Phase (inhalation vs. exhalation) as within-participant factors. The 2×2×2 interaction (System by Attention Focus by Phase) was calculated as with the formula: [(HCT Exhalation – HCT Inhalation) – (C-TCT Exhalation – C-TCT Inhalation)] vs. [(BCT Exhalation – BCT Inhalation) – (B-TCT Exhalation – B-TCT Inhalation)]. The test was performed over the significant time window and electrodes resulting from the previous analysis. Planned t-tests were HCT inhalation vs. HCT exhalation; BCT inhalation vs. BCT exhalation; C-TCT inhalation vs. C-TCT exhalation; B-TCT inhalation vs. B-TCT exhalation; HCT exhalation vs. C-TCT exhalation; HCT exhalation vs. BCT exhalation; HCT inhalation vs. C-TCT inhalation; and HCT inhalation vs. BCT inhalation (number of planned t-tests: 8).

### 2.10.2 Trial-level cardio-respiratory control analyses

We controlled for instantaneous HR influences on HEPs between HCT and C-TCT by assessing trial-level data through linear mixed-effects models on 46903 trials clustered around 32 participants (Ambrosini et al., 2019; Kliegl, 2010; Zaccaro et al., 2022). We also controlled for cardiac influences on HEPs among respiratory phases at the single-trial level during HCT with a linear mixed-effects model on 17406 trials, clustered around 28 participants. Instantaneous HR for each heartbeat was based on the trial-level inter-beat interval. Trial-based ECG amplitude was calculated by averaging

ECG voltage in the significant HEP time window. Single-trial HEP activity was calculated by averaging the voltage of the significant channels and time-window of observed HEP effects. Values lying outside three standard deviations from the mean were excluded. Models were implemented with the General Analyses for the Linear Model (GAMLj) module in jamovi (v2.3.21; The jamovi project, 2022), using the Residual Maximum Likelihood (REML) method. The Akaike Information Criterion (AIC) was used to determine the best fitting model. For each parameter of the best fitting model, we reported the estimated coefficient (b), standard error (SE), t-statistic, and p-value. Degrees of freedom were estimated with the Satterthwaite's method.

### 2.10.3 Respiratory cycle analyses

Circular statistics were performed to assess HEP activity over the entire respiratory cycle, spanning from one inhalation to the subsequent one. We calculated the angular value of each R-peak using the formula (Al et al., 2020):

$$\text{Angular value} = [360 * \frac{(\text{R onset} - \text{previous inhalation onset})}{(\text{subsequent inhalation onset} - \text{previous inhalation onset})}]$$

R-peaks angular values ranged from 0° to 360°, with 0° indicating the onset of inhalation. Single-trial angular values were converted to radians (range 0 - 2π) and the corresponding HEP values were derived from electrodes and time window showing significant changes across the respiratory cycle in the binary analysis. Outliers exceeding three standard deviations from the mean were removed. Using the interquartile range method, HEPs were categorized into low (first quartile) and high-amplitude (fourth quartile) HEPs for each participant (Al et al., 2020, 2021). For each participant, the mean angle direction was calculated for the low and high-amplitude HEPs. At the group level, we tested whether the distribution of low and high-amplitude HEPs deviated from uniform distribution using the Rayleigh test for uniformity (Landler et al., 2018) as implemented in the Circular Statistics Toolbox (Berens, 2009). To assess whether the strength of the respiratory phase-locking differed

between low and high-amplitude HEPs, we applied the Watson-Williams test (Stephens, 1969; Watson & Williams, 1956).

We computed HEPs amplitude based on six equally sized respiration phase bins spanning the 0°-360° interval. A one-way repeated measures ANOVA was conducted to assess changes in HEP amplitude across bins. Planned t-tests were performed between inhalation phase bins (0°-60°, 60°-120°, 120°-180°) and exhalation phase bins (180°-240°, 240°-300°, 300°-360°) (number of planned t-tests: 9).

When appropriate, we used the Benjamini and Yekutieli procedure (FDR; Benjamini & Yekutieli, 2001), to correct for multiple testing with an FDR threshold of p = 0.05. Effect sizes were estimated with Cohen's d and partial eta squared ($\eta$p2) indices. Statistical analyses of behavioural and physiological data were conducted using repeated measures ANOVAs. Correlations between behavioural and psychometric data with HEP values were performed using Pearson's correlation. Statistical analyses were conducted in jamovi (v2.3.21; The jamovi project, 2022).

## 3. Results

### 3.1 Overview

After a baseline resting-state with eyes open, participants underwent four tasks involving interoceptive and exteroceptive attention (Attention Focus factor) focused on the cardiac and the respiratory systems (System factor). Tasks included HCT (Pollatos & Schandry, 2004; Schandry et al., 1986) and the Breath Counting Task (BCT; Herrero et al., 2018) as interoceptive tasks, and the Cardiac-Tone Counting Task (C-TCT; Wiebking et al., 2015) and the Breath-Tone Counting Task (B-TCT; adapted from Herrero et al., 2018) as exteroceptive tasks.

### 3.2 Heartbeat evoked potential activity is related to interoceptive attention

To test whether HEP activity was modulated by attention, we performed a cluster-based permutation test over the whole scalp, with HEP amplitude as the dependent variable and System (cardiac vs. respiratory) and Attention Focus (interoceptive vs. exteroceptive) as within-participant factors. Based on previous research (Baranauskas et al., 2017; Gray et al., 2007; Kumral et al., 2022; Petzschner et al., 2019; Pollatos et al., 2016; Schandry & Montoya, 1996; Schulz et al., 2018; Simor et al., 2021; Villena-González et al., 2017; Zaccaro et al., 2022), we tested HEP amplitude at each electrode and time point separately in an early (100-350 ms) and a late time window (350-600 ms) after the R-peak.

In the early time window, there was no difference in HEP amplitude between interoceptive and exteroceptive attention (Attention Focus: $t_{31} = -1.312$, $p_{clust} = 0.115$, $d = 0.232$) nor between the cardiac and respiratory system (System: $t_{31} = 0.892$, $p_{clust} = 0.234$, $d = 0.158$). However, there was a significant System by Attention Focus interaction from 242 to 313 ms after the R-peak over the following electrodes: Fp1, AF7, AF3, F3, F1, Fpz, AFz, Fz, FCz, Fp2, AF8, AF4, and F2 ($t_{31} = -4.034$, $p_{clust} = 0.018$, $d = 0.713$). However, despite the interaction, none of the planned t-tests were significant, showing no HEP difference when comparing the tasks (HCT vs. C-TCT: $t_{31} = -2.376$, $p_{clust} = 0.069$, $d = 0.42$; HCT vs. BCT: $t_{31} = 2.631$, $p_{clust} = 0.067$, $d = 0.465$; BCT vs. B-TCT: $t_{31} = -0.114$, $p_{clust} = 0.434$, $d = 0.02$; and C-TCT vs. B-TCT: $t_{31} = 2.724$, $p_{clust} = 0.312$, $d = 0.485$).

In the late time window, a higher HEP positivity was observed for interoceptive attention over F3, F1, FC1, C3, C1, CP1, CP3, Fpz, AFz, Fz, FCz, Cz, AF4, F6, F2, FC4, and FC2 from 352 to 508 ms after the R-peak (Attention Focus: $t_{31} = 5.039$, $p_{clust} = 0.017$, $d = 0.891$, Fig. 1A). Neither the main effect of System ($t_{31} = 0.338$, $p_{clust} = 0.738$, $d = 0.06$) nor the System by Attention Focus interaction ($t_{31} = 1.28$, $p_{clust} = 0.872$, $d = 0.227$) were significant. These findings suggest that the impact of attention on late HEP amplitude did not specifically depend on the system being monitored (cardiac vs. respiratory) but was associated with attention directed towards the body. Despite the non-significant interaction, planned t-tests conducted based on previous studies (Coll et al., 2021) revealed increases in HEP activity only during HCT compared to C-TCT from 352 to 539 ms after the R-peak over F1, FC3, FC1, C1, AFz, Fz, FCz, AF4, F6, F4, F2, FC4, and FC2 ($t_{31} = 4.13$, $p_{clust} = 0.013$, $p_{FDR} = 0.039$, $d = 0.73$, Fig. 1B), but not compared to BCT ($t_{31} = 1.34$, $p_{clust} = 0.19$, $d = 0.273$, Fig. 1B). No differences were observed between BCT vs. B-TCT ($t_{31} = 0.627$, $p_{clust} = 0.231$, $d = 0.111$, Fig. 1B), nor between C-TCT vs. B-TCT ($t_{31} = -0.683$, $p_{clust} = 0.5$, $d = 0.121$, Fig. 1B).

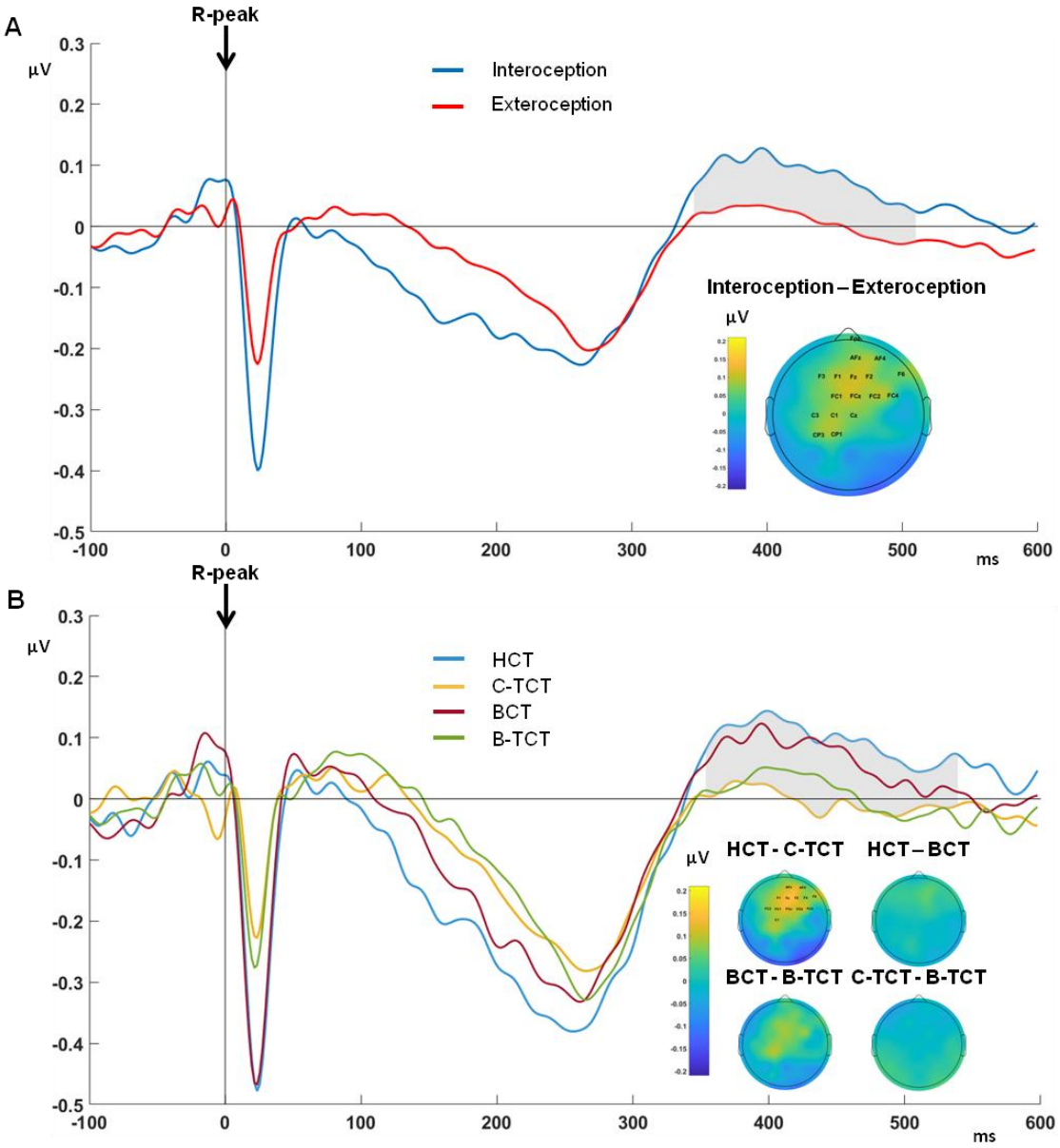



**Figure 1. HEP activity is related to interoceptive attention. A)** Grand-average HEP pooled for significant electrodes illustrating the main effect of Attention Focus. The shaded area marks significant differences between Interoception (blue) and Exteroception (red). The topographical distribution represents HEP differences between Interoception vs. Exteroception. Labels represent significant electrodes (cluster-based t-test: $t_{31} = 5.039$, $p_{clust} = 0.017$, $d = 0.891$). The scale bar unit of measurement is μV. **B)** Grand-average HEP pooled for significant electrodes during HCT (light blue), C-TCT (orange), BCT (purple), and B-TCT (green). The shaded area marks significant differences between HCT and C-TCT. The topographical distributions represent HEP differences between HCT vs. C-TCT, HCT vs. BCT, BCT vs. B-TCT, and C-TCT vs. B-TCT. Labels represent significant electrodes (cluster-based t-test: $t_{31} = 4.13$, $p_{clust} = 0.013$, $p_{FDR} = 0.039$, $d = 0.73$). The scale bar unit of measurement is μV. Abbreviations: HCT-Heartbeat Counting Task, C-TCT-Cardiac-Tone Counting Task, BCT-Breath Counting Task, B-TCT-Breath-Tone Counting Task.

### 3.3 Heartbeat evoked potential activity is related to the respiratory phase

To test whether HEP activity was modulated by the respiratory phase, we differentiated HEPs occurring during inhalation and exhalation. We found more epochs during inhalation than exhalation, likely due to higher Heart Rate (HR) during inhalation, resulting in the detection of more R-peaks. We firstly ran a cluster-based permutation t-test comparing HEP amplitude between inhalation and exhalation during the baseline. In the early time window, the analysis showed a positive posterior cluster of higher HEP amplitude during exhalation compared to inhalation from 195 to 328 ms after the R-peak (CP1, CP3, CP5, P1, P3, P5, PO3, CPz, Pz, POz, C4, CP2, CP4, CP6, P2, P4, P6, and PO4) ($t_{27}$ = 3.9, $p_{clust}$ = 0.012, d = 0.738) and a negative frontal cluster from 195 to 336 ms (Fp1, AF7, AF3, F5, F3, F1, FC5, FC3, C3, C5, Fpz, AFz, Fz, FCz, Fp2, AF8, AF4, F6, F4, F2, FC6, FC4, FC2, and C6) ($t_{27}$ = 3.18, $p_{clust}$ = 0.012, d = 0.601). We found no significant differences in the late time window ($t_{27}$ = 2.7, $p_{clust}$ = 0.303, d = 0.489).

We then conducted two cluster-based permutation tests: one for the early and one for the late time window, both focused on the significant fronto-central cluster observed in the previous analysis that did not consider the respiratory phase. In these analyses, HEP amplitude served as the dependent variable, with System (cardiac vs. respiratory), Attention Focus (interoceptive vs. exteroceptive), and respiratory Phase (inhalation vs. exhalation) as within-participant factors. In the early time window, we found a main effect of Phase from 117 to 266 ms after the R-peak over Fp1, AF7, AF3, F5, F3, F1, FC3, FC1, AFz, Fz, FCz, AF8, AF4, F6, F4, F2, and FC4 ($t_{27}$ = -3.32, $p_{clust}$ = 0.007, d = 0.627, Fig. 2A), indicating that HEP negativity was consistently higher during exhalation compared to inhalation across all tasks. There was no main effect of System ($t_{27}$ = -1.65, $p_{clust}$ = 0.054, d = 0.311) or Attention Focus ($t_{27}$ = -2.71, $p_{clust}$ = 0.472, d = 0.512). Moreover, no interactions were significant (System by Attention Focus by Phase: $t_{27}$ = 0.544, $p_{clust}$ = 0.089, d = 0.103; System by Attention Focus: $t_{27}$ = 1.68, $p_{clust}$ = 0.698, d = 0.318; Attention Focus by Phase: $t_{27}$ = -0.674, $p_{clust}$ = 0.55, d = 0.127; System by Phase: $t_{27}$ = 1.40, $p_{clust}$ = 0.098, d = 0.265).

In the late time window, we found no main effect of System ($t_{27}$ = 0.2, $p_{clust}$ = 0.319, d = 0.038), Attention Focus ($t_{27}$ = 2.057, $p_{clust}$ = 0.857, d = 0.389), or Phase ($t_{27}$ = 0.777, $p_{clust}$ = 0.174, d = 0.147) on HEP. Similarly, there were no significant System by Attention Focus ($t_{27}$ = -1.705, $p_{clust}$ = 0.974, d = 0.322), System by Phase ($t_{27}$ = -0.45, $p_{clust}$ = 0.318, d = 0.085), or Attention Focus by Phase interactions ($t_{27}$ = 1.058, $p_{clust}$ = 0.676, d = 0.199). Crucially, however, the three-way System by Attention Focus by Phase interaction was significant from 430 to 523 ms over Fp1, AF3, F5, F3, F1, FC1, Fpz, AFz, Fz, Fp2, AF8, AF4, F4, F2, FC4, and FC2 ($t_{27}$ = 3.98, $p_{clust}$ = 0.031, d = 0.583). This interaction was explained by the following planned t-tests, which showed that HEP positivity increased during exhalation compared to inhalation specifically in HCT, from 367 to 500 ms after the R-peak, over AF3, F1, FC1, Fpz, AFz, Fz, FCz, Fp2, AF8, F4, F2, and FC2 ($t_{27}$ = 3.8, $p_{clust}$ = 0.005, $p_{FDR}$ = 0.02, d = 0.719, Fig. 2B-C). In contrast, there were no changes in HEP activity between exhalation and inhalation in BCT ($t_{27}$ = -0.357, $p_{clust}$ = 0.129, d = 0.067), C-TCT ($t_{27}$ = 0.116, $p_{clust}$ = 0.667, d = 0.022), or B-TCT ($t_{27}$ = 1.01, $p_{clust}$ = 0.392, d = 0.192). Interestingly, HEPs recorded during exhalation in HCT were higher than those recorded during exhalation in C-TCT from 383 to 508 ms after the R-peak over F3, F1, FC3, FC1, Fpz, AFz, Fz, FCz, Fp2, AF8, AF4, F6, F4, F2, FC4, and FC2 ($t_{27}$ = 3.668, $p_{clust}$ = 0.003, $p_{FDR}$ = 0.02, d = 0.693, Fig. 2C-D), and during exhalation in BCT from 445 to 500 ms over AF3, F5, F3, F1, FC1, AFz, Fz, FCz, Fp2, AF8, AF4, F6, F4, F2, FC4, and FC2 ($t_{27}$ = 3.572, $p_{clust}$ = 0.018, $p_{FDR}$ = 0.048, d = 0.675, Fig. 2C-D). In contrast, there were no changes between HEPs recorded during inhalation in HCT and those recorded during inhalation in C-TCT ($t_{27}$ = 0.428, $p_{clust}$ = 0.654, d = 0.081, Fig. 2D) nor BCT ($t_{27}$ = -1.061, $p_{clust}$ = 0.895, d = 0.2, Fig. 2D). These results showed higher late HEP positivity during exhalation compared to inhalation specifically for HCT. Importantly, they highlight that the observed increases in HEP amplitude during HCT primarily stem from HEPs recorded during exhalation, with minimal contribution from HEPs recorded during inhalation.

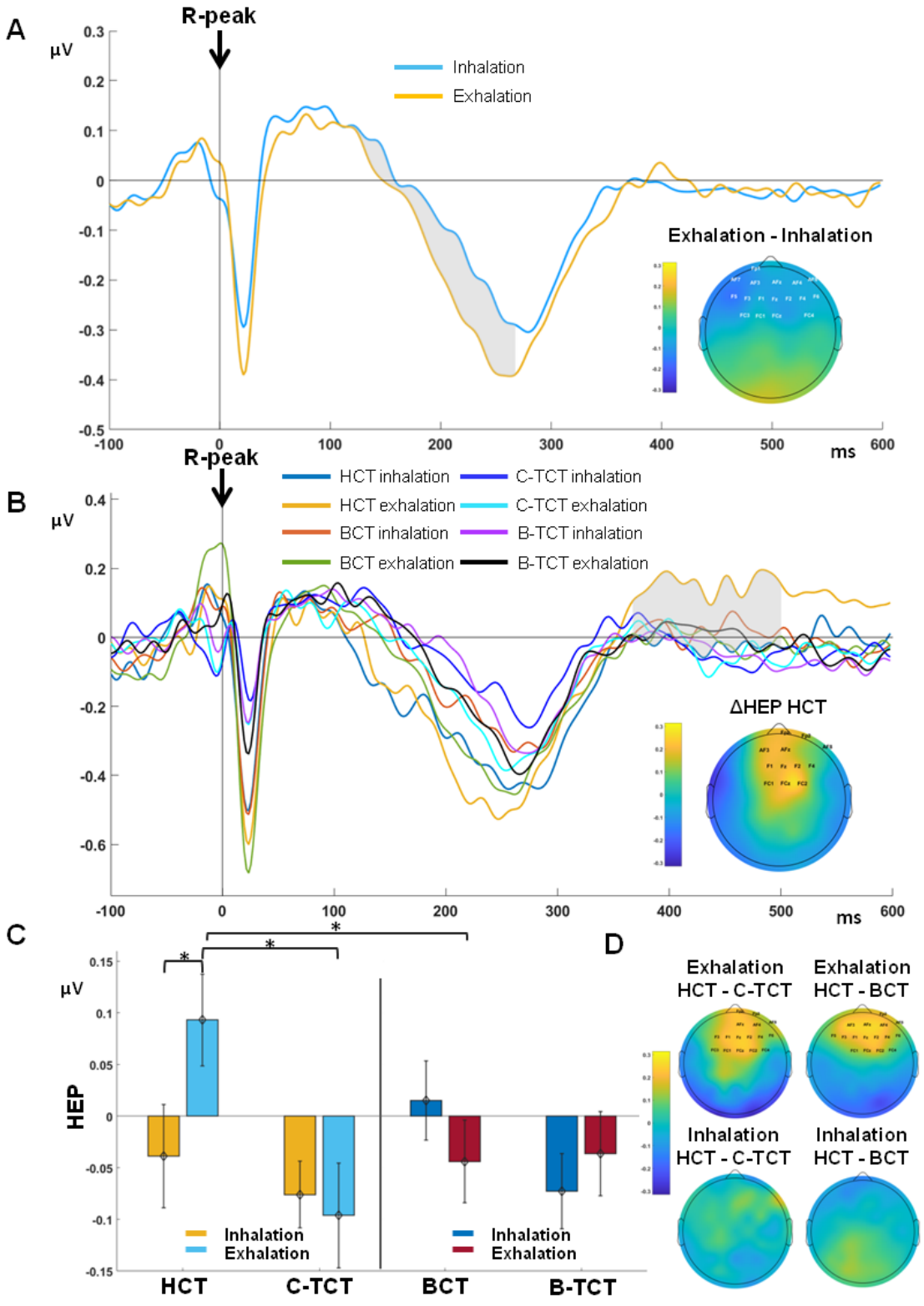



**Figure 2. HEP activity is related to the respiratory phase. A)** Grand-average HEP pooled for significant electrodes illustrating the main effect of Phase. The shaded area marks significant differences between Exhalation (orange) and Inhalation (light blue). The topographical distribution represents HEP differences between Exhalation vs. Inhalation. Labels represent significant electrodes (cluster-based t-test: $t_{27}$ = -3.32, $p_{clust}$ = 0.007, d = 0.627). The scale bar unit of measurement is µV. **B)** Grand-average HEP pooled for significant electrodes during different respiratory phases: HCT-inhalation (dark turquoise), HCT-exhalation (orange), BCT-inhalation (brown), BCT-exhalation

(green), C-TCT-inhalation (blue), C-TCT-exhalation (light blue), B-TCT-inhalation (purple), B-TCT-exhalation (black). The shaded area marks significant differences between exhalation and inhalation (ΔHEP) during HCT. The topographical distribution represents HEP differences between Exhalation vs. Inhalation during HCT. Labels represent significant electrodes (cluster-based t-test: $t_{27} = 3.8$, $p_{clust} = 0.005$, $p_{FDR} = 0.02$, $d = 0.719$). The scale bar unit of measurement is μV. **C)** Mean HEP amplitude over significant electrodes across tasks and respiratory phases. Data are presented as mean +/- standard error. Significant planned t-tests are indicated by asterisks (* $p < 0.05$). **D)** Topographical distributions represent HEP differences during exhalation between HCT vs. C-TCT and HCT vs. BCT, and during inhalation between HCT vs. C-TCT and HCT vs. BCT. Labels represent significant electrodes (Exhalation HCT vs. C-TCT cluster-based t-test: $t_{27} = 3.668$, $p_{clust} = 0.003$, $p_{FDR} = 0.02$, $d = 0.693$; Exhalation HCT vs. BCT cluster-based t-test: $t_{27} = 3.572$, $p_{clust} = 0.018$, $p_{FDR} = 0.048$, $d = 0.675$). The scale bar unit of measurement is μV. Abbreviations: HCT-Heartbeat Counting Task, C-TCT-Cardiac-Tone Counting Task, BCT-Breath Counting Task, B-TCT-Breath-Tone Counting Task.

### 3.4 Heartbeat evoked potential and cardio-respiratory physiology

We performed control analyses at both the participant and trial levels to assess whether observed changes in HEP amplitude were related to cardio-respiratory physiology (Buot et al., 2021; Candia-Rivera et al., 2022; Dirlich et al., 1997; Kern et al., 2013; Leganes-Fonteneau et al., 2021; MacKinnon et al., 2013). Cardio-respiratory features of interest are described in the Materials and Methods section. We found negligible effects of cardio-respiratory physiology on HEP changes across tasks and respiratory phases.

### 3.5 Respiratory cycle analyses during the Heartbeat Counting Task

To capture HEP changes across the respiratory cycle during HCT, we employed circular statistics and divided the respiratory cycle into phase bins. We used the interquartile range to categorize HEPs into low and high-amplitude HEPs. The Rayleigh test rejected the uniform distribution for both low ($z = 11.282$, $p < 0.001$) and high-amplitude HEPs ($z = 3.809$, $p = 0.021$). Low-amplitude HEPs were clustered around the middle phase of inhalation (first and second quadrants; mean angle = 100.45°, Fig. 3A), while high-amplitude HEPs were clustered around the early phase of inhalation (first quadrant) and extended to the exhalation phase (third and fourth quadrant), with the mean direction occurring near the transition from exhalation to inhalation (19.99°, Fig. 3B). The Watson-Williams

test revealed significant differences between low and high-amplitude HEPs ($F_{1,54}$ = 15.665, p < 0.001).

We assessed HEP amplitude changes in HCT across the respiratory cycle using six equally-sized bins covering the 0°-360° interval. A one-way repeated measures ANOVA revealed significant HEP amplitude changes across phase bins ($F_{5,135}$ = 3.23, p = 0.009, $\eta p2$ = 0.107). Planned t-tests showed that HEPs detected in the 60°-120° range (middle inhalation) had lower amplitude than those detected in the 240°-300° range (middle exhalation: $t_{27}$ = -2.995, p = 0.006, $p_{FDR}$ = 0.027, d = 0.566) and the 300°-360° range (late exhalation: $t_{27}$ = -2.43, p = 0.022, $p_{FRD}$ = 0.049, d = 0.459). Furthermore, HEPs detected in the 120°-180° range (late inhalation) had lower amplitude than those detected in the 240°-300° range (middle exhalation: $t_{27}$ = -3.063, p = 0.005, $p_{FRD}$ = 0.027, d = 0.578) and the 300°-360° range (late exhalation: $t_{27}$ = -2.731, p = 0.011, $p_{FRD}$ = 0.033, d = 0.516; Fig. 3C). All the other comparisons did not show significant differences.

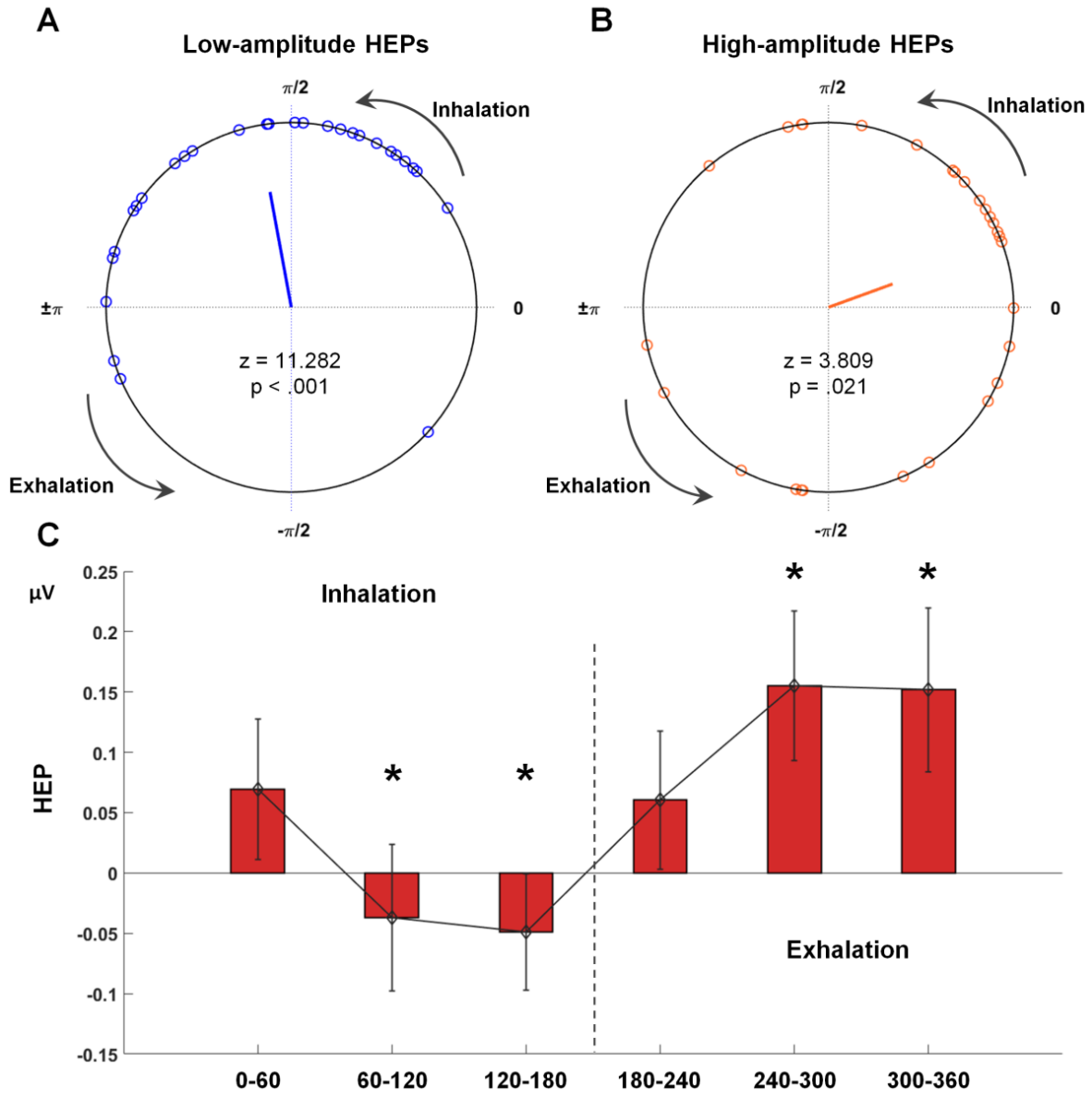



**Figure 3. Respiratory cycle analyses.** Circular distribution of mean angles (HEPs onsets relative to the respiratory cycle) for **A)** low-amplitude HEPs (blue) and **B)** high-amplitude HEPs (orange). Zero degree corresponds to inhalation onset. Each dot indicates the mean angle of one participant. Line direction indicates the mean angle across the participants. Arrow length represents the mean resultant length. **C)** The mean amplitude of HEPs as a function of six equally sized bins of the respiratory phase. Error bars represent the standard error. Significant t-tests comparing inhalation and exhalation phase bins are indicated by asterisks (* $p < 0.05$).

### 3.6 Correlation between the Heartbeat Evoked Potential, behavioural and psychometric data

Task accuracy changed across tasks. A 2×2 repeated measures ANOVA revealed a main effect of System ($F_{1,31} = 73.1$, $p < 0.001$, $\eta p2 = 0.702$) and Attention Focus ($F_{1,31} = 108.5$, $p < 0.001$, $\eta p2 = 0.778$), with lower accuracy in the cardiac than respiratory condition and in the interoceptive than

exteroceptive condition. We also found a significant System by Attention Focus interaction ($F_{1,31}$ = 110.7, $p < 0.001$, $\eta p2 = 0.781$). Planned t-tests revealed lower task accuracy in HCT compared to C-TCT ($t_{31}$ = -10.78, $p < 0.001$, d = 1.91) and BCT ($t_{31}$ = -9.66, $p < 0.001$, d = 1.71), and lower task accuracy in B-TCT compared to C-TCT ($t_{31}$ = -2.6, p = 0.048, d = 0.365). No differences were observed between BCT and B-TCT ($t_{31}$ = -1.81, p = 0.08, d = 0.32). Correlations with HEP amplitude showed no relationship with HCT accuracy (r = 0.117, p = 0.524) or confidence (r = 0.108, p = 0.558). Similarly, HEPs amplitude during inhalation or exhalation did not correlate with HCT accuracy (inhalation: r = 0.074, p = 0.708; exhalation: r = -0.047, p = 0.812) or confidence (inhalation: r = 0.183, p = 0.352; exhalation: r = -0.086, p = 0.663). The absence of correlation might arise from the inherent limitations of HCT in assessing accuracy (Brener & Ring, 2016; Desmedt et al., 2018; Zamariola et al., 2018). In addition, while interoceptive accuracy is related to conscious perception of heartbeats, HEP changes may also be attributed to unconscious processes (Villena-González et al., 2017).

Given previous associations of HEP activity with specific self-reported interoceptive sensibility and trait mindfulness (Baranauskas et al., 2017; Billeci et al., 2021; Verdonk et al., 2021), we examined the correlations between scores obtained on the Trusting and Not-Worrying scales of the Multidimensional Assessment of Interoceptive Awareness (MAIA) and the total score of the Five Facet Mindfulness Questionnaire (FFMQ) with HEP amplitude recorded during inhalation and exhalation during HCT. HEPs recorded during inhalation did not correlate with any of the scales (FFMQ Total Score: r = -0.01, p = 0.963, Fig. 4A; MAIA Trusting: r = 0.163, p = 0.437, Fig 4B; MAIA Not-Worrying: r = -0.348, p = 0.088, Fig. 4C). In contrast, HEPs recorded during exhalation exhibited a positive correlation with FFMQ total score (r = 0.407, p = 0.044, Fig. 4D) and MAIA Trusting scale (r = 0.399, p = 0.048, Fig. 4E), but not with MAIA Not-Worrying scale (r = 0.139, p = 0.506, Fig. 4F). None of the other MAIA scales correlated with HEP values. These findings suggest that the relationship between HEP amplitude, interoceptive sensibility, and trait mindfulness is related to HEPs recorded during exhalation.

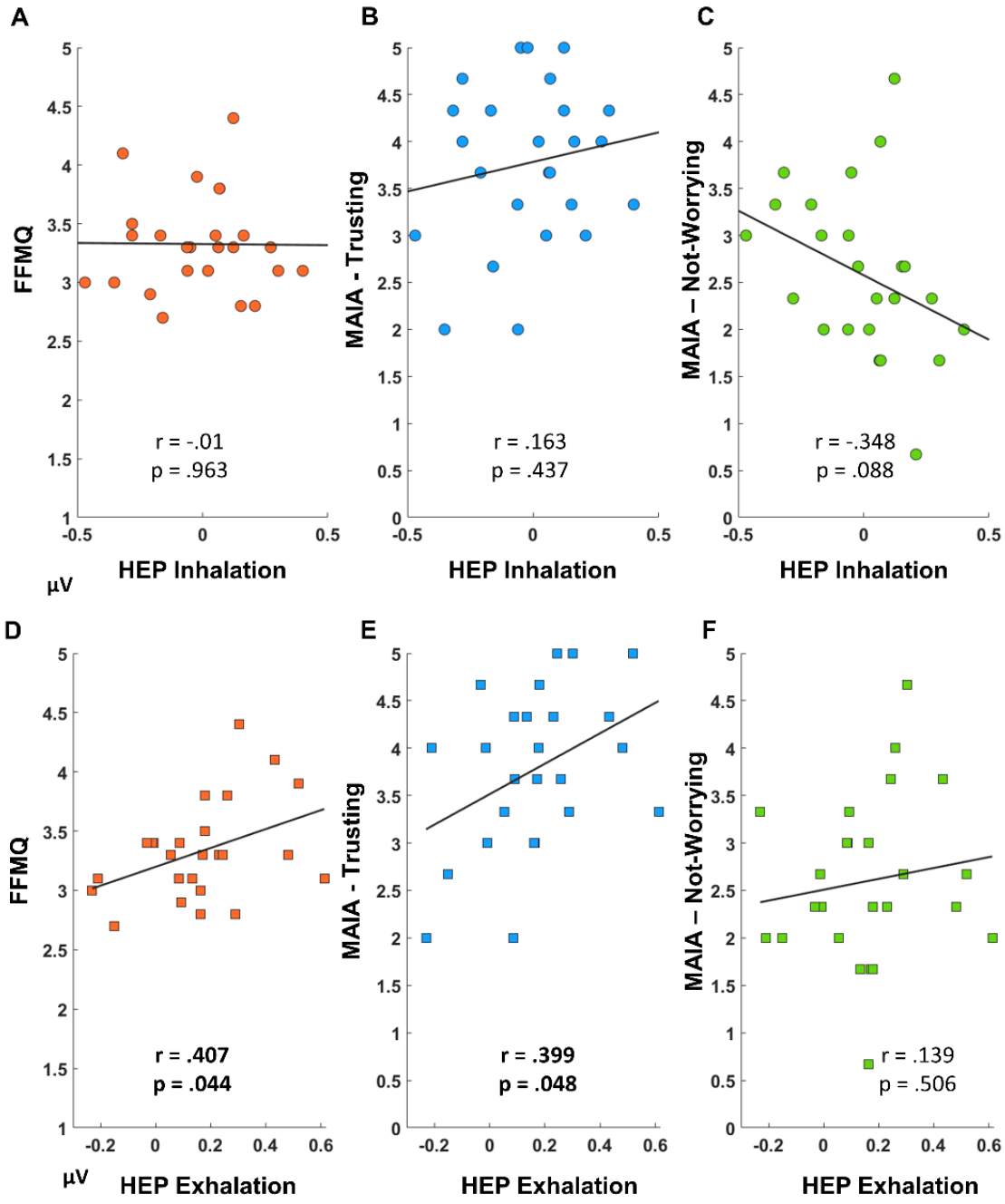



**Figure 4. Correlation between questionnaires and HEPs recorded at inhalation and exhalation.** Scatter plots of the linear relationships (Pearson's correlation) between the FFMQ total score, MAIA Trusting scale, and MAIA Not-Worrying scale and mean HEP amplitude recorded during inhalation **(A, B, C)** and exhalation **(D, E, F)**.

## 4. Discussion

We assessed HEP activity in healthy volunteers during tasks prompting either interoceptive or exteroceptive attention. Our aim was to investigate HEP and ΔHEP (respiratory phase-related HEP modulations) changes across different interoceptive and exteroceptive attention tasks. The results revealed late HEP amplitude increases during the interoceptive tasks at fronto-central electrodes, while only partially supporting the idea that HEP increases are specifically induced by cardiac interoceptive attention. Crucially, when respiratory phases were taken into account, a specific modulation of HEP amplitude induced by cardiac interoceptive attention clearly emerged. When comparing the respiratory phase-induced modulations of HEPs between the different tasks (HCT, BCT, C-TCT, and B-TCT), results revealed increased HEP positivity during exhalation compared to inhalation only during the cardiac interoceptive task (HCT). In contrast, no changes in HEP activity were observed between exhalation and inhalation during the other tasks. Circular statistics showed that in HCT low-amplitude HEPs were clustered around the middle part of inhalation and high-amplitude HEPs were concentrated around exhalation and the transition from exhalation to inhalation. We also observed a gradual increase in HEP amplitude throughout the respiratory cycle, peaking at the end of exhalation (240°-360° respiratory phase bins). Importantly, the experimental design allowed a direct comparison of HEP amplitude between inhalation and exhalation among tasks. We found that HEPs recorded during exhalation in HCT showed higher amplitude than HEPs recorded during exhalation in C-TCT and BCT. Notably, no differences were found when comparing HEPs recorded during inhalation in HCT with HEPs recorded during inhalation in C-TCT nor BCT. These results extend our previous findings regarding changes in HEP amplitude between respiratory phases (Zaccaro et al., 2022). Firstly, they corroborate previous results using HCT in addition to HBD. Secondly, they establish that late HEP modulations related to the respiratory phase are specific to the *cardiac* interoceptive task and do not extend to *non-cardiac* interoceptive tasks (BCT). This also suggests that ΔHEP modulation is a more specific index for cardiac interoceptive attention than HEP amplitude alone, when respiratory phases are not taken into account. Lastly, the results indicate that,

during HCT, the brain does not enhance heartbeat sensations during inhalation, but enhances heartbeat sensations exclusively during exhalation.

An additional finding is the association between HEP activity and interoceptive sensibility and trait mindfulness. During HCT, HEP amplitude recorded during exhalation was related to the Trusting and Not-Worrying scales of MAIA and FFMQ total score. In contrast, no association was found between HEP amplitude during inhalation and these indices. This suggests that only HEPs assessed during exhalation are linked to interoceptive sensibility and mindfulness, which are important indicators of well-being and mental health (Bonaz et al., 2021; Hölzel et al., 2011; Khalsa et al., 2018; Paulus, 2013; Tang et al., 2015; Tsakiris & Critchley, 2016). These results could explain non-significant findings regarding cardiac interoceptive accuracy changes in mindfulness practitioners (see Khalsa et al., 2020 and Treves et al., 2019 for meta-analyses) that might be attributed to the failure to consider respiratory phases. It is possible that cardiac interoception in experienced meditators is specifically improved during exhalation. These findings may also provide an explanation for previously reported null associations between trait mindfulness and HEP (Verdonk et al., 2021), a link that may be evident only during exhalation. Future studies may shed light on this topic.

Our results show that late HEP amplitude increases only when attention is focused on the heart *and* during exhalation. In other words, exhalation may not only serve as a respiratory phase that enhances attention to cardiac interoception compared to inhalation; it may also be a necessary condition for directing attention to heartbeat sensations during cardiac interoceptive tasks. If the first scenario were true, we would also expect to find higher HEP amplitude during inhalation in HCT compared to the other tasks (C-TCT and BCT), which was not observed. Several factors could explain this phenomenon. A higher-level explanation is in line with a recent hypothesis regarding the role of respiration in interoceptive perception (Molle & Coste, 2022). According to this hypothesis, the brain is constantly engaged in a trade-off between directing attention towards interoceptive or exteroceptive stimuli. Inhalation can hence give priority to external perception by redirecting attention to the

environment, while exhalation can optimize interoception by allocating attentional resources to bodily sensations. Alternatively, a peripheral explanation may involve Respiratory Sinus Arrhythmia (RSA; Brecher & Hubay, 1955), which produces faster but weaker heartbeats during inhalation (Larsson et al., 2021), thereby reducing HEP amplitude compared to exhalation. The non-specific increase observed in the early time window across all tasks, irrespective of attentional focus, could be precisely attributed to this bottom-up mechanism. However, control analyses on late HEP amplitude and cardio-respiratory physiology seem to rule out the substantial contribution of these bottom-up components. Nevertheless, changes in cardiac physiology between respiratory phases do not exclude a concomitant top-down modulation of attention: heartbeats strength reduction during inhalation may enhance exteroceptive attention also due to reduced interference of cardiac signals, while exhalation may facilitate interoceptive attention also due to already increased cardiac sensations.

In conclusion, our data suggest that respiratory phases play a crucial role in influencing cardiac interoception. It is crucial for future studies to investigate the impact of respiratory phases on other aspects of interoception beyond cardiac sensations. These domains include gastric interoception (Khalsa et al., 2022; Porciello et al., 2018; Rebollo et al., 2018), interoceptive touch (Crucianelli et al., 2018, 2022; Di Lernia et al., 2018), and pain perception (Arsenault et al., 2013; Iwabe et al., 2014; Martin et al., 2012; Parrotta et al., 2024). Recognizing the role of respiration in shaping other interoceptive processes will be critical for developing a comprehensive understanding of reciprocal interactions between the body and the brain (Allen et al., 2023; Boyadzhieva & Kayhan, 2021; Brændholt et al., 2023; Corcoran et al., 2023; Criscuolo et al., 2022; Tort et al., 2018).

Some limitations of this study deserve consideration. Firstly, potential variations in task difficulty across tasks could have impacted HEP amplitude when comparing interoceptive and exteroceptive tasks (Coll et al., 2021). Secondly, the inherent ease of BCT, driven by the salience of respiratory sensations, poses a challenge when comparing it with HCT, characterized by greater ambiguity in cardiac sensations, raising questions about whether BCT qualifies as a true interoceptive task.

Nonetheless, the use of BCT was necessary to ensure comparability with HCT, and previous research has suggested that breath counting can indeed elicit interoceptive attention (F. Wong et al., 2018; Herrero et al., 2018; Levinson et al., 2014). Future studies exploring this topic could consider employing alternative tasks, such as the filter detection task (Harrison et al., 2021), respiratory resistance sensitivity task (Nikolova et al., 2022), respiratory tracking task (Daubenmier et al., 2013), or interoceptive/exteroceptive attention task (Farb et al., 2023).

# Study 3

## Cardio-respiratory interactions in interoceptive perception: The role of heartbeat-modulated cortical oscillations

This study has been published as:

Zaccaro A., della Penna F., Bubbico F., Bayram B., Perrucci M.G., Costantini M., Ferri F. (2026). Cardio-respiratory interactions in interoceptive perception: The role of heartbeat-modulated cortical oscillations. *NeuroImage*. https://doi.org/10.1016/j.neuroimage.2026.121711

The version presented in this thesis has been adapted to fit the overall structure of the dissertation. The original published version is provided in Appendix C.

## 1. Introduction

We have previously highlighted cardio-respiratory interoceptive interactions as reflected in the heartbeat-evoked potential (HEP; Coll et al., 2021; Schandry et al., 1986). In two independent samples of healthy individuals, we found increased late HEP positivity (emerging after 300 ms from the R-peak) during exhalation compared to inhalation while participants engaged in two cardiac interoceptive tasks: the heartbeat detection task (HBD; Zaccaro et al., 2022) and the heartbeat counting task (HCT; Zaccaro et al., 2024). In the HBD, greater HEP amplitudes during exhalation compared to inhalation were positively correlated with greater interoceptive accuracy (Zaccaro et al., 2022). In the HCT, late HEP enhancements relative to the C-TCT were predominantly driven by exhalation, with no significant contribution from inhalation (Zaccaro et al., 2024). Together, these results supported the hypothesis that exhalation may enhance cardiac interoception compared to inhalation. They were also consistent with evidence that breathing dynamically shapes neural processing in different domains. The respiratory cycle interacts with both resting (Herrero et al., 2018; Kluger et al., 2023; Kluger & Gross, 2021) and task-related brain activity, modulating perceptual (Flexman et al., 1974; Gallego et al., 1991; Goheen et al., 2024; Grund et al., 2022; Harting et al., 2025; Johannknecht & Kayser, 2022; Kluger et al., 2021; Leupin & Britz, 2024; Mizuhara et al., 2024, 2025; Mizuhara & Nittono, 2022; Saltafossi et al., 2025; Stetza et al., 2025), cognitive-emotional (Arshamian et al., 2018; Belli & Fischer, 2024; Brændholt et al., 2025; Huijbers et al., 2014; Mizuhara & Nittono, 2023; Molle et al., 2023; Nakamura et al., 2018; Perl et al., 2019; Schaefer et al., 2024; Waselius et al., 2019; Zelano et al., 2016), and motor functions (Engelen et al., 2025; Kluger & Gross, 2020; Park et al., 2020, 2022; see Tort et al., 2025 for an extensive review). However, despite its well-established role in exteroceptive functions, the precise influence of respiration on cardiac interoception remains unclear, particularly due to the strong physiological coupling between heartbeat dynamics and respiratory cycles, which introduces potential confounds and complicates interpretation.

A growing body of evidence suggests that, beyond time-domain HEPs, heartbeat-modulated cortical oscillations in the time-frequency domain may be used as more precise electrophysiological markers of cardiac interoception. A landmark electrocorticography study (Kern et al., 2013) identified heartbeat-modulated power fluctuations over somatosensory areas at rest, predominantly occurring in the low-frequency band (< 12 Hz). Similarly, an intracranial EEG (iEEG) study (Park et al., 2018) identified heartbeat-modulated increases in inter-trial coherence (ITC) in the theta band within the insula and frontotemporal regions. These increases were observed both at rest and during a task designed to modulate bodily self-awareness (a full-body illusion paradigm), while no heartbeat-modulated power changes were detected in the same areas. In contrast, an iEEG study by Treves (2020) employing independent component analysis-based denoising reported heartbeat-modulated increases in alpha power but found no changes in ITC. Several EEG studies have investigated heartbeat-modulated modulations in power, ITC, and functional connectivity (FC) across a range of conditions, including sleep stages (Lechinger et al., 2015; Simor et al., 2025), states of consciousness (Liuzzi et al., 2024), resting-state (Kim & Jeong, 2019), emotions (Kato et al., 2020; Kim et al., 2019), interoceptive metacognitive awareness (Canales-Johnson et al., 2015), interoceptive-exteroceptive processing (Fló et al., 2024; García-Cordero et al., 2017; Pultsina et al., 2025), and meditation expertise (Jiang et al., 2020). Recently, Lee et al. (2024) employed a classification approach to highlight the role of heartbeat-related spectral perturbations in the alpha and theta bands in distinguishing interoceptive (heartbeat-focused) from exteroceptive (sound-focused) attentional states. Their results suggest that time-frequency measures may be less susceptible to physiological artifacts, such as the cardiac field artifact. Taken together, these findings indicate that studying heartbeat-modulated cortical oscillations in the time-frequency domain may help to overcome the limitations of time-domain HEP analysis and may provide deeper insights into the neural mechanisms of cardiac interoception. In this study, we re-analyzed our previously collected dataset (Zaccaro et al., 2024) comprising 28 healthy participants. Our investigation focused on heartbeat-modulated activity during the HCT and its exteroceptive control task (C-TCT), analyzing heartbeats separately during

inhalation and exhalation. Our central hypothesis was that heartbeat-modulated power and ITC would be differentially shaped by respiratory phase and task demands: based on the findings of Lee et al. (2024) and our previous work (Zaccaro et al., 2024), we predicted selective increases in theta (4–8 Hz) and alpha (8–13 Hz) activity during exhalation, emerging in a late post-R-peak window (from 300 ms onward) and specifically during the HCT.

To further investigate the relationship between HEPs and time-frequency measures, we adopted a methodology from a study that reported a negative association between auditory-evoked P300 responses and alpha activity (Studenova et al., 2023). We then applied linear mixed-effects models to assess trial-level relationships between HEP, power, and ITC across respiratory phases, as well as their associations with interoceptive accuracy and cardio-respiratory physiology. Based on prior research identifying alpha power as a marker of interoceptive attention that has been shown to correlate with emotional arousal-related HEP modulations (Luft & Bhattacharya, 2015), interoceptive accuracy (Rominger et al., 2025; Villena-González et al., 2017), and to increase during heartbeat-focused tasks (Crivelli & Balconi, 2025; Kritzman et al., 2022; Villena-González et al., 2017), we expected to find positive associations between HEPs, heartbeat-modulated cortical oscillations in the alpha band, and interoceptive accuracy. Finally, we conducted exploratory analyses to evaluate changes in heartbeat-modulated FC and graph theory metrics within the alpha and theta frequency bands, across tasks and respiratory phases. As with power and ITC, we expected to observe increases in heartbeat-modulated FC and graph theory metrics during exhalation compared to inhalation in the HCT. We interpreted our findings within the interoceptive predictive coding framework, examining how respiration shapes predictive processes underlying cardiac interoception and how cardio-respiratory interoceptive interactions may modulate the precision-weighting of cardiac prediction errors.

## 2. Materials and methods

### 2.1 Ethics statement

The study from which the original dataset was derived (Zaccaro et al., 2024) was approved by the Institutional Review Board of the Department of Psychology at the "G. d'Annunzio" University of Chieti-Pescara, Italy (Protocol Number 44_26_07_2021_21016). The study adhered to the ethical guidelines of the Italian Association of Psychology and the Declaration of Helsinki, including its amendments. All participants provided their written informed consent and were unaware of the experimental aims prior to data collection.

### 2.2 Participants

Twenty-eight healthy volunteers (13 female; 1 left-handed; mean age: 27.88 ±4.46 years) were analyzed. Eligibility was determined based on self-reported criteria: (1) no personal or family history of psychiatric, neurological or somatic disorders; (2) no chronic or acute respiratory diseases; (3) no use of central nervous system-affecting substances in the previous week; and (4) no previous experience with mindfulness-based meditation or breath control practices. All participants were of normal weight and had normal or corrected-to-normal vision.

### 2.3 Experimental procedure

As described in Zaccaro et al. (2024), the tasks were administered using the E-Prime 3.0 software (Psychology Software Tools, Pittsburgh, PA, USA). Participants were seated comfortably in front of a computer screen positioned approximately 60 cm away for optimal keyboard use and screen visibility. Room lighting and noise levels were minimised, and the temperature was maintained at a comfortable level. Written instructions were presented before each task. The experimenter then ensured that participants understood the instructions well and invited them to ask questions if necessary. EEG, ECG and respiratory signals were continuously recorded throughout the experiment.

The resting-state condition was recorded first. Participants sat for 10 min resting with their eyes open, looking at a fixation cross in the centre of the screen and allowing their thoughts to wander without focusing on anything in particular. They were also instructed to breathe spontaneously.

The cardiac interoceptive task used was the heartbeat counting task (HCT; Pollatos et al., 2005; Schandry et al., 1986). Participants were given the following instructions, adapted from Desmedt et al. (2018): "*In this task, direct your attention to your heart and the associated physical sensations. You are required to sustain your focus on your heart for various durations and count the number of heartbeats you perceive. Begin silently counting when the heart symbol appears on the screen. When the heart symbol disappears, report the number of heartbeats you are sure you felt. Only report the number of heartbeats you are sure about, without trying to estimate your heart rate. During each trial, keep your eyes open, gaze at the screen and avoid moving. Refrain from guiding your responses by checking your pulse in your wrists or neck. Breathe spontaneously and avoid changing your breathing frequency or holding your breath*". The HCT consisted of three blocks of four randomized trials lasting 25, 35, 45 and 100 s (Ardizzi & Ferri, 2018; Di Lernia et al., 2018; Ueno et al., 2020), for a total of 12 trials. After each trial, participants reported the number of perceived heartbeats and rated their confidence (HCT confidence) on a 10-point Likert scale, ranging from 0 (very poor) to 9 (excellent). They did not receive any feedback on their performance.

The exteroceptive task used was the cardiac-tone counting task (C-TCT). Participants were presented with digitally generated heartbeat sounds and instructed to count and report the number of heartbeats they heard (Wiebking et al., 2015). The C-TCT consisted of three blocks of four randomized trials lasting 25, 35, 45 and 100 s. The heartbeat sounds were presented at irregular intervals, with an average frequency of 60 bpm. After each trial, participants reported the number of heartbeats they heard and rated their confidence (C-TCT confidence). Before starting the experiment, participants completed a short training session and verbally confirmed that they could not perceive their heartbeat through the breathing belt to ensure that it was not too tight.

### 2.4 Electrophysiological recording and pre-processing

Respiratory activity was recorded using a respiratory belt placed around the chest (Respiratory Transducer TSD201, BIOPAC Systems Inc, Goleta, CA, USA). EEG signals were recorded using a 64-channel BrainAmp MR EEG system (BrainCap, BrainVision LLC, Garner, NC, USA) with electrodes positioned according to the International 10–20 system. Electrode impedance was kept below 10 kΩ for all channels. The ECG was recorded using three electrodes: two placed over the left costal margin and the right clavicle, with the ground electrode placed over the right costal margin (MP160, BIOPAC Systems Inc, Goleta, CA, USA). Three additional backup electrodes were integrated into the EEG recording system via an external electrode input box (BrainProducts GmbH, BrainVision LLC, Gilching, Germany) and placed over the left and right clavicles, with the ground at the left costal margin. The BrainAmp MR EEG, MP160 and TSD201 systems were synchronised with the E-Prime 3.0 software using a TriggerStation™ (BRAINTRENDS LTD 2010, Italy). All signals were sampled at 2.5 kHz with a 0.016 to 250 Hz bandpass filter and a 50 Hz notch filter. Signals were then filtered and down-sampled to 256 Hz.

Respiratory data were processed using custom MATLAB scripts (R2021a, MathWorks Inc, Natick, MA, USA). The respiratory signal was high-pass filtered at 0.1 Hz to remove baseline drift. Respiratory phases were detected using a validated method (Grund et al., 2022; Power et al., 2020; Zaccaro et al., 2024). Outliers exceeding three scaled median absolute deviations from the local median within a 1-s moving window were linearly interpolated with the adjacent values. Data were then smoothed with a 1-s window filter (Savitzky & Golay, 1964) and z-scored. Inhalation and exhalation onsets were identified as local minima (troughs) and maxima (peaks), respectively. Peaks and troughs had to be at least 2 s apart, and the minimum prominence of the interquartile range of the z-scored data was multiplied by a factor ranging from 0.3 to 0.8, depending on the participant's respiratory trace (Grund et al., 2022). A breath cycle was defined as the interval between successive inhalations (i.e. from one trough to the next).

EEG data were pre-processed using the EEGLAB toolbox (v2022.1; Delorme and Makeig, 2004). Data were filtered using a Hamming windowed FIR filter between 0.5 and 45 Hz (Al et al., 2020; 2021). EEG segments with poor signal quality were manually rejected. Independent component analysis (ICA) was performed to remove artefacts related to heartbeat, eye and muscle activity (FastICA; Hyvarinen, 1999). The ECG, respiratory channels and excessively noisy channels were excluded from the ICA decomposition. A few noisy channels (<5), typically peripheral and not known to contribute to heartbeat-evoked potential (HEP) generation (Coll et al., 2021), were identified. Independent components (ICs) were rejected based on IC time series, scalp maps, and power spectra (Delorme and Makeig, 2004). Special attention was given to the cardiac field artifact (CFA) and the pulse-related artifact (PA) as they significantly affect HEP activity (Coll et al., 2021). ICs contaminated by CFA and PA were identified by plotting R-peaks over IC time series, and ICs with activation time-locked to the ECG R-peak were removed (Zaccaro et al., 2024). The number of ICs removed ranged from 1 to 6 (3 ±1 [mean ±SD]), with CFA-related ICs ranging from 0 to 3 (1 ±1 [mean ±SD]). After ICA, previously identified noisy channels were interpolated using adjacent electrodes (Jungh¨ofer et al., 2000). The cleaned EEG signals were then referenced to the mean reference (Antonacci et al., 2023; Barà et al., 2023; Zaccaro et al., 2024) as recommended (Candia-Rivera et al., 2021). ECG R-peaks were identified using the HEPLAB toolbox (Perakakis, 2019), with manual correction of mis-detected peaks (Al et al., 2021; Zaccaro et al., 2022). EEG data were epoched from -2 to 2 s around each R-peak (Kern et al., 2013). Epochs were averaged within participants for each task and were further classified based on the respiratory phase in which the corresponding R-peak occurred. This resulted in four epoch bins: HCT inhalation and exhalation, and C-TCT inhalation and exhalation. The average number of heartbeats per participant (mean ±SD) was as follows: HCT – inhalation (315.86 ± 73.83) and exhalation (273.71 ± 76.48); C-TCT – inhalation (334.82 ± 52.12) and exhalation (297.96 ± 53.01). At the group level, a greater number of heartbeats was observed during inhalation than exhalation in both tasks, likely reflecting the higher heart rate (HR) during inhalation associated with respiratory sinus arrhythmia. This difference was significant

for both HCT (inhalation vs. exhalation: $t_{27} = 3.00$, $p = 0.006$, $d = 0.57$) and C-TCT ($t_{27} = 3.33$, $p = 0.003$, $d = 0.63$).

### 2.5 Heartbeat-modulated cortical oscillations

Heartbeat-modulated cortical oscillations were calculated using the FieldTrip toolbox (version 20231025; Oostenveld et al., 2011) according to established procedures (Park et al., 2018). Time-frequency analysis was performed on the time-series data for each experimental condition. For each trial, we convolved the signal with a complex wavelet constructed by pointwise multiplying the real cosine and imaginary sine components at each frequency with a Hann taper. Both the data and the tapered wavelet were then Fourier transformed, and their element-wise multiplication in the frequency domain, followed by an inverse Fourier transform, yielded the convolution in the time domain. A sliding window with a Hann taper was used, maintaining a constant number of cycles per time window for all frequencies (4 cycles per time window). Zero padding was applied to round the maximum trial length to the nearest power of 2. Power was then extracted from the resulting complex representation by computing the squared magnitude of the signal. Time-frequency analysis was performed on each EEG channel from 1 Hz to 45 Hz, with a step size of 0.5 Hz, and from -1.5 s to 2 s after the R-peak, with steps of 0.01 s. The mean power value of the pre-R-peak time window (-300 ms to -100 ms) was designated as the baseline and used to normalize the post-R-peak power values in each frequency bin (relative heartbeat-modulated power; Park et al., 2018). This baseline normalization was intended to prevent smearing of post-R-peak activity into baseline and to mitigate the potential influence of CFA around the ECG P-wave (Park et al., 2018).

To compute heartbeat-modulated inter-trial coherence (ITC), we first normalized the complex Fourier coefficients by their magnitude to focus on the phase information. To derive the average ITC, the resulting phase information was summed and normalized by the number of trials. ITC reflects the consistency of phase across multiple trials at different times and frequencies, with values ranging from 0 to 1, with higher values indicating more consistent phase alignment across trials. Similar to

power values, we used the baseline window to normalize ITC values (relative heartbeat-modulated ITC; Park et al., 2018). To remove components reflecting PA and its harmonics, we excluded frequency bands below 4 Hz (Kern et al., 2013; Park et al., 2018).

To extract the heartbeat-modulated functional connectivity (FC), we computed the complex Fourier spectra from 1 Hz to 45 Hz (all settings were the same as for power calculation). Fourier spectra were calculated between -300 and -100 ms before the R-peak (baseline) and between 300 and 600 ms after the R-peak (active period of heartbeat effects; Liuzzi et al., 2024; Zaccaro et al., 2024). The imaginary part of coherency (iCOH) was used as a measure of undirected FC between electrodes in the sensor space, resulting in a connectivity matrix between all pairs of electrodes. The iCOH suppresses spurious coherence due to electromagnetic field propagation, which is indicated by zero-phase synchronization between sensors (Nolte et al., 2004). We hypothesized that FC would change in the theta (4-8 Hz) and alpha (8-13 Hz) bands, according to previous studies (Fló et al., 2024; Kern et al., 2013; Kim & Jeong, 2019). Correlation matrices were calculated across trials, resulting in a correlation matrix for each participant, task (HCT and C-TCT), cardiac time window (baseline and active), respiratory phase (inhalation and exhalation), and frequency band (alpha and theta). To assess heartbeat-modulated FC, we calculated the ratio of connectivity during the active cardiac time window to that of the baseline cardiac time window (relative heartbeat-modulated FC).

To extract undirected graph theory metrics, we thresholded the iCOH matrices using a proportional threshold that preserves a percentage of the strongest matrix weights (Perl et al., 2019). In graph theory, a network is represented by nodes (each EEG channel) and edges indicating the strength of the connection (the iCOH values for each pair of EEG channels). We used six incremental thresholds ranging from 5 % to 30 % as cutoffs (e.g., a threshold of 5 % means that out of 100 nodes, each node is connected to five other nodes on average; Perl et al., 2019). All edges that did not reach the threshold were removed. We extracted the following network connectivity measures for each participant, threshold, task, cardiac time window, respiratory phase, and frequency band using the brain connectivity toolbox (Rubinov & Sporns, 2010): i) density: the ratio of current connections to

all possible connections, reflecting the overall interconnectivity of the network; ii) clustering coefficient: the ratio of triangles formed around each node, illustrating the degree of dense interconnectivity among neighbouring nodes; iii) global efficiency: a measure of network integration that reflects the network's ability to facilitate long-range information transfer; and iv) local efficiency: a measure of the network's capacity to support short-range information transfer and its resilience to incremental disconnections.

**2.6 Statistical analyses of heartbeat-modulated cortical oscillations**

Changes in heartbeat-modulated cortical oscillations were assessed using the FieldTrip toolbox (v.20231025; Oostenveld et al., 2011). The analysis focused on the cluster mass rather than individual electrodes or time points. Initially, spatial (neighbouring channels) and temporal (adjacent time points) points with a p-value below 0.05 were included in a cluster. A cluster statistic was calculated by summing the t-values within each cluster. The null distribution was estimated by Monte Carlo permutations, with condition labels randomly shuffled 5000 times. The largest cluster-level statistic from each randomization was included in the null distribution. Statistical significance was determined by comparing the experimentally observed cluster-level statistics with the randomly generated null distribution. Clusters exceeding the 1 - α percentile of this distribution (two-tailed) were considered significant. The minimum number of adjacent channels required to form a cluster was set to 2. To test for interaction effects, we used the permutation of residuals method (Anderson & Braak, 2003; Still & White, 1981; Winkler et al., 2014). For instance, to test the 2×2 interaction (task×respiratory phase), we calculated the difference between the two levels of phase for each level of task and conducted paired cluster-based permutation t-tests comparing difference values (HCT-exhalation minus HCT-inhalation vs. C-TCT-exhalation minus C-TCT-inhalation). Based on Zaccaro et al. (2024), tests were performed at each electrode and time point for the whole late time window (300-600 ms) following the R-peak. We tested each frequency band of interest separately, averaging over their respective frequency bins: theta (4-8 Hz), alpha (8-13 Hz), beta (13-30 Hz), and low-gamma (30-45 Hz). We

excluded external electrodes (F7, F8, FT7, FT8, T7, T8, TP7, TP8, P7, P8, PO7, PO8, O1, O2, Oz, TP9, and TP10), which are prone to noise contamination, in line with a recent meta-analysis (Coll et al., 2021). Cluster-based permutation t-tests were conducted on the time-frequency data, with heartbeat-modulated power and ITC values as dependent variables. Even in the absence of significant task × phase interactions, we conducted exploratory planned comparisons to specifically test exhalation versus inhalation differences within each task (HCT: exhalation versus inhalation; C-TCT: exhalation versus inhalation), as motivated by our previous findings (Zaccaro et al., 2024). As cluster-based permutation testing intrinsically controls for multiple comparisons across the time × electrode space, we applied an additional Benjamini-Yekutieli false discovery rate (FDR) correction only across the theta and alpha frequency bands, which constituted our a priori hypotheses. Importantly, as respiratory-phase effects were theoretically expected only during interoceptive processing (HCT), FDR correction was restricted to these two planned contrasts (HCT exhalation vs. inhalation for alpha; HCT exhalation vs. inhalation for theta). Analyses in the beta and gamma bands, as well as all comparisons within the C-TCT, were conducted for completeness but were considered exploratory and therefore not corrected for multiple comparisons.

To examine the interaction effects between tasks and respiratory phases on heartbeat-modulated FC, we applied the same permutation-of-residuals method used for power and ITC. We excluded from the FC analysis the same external electrodes omitted in the power and ITC analyses, as they are particularly susceptible to noise contamination. Relative iCOH values between electrode pairs for each frequency band (theta and alpha) were used as the dependent variable. Planned permutation-based t-tests were performed for both the theta and alpha bands, comparing HCT exhalation vs. HCT inhalation, and C-TCT exhalation vs. C-TCT inhalation. Significance was assessed using a single-threshold permutation test for the maximum t-statistics (5000 permutations). Connectivity values showing a significant effect with a p-value $\leq 0.01$ (uncorrected) were used to construct symmetric connectivity matrices for theta and alpha using the BrainNet Viewer toolbox (Xia et al., 2013).

Undirected graph connectivity metrics were analyzed using a series of linear mixed-effects models (LMEMs), implemented in jamovi (v2.3.21; GAMLj module; Gallucci, 2019) with restricted maximum likelihood (REML) estimation. Separate models were estimated for the theta and alpha frequency bands. Fixed factors included task (HCT, C-TCT), respiratory phase (inhalation, exhalation), cardiac time window (baseline, active), and threshold (5%, 10%, 15%, 20%, 25%, 30%). Degrees of freedom were estimated using the Satterthwaite method. For each graph-theory metric, the full model included a three-way interaction (task × time × phase), with subject-specific random intercepts and random slopes for the interaction terms. Even in the absence of a significant three-way interaction, we conducted exploratory planned contrasts to probe condition-specific effects that may not be detectable at the omnibus level. Planned pairwise t-tests were computed separately for each task and respiratory phase. To control for multiple comparisons, we applied FDR correction across the eight planned contrasts within each frequency band (four contrasts in HCT and four in C-TCT, considered separately for the alpha and theta bands). Specifically, we tested the following comparisons: (i) baseline inhalation versus baseline exhalation, (ii) active inhalation versus active exhalation, (iii) baseline versus active during inhalation, and (iv) baseline versus active during exhalation, each assessed within both the HCT and C-TCT.

### 2.7 Correlational and mixed-effects analyses of heartbeat-modulated EEG activity and interoceptive performance

Based on prior research (Crivelli & Balconi, 2025; Kritzman et al., 2022; Luft & Bhattacharya, 2015; Rominger et al., 2025; Villena-González et al., 2017), we assessed relationships between changes in HEP amplitude across respiratory phases and corresponding differences in heartbeat-modulated alpha power during HCT. Single-trial epochs around each R peak (from -300 to 600 ms) were filtered between 0.5 and 3 Hz (Studenova et al., 2023). To assess the spatial overlap between the distributions of significant heartbeat-modulated alpha power and HEP amplitude changes across respiratory phases, a full-scalp cluster-based permutation t-test was performed, using HEP amplitude as the

dependent variable, comparing inhalation and exhalation in the late time window (300-600 ms after the R-peak; Zaccaro et al., 2024). HEP amplitude and heartbeat-modulated alpha power values were averaged for each participant, and Δ values between respiratory phases were extracted. Mean values were obtained by averaging across the time windows that previously showed significant power differences between respiratory phases. We computed Spearman's rho and p-values for each channel ($\alpha = 0.05$, two-tailed) by correlating participant-level mean heartbeat-modulated Δalpha power with the corresponding mean ΔHEP values. We applied the FDR correction procedure to control for multiple comparisons across channels. The analysis was repeated for other frequency bands during both HCT and C-TCT, and we also assessed correlations between ΔHEP amplitude and ΔITC, as well as between Δpower and ΔITC across all frequency bands. Finally, we examined correlations between HEP, power, and ITC across all frequency bands during HCT and C-TCT by analyzing their absolute values, rather than Δ values. We then computed the instantaneous group-level correlation between Δalpha power and the corresponding ΔHEP values for each time point and frequency bin, yielding a time-frequency representation of Spearman's rho and p-values ($\alpha = 0.05$, two-tailed). The analysis focused on channels that had previously shown a significant participant-level correlation between ΔHEP amplitude and Δalpha power. We compared instantaneous correlations between HCT and C-TCT by applying Fisher's z-normalization to Spearman's rho values averaged across the previously selected channels. Statistical significance at each time point was determined using the cumulative distribution function of the standard normal distribution to evaluate the probability of observing extreme z-differences under the null hypothesis. We applied the FDR correction procedure to control for multiple comparisons across time points.

To examine the relationships between HCT/C-TCT trial-level changes in HEP, heartbeat-modulated power and ITC across respiratory phases, as well as their associations with accuracy and cardiac physiology, we applied multiple LMEMs. For each HCT and C-TCT trial (12 trials per participant per task), we computed the changes across respiratory phases (Δ) in HEP, heartbeat-modulated power, and ITC within the alpha band, along with accuracy and confidence. HCT/C-TCT trial-level Δ values

were derived by first extracting the mean values from significant channels and time windows during exhalation and inhalation and then calculating the Δ (exhalation minus inhalation). To account for the influence of cardiac physiology, we also computed ΔHR, which was derived by subtracting the HCT/C-TCT trial-level mean HR during inhalation from that during exhalation.

As an additional control, we modelled instantaneous HR as a covariate in the LMEMs to quantify its contribution to heartbeat-modulated power. Heartbeat-modulated alpha and theta power were computed on a trial-by-trial basis by averaging the significant channels and time points identified in the group-level contrasts. Specifically, we extracted heartbeat-modulated alpha power from the task × respiratory-phase interaction, and heartbeat-modulated alpha and theta power from the exhalation-inhalation contrast during the HCT.

All LMEMs were implemented using the GAMLj module in jamovi (v2.3.21; the jamovi project, 2022; Gallucci, 2019), with REML estimation. For each analysis, we started from a model with the full fixed-effects structure dictated by our experimental design and an initially maximal random-effects structure (random intercepts and slopes). We then simplified the random-effects structure in a stepwise manner by iteratively removing random components that either led to non-convergence or did not improve model fit (as assessed by a reduction of the Akaike information criterion, AIC). The final models retained the full fixed-effects structure and a parsimonious random-effects structure that ensured convergence and adequate fit. The dependent variables were z-scored prior to modelling, and the instantaneous HR covariate was z-scored within participants (clusterwise centering) to preserve within-subject variability. Degrees of freedom were estimated using the Satterthwaite method. For each parameter of the best-fitting model, we reported the estimated coefficient (b), standard error (SE), 95 % confidence intervals, t-statistic, and p-value.

## 3. Results

### 3.1 Main findings

#### 3.1.1 Task-and respiratory phase-dependent changes in heartbeat-modulated power

Following an eyes-open resting-state condition, participants engaged in tasks requiring either cardiac interoceptive (heartbeat counting task - HCT) or exteroceptive (cardiac-tone counting task - C-TCT) attention. We performed a full-scalp cluster-based permutation test using heartbeat-modulated power as dependent variable and task (HCT vs. C-TCT), respiratory phase (inhalation vs. exhalation), and their interaction as within-participant factors. The test revealed a significant task × phase interaction in the alpha band from 300 to 600 ms over electrodes C4, C6, CP4, and CP6 ($t_{27}$ = 3.165, $p_{clust}$ = 0.037, d = 0.598), but no interaction in the theta band ($t_{27}$ = 1.933, $p_{clust}$ = 0.14, d = 0.365). The interaction was explained by planned t-test, which showed significantly higher heartbeat-modulated alpha power during HCT from 391 to 600 ms over FCz, FC2, FC4, Cz, C2, C4, C6, CP2, CP4, and CP6 ($t_{27}$ = 3.049, $p_{clust}$ = 0.039, $p_{FDR}$ = 0.039, d = 0.576; Fig. 1A) during exhalation compared to inhalation. Despite the absence of a significant task × phase interaction in the theta band, an exploratory planned comparison (see Section 2.6) revealed increased heartbeat-modulated theta power during exhalation than inhalation from 300 to 469 ms after the R-peak over F6, FC4, FC6, Cz, C2, C4, C6, CP3, CP1, CPz, CP2, and P1 ($t_{27}$ = 3.896, $p_{clust}$ = 0.039, $p_{FDR}$ = 0.039, d = 0.736). No significant interaction was observed in other frequency bands, which were exploratory and are reported for completeness (beta: $t_{27}$ = 1.714, $p_{clust}$ = 0.122, d = 0.324; gamma: $t_{27}$ = -0.525, $p_{clust}$ = 0.276, d = 0.099). No significant differences were found between respiratory phases for beta ($t_{27}$ = 0.793, $p_{clust}$ = 0.343, d = 0.149) or gamma ($t_{27}$ = -1.375, $p_{clust}$ = 0.264, d = 0.259) bands. During C-TCT, we found no change in heartbeat-modulated power between exhalation and inhalation in any of the investigated frequency bands (theta: $t_{27}$ = 0.261, $p_{clust}$ = 1, d = 0.049; alpha: $t_{27}$ = -0.448, $p_{clust}$ = 1, d = 0.085; beta: $t_{27}$ = -2.661, $p_{clust}$ = 0.09, d = 0.503; gamma: $t_{27}$ = 1.659, $p_{clust}$ = 0.052, d = 0.314; Fig. 1B). A subsampling-based sensitivity analysis confirmed that the observed task-by-phase effects were not driven by differences in heartbeat counts across respiratory phases. These results suggest that

heartbeat-modulated alpha and theta power only increase during exhalation when attention is focused on internal cardiac signals. By contrast, no respiratory phase-dependent modulation emerged during the exteroceptive task.

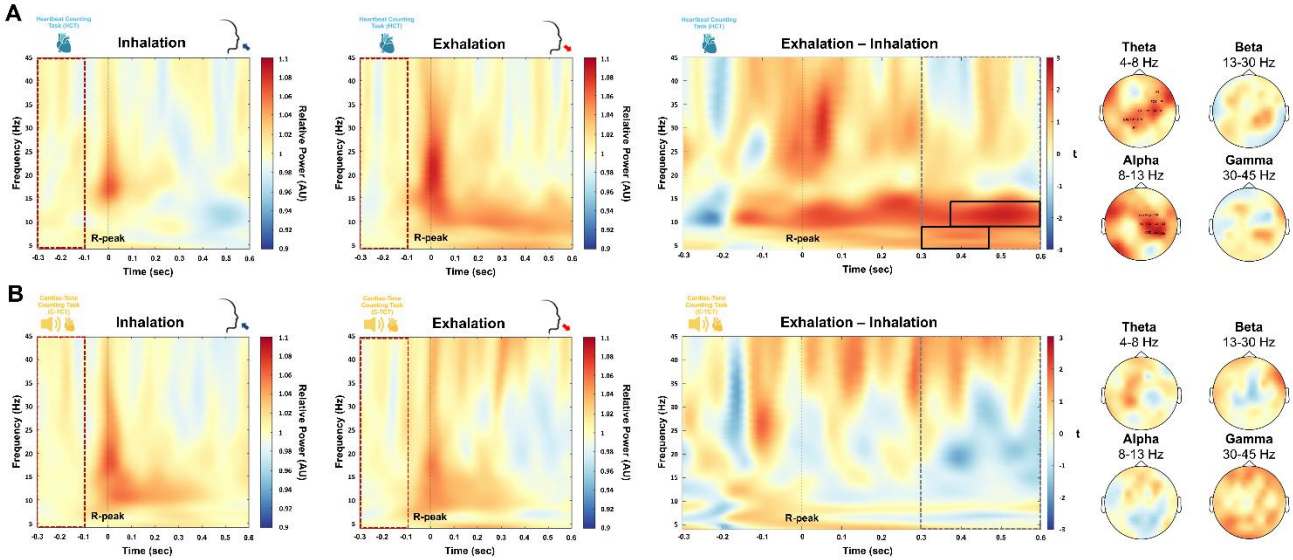



**Figure 1. Heartbeat-modulated power changes across respiratory phases and tasks. A)** Grand-averaged heartbeat-modulated power in the heartbeat counting task during inhalation (left), exhalation (middle), and the exhalation-minus-inhalation difference (right). The black rectangle marks significant differences between exhalation and inhalation (cluster-corrected). Topographical distributions illustrate differences, with labels indicating significant electrodes. **B)** Grand-averaged heartbeat-modulated power in the cardiac-tone counting task during inhalation (left), exhalation (middle), and the exhalation-minus-inhalation difference (right). The red dotted area represents the baseline window (-300 to -100 ms relative to R-peak onset). The grey dotted area marks the temporal window of interest for statistical analysis (300-600 ms after the R-peak). Abbreviations: AU = arbitrary unit.

### 3.1.2 Task- and respiratory phase–dependent changes in heartbeat-modulated inter-trial coherence

We performed a full-scalp cluster-based permutation test using heartbeat-modulated inter-trial coherence (ITC) as dependent variable and task (HCT vs. C-TCT), respiratory phase (inhalation vs. exhalation), and their interaction as within-participant factors. No significant task × phase interaction was observed for ITC in any of the frequency bands (theta: $t_{27} = 0.129$, $p_{clust} = 0.132$, $d = 0.024$; alpha: $t_{27} = 2.104$, $p_{clust} = 0.072$, $d = 0.398$; beta: $t_{27} = 0.934$, $p_{clust} = 0.432$, $d = 0.177$; gamma: $t_{27} = 2.223$,

$p_{clust}$ = 0.347, d = 0.421). We conducted exploratory planned comparisons to specifically test exhalation versus inhalation differences within the HCT in theta and alpha bands (see Section 2.6). We found a significant increase in alpha-band heartbeat-modulated ITC during exhalation compared to inhalation from 422 to 559 ms after the R-peak over C2, C4, CP2, CP4, and CP6 ($t_{27}$ = 3.238, $p_{clust}$ = 0.023, $p_{FDR}$ = 0.046, d = 0.612; Fig. 2A), but no changes in the theta band ($t_{27}$ = 0.229, $p_{clust}$ = 1, $p_{FDR}$ = 1, d = 0.043). For completeness, we also report a significant increase in gamma band ITC from 441 to 469 ms over C3, C5, CP3, CP5, and P5 ($t_{27}$ = 3.825, $p_{clust}$ = 0.038, d = 0.723). However, this effect was brief (28 ms) and localized over electrodes not typically associated with cardiac interoception (Coll et al., 2021). No significant ITC differences between respiratory phases were found for the other frequency bands (beta: $t_{27}$ = 0.629, $p_{clust}$ = 0.345, d = 0.119). Similarly, no phase-related ITC changes were observed during the C-TCT across all frequency bands (theta: $t_{27}$ = 0.013, $p_{clust}$ = 1, d = 0.003; alpha: $t_{27}$ = 0.256, $p_{clust}$ = 0.186, d = 0.048; beta: $t_{27}$ = -0.669, $p_{clust}$ = 1, d = 0.127; gamma: $t_{27}$ = 0.324, $p_{clust}$ = 0.289, d = 0.061; Fig. 2B). A subsampling-based sensitivity analysis confirmed that the observed phase effects were not driven by differences in heartbeat counts across respiratory phases. These tests were exploratory and uncorrected for multiple comparisons, and are reported for completeness. Overall, heartbeat-modulated ITC was selectively shaped by respiratory phase in the alpha range during interoceptive attention, while no corresponding modulation was observed during the exteroceptive task.

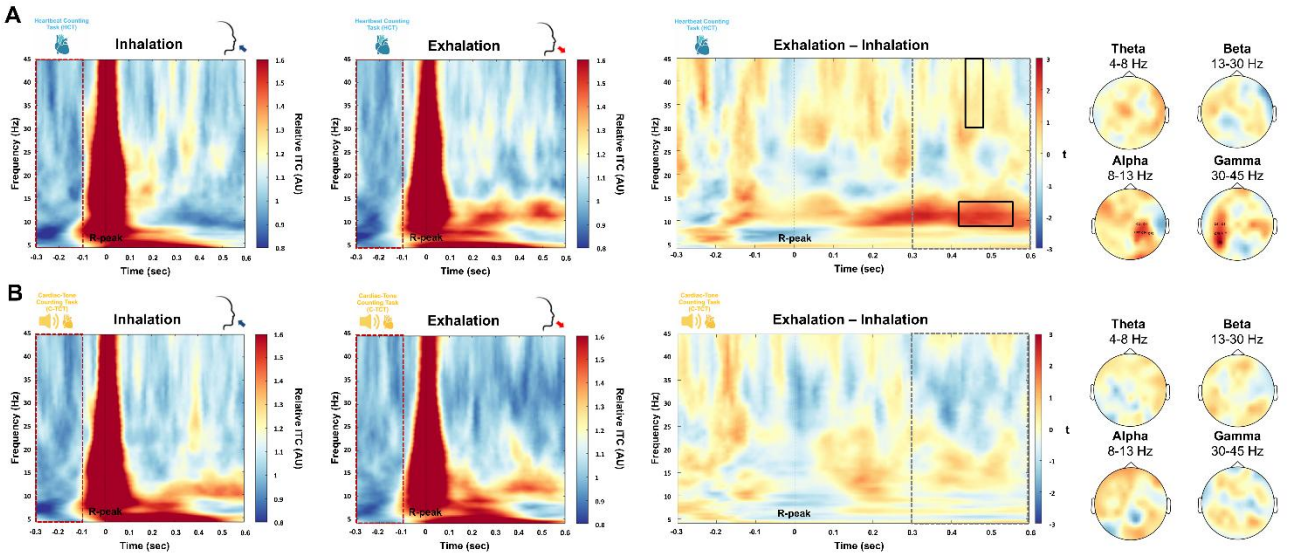



**Figure 2. Heartbeat-modulated inter-trial coherence changes across respiratory phases and tasks. A)** Grand-averaged heartbeat-modulated inter-trial coherence in the heartbeat counting task during inhalation (left), exhalation (middle), and the exhalation-minus-inhalation difference (right). The black rectangle marks significant differences between exhalation and inhalation (cluster-corrected). Topographical distributions illustrate differences, with labels indicating significant electrodes. **B)** Grand-averaged heartbeat-modulated inter-trial coherence in the cardiac-tone counting task during inhalation (left), exhalation (middle), and the exhalation-minus-inhalation difference (right). The red dotted area represents the baseline window (-300 to -100 ms relative to R-peak onset). The grey dotted area marks the temporal window of interest for statistical analysis (300-600 ms after the R-peak). Abbreviations: ITC = inter-trial coherence, AU = arbitrary unit.

### 3.1.3 Heartbeat-modulated oscillations and heartbeat-evoked potentials

We assessed the spatial overlap between the distributions of significant heartbeat-modulated alpha power and heartbeat-evoked potential (HEP) amplitude changes across respiratory phases (Δalpha power and ΔHEP). As previously reported (Zaccaro et., 2024), significant ΔHEP changes were localized to right centro-frontal electrodes (AFz, F1, Fz, F2, F4, FC1, FCz, FC2, FC4, C1, Cz, C2, and C4) from 360 to 528 ms after the R-peak ($t_{27} = 3.29$, $p_{clust} = 0.016$, $d = 0.621$; Fig. 3A). Although ΔHEP differences occurred in more anterior regions of the scalp compared to the more central Δalpha power differences (same cluster as in Section 3.1.1; Fig. 3B), both distributions converged spatially in fronto-central areas, slightly lateralized to the right hemisphere. To statistically quantify this relationship, we computed Spearman's correlation between participant-level mean heartbeat-modulated Δalpha power with the corresponding mean ΔHEP values within the late significant time

window of heartbeat-modulated power effects (390-600 ms after the R-peak). A significant positive correlation was found over frontal electrodes (Fig. 3C), including AFz (rho = 0.519, $p_{FDR}$ = 0.044), AF3 (rho = 0.521, $p_{FDR}$ = 0.044), AF4 (rho = 0.522, $p_{FDR}$ = 0.044), F4 (rho = 0.577, $p_{FDR}$ = 0.038), and Fz (rho = 0.573, $p_{FDR}$ = 0.038). A negative correlation was also observed over channel P6 (rho = -0.512, $p_{FDR}$ = 0.044). When examining correlations between ΔHEP amplitude and heartbeat-modulated Δpower in other frequency bands during both HCT and C-TCT, no significant results were found, confirming that the effects were specific to the alpha band during HCT. Additionally, no significant correlations were observed between ΔHEP amplitude and ΔITC, nor between Δpower and ΔITC across any frequency band in either task (during HCT or C-TCT). Finally, no correlations were found between HEP, power, or ITC in any frequency band when analyzing their absolute values recorded separately for inhalation and exhalation in either task.

We then computed the instantaneous group-level Spearman's correlation between heartbeat-modulated Δpower and the corresponding ΔHEP values for each time point and frequency band, averaged across the previously identified channels (AFz, AF3, AF4, F4, and Fz), during both the HCT and C-TCT tasks. A significant correlation emerged in the alpha band exclusively during HCT, within a late time window from 422 to 600 ms post-R-peak (Fig. 3D, E). We compared instantaneous correlations between HCT and C-TCT by applying Fisher's z-transformation to Spearman's rho values averaged across the previously selected channels in the alpha band. This analysis revealed significantly stronger correlations for HCT relative to C-TCT between 512 and 600 ms post-R-peak (Fig. 3F). Together, these findings indicate that the coupling between ΔHEP amplitude and heartbeat-modulated Δalpha power is selectively enhanced during cardiac interoceptive attention.

### 3.1.4 Heartbeat-modulated oscillations and task accuracy

To examine the relationships between HCT trial-level changes in HEP and heartbeat-modulated alpha power and ITC across respiratory phases, as well as their associations with accuracy, we applied multiple linear mixed-effects models (LMEMs). Following previous studies (Fló et al., 2024; Park et

al., 2018), we first tested the relationship between changes in heartbeat-modulated alpha power and ITC across respiratory phases and confirmed that no significant relationship was found between the two measures (b = 0.022, SE = 0.056, CI 95% = [-0.087 0.132], t = 0.399, p = 0.69). Using ΔHEP as the dependent variable, the model revealed a significant interaction between Δalpha power and Δalpha ITC (b = 0.118, SE = 0.056, CI 95% = [0.008 0.229], t = 2.096, p = 0.037; Fig. 3G), suggesting that Δalpha power moderates the effects of Δalpha ITC on ΔHEP. A simple effects analysis of the interaction indicated a significant relationship between Δalpha ITC and ΔHEP only when Δalpha power was high (mean + 1SD: b = 0.18, SE = 0.079, CI 95% = [0.026 0.335], t = 2.294, p = 0.023). No main effects were observed for Δalpha power or Δalpha ITC. Notably, no significant effects involving ΔHR were found (b = 0.015, SE = 0.059, CI 95% = [-0.101 0.132], t = 0.258, p = 0.797).

When we used the HCT trial-level accuracy as the dependent variable, the model revealed a significant three-way interaction between ΔHEP, Δalpha power, and confidence (b = 0.084, SE = 0.032, CI 95% = [0.021 0.147], t = 2.603, p = 0.009; Fig. 3H), indicating that changes in alpha power and confidence together moderated the effect of ΔHEP on task accuracy. Simple effects analysis showed a significant relationship between ΔHEP and accuracy only when both Δalpha power and confidence were high (mean + 1SD: b = 0.129, SE = 0.052, CI 95% = [0.028 0.232], t = 2.503, p = 0.013). Additionally, significant main effects were observed for confidence (b = 0.352, SE = 0.077, CI 95% = [0.202 0.503], t = 4.578, p < 0.001) and Δalpha power (b = -0.064, SE = 0.031, CI 95% = [-0.126 -0.003], t = -2.041, p = 0.042) on accuracy. No other main effects or significant interactions were found. Notably, no effect of ΔHR on accuracy (b = 0.029, SE = 0.044, CI 95% = [-0.056 0.115], t = 0.686, p = 0.493) was found (Fig. 3I).

Performing an LMEM for C-TCT with ΔHEP as the dependent variable was not feasible due to insufficient random coefficient variance. A general linear model revealed no significant interaction between Δalpha power and Δalpha ITC (b = -0.112, SE = 0.062, CI 95% = [-0.233 0.009], t = -1.815, p = 0.071), nor any main effects for Δalpha power (b = 0.003, SE = 0.058, CI 95% = [-0.111 0.117], t = 0.046, p = 0.964) or Δalpha ITC (b = 0.004, SE = 0.058, CI 95% = [-0.11 0.118], t = 0.066, p =

0.947). No role of ΔHR was observed (b = 0.092, SE = 0.057, CI 95% = [-0.021 0.205], t = 1.6, p = 0.111). Finally, using the trial-level C-TCT accuracy as the dependent variable, the model indicated that only confidence (b = 0.347, SE = 0.093, CI 95% = [0.165 0.528], t = 3.737, p = 0.002) significantly predicted task accuracy. Again, no role of ΔHR emerged (b = 0.075, SE = 0.064, CI 95% = [-0.052 0.201], t = 1.59, p = 0.251).

Collectively, these results demonstrate selective coupling between HEPs and heartbeat-modulated alpha power during interoceptive attention, particularly in the late post-R-peak interval. Importantly, these associations occurred exclusively within the alpha band, only during interoceptive attention, and were driven by respiratory phase-dependent differences and not by absolute amplitude changes. This pattern rules out trivial mathematical or preprocessing artifacts and points to a mechanism specific to the task and physiological state. Moreover, when confidence was high, alpha-related modulation of HEPs predicted interoceptive accuracy, suggesting that coordinated cortical processing of cardiac signals supports accurate perception of internal bodily sensations during exhalation. Notably, HR did not explain these effects. Additional analyses on cardiac and respiratory contributions are presented in the following section.

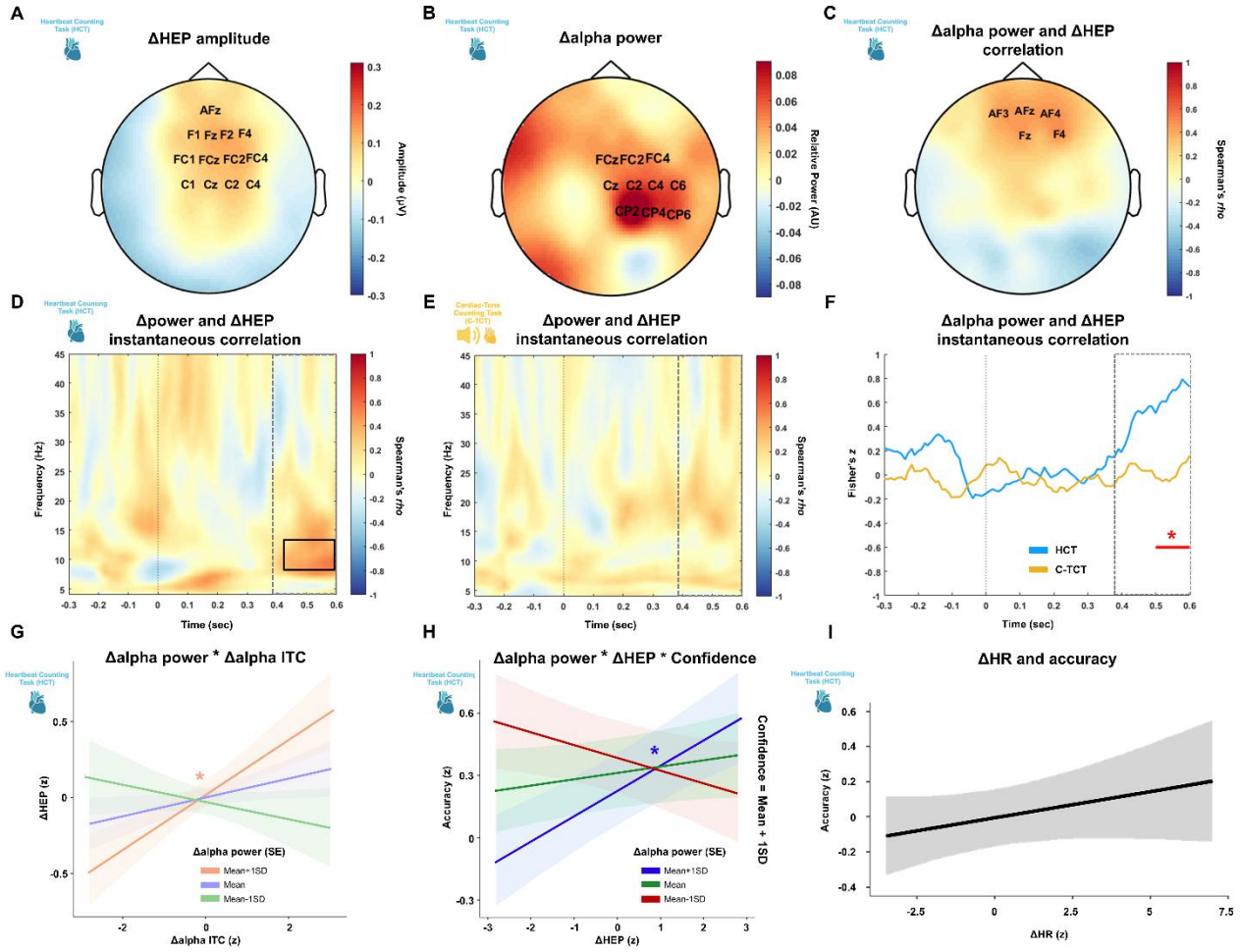



**Figure 3. Relationships between heartbeat-modulated cortical oscillations, heartbeat-evoked potentials, and task performance. A)** Topographical distribution of HEP differences between exhalation and inhalation during HCT. **B)** Topographical distribution of heartbeat-modulated alpha power differences between exhalation and inhalation during HCT. **C)** Topographical distribution of the Spearman correlation between ΔHEP and Δalpha power across channels during HCT. Labels indicate significant electrodes. **D-E)** Time-frequency representations of the instantaneous Spearman correlation between Δpower and ΔHEP during HCT (D) and the C-TCT (E). The grey dotted region marks the temporal window of interest for statistical analysis (390-600 ms post R-peak), and the black rectangle indicates significant differences (FDR-corrected). **F)** Fisher's z-transformed instantaneous Spearman correlation values (alpha band) comparing HCT and C-TCT. Asterisks indicate significant differences (*$p < 0.05$, FDR-corrected). **G)** Linear mixed-effects model showing that the relationship between Δalpha ITC and ΔHEP was moderated by Δalpha power during HCT. Asterisks indicate significant effects (*$p < 0.05$). **H)** Linear mixed-effects model demonstrating that the interaction between Δalpha power, ΔHEP, and confidence predicted interoceptive accuracy during HCT. **I)** Linear mixed-effects model showing that changes in heart rate (ΔHR) did not predict interoceptive accuracy during HCT. Abbreviations: HEP = heartbeat-evoked potential, ITC = inter-trial coherence, HCT = heartbeat counting task, C-TCT = cardiac-tone counting task, ECG = electrocardiogram, SD = standard deviation, SE = standard error, AU = arbitrary unit.

### 3.2 Control analyses addressing physiological and respiratory confounds

#### 3.2.1 Resting-state and task-level comparisons (without respiratory phase)

To determine whether heartbeat-modulated cortical oscillations varied across respiratory phases during the resting-state, we conducted full-scalp cluster-based permutation tests comparing inhalation to exhalation. Across all frequency bands, we found no significant differences in heartbeat-modulated power (theta: $t_{27} = 2.085$, $p_{clust} = 0.097$, $d = 0.394$; alpha: $t_{27} = 0.013$, $p_{clust} = 0.989$, $d = 0.003$; beta: $t_{27} = 0.089$, $p_{clust} = 0.929$, $d = 0.017$; gamma: $t_{27} = 2.12$, $p_{clust} = 0.15$, $d = 0.401$) or ITC (theta: $t_{27} = -0.915$, $p_{clust} = 0.369$, $d = 0.173$; alpha: $t_{27} = -2.381$, $p_{clust} = 0.096$, $d = 0.45$; beta: $t_{27} = 1.161$, $p_{clust} = 0.178$, $d = 0.219$; gamma: $t_{27} = 1.46$, $p_{clust} = 0.156$, $d = 0.276$). Similarly, when not accounting for respiratory phases (i.e., averaging heartbeats occurring during both inhalation and exhalation), we observed no significant differences between HCT and C-TCT in heartbeat-modulated power (theta: $t_{27} = 0.162$, $p_{clust} = 0.872$, $d = 0.031$; alpha: $t_{27} = -0.163$, $p_{clust} = 0.872$, $d = 0.031$; beta: $t_{27} = 0.718$, $p_{clust} = 0.108$, $d = 0.136$; gamma: $t_{27} = 0.129$, $p_{clust} = 0.899$, $d = 0.024$) or ITC (theta: $t_{27} = -1.4$, $p_{clust} = 0.174$, $d = 0.264$; alpha: $t_{27} = -2.28$, $p_{clust} = 0.215$, $d = 0.431$; beta: $t_{27} = 1.12$, $p_{clust} = 0.075$, $d = 0.212$; gamma: $t_{27} = 1.7$, $p_{clust} = 0.359$, $d = 0.322$). These findings suggest that heartbeat-modulated cortical oscillations are not linked to the respiratory cycles at rest. Furthermore, they suggest that cardiac interoceptive and exteroceptive attention tasks elicit similar changes in heartbeat-modulated power and ITC when respiratory phases are not taken into account.

#### 3.2.2 Controlling for heart rate

To examine whether modulation of heartbeat-modulated responses varied as a function of cardiac physiology, we first assessed changes in instantaneous HR across tasks and respiratory phases. The LMEM revealed significant main effects of phase ($b = -0.338$, $SE = 0.032$, CI 95% [-0.401 -0.275], $t = -10.45$, $p < 0.001$) and task ($b = 0.153$, $SE = 0.051$, CI 95% [0.053 0.253], $t = 3.00$, $p = 0.006$), but no task × phase interaction ($b = 0.031$, $SE = 0.032$, CI 95% [-0.032 0.094], $t = 0.96$, $p = 0.348$).

Overall, HR was lower during exhalation than inhalation and during interoceptive relative to exteroceptive attention.

We then quantified the extent to which instantaneous HR accounted for the task × phase modulation of heartbeat-modulated alpha power. The LMEM confirmed a significant task × phase interaction (b = -0.040, SE = 0.019, CI 95% [-0.078 -0.003], t = -2.11, p = 0.035). No additional main effects or interactions reached significance, including HR (b = -0.001, SE = 0.007, CI 95% [-0.015 0.012], t = -0.21, p = 0.835), task × HR (b = -0.024, SE = 0.014, CI 95% [-0.050 0.003], t = -1.75, p = 0.080), phase × HR (b = 0.005, SE = 0.013, CI 95% [-0.021 0.032], t = 0.40, p = 0.691), or the task × phase × HR interaction (b = 0.044, SE = 0.027, CI 95% [-0.008 0.097], t = 1.65, p = 0.099).

Finally, we estimated the contribution of instantaneous HR within the HCT, separately for the alpha and theta frequency bands. For theta power, the LMEM replicated the significant main effect of respiratory phase (b = 0.027, SE = 0.01, CI 95% = [0.007 0.047], t = 2.645, p = 0.008). In contrast, neither the main effect of instantaneous HR (b < 0.001, SE = 0.007, CI 95% = [-0.014 0.015], t = 0.083, p = 0.934) nor the phase × HR interaction (b = -0.009, SE = 0.015, CI 95% = [-0.037 0.019], t = -0.593, p = 0.553) reached significance. For alpha power, the LMEM replicated the significant main effect of respiratory phase (b = 0.038, SE = 0.017, CI 95% = [0.005 0.071], t = 2.238, p = 0.025). Again, neither the main effect of instantaneous HR (b = -0.005, SE = 0.014, CI 95% = [-0.032 0.022], t = -0.374, p = 0.709) nor the phase × HR interaction (b = 0.009, SE = 0.024, CI 95% = [-0.039 0.056], t = 0.35, p = 0.726) were significant. Taken together, these analyses show that although HR varies systematically across tasks and respiratory phases, such fluctuations do not account for the observed task × phase modulation of heartbeat-modulated power.

### 3.2.3 Controlling for the cardiac field artifact

We verified that changes in alpha and theta heartbeat-modulated power did not reflect an artificial increase induced by cardiac field artifact (CFA) changes by testing the interaction between tasks and respiratory phases on the time-frequency decomposed ECG signal, time-locked to the R-peak (Daoui

et al., 2022; Tsutsumi et al., 2014). This was done using a repeated-measures, FDR-corrected two-tailed t-test within the time window and frequency bands where significant effects were observed. We first tested the task × phase interaction from 300 to 600 ms over the time-frequency decomposed averaged ECG signal and found no significant effects in either frequency band (theta: $t_{27}$ = -1.258, $p_{FDR}$ = 0.11, d = 0.238, CI 95% = [-0.61 0.14]; alpha: $t_{27}$ = 1.043, $p_{FDR}$ = 0.19, d = 0.197, CI 95% = [-0.18 0.57]). We then examined exhalation–inhalation differences in the time-frequency-decomposed averaged ECG signal within the time window corresponding to the significant heartbeat-modulated alpha effects observed during HCT and C-TCT (391-600 ms). Again, no significant effects were detected (HCT: $t_{27}$ = 0.442, $p_{FDR}$ = 0.338, d = 0.084, CI 95% = [-0.29 0.45]; C-TCT: $t_{27}$ = -1.037, $p_{FDR}$ = 0.164, d = 0.196, CI 95% = [-0.57 0.18]). Together, these null results indicate that the respiratory-phase effects observed in EEG power cannot be attributed to the CFA and instead reflect genuine neural modulation.

### 3.2.4 Breathing adjustments during interoceptive attention

To evaluate whether participants systematically adjusted their breathing during the interoceptive task, we extracted for each HCT trial the average respiratory rate and the inhalation-exhalation ratio (I/E ratio) across the full dataset. LMEMs were used to test within-task changes across trials and to examine whether these respiratory parameters predicted interoceptive accuracy and heartbeat-modulated alpha power and ITC. To avoid overparameterizing models that already included multiple higher-order interactions, respiratory rate and the I/E ratio were evaluated as independent predictors in separate LMEMs. Respiratory rate did not change over the course of the task (omnibus test: $F_{11,297}$ = 0.92, p = 0.52), whereas the I/E ratio showed a significant modulation across trials ($F_{11,297}$ = 3.78, p < 0.001), increasing gradually from early to mid-blocks before returning to baseline levels toward the end. We next examined whether respiratory rate and I/E ratio predicted interoceptive accuracy, Δalpha power, or Δalpha ITC. Respiratory rate significantly predicted interoceptive accuracy ($F_{1,297}$ = 4.16, p = 0.042), such that slower breathing was associated with higher accuracy. No effects of trial

number ($F_{11,255}$ = 0.468, p = 0.922) or trial × respiratory rate interaction emerged ($F_{11,255}$ = 0.949, p = 0.494). The I/E ratio did not predict accuracy ($F_{1,269}$ = 0.002, p = 0.969), nor did trial × I/E ratio interaction ($F_{11,258}$ = 0.974, p = 0.471). For Δalpha power, neither respiratory rate ($F_{1,85}$ = 1.91, p = 0.171), trial number ($F_{11,258}$ = 1.15, p = 0.326), nor their interaction ($F_{11,268}$ = 1.08, p = 0.380) were significant. Likewise, I/E ratio ($F_{1,172}$ = 0.340, p = 0.561) and its interaction with trial number ($F_{11,272}$ = 1.172, p = 0.307) did not predict Δalpha power. For Δalpha ITC, neither respiratory rate ($F_{1,74}$ = 0.075, p = 0.785), trial number ($F_{11,260}$ = 0.465, p = 0.924), nor their interaction ($F_{11,271}$ = 0.995, p = 0.451) reached significance. Similarly, neither the main effect of the I/E ratio ($F_{1,21}$ = 3.612, p = 0.071), nor its interaction with trial number ($F_{11,250}$ = 1.100, p = 0.362) was significant. These analyses indicate that participants did not systematically slow their breathing over the course of the task, although the I/E ratio showed modest variation across trials. While lower respiratory rate was associated with higher interoceptive accuracy, such respiratory adaptations did not explain or attenuate the primary task- and phase-dependent effects reported in this study.

### 3.2.5 Respiratory bins and phase transitions

To examine whether heartbeat-modulated alpha power varies continuously across the respiratory cycle or shows abrupt changes at phase transitions, we performed an analysis using a finer-grained representation of respiratory phase. For each breathing cycle in the interoceptive task (HCT), the interval between two consecutive inhalations was divided into four equidistant phase bins (90°), which were subsequently grouped into the following respiratory segments: exhalation-to-inhalation transition (315-45°), inhalation (45-135°), inhalation-to-exhalation transition (135-225°), and exhalation (225-315°). Heartbeat-modulated alpha power was extracted from the significant cluster identified in the exhalation vs. inhalation contrast and averaged across trials for each participant. A repeated-measures ANOVA with phase (four levels) as a within-subject factor replicated the significant main effect of Phase ($F_{3,81}$ = 3.18, p = 0.029, $\eta^2p$ = 0.105). Post-hoc comparisons indicated that heartbeat-modulated alpha power during inhalation was significantly lower than during the

inhalation-to-exhalation transition (mean difference = -0.062, SE = 0.022, $t_{27}$ = -2.89, p = 0.008) and exhalation (mean difference = -0.070, SE = 0.024, $t_{27}$ = -2.93, p = 0.007). This analysis confirmed that heartbeat-modulated alpha power varies systematically across the respiratory cycle, with a specific reduction during inhalation.

### 3.3 Exploratory analyses of network-level dynamics

#### 3.3.1 Heartbeat-modulated functional connectivity

We conducted an exploratory assessment of heartbeat-modulated functional connectivity (FC) between all pairs of electrodes, estimated for each participant, task, and respiratory phase separately in the alpha and theta bands. We focused on these frequency bands because they showed significant modulation of heartbeat-modulated power and ITC between respiratory phases. We conducted permutation-based t-tests across the entire scalp, using the relative (i.e., active divided by baseline cardiac time-window, see Section 2.5) imaginary part of coherency (iCOH) as the dependent variable, with task (HCT vs. C-TCT), respiratory phase (inhalation vs. exhalation) and their interaction as within-participant factors. The analysis revealed a significant task × phase interaction in the theta band over the parieto-occipital cortices, alongside a negative effect in frontal regions. Planned t-tests (see Section 2.6) indicated greater theta-band FC during HCT in exhalation compared to inhalation, predominantly lateralized to the right hemisphere, spanning from prefrontal to parieto-occipital areas. During C-TCT, while some theta-band FC increases were observed during exhalation relative to inhalation, these were accompanied by a marked reduction in connectivity in the right hemisphere. In the alpha band, we observed a significant task × phase interaction, which was most pronounced over the right frontal cortices. This effect was driven by a significant increase in FC between right frontal and central regions during exhalation compared to inhalation during HCT. On the other hand, during C-TCT, FC was significantly reduced during exhalation relative to inhalation, particularly over the right frontal and prefrontal regions.

We also ensured that any significant changes in iCOH did not represent an artificial increase in phase synchronisation caused by CFA. Following the procedure outlined in Kim et al., 2019, we tested whether the relative alpha and theta iCOH increased during exhalation compared to inhalation between the ECG and EEG electrodes that showed significant iCOH changes, using permutation-based dependent samples t-tests. Comparing relative iCOH between exhalation and inhalation during HCT revealed a significant increase between the ECG and F3 electrode in the theta band ($t_{27}$ = 1.07, p = 0.004, d = 0.2, CI 95% = [-0.19 0.59]), as well as between the ECG and Fpz electrode in the alpha band ($t_{27}$ = 1.85, p = 0.006, d = 0.35, CI 95% = [-0.05 0.75]). No significant changes in ECG connectivity were found during C-TCT. These results show that the widespread functional connectivity changes observed between respiratory phases were not attributable to CFA-related connectivity effects. In summary, heartbeat-modulated FC was selectively enhanced during exhalation when attention was directed inward (HCT), particularly in right-lateralized alpha and theta networks, highlighting a task-dependent reconfiguration of large-scale cortical networks.

### 3.3.2 Heartbeat-modulated graph-theory metrics

To exploratorily assess heartbeat-modulated graph-theory metrics, we estimated a total of eight LMEMs across each frequency band (alpha, theta). Each model included the graph metric as the dependent variable and incorporated task, time, and respiratory phase, as well as their three-way interaction (task × time × phase) as fixed effects. Threshold was included as a fixed factor. All models included participant-specific random intercepts and random slopes for fixed effects (maximal random structure). Models were estimated separately for four graph metrics: density, clustering coefficient, global efficiency, and local efficiency. In the theta frequency band, beyond the expected main effect of the threshold factor, we observed a significant main effect of time (i.e., baseline vs. active cardiac time-windows) across all four graph theory metrics (density: b = 0.037, SE = 0.015, t = 2.402, p = 0.023; clustering coefficient: b = 0.039, SE = 0.014, t = 2.781, p = 0.009; local efficiency: b = 0.065, SE = 0.023, t = 2.834, p = 0.008; global efficiency: b = 0.048, SE = 0.019, t = 2.504, p = 0.019; Fig.

4A-D). This suggests that the heartbeat generally reduces connectivity in the theta band. Despite the three-way interaction between task, time, and phase was not significant (b = 0.041, SE = 0.062, t = 0.664, p = 0.512), exploratory planned t-tests (see Section 2.6) revealed a significant heartbeat-modulated reduction in network density during inhalation in HCT (t = -3.566, p = 0.001, $p_{FDR}$ = 0.010), resulting in higher density during exhalation compared to inhalation in the active cardiac time-window (t = 2.672, p = 0.012, $p_{FDR}$ = 0.050; Fig. 4A). A similar pattern was observed for the clustering coefficient in HCT, where t-tests indicated a heartbeat-modulated reduction during inhalation (t = -4.01, p < 0.001, $p_{FDR}$ = 0.003), leading to higher theta clustering coefficients during exhalation than inhalation in the active cardiac time-window (t = 2.383, p = 0.024, $p_{FDR}$ = 0.096; Fig. 4B), the latter reflecting a trend-level effect following FDR correction. Furthermore, both heartbeat-modulated local and global efficiency significantly decreased during inhalation in HCT (local efficiency: t = -3.988, p < 0.001, $p_{FDR}$ = 0.003, Fig. 4C; global efficiency: t = -3.793, p < 0.001, $p_{FDR}$ = 0.005, Fig. 4D). However, no significant differences were observed between inhalation and exhalation in the active cardiac time-window (local efficiency: t = 1.967, p = 0.059; global efficiency: t = 1.444, p = 0.160). In the alpha band, the heartbeat consistently induced a significant increase in alpha connectivity metrics (main effect of time for density: b = -0.036, SE = 0.007, t = -4.72, p < 0.001; clustering coefficient: b = -0.034, SE = 0.009, t = -3.73, p < 0.001; local efficiency: b = -0.052, SE = 0.013, t = -4.11, p < 0.001; global efficiency: b = -0.041, SE = 0.009, t = -4.34, p < 0.001). Additionally, a significant main effect of task was observed, indicating higher alpha connectivity during HCT compared to C-TCT (density: b = 0.056, SE = 0.026, t = 2.13, p = 0.043; clustering coefficient: b = 0.061, SE = 0.029, t = 2.06, p = 0.049; local efficiency: b = 0.096, SE = 0.045, t = 2.18, p = 0.038; global efficiency: b = 0.076, SE = 0.032, t = 2.35, p = 0.026; as can be inferred from Fig. 4E–H). Despite the three-way interaction between task, time, and phase was not significant (b = 0.04, SE = 0.039, t = 1.55, p = 0.3), exploratory planned t-tests (see Section 2.6) for graph density revealed a significant heartbeat-modulated increase in density during exhalation in HCT (t = 2.82, p = 0.008, $p_{FDR}$ = 0.035), leading to higher alpha density at exhalation compared to inhalation within the active

cardiac time-window (t = 2.497, p = 0.018, $p_{FDR}$ = 0.050; Fig. 4E). In contrast, during C-TCT, the heartbeat increased alpha density only during inhalation (t = 3.188, p = 0.003, $p_{FDR}$ = 0.028) and resulted in no significant differences between respiratory phases (t = -0.132, p = 0.896). For the clustering coefficient, no significant heartbeat-modulated differences between respiratory phases were significant (HCT: t = 1.615, p = 0.117; C-TCT: t = -0.214, p = 0.832; Fig. 4F). For local efficiency, heartbeat-induced increases in the alpha band were observed only during inhalation in C-TCT (t = 2.871, p = 0.007, $p_{FDR}$ = 0.056, Fig. 4G), reflecting a trend-level effect following FDR correction. Finally, for global efficiency, the heartbeat evoked increased connectivity during exhalation (t = 2.62, p = 0.014, $p_{FDR}$ = 0.048), leading to higher alpha global efficiency at exhalation compared to inhalation in the active cardiac time-window during HCT (t = 2.499, p = 0.018, $p_{FDR}$ = 0.048; Fig. 4H). Conversely, in C-TCT, global efficiency was enhanced by the heartbeat only during inhalation (t = 3.751, p < 0.001, $p_{FDR}$ = 0.006), but no significant differences were found between respiratory phases in the active phase of the cardiac cycle (t = -0.292, p = 0.772). Overall, these findings revealed that heartbeat-modulated network organization is selectively enhanced during exhalation when attention is directed inward, particularly within theta and alpha frequency bands.

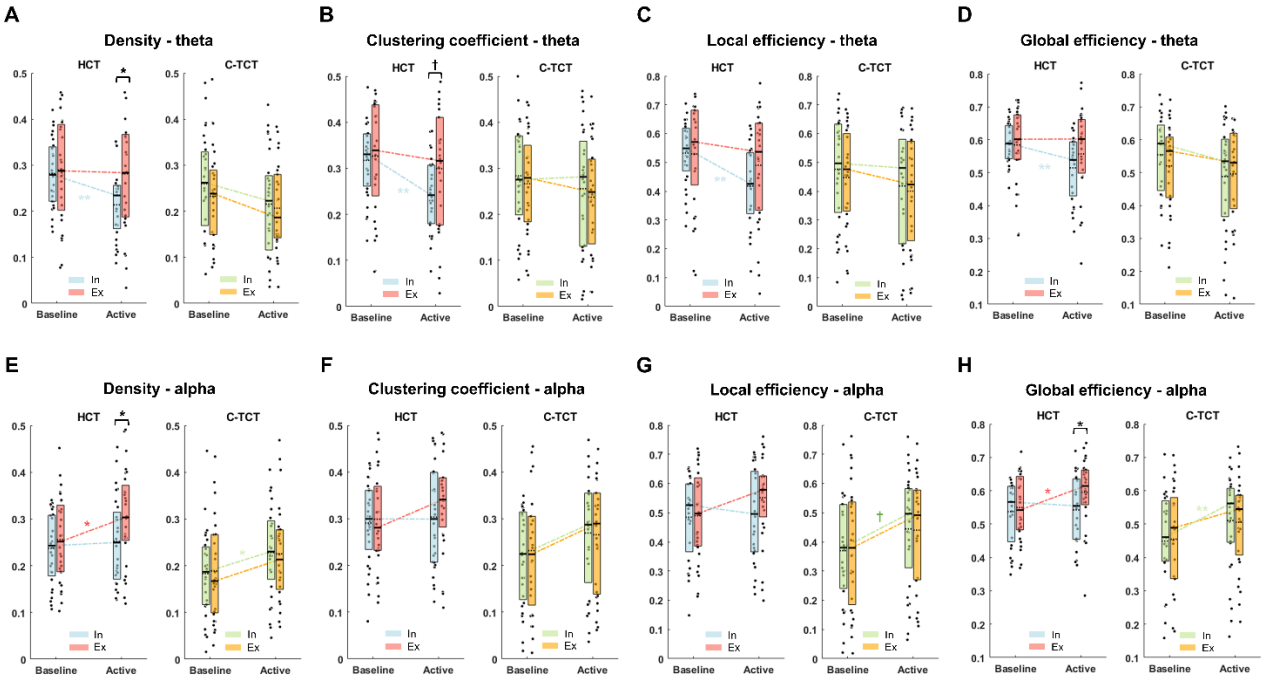


**Figure 4. Graph theory metrics across respiratory phases and tasks.** Box plots displaying descriptive statistics for graph-theoretic metrics before (baseline) and after (active) the heartbeat during inhalation and exhalation in the heartbeat counting task and the cardiac-tone counting task. **A)** Network density in the theta band. **B)** Network clustering coefficient in the theta band. **C)** Network local efficiency in the theta band. **D)** Network global efficiency in the theta band. **E)** Network density in the alpha band. **F)** Network clustering coefficient in the alpha band. **G)** Network local efficiency in the alpha band. **H)** Network global efficiency in the alpha band. Significant planned t-tests are indicated by asterisks (**$p_{FDR} \leq 0.01$, *$p_{FDR} \leq 0.05$, †$p_{FDR} \leq 0.1$). The y-axis units reflect normalized ratios (arbitrary units). Abbreviations: In = inhalation, Ex = exhalation, HCT = heartbeat counting task, C-TCT = cardiac-tone counting task.

## 4. Discussion

In previous studies, we found greater late heartbeat-evoked potential (HEP) positivity during exhalation compared to inhalation in healthy participants performing two cardiac interoceptive tasks (HBD and HCT; Zaccaro et al., 2022, 2024). In the present study, we aimed to extend previous findings to the time-frequency domain by re-analyzing the same dataset and focusing on the interoceptive HCT and the exteroceptive C-TCT (Zaccaro et al., 2024). As hypothesized, and consistent with previous time-domain results, we observed increased late heartbeat-modulated power and inter-trial coherence (ITC) in exhalation compared to inhalation during the HCT. These effects were observed in the alpha and theta frequency bands over right fronto-centro-parietal electrodes. In contrast, no differences were found between exhalation and inhalation during the cardiac-tone counting task (C-TCT). At the participant level, heartbeat-modulated alpha power and HEP changes across respiratory phases (Δalpha power and ΔHEP) were positively correlated over frontal electrodes. This relationship was specific to HCT and was not observed for theta or other frequency bands, nor ITC changes across respiratory phases (ΔITC). At the HCT-trial level, Δalpha ITC predicted ΔHEP only when Δalpha power was high, whereas ΔHEP predicted interoceptive accuracy only when both Δalpha power and confidence were high. Crucially, these relationships were independent of cardiac and physiology and were absent during C-TCT. Overall, these results indicate that when participants focus on their cardiac sensations, the heartbeat elicits higher power and ITC during exhalation compared to inhalation, primarily in the alpha band, which in turn predicts cardiac

interoceptive accuracy. The predominance of effects at fronto-centro-parietal electrodes aligns with the canonical topography of the HEP, which reliably shows maximal amplitudes in these regions across studies. This spatial pattern reflects source contributions from insula, cingulate, somatosensory, and medial prefrontal cortices (Coll et al., 2021; Park & Blanke, 2019), and has also emerged in our previous works (Zaccaro et al., 2022, 2024). These findings further indicate that respiratory-phase modulation of cardiac processing is not an automatic physiological consequence of breathing, but a task-dependent phenomenon that emerges only when interoceptive information is behaviourally prioritized.

During HCT, we also exploratively observed a widespread increase in heartbeat-modulated functional connectivity (FC) in the alpha and theta bands during exhalation compared to inhalation, mostly lateralized to the right fronto-central regions. Conversely, during C-TCT, alpha and theta FC in the right hemisphere decreased during exhalation compared to inhalation. Graph theory analysis further clarified these findings. During HCT, the heartbeat induced a reduction in theta-band graph connectivity during inhalation and increased alpha-band graph connectivity during exhalation. Consequently, both theta-band (density and clustering coefficient) and alpha-band (density and global efficiency) heartbeat-modulated graph connectivity metrics were higher during exhalation than inhalation. No changes were observed in the theta-band graph connectivity during C-TCT, whereas in the alpha band the heartbeat caused some inhalation-related increases that did not result in significant differences between respiratory phases.

We propose that reduced cortical excitability during exhalation, particularly in the insula and somatosensory regions, may enhance cardiac interoception, as reflected in increased heartbeat-modulated cortical oscillations in the alpha range. Studies using both periodic and aperiodic MEG/EEG signal analysis have found higher cortical inhibition in the late phase of exhalation and in the transition from exhalation to inhalation (Karjalainen et al., 2025; Kluger et al., 2023; Nakamura et al., 2024). Furthermore, neuroimaging studies have found that interoceptive accuracy is mediated by insula inhibition, suggesting an “addition by subtraction” mechanism for interoceptive attention

(Farb et al., 2023; Kuehn et al., 2016; Wiebking et al., 2015). Complementary EEG evidence has shown enhanced alpha power during interoceptive tasks (Crivelli & Balconi, 2025; Kritzman et al., 2022), which correlates with task accuracy (Rominger et al., 2025; Villena-González et al., 2017). This has been interpreted as an active inhibitory mechanism that suppresses the processing of distracting signals (Cooper et al., 2003; Foxe & Snyder, 2011; Jensen & Mazaheri, 2010; Klimesch et al., 2007; Neri et al., 2024; Van Diepen et al., 2019). Additionally, in the context of predictive coding, alpha activity has been linked to the precision-weighting of prediction errors and prior updating (Bastos et al., 2012; Brændholt et al., 2023; Friston, 2019; Friston et al., 2015; Sherman et al., 2016). Therefore, synthesizing this body of literature, our findings of increased heartbeat-modulated alpha power, ITC, and FC during exhalation can be interpreted as neurophysiological signatures of enhanced cardiac interoception. This enhancement likely reflects a state of increased top-down attentional allocation toward interoceptive signals (Molle & Coste, 2022), supported by active inhibition of irrelevant sensory input facilitated by heightened cortical inhibition (particularly in insular and somatosensory regions) during the exhalation phase. Such a configuration may optimize the precision-weighting of cardiac prediction errors, ultimately contributing to improved heartbeat perception and confidence. This interpretation is consistent with the null results observed during the C-TCT: when attention is allocated to an external cue, sensory precision is directed toward exteroceptive stimuli, reducing the salience of cardiac input and abolishing phase-dependent modulations.

As we observed increases in both heartbeat-modulated alpha power and ITC during exhalation, we cannot conclusively determine whether the observed HEP modulations between respiratory phases result from an enhanced phase-reset mechanism. Such modulations would be supported by ITC increases without concurrent power increases (Lopour et al., 2013; Park et al., 2018). We propose that respiration modulates HEP amplitude through increases in both evoked amplitude and phase-reset mechanisms in the alpha band. This interpretation is supported by the moderating effect of heartbeat-modulated power changes on the ITC-HEP relationship: while power and ITC changes across

respiratory phases did not correlate (as in Park et al., 2018), ITC increases were positively associated with HEP enhancements only when power increases were also high. This suggests that the two processes (alpha power and ITC increases) stem from distinct yet interactive mechanisms, both essential for cardiac perception. We speculate that positive Δalpha power may serve as an index of interoceptive sensory gating mediated by top-down attention (Crivelli & Balconi, 2025; Kritzman et al., 2022; Molle & Coste, 2022; Rominger et al., 2025; Villena-González et al., 2017), whereas increased Δalpha ITC may reflect increased precision-weighting of cardiac prediction errors (Park et al., 2018; Petzschner et al., 2019).

Several additional questions remain to be answered. First, the breathing pathway (nasal vs. mouth) may play a role in cardio-respiratory interoceptive interactions (Fontanini & Bower, 2006; Tort et al., 2018). Further investigation is needed to determine whether inhalation disrupts cardiac interoception specifically during nasal breathing or whether this effect persists during mouth breathing. Second, directing attention to the heart reduces respiratory rate, likely as a form of respiratory active inference to increase cardiac salience (Candia-Rivera et al., 2022; Zaccaro et al., 2022, 2024). Future studies should investigate the role of voluntary respiratory modulation (in depth, phase, or frequency) in shaping cardiac interoceptive accuracy, emphasizing the contribution of respiratory active inference to cardiac interoceptive attention (Stoupi et al., 2024).

In conclusion, our findings indicate that cardio-respiratory interactions occur at high levels of the interoceptive hierarchy (R. Smith et al., 2017; Suksasilp & Garfinkel, 2022). We propose that these interactions are fundamental to understanding cardiac interoception, as they provide additional explanatory power for how the central nervous system optimizes the interplay between interoceptive processes. Furthermore, we suggest that such interactions extend beyond the cardiac and respiratory systems and that the predictive coding framework offers valuable insights for their investigation. Finally, we hypothesize that the dynamic interplay between the cardio-respiratory system and the brain has functional significance and may be altered in clinical conditions. This is supported by evidence showing that a respiratory perturbation (breath-holding) enhanced the interoceptive

precision assigned to cardiac signals only in healthy individuals, whereas no such effect was observed in individuals with various psychiatric disorders, including depression, anxiety, substance use, and eating disorders (Lavalley et al., 2024; R. Smith et al., 2020, 2021). Thus, difficulties in adjusting the precision of afferent cardiac signals across respiratory phases during spontaneous breathing may represent a transdiagnostic marker of vulnerability to somatic and mental health disorders.

# Study 4

## Interoception and fatigue: preliminary data from an ongoing study

*This study is currently ongoing. Data collection has been completed; however, not all planned analyses have been performed. Accordingly, the results presented here should be considered preliminary and subject to further verification and refinement in subsequent analyses.*

## 1. Rationale

Studies 1-3 provided converging evidence that respiratory phase systematically modulates the cortical and behavioral processing of cardiac interoceptive signals. Across electrophysiological, time-frequency and behavioral measures, exhalation was consistently associated with enhanced heartbeat-evoked potentials, increased heartbeat-modulated oscillatory power and inter-trial phase coherence and higher interoceptive cardiac accuracy. Moreover, participants were found to actively adjust their respiratory rhythm to align the expected onset of stimuli with specific respiratory phases, suggesting that breathing is not merely a passive physiological background but an active control variable that regulates the precision of interoceptive and exteroceptive signals.

These findings are naturally framed within interoceptive predictive processing models, according to which perception of the body arises from the integration of afferent bodily signals with top-down generative predictions weighted by their estimated precision (Greenhouse-Tucknott et al., 2022). Within this framework, the respiratory cycle appears to operate as a precision-modulating mechanism, with exhalation selectively increasing the gain assigned to cardiac afferents, thereby facilitating interoceptive processing and improving perceptual performance.

However, Studies 1-3 were conducted in healthy participants performing brief, highly controlled laboratory tasks. While these experiments establish the existence of respiration-dependent modulation of interoceptive processing, they leave a critical theoretical question unresolved: does this respiratory control of interoceptive precision play a functional role when the body is challenged by sustained physiological demands, such as during physical exertion or fatigue?

Fatigue is conceptualized as the inability of muscle to sustain the expected force output in response to a given motor drive, arising from metabolic alterations, such as reduced glycogen availability, as well as impairments in excitation-contraction coupling, including decreased $Ca^{2+}$ release from the sarcoplasmic reticulum (Ørtenblad et al., 2013). However, in contemporary accounts of fatigue grounded in interoception and predictive processing (Stephan et al., 2016), fatigue is not conceived merely as metabolic depletion, but as the subjective consequence of persistent interoceptive

prediction errors and the progressive loss of confidence in the brain's ability to control bodily states (Greenhouse-Tucknott et al., 2022; Hess et al., 2024). Under conditions of prolonged exertion or pathological dysregulation, increasing physiological instability leads to increasingly imprecise bodily signals and larger prediction errors (Barrett & Simmons, 2015), which in turn undermine allostatic control and give rise to the phenomenology of fatigue (Stephan et al., 2016). Within this framework, although transient and pathological fatigue have traditionally been conceptualized as distinct phenomena, they can be understood as arising from a common underlying mechanism: transient fatigue reflects temporary mismatches between expected and actual bodily states, whereas pathological fatigue is associated with persistent prediction errors and chronic dyshomeostasis (Greenhouse-Tucknott et al., 2022).

From this perspective, the respiratory modulation of interoceptive precision observed in Studies 1-3 should become especially relevant under conditions of fatigue. If exhalation indeed enhances the precision weighting of cardiac signals, then this mechanism should play a critical role when the interoceptive system is under stress conditions. Study 4 was therefore designed to test whether the cardio-respiratory mechanisms identified in controlled laboratory settings extend to contexts of transient or pathological fatigue, probing whether respiratory phase continues to regulate interoceptive precision when the organism operates under conditions of elevated metabolic demand, physiological instability and altered interoception.

## 2. Materials and methods

### 2.1 Ethics statement

The study was approved by the Ethics Committee of the Department of Psychology, "G. d'Annunzio" University of Chieti-Pescara. The study was conducted in accordance with the guidelines of the Italian Association of Psychology and the Declaration of Helsinki and its later amendments. Participants were unaware of the specific aims of the experiment. After reading the consent form, all participants provided written informed consent.

### 2.2 Participants

Forty healthy volunteers (25 females; 6 left-handed; mean age: 24 ± 3.4 years [mean ± SD]) participated in the study. Eligibility was determined based on self-reported criteria, including: (1) no personal or family history of psychiatric, neurological, or somatic disorders; (2) no chronic or acute respiratory conditions; (3) no use of medications affecting pulmonary or cardiovascular function; and (4) no smoking habits. All participants had a body mass index (BMI) within the normal range (22.05 ± 2.4 [mean ± SD]) and normal or corrected-to-normal vision.

### 2.3 Apparatus and stimuli

The experiment was conducted at the Behavioral Imaging and Neural Dynamics Center (BIND) of the "G. d'Annunzio" University of Chieti-Pescara. Participants were recruited via flyers and social media advertisements. Electrophysiological data were recorded using LabChart (LabChart v7.1, ADInstruments, Oxford, UK). Electrocardiogram (ECG) data were acquired using three Ag/AgCl pre-gelled electrodes positioned over the left and right clavicles and the right costal margin (ground electrode). Respiration was recorded via a chest-placed respiratory transducer (ABioHarness, Zephyr Technology).

All tasks were administered using E-Prime 3.0 (Psychology Software Tools, Pittsburgh, PA, USA).

## 2.4 Experimental design

The experimental procedure consisted of two sessions, scheduled 2 to 7 days apart. Each session began with a 5-minute resting-state period with eyes open, followed by either the interoceptive cardiac task (HCT) or the respiratory task (BCT), with task presentation order randomized across participants. Each session lasted approximately 1 hour. Room lighting and noise were minimized, and temperature and humidity were maintained at a comfortable level. The experimental procedures are depicted in Figure 1.

On day 1, participants sat comfortably in front of a computer at an optimal distance (approximately 60 cm) for screen visibility. They then underwent the montage of the EEG cap, respiratory belt, and ECG electrodes. After completing the Fatigue Severity Scale (FSS), the 5-minute resting-state period began, followed by the assessment of the Rate of Fatigue (ROF). The tasks were then administered in randomized order, and the ROF was assessed between tasks and at the end of the session (three time points in total). After task completion, the experimenter removed all physiological recording devices (EEG cap, respiratory belt, and ECG electrodes) and placed a heart-rate monitor (XAND Heart Rate Monitor, Futurum BV, Apeldoorn, Netherlands) on the participant's chest. Participants then performed a procedure on the cycle ergometer (LODE Excalibur Sport with Pedal Force Measurement (Lode BV, Groningen, NL; software: Lode Ergometry Manager v10.14)) to assess the individual anaerobic threshold, which was required for Day 2. The saddle and handlebars were adjusted individually to ensure an optimal pedaling position. Details regarding the anaerobic threshold assessment are provided in the section *"2.5 Individual anaerobic threshold assessment"*.

On day 2, after completing the full montage setup (EEG, ECG, respiratory belt and heart-rate monitor), participants sat on the cycle ergometer and performed a 5-minute resting-state period with eyes open, followed by a warm-up with a ramp protocol, increasing from 80% of body-weight-adjusted wattage to the threshold determined on Day 1 over 4 minutes. This was followed by a 3-minute baseline phase in which pedal resistance was kept constant. After the baseline, the Time to Exhaustion (TTE) task began, during which participants also completed the HCT and BCT (order

randomized across participants). Rate of Perceived Exertion (RPE) and ROF were collected at the end of the warm-up, once per minute during the 3-minute baseline, and after each HCT and BCT trial. Participants maintained a constant pedaling cadence of 70 revolutions per minute (RPM) (Hunt & Hurni, 2019) for the entire duration of the cycling session, including warm-up, baseline and all experimental tasks.

This manuscript reports only the preliminary results from Day 1, during the resting condition.

### 2.5 Individual anaerobic threshold assessment

To determine the anaerobic threshold, participants performed an incremental test on a cycle ergometer while wearing a heart rate monitor placed on their chest. The protocol consisted of a warm-up phase (i.e., 3 minutes at a workload corresponding to 80% of the participant's body mass, start load), followed by a stepwise ramp protocol with increments of 10 W per minute until exhaustion (end load). The test was terminated when participants reached their age-predicted maximal heart rate (220 minus age; Fox et al., 1971) or when they were no longer able to maintain the required pedaling rate of 70 RPM (Hunt & Hurni, 2019). Participants had a monitor in front of them displaying real-time feedback for the cadence. At the end of each minute, participants reported their Rate of Fatigue (ROF) and Rate of Perceived Exertion (RPE). Mean start load was 50.2 ± 7.6 W (mean ± SD), while mean end load was 114.8 ± 32.1 W (mean ± SD).

Heart rate data were used to detect anaerobic threshold (VT2) using a non-invasive method based on HR deflection (Conconi et al., 1982; Dantas et al., 2015). After exhaustion, the HR-Watt relationship obtained on the monitor through the test was evaluated and the Watt at which the linearity of this relationship was lost (i.e., HR deflection) was considered as the anaerobic threshold (Di Fronso et al., 2020).

### 2.6 Interoceptive tasks

In the HCT (Desmedt et al., 2018), participants were asked to focus on their heartbeat, trying to perceive it, and silently count the number of perceived heartbeats during 4 time intervals (60, 70, 80 and 90 seconds). Participants were specifically instructed not to guess the number of heartbeats and were encouraged to report 0 if they were unable to perceive any. After each trial, participants were asked to verbally report their confidence level on a 9-point Likert scale.

In the BCT (Zaccaro et al., 2024), participants were asked to focus on their breathing sensations and silently count the number of perceived breaths during two 150-second intervals. After each trial, participants were asked to verbally report their confidence level and to rate how easy it was to perform the task without altering their breathing on a 9-point Likert scale.

### 2.7 Psychometric questionnaires

Body Perception Questionnaire (BPQ), International Physical Activity Questionnaire (IPAQ), Fatigue Severity Scale (FSS), Psychological General Well-Being Index (PGWBI), Perceived Physical Ability Scale (PPAS) were administered via Qualtrics online platform (Qualtrics, Provo, UT, USA) in their Italian validated versions.

The Body Perception Questionnaire (BPQ; Cerritelli et al., 2021) measures interoceptive sensibility, the self-reported tendency to notice and be aware of bodily signals. It focuses on perceived awareness of internal physiological processes such as heartbeats, breathing, hunger, satiety, temperature, and visceral sensations. The BPQ is grounded in contemporary models of interoception and autonomic regulation and includes subscales related to bodily awareness and autonomic reactivity: the BPQ-BOA subscale measures subjective awareness of internal bodily sensations including heartbeat, respiration, muscular tension, thirst, hunger and temperature; the BPQ-SUP subscale measures the supradiaphragmatic autonomic reactivity and reflects both sympathetic and parasympathetic activation, encompassing sensations such as palpitations, respiratory discomfort and dry mouth. The BPQ-SUB subscale measures subdiaphragmatic autonomic reactivity including sensations such as

nausea, abdominal cramps, and other visceral gastrointestinal symptoms. In the present study, the BPQ-BOA and BPQ-SUB subscales were combined into a single index (BPQ-BOA/SUB; Poli et al., 2021). Higher scores indicate greater subjective sensitivity to bodily signals. The questionnaire was administered in its short form (22 items).

The International Physical Activity Questionnaire (IPAQ; Mannocci et al., 2010) is a standardized self-report measure of habitual physical activity over the previous seven days. It quantifies time spent in vigorous activity, moderate activity, walking, and sedentary behavior, producing estimates of activity-related metabolic load expressed in MET-minutes per week, where MET (Metabolic Equivalent of Task) represents the energy cost of a physical activity relative to resting metabolic rate. IPAQ allows classification of participants into low, moderate, or high physical activity levels. Higher MET scores indicate higher levels of physical activity.

The Fatigue Severity Scale (FSS; Ottonello et al., 2016) is a 9-item questionnaire measuring the impact of fatigue on daily functioning, motivation, physical activity, and cognitive effort. Items are rated on a Likert scale, with higher scores indicating more severe and disabling fatigue. The FSS is widely used in clinical and non-clinical populations and captures the subjective burden of fatigue.

The Psychological General Well-Being Index (PGWBI; Grossi et al., 2006) is a 22-item questionnaire that assesses psychological well-being and distress across six domains: anxiety, depressed mood, positive well-being, self-control, general health, and vitality. It provides a global index of subjective mental health and emotional functioning. Higher scores indicate better psychological well-being and lower psychological distress.

The Perceived Physical Ability Scale (PPAS; Bortoli & Robazza, 1997) measures individuals' attitudes, motivation, and affective orientation towards physical activity. It assesses how positively or negatively participants relate to exercise, including enjoyment, perceived competence, and motivational engagement. It consists of two subscales: *motor efficiency*, which reflects the individual's perceived physical competence and ease of movement during physical activity (higher scores indicate that physical activity is experienced as effective and under control, whereas lower

scores reflect a sense of awkwardness, clumsiness, or physical inefficiency) and *perceived difficulty*, which measures how effortful and unpleasant physical activity feels, independently of actual performance (higher scores indicate that physical exertion is experienced as more difficult and exhausting, whereas lower scores indicate that activity feels manageable).

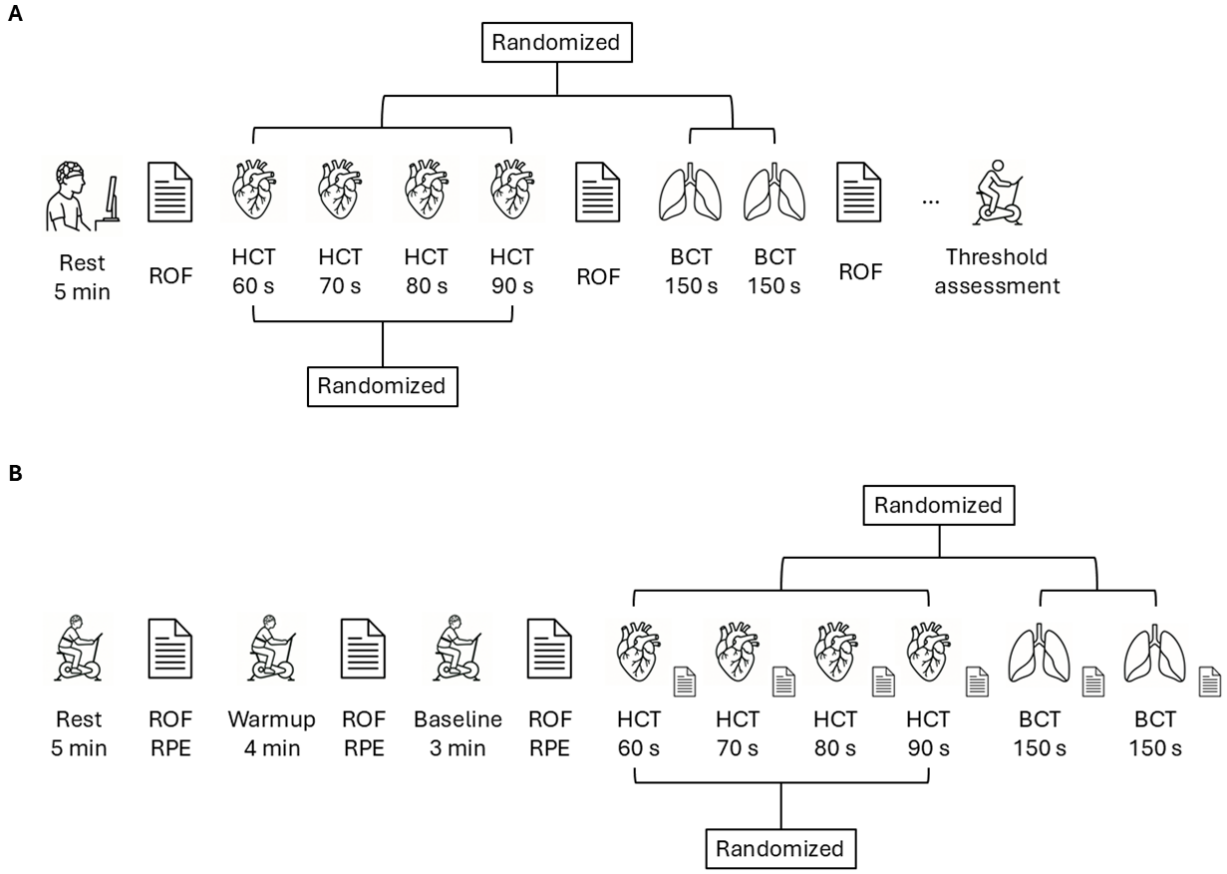



**Figure 5. Experimental procedures**. **A)** Day 1: after 5 minutes of resting-state with eyes open, participants underwent 4 trials of HCT and two trials of BCT; the two tasks were administered randomly. The ROF was asked during three time points: after the resting state, after the 4 HCT trials and after the 2 BCT trials. Once the tasks were completed, participants got on the cycle ergometer for the assessment of their individual anaerobic threshold. **B)** Day 2: participants got on the cycle ergometer and performed 5 minutes of resting-state with eyes open, followed by a 4-minute ramp warm-up, in which the pedal resistance increased from 80% of body weight (in watts) up to the anaerobic threshold assessed on Day 1; once the threshold was reached, they kept pedaling at a constant resistance for 3 minutes of baseline. After baseline, they completed HCT and BCT trials in a randomized order. ROF and RPE were collected after rest, after the warm-up, after each of the three baseline minutes, and after each HCT and BCT trial.

### 2.8 EEG data acquisition and pre-processing

EEG signals were acquired using a 32-channel ASALAB system with Waveguard cap (Advanced Neuro Technology, Enschede, Netherlands). Electrodes were positioned on the scalp following the International 10-5 system (Oostenveld & Praamstra, 2001). Electrode impedance was kept below 10 kΩ for all channels. The sampling rate was 1024 Hz. EEG preprocessing was carried out in EEGLAB (v2022.1) (Delorme & Makeig, 2004). The continuous signal was band-pass filtered between 0.5 and 45 Hz using a Hamming-windowed FIR filter (Al et al., 2020, 2021) and down-sampled to 256 Hz. Periods affected by excessive noise were identified through visual inspection and manually removed. To remove noise and non-neural related artifacts, an Independent Component Analysis was performed using the RunICA algorithm (Hyvarinen, 1999) excluding highly contaminated EEG channels. Fewer than four EEG electrodes were typically removed, all located in peripheral scalp areas that do not contribute to HEP generation (Coll et al., 2021). The resulting independent components (ICs) were inspected by combining information from their scalp distributions, spectral profiles, and temporal dynamics (Delorme & Makeig, 2004). Cardiac field artefact (CFA) components, which are known to strongly affect HEP measurements (Coll et al., 2021), were detected by overlaying ECG R-peaks onto ICs' time courses: components showing systematic R-peak locking were excluded from further analysis (Al et al., 2020, 2021; Zaccaro et al., 2022). Overall, between 1 and 6 ICs were removed per participant (3 ± 2 [mean ± SD]), of which 0 to 2 corresponded to CFA-related activity (1 ± 1 [mean ± SD]). After ICA correction, channels that had been previously removed were interpolated with their neighbouring electrodes (Junghöfer et al., 2000), and the data were re-referenced to the average reference (Zaccaro et al., 2022).

### 2.9 Cardio-respiratory data acquisition and pre-processing

Cardio-respiratory signals were recorded at a sampling rate of 2 kHz. A band-pass filter (0.1–50 Hz) and a 50-Hz notch filter were applied. The signals were then down-sampled to 256 Hz. Data analysis was conducted using custom MATLAB scripts (R2023b, MathWorks Inc.). R-peaks were detected

using the Pan-Tompkins algorithm (Pan & Tompkins, 1985). Respiratory phases (inhalation and exhalation) were identified using the *findpeaks* function. Inhalation onsets were marked at local minima (troughs), whereas exhalation onsets were marked at local maxima (peaks). A complete respiratory cycle was defined as the interval between two consecutive troughs. Outliers, defined as values exceeding three scaled median absolute deviations from the local median within a moving 1-second window, were linearly interpolated using neighboring values. The data were subsequently smoothed with a 1-second window filter (Savitzky & Golay, 1964) and z-scored.

### 2.10 Task accuracy assessment

HCT accuracy was evaluated using validated procedures (Candia-Rivera et al., 2022; Garfinkel et al., 2015; Schandry, 1981) based on the number of counted heartbeats in relation to the heartbeats recorded with ECG:

$$\text{HCT accuracy} = 1 - \frac{|(\text{Recorded heartbeats} - \text{Counted heartbeats})|}{\text{Recorded heartbeats}}$$

The accuracy of each trial was then averaged over the 4 HCT trials (Candia-Rivera et al., 2022; Garfinkel et al., 2015). Similarly, BCT accuracy was calculated based on the number of counted respiratory cycles in relation to performed respiratory cycles (Zaccaro et al., 2024):

$$\text{BCT accuracy} = 1 - \frac{|(\text{Recorded breaths} - \text{Counted breaths})|}{\text{Recorded breaths}}$$

The accuracy of each trial was then averaged over the 2 BCT trials (Zaccaro et al., 2024).

### 2.11 HEP analysis

Heartbeat-evoked potentials were computed using the FieldTrip toolbox (Oostenveld et al., 2011). R-peaks were detected with the HEPLAB toolbox (Perakakis, 2019) and subsequently visually inspected and corrected (Al et al., 2021; Zaccaro et al., 2022). EEG data were segmented into epochs extending from -100 to 600 ms around each R-peak (Coll et al., 2021) and were baseline-corrected by subtracting the mean voltage in a prestimulus interval from -300 to -100 ms (demean correction). For

each participant, epochs were averaged separately for each experimental condition, yielding three HEP waveforms corresponding to the heartbeat counting task (HCT), the breath counting task (BCT), and the resting-state condition. Finally, each heartbeat-locked epoch was classified as occurring during inhalation or exhalation based on the respiratory phase at the time of the R-peak.

## 3. Preliminary results

### 3.1 Attentional and respiratory modulation of heartbeat-evoked potentials

To assess whether HEPs were modulated by attentional focus, we conducted cluster-based permutation tests over the full scalp, comparing HEPs recorded during 1) resting state (resting-state HEP), 2) the heartbeat counting task (cardiac HEP), and 3) the breath counting task (respiratory HEP). Based on previous literature (Baranauskas et al., 2017; Gray et al., 2007; Petzschner et al., 2019; Pollatos et al., 2016; Schandry et al., 1986; Zaccaro et al., 2022), analyses were performed separately within an early (100-350 ms) and a late (350-600 ms) time window following the R-peak.

Comparisons between the resting-state HEP and the cardiac HEP revealed no significant differences in amplitude in either the early or the late time window (Fig. 2). In contrast, the comparison between the cardiac HEP and the respiratory HEP showed significant amplitude differences in both time windows (Fig. 3). Specifically, a significant positive cluster was observed in the early window ($t_{clust}$ = 151.6, $p_{clust}$ = 0.02) and in the late window ($t_{clust}$ = 458.9, $p_{clust}$ = 0.0002), indicating differential heartbeat-related cortical processing between the two task conditions. This effect was observed over frontal and frontocentral electrodes (Fp1, Fpz, Fp2, F3, Fz, F4, FC1, FC2). Additionally, the comparison between the respiratory HEP and the resting-state HEP also revealed significant amplitude differences in both the early and late time windows (Fig. 4). A significant positive cluster was observed in the early window ($t_{clust}$ = 90.9, $p_{clust}$ = 0.02) and in the late window ($t_{clust}$ = 85.3, $p_{clust}$ = 0.02). This effect was observed over electrodes distributed over central regions. (Fz, F4, FC1, FC2).

To investigate whether HEPs were modulated by respiratory phase, epochs were classified as occurring during inhalation or exhalation based on the respiratory phase at the time of each R-peak.

HEPs during exhalation and inhalation were then compared separately for each experimental condition. A significant effect of respiratory phase was observed for the cardiac HEP. HEP amplitude during exhalation was significantly larger than during inhalation, as reflected by a negative cluster in the early time window ($t_{clust}$ = -146.7, $p_{clust}$ = 0.02, Fig. 5). This effect was present across frontal, frontocentral and central electrodes (Fp1, Fpz, Fp2, F3, Fz, FC1, FC2, Cz, CP1).

In contrast, no significant respiratory-phase modulation was detected for the respiratory HEP (BCT) in either the early or late window. Similarly, for the resting-state condition, no significant differences between inhalation and exhalation were observed in either the early or the late time window. Figure 6 illustrates HEP waveforms across the three conditions (HCT, BCT, and resting-state) separately for inhalation and exhalation.

All analyses were performed on the full sample (N = 40).

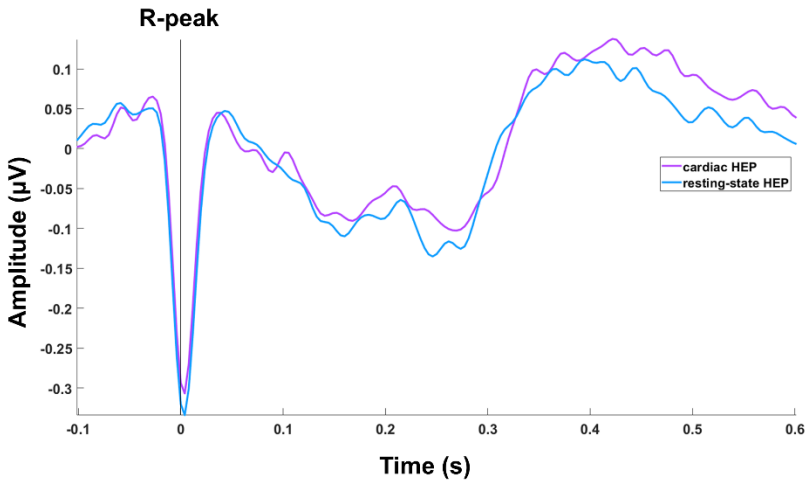



**Figure 2**. Grand-average HEP pooled for significant electrodes in the cardiac task (violet) and the resting-state condition (blue).

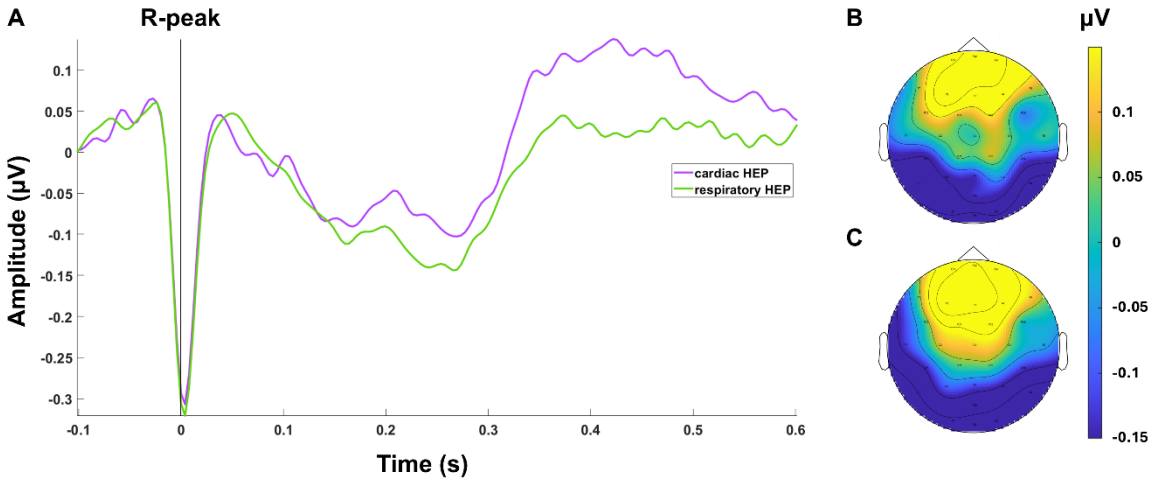



**Figure 3**. **A)** Grand-average HEP pooled for significant electrodes in the cardiac task (violet) and the respiratory task (green). The topographical distributions represent HEP differences between HCT vs. BCT in the **B)** early and **C)** late window of analysis.

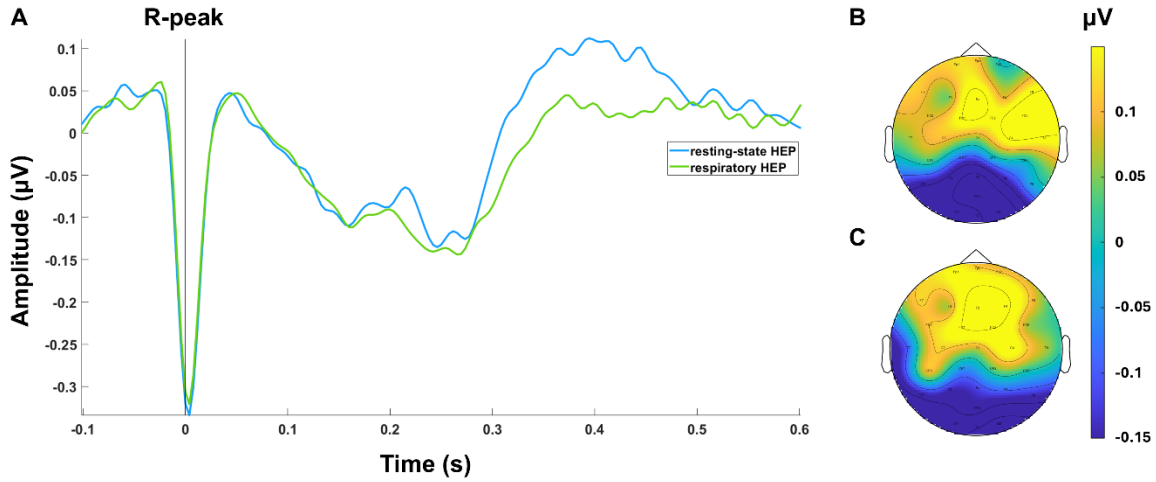



**Figure 4**. **A)** Grand-average HEP pooled for significant electrodes in the resting-state condition (blue) and the respiratory task (green). The topographical distributions represent HEP differences between resting-state vs. BCT in the **B)** early and **C)** late window of analysis.

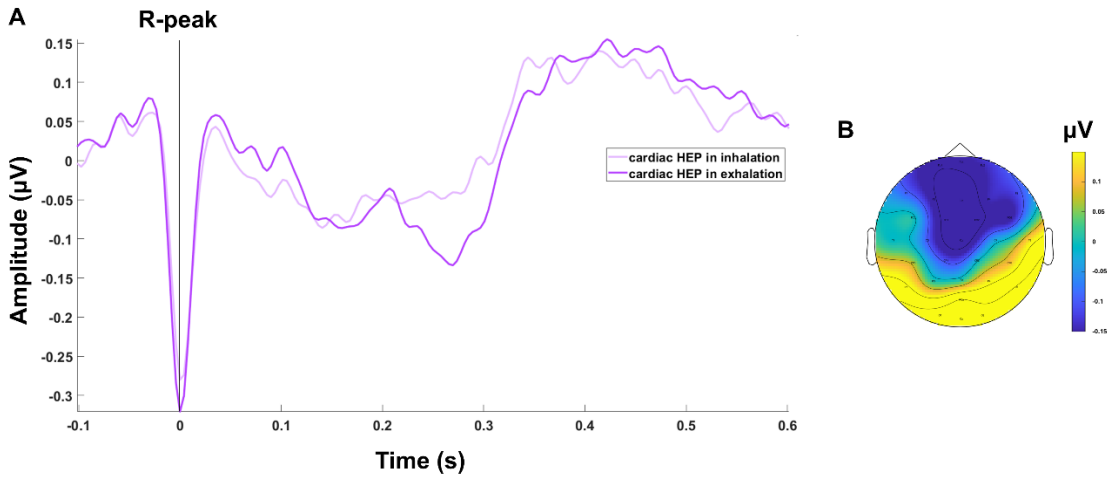



**Figure 5**. **A)** Grand-average HEP pooled for significant electrodes, plotted separately for inhalation (pink) and exhalation (violet) in the cardiac task (HCT). **B)** Topographical distribution of HEP differences between inhalation vs. exhalation in the early window of analysis.

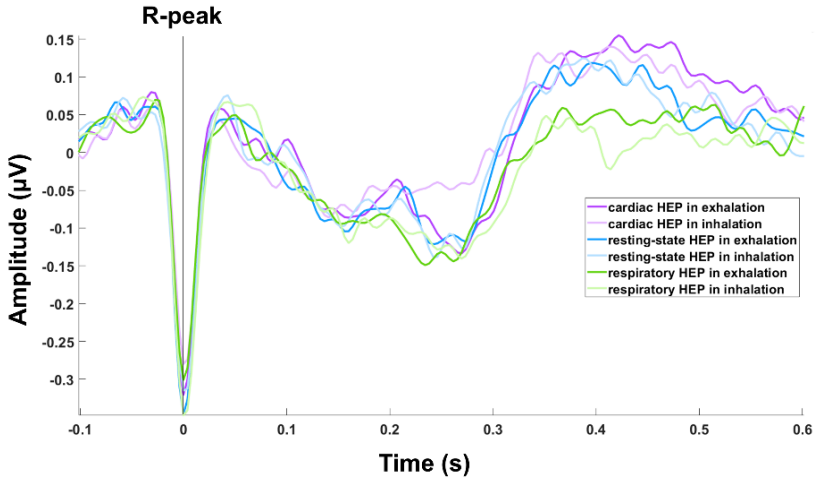



**Figure 6.** Grand-average HEP pooled for significant electrodes, plotted separately for inhalation (lighter colors) and exhalation (darker colors) in the cardiac task (HCT), respiratory task (BCT), and resting-state condition.

### 3.2 Pearson correlation analysis

Pearson correlation analyses were conducted in Jamovi (version 2.4) to examine relationships between demographic, physiological, behavioral and questionnaire measures.

Body size was significantly related to cardiac activity. Body weight was negatively correlated with heart rate (HR; r = -0.35, p = 0.026), and height was also negatively associated with HR (r = -0.41, p

= 0.008). Height was further negatively correlated with interoceptive sensibility as measured by the BPQ-BOA/SUB subscale (r = -0.46, p = 0.008).

Several significant associations emerged for the PPAS motor efficiency subscale. Higher motor efficiency scores were associated with lower HR (r = -0.41, p = 0.004), higher cardiac accuracy (r = 0.39, p = 0.015), and greater height (r = 0.34, p = 0.039). The PPAS difficulty subscale showed a consistent pattern of associations, being negatively correlated with HR (r = -0.5, p = 0.002), respiratory rate (r = -0.39, p = 0.016), fatigue severity as indexed by the FSS (r = -0.38, p = 0.018), and both BPQ-SUP (r = -0.37, p = 0.021) and BPQ-BOA/SUB (r = -0.37, p = 0.022). In contrast, PPAS difficulty was positively related to cardiac accuracy (r = 0.41, p = 0.011) and height (r = 0.34, p = 0.036).

Interoceptive sensibility was also associated with behavioral performance: BPQ-BOA/SUB was negatively correlated with cardiac accuracy (r = -0.33, p = 0.043).

Physical activity level, as assessed by IPAQ, was positively correlated with age (r = 0.409, p = 0.011) and cardiac accuracy (r = 0.34, p = 0.038), and negatively correlated with HR (r = -0.39, p = 0.015).

Finally, ROF score was negatively associated with respiratory accuracy (r = -0.37, p = 0.017) and positively correlated with BPQ-SUP (r = 0.36, p = 0.025).

**4. Ongoing analyses and future directions**

Beyond the preliminary EEG and behavioral results reported above, two complementary analyses are currently being implemented: network physiology and epigenetic profiling. Network physiology analyses will be used to characterize how brain activity, cardiac dynamics, and respiratory signals interact as a coupled multiscale system, rather than as independent physiological processes (Faes et al., 2016, 2017). This approach quantifies the degree of synchronization, information exchange, and dynamic coupling between neural oscillations, heart rate variability, and respiratory rhythms, thereby allowing the identification of brain-interoceptive system interaction patterns associated with perceived fatigability. These multivariate interaction patterns will be used to predict individual

differences in fatigue both at rest and during physical exertion, and to assess how they are modulated by cognitive factors such as interoceptive awareness.

In parallel, epigenetic analyses are being conducted to investigate whether individual differences in fatigue and interoceptive processing are associated with DNA methylation patterns in fatigue-relevant genes, involved in neural plasticity, stress regulation, and inflammatory processes, such as BDNF and NR3C1, whose methylation status has been linked to pathological fatigue (Vangeel et al., 2018). It remains unclear, however, whether similar mechanisms also contribute to transient fatigue in healthy individuals. Although with distinct origins, it has been recently proposed that both pathological and transient fatigue arise from inference processes grounded in interoception (Greenhouse-Tucknott et al., 2022), when persistent mismatches between predicted and actual bodily states occur. Within this framework, inter-individual variability in DNA methylation may represent a marker of vulnerability or susceptibility to fatigue even in non-clinical populations.

These molecular markers will be integrated with network-physiology metrics in order to test whether epigenetic variability modulates the strength and organization of brain-cardio-respiratory interactions underlying fatigue.

# Chapter 3

# General Discussion and Conclusions

## General Discussion and Conclusions

The overarching aim of the studies included in this thesis was to investigate whether and how respiration shapes perceptual processing across interoceptive and exteroceptive domains in a phase-dependent manner, and to identify the behavioral and neural mechanisms underlying such modulation. When considered together, our findings provide converging evidence that respiration is not a passive physiological background signal, but an active and functionally relevant rhythm that shapes cardiac interoceptive processing, with more limited effects on exteroception. Across studies, perceptual accuracy was systematically modulated by the phase of the respiratory cycle, with performance consistently optimized during exhalation. In the interoceptive domain, exhalation was associated with increased HEP amplitude only when attention was directed towards heartbeat sensations, suggesting enhanced cortical processing of cardiac signals during this respiratory phase and supporting the view that the HEP indexes a selective amplification of cardiac signal processing that emerges only when both respiratory conditions and attentional demands are aligned. At the physiological level, exhalation is associated with enhanced baroreceptor signalling due to respiratory sinus arrhythmia, which amplifies the afferent cardiac signal reaching the central nervous system (Brecher & Hubay, 1955; Larsson et al., 2021). Conversely, during inhalation, respiratory-related afferent activity may introduce interoceptive noise that interferes with the cortical processing of cardiac signals. This interpretation is further supported by the shared afferent pathways of respiratory and cardiac signals, which converge at multiple levels of the central nervous system (Craig, 2002). Importantly, the observed respiratory modulation was specific to cardiac interoceptive tasks and was consistently replicated across different task implementations, including heartbeat counting, detection, and discrimination tasks. This convergence across paradigms strengthens the interpretation that respiratory phase selectively gates the neural processing of cardiac signals.

Beyond passive modulation, results further indicate that participants actively regulate their breathing behavior to optimize performance. Respiratory patterns were dynamically adjusted in relation to task

demands, suggesting that respiration itself may constitute a regulatory mechanism through which individuals enhance sensory processing. At the neural level, respiration was found to modulate heartbeat-modulated alpha power, supporting the notion that respiratory phase influences cortical excitability (Kluger et al., 2021). In particular, heartbeat-modulated alpha power was enhanced during exhalation exclusively during cardiac interoceptive attention. This pattern can be interpreted within a predictive coding framework, as potentially reflecting respiration-dependent modulation of precision weighting (Brown & Friston, 2012; Kanai et al., 2015), with respiration potentially influencing the processing of sensory inputs to match predictions and minimize prediction errors (Barrett & Simmons, 2015). Alpha oscillations are widely interpreted as reflecting active inhibitory control, suppressing task-irrelevant input and reducing cortical noise (Cooper et al., 2003; Foxe & Snyder, 2011; Jensen & Mazaheri, 2010; Klimesch et al., 2007; Neri et al., 2024; Van Diepen et al., 2019), thereby facilitating interoceptive processing. In the present context, increased alpha activity during exhalation may therefore facilitate cardiac signal processing by reducing cortical noise and limiting interference from competing sensory inputs.

Crucially, results point to a functional dissociation between phases of the respiratory cycle. Inhalation is associated with anticipatory processes (Harting et al., 2025; Johannknecht & Kayser, 2022) and motor behavior (Brændholt et al., 2025; Molle et al., 2023), whereas exhalation consistently supports perceptual optimization (Grund et al., 2022). This dissociation suggests that distinct respiratory phases may preferentially support different functional roles, with inhalation facilitating anticipatory behavior and exhalation promoting enhanced perceptual accuracy. In addition to these phase-dependent effects, respiration was also modulated in its temporal and amplitude characteristics as a function of task demands. Specifically, inhalation duration was longer during the interoceptive (HDT) compared to the exteroceptive (TDT) task, indicating that breathing dynamics were adjusted according to the nature of the perceptual target. This pattern suggests that respiration is not merely passively coupled to perception but is systematically modulated to support the detection of weak or ambiguous sensory inputs, including near-threshold tactile stimuli and cardiac signals, which are

intrinsically difficult to perceive (Garfinkel et al., 2015; Larsson et al., 2021). However, rather than reflecting a simple inhalation-exhalation dichotomy, these findings point to a more complex functional organization of the respiratory cycle in shaping perception. This functional dissociation should be interpreted as a dynamic coordination of respiratory phases, phase transitions, phase-locking dynamics, amplitude modulations and associated neural states that differentially shape perception. Taken together, these findings support a broader integrative framework in which respiration influences behavioral performance and neural processing, shaping perception through both bottom-up physiological mechanisms and top-down adaptive strategies.

While the results described above establish a consistent pattern of respiratory-dependent effects on perception and neural processing, an important question concerns the mechanisms through which respiration exerts this influence, and why such effects emerge preferentially during interoceptive processing. Across studies, respiratory phase effects on perceptual accuracy and neural markers consistently emerged in the interoceptive cardiac tasks (HCT and HDT), whereas comparable effects were absent or markedly reduced in the exteroceptive tasks (C-TCT, B-TCT and TDT). In particular, trial-locked analyses revealed significant differences in respiratory modulation between correct and incorrect trials in the HDT, while no such difference was observed in the TDT. Moreover, in the HDT, phase-clustering was selectively present for correct but not for incorrect trials; by contrast, in the TDT, respiratory phase-clustering was observed regardless of trial accuracy. Together, these findings support the view that respiration plays a more prominent and functionally specific role in shaping perceptual accuracy when the task requires access to weak and noisy interoceptive signals.

The studies included in this thesis demonstrate that respiration represents an active mechanism able to shape perceptual processing, particularly in the interoceptive domain. Within an interoceptive predictive coding framework, respiration may contribute to the allocation of precision weights to bodily signals, with inhalation supporting anticipatory behavior and exhalation providing a low-noise context that optimizes the cortical processing of cardiac information. Rather than acting as a

background physiological rhythm, breathing dynamically interacts with attention and neural excitability to modulate the precision with which bodily signals are processed.

Beyond perceptual mechanisms, these results have broader implications for conditions associated with altered interoceptive processing, such as fatigue, anxiety, and stress-related disorders. The present findings indicate that modulation of interoceptive precision by respiration may support both adaptive and maladaptive forms of regulation, depending on task demands and individual factors.

Despite the strengths of the studies included in this thesis, several limitations should be acknowledged. First, the present thesis comprises four studies that rely on only two experimental paradigms to assess interoceptive performance: the HCT and the HDT, both of which have been criticized in the literature. Specifically, the HCT does not allow distinguishing whether participants are genuinely perceiving and counting their heartbeats (Desmedt et al., 2018; Körmendi et al., 2021, 2022) or instead relying on estimates based on prior beliefs about their heart rate (Brener & Ring, 2016; Ring et al., 2015) and time estimation abilities (Murphy et al., 2018). Although the HDT has been proposed as a more reliable measure of interoception compared to the HCT, it is not without limitations. In particular, the HDT is not a purely interoceptive measure, as it requires the integration of interoceptive and exteroceptive signals (Hickman et al., 2020), and involves multisensory, decisional, and temporal discrimination processes. Nevertheless, HDT performance is less susceptible to confounding factors such as prior knowledge of one's resting heart rate or time estimation abilities (Phillips et al., 1999; Tanaka et al., 2021). Moreover, given that heartbeat perception varies across individuals (Betka et al., 2021), the use of fixed temporal windows may not be appropriate for all participants and may lead to misclassification of synchronous and asynchronous trials (Brener & Ring, 2016).

Another important limitation concerns the study samples, which consisted exclusively of healthy participants, potentially limiting the generalizability of the findings. Finally, the fourth study included in this thesis is ongoing and analyses are still in progress. Therefore, the results reported for this study should be considered preliminary and interpreted with caution.

Future studies should aim to address these limitations by developing experimental paradigms that more selectively capture interoceptive processing, reducing the influence of non-interoceptive and decisional components. Moreover, extending these findings to clinical populations characterized by altered interoceptive processing would help to improve their generalizability and clinical relevance. Within this framework, future research should investigate whether targeted modulation of respiratory dynamics can causally influence interoceptive precision and perceptual performance, and how individual biological factors may interact with and shape this coupling. Addressing these questions will further clarify the role of respiration as a central organizing rhythm in brain-body interactions.

# References


Ainley, V., Apps, M. A. J., Fotopoulou, A., & Tsakiris, M. (2016). 'Bodily precision': A predictive coding account of individual differences in interoceptive accuracy. *Philosophical Transactions of the Royal Society B: Biological Sciences*, *371*(1708), 20160003. https://doi.org/10.1098/rstb.2016.0003

Al, E., Iliopoulos, F., Forschack, N., Nierhaus, T., Grund, M., Motyka, P., Gaebler, M., Nikulin, V. V., & Villringer, A. (2020). Heart–brain interactions shape somatosensory perception and evoked potentials. *Proceedings of the National Academy of Sciences*, *117*(19), 10575–10584. https://doi.org/10.1073/pnas.1915629117

Al, E., Iliopoulos, F., Nikulin, V. V., & Villringer, A. (2021). Heartbeat and somatosensory perception. *NeuroImage*, *238*, 118247. https://doi.org/10.1016/j.neuroimage.2021.118247

Alday, P. M. (2019). How much baseline correction do we need in ERP research? Extended GLM model can replace baseline correction while lifting its limits. *Psychophysiology*, *56*(12), e13451. https://doi.org/10.1111/psyp.13451

Allen, M., Levy, A., Parr, T., & Friston, K. J. (2022). In the Body's Eye: The computational anatomy of interoceptive inference. *PLOS Computational Biology*, *18*(9), e1010490. https://doi.org/10.1371/journal.pcbi.1010490

Allen, M., Varga, S., & Heck, D. H. (2023). Respiratory rhythms of the predictive mind. *Psychological Review*, *130*(4), 1066–1080. https://doi.org/10.1037/rev0000391

Ambrosini, E., Finotti, G., Azevedo, R. T., Tsakiris, M., & Ferri, F. (2019). Seeing myself through my heart: Cortical processing of a single heartbeat speeds up self-face recognition. *Biological Psychology*, *144*, 64–73. https://doi.org/10.1016/j.biopsycho.2019.03.006

Anderson, M., & Braak, C. T. (2003). Permutation tests for multi-factorial analysis of variance. *Journal of Statistical Computation and Simulation*, *73*(2), 85–113. https://doi.org/10.1080/00949650215733

Andresen, M. C., & Kunze, D. L. (1994). Nucleus Tractus Solitarius—Gateway to Neural Circulatory Control. *Annual Review of Physiology*, *56*(1), 93–116. https://doi.org/10.1146/annurev.ph.56.030194.000521

Antonacci, Y., Barà, C., Zaccaro, A., Ferri, F., Pernice, R., & Faes, L. (2023). Time-varying information measures: An adaptive estimation of information storage with application to brain-heart interactions. *Frontiers in Network Physiology*, *3*, 1242505. https://doi.org/10.3389/fnetp.2023.1242505

Ardizzi, M., Ambrosecchia, M., Buratta, L., Ferri, F., Peciccia, M., Donnari, S., Mazzeschi, C., & Gallese, V. (2016a). Interoception and Positive Symptoms in Schizophrenia. *Frontiers in Human Neuroscience*, *10*. https://doi.org/10.3389/fnhum.2016.00379

Ardizzi, M., Ambrosecchia, M., Buratta, L., Ferri, F., Peciccia, M., Donnari, S., Mazzeschi, C., & Gallese, V. (2016b). Interoception and Positive Symptoms in Schizophrenia. *Frontiers in Human Neuroscience*, *10*. https://doi.org/10.3389/fnhum.2016.00379

Ardizzi, M., & Ferri, F. (2018). Interoceptive influences on peripersonal space boundary. *Cognition*, *177*, 79–86. https://doi.org/10.1016/j.cognition.2018.04.001

Arsenault, M., Ladouceur, A., Lehmann, A., Rainville, P., & Piché, M. (2013). Pain modulation induced by respiration: Phase and frequency effects. *Neuroscience*, *252*, 501–511. https://doi.org/10.1016/j.neuroscience.2013.07.048

Arshamian, A., Iravani, B., Majid, A., & Lundström, J. N. (2018). Respiration Modulates Olfactory Memory Consolidation in Humans. *The Journal of Neuroscience*, *38*(48), 10286–10294. https://doi.org/10.1523/JNEUROSCI.3360-17.2018

Azzalini, D., Rebollo, I., & Tallon-Baudry, C. (2019). Visceral Signals Shape Brain Dynamics and Cognition. *Trends in Cognitive Sciences*, *23*(6), 488–509. https://doi.org/10.1016/j.tics.2019.03.007

Babo-Rebelo, M., Buot, A., & Tallon-Baudry, C. (2016). Neural responses to heartbeats distinguish self from other during imagination. *NeuroImage*, *191*, 10–20. https://doi.org/10.1016/j.neuroimage.2019.02.012

Babo-Rebelo, M., Wolpert, N., Adam, C., Hasboun, D., & Tallon-Baudry, C. (2016). Is the cardiac monitoring function related to the self in both the default network and right anterior insula? *Philosophical Transactions of the Royal Society of London. Series B, Biological Sciences*, *371*(1708), 20160004. https://doi.org/10.1098/rstb.2016.0004

Baer, R. A., Smith, G. T., Hopkins, J., Krietemeyer, J., & Toney, L. (2006). Using Self-Report Assessment Methods to Explore Facets of Mindfulness. *Assessment*, *13*(1), 27–45. https://doi.org/10.1177/1073191105283504

Bailey, N. W., Biabani, M., Hill, A. T., Miljevic, A., Rogasch, N. C., McQueen, B., Murphy, O. W., & Fitzgerald, P. B. (2023). Introducing RELAX: An automated pre-processing pipeline for cleaning EEG data - Part 1: Algorithm and application to oscillations. *Clinical Neurophysiology*, *149*, 178–201. https://doi.org/10.1016/j.clinph.2023.01.017

Bailey, N. W., Hill, A. T., Biabani, M., Murphy, O. W., Rogasch, N. C., McQueen, B., Miljevic, A., & Fitzgerald, P. B. (2023). RELAX part 2: A fully automated EEG data cleaning algorithm that is applicable to Event-Related-Potentials. *Clinical Neurophysiology*, *149*, 202–222. https://doi.org/10.1016/j.clinph.2023.01.018

Balnis, J., Madrid, A., Hogan, K. J., Drake, L. A., Chieng, H. C., Tiwari, A., Vincent, C. E., Chopra, A., Vincent, P. A., Robek, M. D., Singer, H. A., Alisch, R. S., & Jaitovich, A. (2021). Blood DNA methylation and COVID-19 outcomes. *Clinical Epigenetics*, *13*(1), 118. https://doi.org/10.1186/s13148-021-01102-9

Baltazar, M., Grezes, J., Geoffray, M.-M., Picq, J.-L., & Conty, L. (2021). Neural correlates of interoceptive accuracy: Beyond cardioception. *The European Journal of Neuroscience*, *54*(10), 7642–7653. https://doi.org/10.1111/ejn.15510

Barà, C., Zaccaro, A., Antonacci, Y., Dalla Riva, M., Busacca, A., Ferri, F., Faes, L., & Pernice, R. (2023). Local and global measures of information storage for the assessment of heartbeat-evoked cortical responses. *Biomedical Signal Processing and Control*, *86*, 105315. https://doi.org/10.1016/j.bspc.2023.105315

Baranauskas, M., Grabauskaitė, A., & Griškova-Bulanova, I. (2017). Brain responses and self-reported indices of interoception: Heartbeat evoked potentials are inversely associated with worrying about body sensations. *Physiology & Behavior*, *180*, 1–7. https://doi.org/10.1016/j.physbeh.2017.07.032

Barnes, P. J., Szefler, S. J., Reddel, H. K., & Chipps, B. E. (2019). Symptoms and perception of airway obstruction in asthmatic patients: Clinical implications for use of reliever medications. *Journal of Allergy and Clinical Immunology*, *144*(5), 1180–1186. https://doi.org/10.1016/j.jaci.2019.06.040

Barrett, L. F., & Simmons, W. K. (2015). Interoceptive predictions in the brain. *Nature Reviews Neuroscience*, *16*(7), 419–429. https://doi.org/10.1038/nrn3950

Bastos, A. M., Usrey, W. M., Adams, R. A., Mangun, G. R., Fries, P., & Friston, K. J. (2012). Canonical Microcircuits for Predictive Coding. *Neuron*, *76*(4), 695–711. https://doi.org/10.1016/j.neuron.2012.10.038

Belli, F., & Fischer, M. H. (2024). Breathing shifts visuo-spatial attention. *Cognition*, *243*, 105685. https://doi.org/10.1016/j.cognition.2023.105685

Benjamini, Y., & Yekutieli, D. (2001). The Control of the False Discovery Rate in Multiple Testing under Dependency. *The Annals of Statistics*, *29*(4), 1165–1188. JSTOR.

Berchicci, M., Menotti, F., Macaluso, A., & Di Russo, F. (2013). The neurophysiology of central and peripheral fatigue during sub-maximal lower limb isometric contractions. *Frontiers in Human Neuroscience*, *7*, 135. https://doi.org/10.3389/fnhum.2013.00135

Berens, P. (2009). **CircStat**: A *MATLAB* Toolbox for Circular Statistics. *Journal of Statistical Software*, *31*(10). https://doi.org/10.18637/jss.v031.i10

Bernasconi, P., & Kohl, J. (1993). Analysis of co-ordination between breathing and exercise rhythms in man. *The Journal of Physiology*, *471*, 693–706. https://doi.org/10.1113/jphysiol.1993.sp019923

Berntson, G. G., & Khalsa, S. S. (2021). Neural Circuits of Interoception. *Trends in Neurosciences*, *44*(1), 17–28. https://doi.org/10.1016/j.tins.2020.09.011

Betka, S., Łukowska, M., Silva, M., King, J., Garfinkel, S., & Critchley, H. (2021). Evidence toward the potential absence of relationship between temporal and spatial heartbeats perception. *Scientific Reports*, *11*(1), 10759. https://doi.org/10.1038/s41598-021-90334-z

Billeci, L., Faraguna, U., Santarcangelo, E. L., d'Ascanio, P., Varanini, M., & Sebastiani, L. (2021). Heartbeat-Evoked Cortical Potential during Sleep and Interoceptive Sensitivity: A Matter of Hypnotizability. *Brain Sciences*, *11*(8), 1089. https://doi.org/10.3390/brainsci11081089

Blankenship, C. M., Hunter, L. L., Keefe, D. H., Feeney, M. P., Brown, D. K., McCune, A., Fitzpatrick, D. F., & Lin, L. (2018). Optimizing Clinical Interpretation of Distortion Product Otoacoustic Emissions in Infants. *Ear & Hearing*, *39*(6), 1075–1090. https://doi.org/10.1097/AUD.0000000000000562

Bonaz, B., Lane, R. D., Oshinsky, M. L., Kenny, P. J., Sinha, R., Mayer, E. A., & Critchley, H. D. (2021). Diseases, Disorders, and Comorbidities of Interoception. *Trends in Neurosciences*, *44*(1), 39–51. https://doi.org/10.1016/j.tins.2020.09.009

Bortoli, L., & Robazza, C. (1997). Italian Version of the Perceived Physical Ability Scale. *Perceptual and Motor Skills*, *85*(1), 187–192. https://doi.org/10.2466/pms.1997.85.1.187

Boyadzhieva, A., & Kayhan, E. (2021). Keeping the Breath in Mind: Respiration, Neural Oscillations, and the Free Energy Principle. *Frontiers in Neuroscience*, *15*, 647579. https://doi.org/10.3389/fnins.2021.647579

Brændholt, M., Kluger, D. S., Varga, S., Heck, D. H., Gross, J., & Allen, M. G. (2023). Breathing in waves: Understanding respiratory-brain coupling as a gradient of predictive oscillations. *Neuroscience & Biobehavioral Reviews*, *152*, 105262. https://doi.org/10.1016/j.neubiorev.2023.105262

Brændholt, M., Nikolova, N., Vejlø, M., Banellis, L., Fardo, F., Kluger, D. S., & Allen, M. (2025). The respiratory cycle modulates distinct dynamics of affective and perceptual decision-making. *PLOS Computational Biology*, *21*(5), e1013086. https://doi.org/10.1371/journal.pcbi.1013086

Brecher, G. A., & Hubay, C. A. (1955). Pulmonary Blood Flow and Venous Return During Spontaneous Respiration. *Circulation Research*, *3*(2), 210–214. https://doi.org/10.1161/01.RES.3.2.210

Brener, J., & Kluvitse, C. (1988). Heartbeat detection: Judgments of the simultaneity of external stimuli and heartbeats. *Psychophysiology*, *25*(5), 554–561. https://doi.org/10.1111/j.1469-8986.1988.tb01891.x

Brener, J., & Ring, C. (2016). Towards a psychophysics of interoceptive processes: The measurement of heartbeat detection. *Philosophical Transactions of the Royal Society of London. Series B, Biological Sciences*, *371*(1708), 20160015. https://doi.org/10.1098/rstb.2016.0015

Brener, J., Ring, C., & Liu, X. (1994). Effects of data limitations on heartbeat detection in the method of constant stimuli. *Psychophysiology*, *31*(3), 309–312. https://doi.org/10.1111/j.1469-8986.1994.tb02219.x

Brown, H. R., & Friston, K. J. (2012). Dynamic causal modelling of precision and synaptic gain in visual perception—An EEG study. *NeuroImage*, *63*(1), 223–231. https://doi.org/10.1016/j.neuroimage.2012.06.044

Buot, A., Azzalini, D., Chaumon, M., & Tallon-Baudry, C. (2021). Does stroke volume influence heartbeat evoked responses? *Biological Psychology*, *165*, 108165. https://doi.org/10.1016/j.biopsycho.2021.108165

Burri, A., Marinova, Z., Robinson, M. D., Kühnel, B., Waldenberger, M., Wahl, S., Kunze, S., Gieger, C., Livshits, G., & Williams, F. (2016). Are Epigenetic Factors Implicated in Chronic Widespread Pain? *PLOS ONE*, *11*(11), e0165548. https://doi.org/10.1371/journal.pone.0165548

Cabrera, A., Kolacz, J., Pailhez, G., Bulbena-Cabre, A., Bulbena, A., & Porges, S. W. (2018). Assessing body awareness and autonomic reactivity: Factor structure and psychometric properties of the Body Perception Questionnaire-Short Form (BPQ-SF). *International Journal of Methods in Psychiatric Research*, *27*(2), e1596. https://doi.org/10.1002/mpr.1596

Calderone, D. J., Lakatos, P., Butler, P. D., & Castellanos, F. X. (2014). Entrainment of neural oscillations as a modifiable substrate of attention. *Trends in Cognitive Sciences*, *18*(6), 300–309. https://doi.org/10.1016/j.tics.2014.02.005

Calì, G., Ambrosini, E., Picconi, L., Mehling, W. E., & Committeri, G. (2015). Investigating the relationship between interoceptive accuracy, interoceptive awareness, and emotional susceptibility. *Frontiers in Psychology*, *6*. https://doi.org/10.3389/fpsyg.2015.01202

Cameron, O. G. (2001). Interoception: The Inside Story—A Model for Psychosomatic Processes: *Psychosomatic Medicine*, *63*(5), 697–710. https://doi.org/10.1097/00006842-200109000-00001

Canales-Johnson, A., Silva, C., Huepe, D., Rivera-Rei, Á., Noreika, V., Garcia, M. D. C., Silva, W., Ciraolo, C., Vaucheret, E., Sedeño, L., Couto, B., Kargieman, L., Baglivo, F., Sigman, M., Chennu, S., Ibáñez, A., Rodríguez, E., & Bekinschtein, T. A. (2015). Auditory Feedback Differentially Modulates Behavioral and Neural Markers of Objective and Subjective Performance When Tapping to Your Heartbeat. *Cerebral Cortex*, *25*(11), 4490–4503. https://doi.org/10.1093/cercor/bhv076

Candia-Rivera, D., Catrambone, V., & Valenza, G. (2021). The role of electroencephalography electrical reference in the assessment of functional brain–heart interplay: From methodology to user guidelines. *Journal of Neuroscience Methods*, *360*, 109269. https://doi.org/10.1016/j.jneumeth.2021.109269

Candia-Rivera, D., Sappia, M. S., Horschig, J. M., Colier, W. N. J. M., & Valenza, G. (2022). Confounding effects of heart rate, breathing rate, and frontal fNIRS on interoception. *Scientific Reports*, *12*(1), 20701. https://doi.org/10.1038/s41598-022-25119-z

Caseras, X., Murphy, K., Mataix-Cols, D., López-Solà, M., Soriano-Mas, C., Ortriz, H., Pujol, J., & Torrubia, R. (2013). Anatomical and functional overlap within the insula and anterior cingulate cortex during interoception and phobic symptom provocation. *Human Brain Mapping*, *34*(5), 1220–1229. https://doi.org/10.1002/hbm.21503

Castro de Moura, M., Davalos, V., Planas-Serra, L., Alvarez-Errico, D., Arribas, C., Ruiz, M., Aguilera-Albesa, S., Troya, J., Valencia-Ramos, J., Vélez-Santamaria, V., Rodríguez-Palmero, A., Villar-Garcia, J., Horcajada, J. P., Albu, S., Casasnovas, C., Rull, A., Reverte, L., Dietl, B., Dalmau, D., … Esteller, M. (2021). Epigenome-wide association study of COVID-19 severity with respiratory failure. *EBioMedicine*, *66*, 103339. https://doi.org/10.1016/j.ebiom.2021.103339

Celarain, N., & Tomas-Roig, J. (2020). Aberrant DNA methylation profile exacerbates inflammation and neurodegeneration in multiple sclerosis patients. *Journal of Neuroinflammation*, *17*(1), 21. https://doi.org/10.1186/s12974-019-1667-1

Cerritelli, F., Galli, M., Consorti, G., D'Alessandro, G., Kolacz, J., & Porges, S. W. (2021). Cross-cultural adaptation and psychometric properties of the Italian version of the Body Perception Questionnaire. *PloS One*, *16*(5), e0251838. https://doi.org/10.1371/journal.pone.0251838

Ceunen, E., Van Diest, I., & Vlaeyen, J. W. S. (2013). Accuracy and awareness of perception: Related, yet distinct (commentary on Herbert et al., 2012). *Biological Psychology*, *92*(2), 426–427. https://doi.org/10.1016/j.biopsycho.2012.09.012

Ceunen, E., Vlaeyen, J. W. S., & Van Diest, I. (2016). On the Origin of Interoception. *Frontiers in Psychology*, *7*. https://doi.org/10.3389/fpsyg.2016.00743

Chan, P.-Y. S., Lee, L.-Y., & Davenport, P. W. (2024). Neural mechanisms of respiratory interoception. *Autonomic Neuroscience*, *253*, 103181. https://doi.org/10.1016/j.autneu.2024.103181

Chaudhuri, A., & Behan, P. O. (2004). Fatigue in neurological disorders. *Lancet (London, England)*, *363*(9413), 978–988. https://doi.org/10.1016/S0140-6736(04)15794-2

Chen, W. G., Schloesser, D., Arensdorf, A. M., Simmons, J. M., Cui, C., Valentino, R., Gnadt, J. W., Nielsen, L., Hillaire-Clarke, C. S., Spruance, V., Horowitz, T. S., Vallejo, Y. F., & Langevin, H. M. (2021). The Emerging Science of Interoception: Sensing, Integrating, Interpreting, and Regulating Signals within the Self. *Trends in Neurosciences*, *44*(1), 3–16. https://doi.org/10.1016/j.tins.2020.10.007

Ciampi de Andrade, D., Maschietto, M., Galhardoni, R., Gouveia, G., Chile, T., Victorino Krepischi, A. C., Dale, C. S., Brunoni, A. R., Parravano, D. C., Cueva Moscoso, A. S., Raicher, I., Kaziyama, H. H. S., Teixeira, M. J., & Brentani, H. P. (2017). Epigenetics insights into chronic pain: DNA hypomethylation in fibromyalgia-a controlled pilot-study. *Pain*, *158*(8), 1473–1480. https://doi.org/10.1097/j.pain.0000000000000932

Citi, L., Brown, E. N., & Barbieri, R. (2012). A Real-Time Automated Point-Process Method for the Detection and Correction of Erroneous and Ectopic Heartbeats. *IEEE Transactions on Biomedical Engineering*, *59*(10), 2828–2837. https://doi.org/10.1109/TBME.2012.2211356

Coll, M.-P., Hobson, H., Bird, G., & Murphy, J. (2021). Systematic review and meta-analysis of the relationship between the heartbeat-evoked potential and interoception. *Neuroscience & Biobehavioral Reviews*, *122*, 190–200. https://doi.org/10.1016/j.neubiorev.2020.12.012

Conconi, F., Ferrari, M., Ziglio, P. G., Droghetti, P., & Codeca, L. (1982). Determination of the anaerobic threshold by a noninvasive field test in runners. *Journal of Applied Physiology: Respiratory, Environmental and Exercise Physiology*, *52*(4), 869–873. https://doi.org/10.1152/jappl.1982.52.4.869

Cooper, N. R., Croft, R. J., Dominey, S. J. J., Burgess, A. P., & Gruzelier, J. H. (2003). Paradox lost? Exploring the role of alpha oscillations during externally vs. internally directed attention and the implications for idling and inhibition hypotheses. *International Journal of Psychophysiology*, *47*(1), 65–74. https://doi.org/10.1016/S0167-8760(02)00107-1

Corcoran, A. W., Perrykkad, K., Feuerriegel, D., & Robinson, J. E. (2023). Body as First Teacher: The Role of Rhythmic Visceral Dynamics in Early Cognitive Development. *Perspectives on Psychological Science*, *20*(1), 45–75. https://doi.org/10.1177/17456916231185343

Corcoran, A. W., Pezzulo, G., & Hohwy, J. (2018). Commentary: Respiration-Entrained Brain Rhythms Are Global but Often Overlooked. *Frontiers in Systems Neuroscience*, *12*, 25. https://doi.org/10.3389/fnsys.2018.00025

Corley, M. J., Pang, A. P. S., Dody, K., Mudd, P. A., Patterson, B. K., Seethamraju, H., Bram, Y., Peluso, M. J., Torres, L., Iyer, N. S., Premeaux, T. A., Yeung, S. T., Chandar, V., Borczuk, A., Schwartz, R. E., Henrich, T. J., Deeks, S. G., Sacha, J. B., & Ndhlovu, L. C. (2021). Genome-wide DNA methylation profiling of peripheral blood reveals an epigenetic

signature associated with severe COVID-19. *Journal of Leukocyte Biology*, *110*(1), 21–26. https://doi.org/10.1002/JLB.5HI0720-466R

Craig, A. D. (2002). How do you feel? Interoception: the sense of the physiological condition of the body. *Nature Reviews Neuroscience*, *3*(8), 655–666. https://doi.org/10.1038/nrn894

Craig, A. D. B. (2009). How do you feel--now? The anterior insula and human awareness. *Nature Reviews. Neuroscience*, *10*(1), 59–70. https://doi.org/10.1038/nrn2555

Criscuolo, A., Schwartze, M., & Kotz, S. A. (2022). Cognition through the lens of a body–brain dynamic system. *Trends in Neurosciences*, *45*(9), 667–677. https://doi.org/10.1016/j.tins.2022.06.004

Critchley, H. D., & Garfinkel, S. N. (2016). Bodily arousal differentially impacts stimulus processing and memory: Norepinephrine in interoception. *The Behavioral and Brain Sciences*, *39*, e205. https://doi.org/10.1017/S0140525X15001764

Critchley, H. D., & Harrison, N. A. (2013). Visceral influences on brain and behavior. *Neuron*, *77*(4), 624–638. https://doi.org/10.1016/j.neuron.2013.02.008

Critchley, H. D., Wiens, S., Rotshtein, P., Ohman, A., & Dolan, R. J. (2004). Neural systems supporting interoceptive awareness. *Nature Neuroscience*, *7*(2), 189–195. https://doi.org/10.1038/nn1176

Crivelli, D., & Balconi, M. (2025). Electrophysiological signature of interoceptive attention: A spectral and source localization analysis. *Cognitive, Affective, & Behavioral Neuroscience*, *25*(2), 402–414. https://doi.org/10.3758/s13415-024-01235-3

Crucianelli, L., Enmalm, A., & Ehrsson, H. H. (2022). Interoception as independent cardiac, thermosensory, nociceptive, and affective touch perceptual submodalities. *Biological Psychology*, *172*, 108355. https://doi.org/10.1016/j.biopsycho.2022.108355

Crucianelli, L., Krahé, C., Jenkinson, P. M., & Fotopoulou, A. (Katerina). (2018). Interoceptive ingredients of body ownership: Affective touch and cardiac awareness in the rubber hand illusion. *Cortex*, *104*, 180–192. https://doi.org/10.1016/j.cortex.2017.04.018

Dantas, J. L., Doria, C., Rossi, H., Rosa, G., Pietrangelo, T., Fanò-Illic, G., & Nakamura, F. Y. (2015). Determination of Blood Lactate Training Zone Boundaries With Rating of Perceived Exertion in Runners. *Journal of Strength and Conditioning Research*, *29*(2), 315–320. https://doi.org/10.1519/JSC.0000000000000639

Dantzer, R., Heijnen, C. J., Kavelaars, A., Laye, S., & Capuron, L. (2014). The neuroimmune basis of fatigue. *Trends in Neurosciences*, *37*(1), 39–46. https://doi.org/10.1016/j.tins.2013.10.003

Daoui, A., Karmouni, H., Sayyouri, M., & Qjidaa, H. (2022). New method for bio—Signals zero—Watermarking using quaternion shmaliy moments and short-time fourier transform. *Multimedia Tools and Applications*, *81*(12), 17369–17399. https://doi.org/10.1007/s11042-022-12660-2

Daubenmier, J., Sze, J., Kerr, C. E., Kemeny, M. E., & Mehling, W. (2013). Follow your breath: Respiratory interoceptive accuracy in experienced meditators. *Psychophysiology*, *50*(8), 777–789. https://doi.org/10.1111/psyp.12057

Del Negro, C. A., Funk, G. D., & Feldman, J. L. (2018). Breathing matters. *Nature Reviews Neuroscience*, *19*(6), 351–367. https://doi.org/10.1038/s41583-018-0003-6

Delorme, A., & Makeig, S. (2004). EEGLAB: An open source toolbox for analysis of single-trial EEG dynamics including independent component analysis. *Journal of Neuroscience Methods*, *134*(1), 9–21. https://doi.org/10.1016/j.jneumeth.2003.10.009

Desmedt, O., Luminet, O., & Corneille, O. (2018). The heartbeat counting task largely involves non-interoceptive processes: Evidence from both the original and an adapted counting task. *Biological Psychology*, *138*, 185–188. https://doi.org/10.1016/j.biopsycho.2018.09.004

Dhingra, R. R., Furuya, W. I., Yoong, Y. K., & Dutschmann, M. (2024). The pre-Bötzinger complex is necessary for the expression of inspiratory and post-inspiratory motor discharge of the vagus. *Respiratory Physiology & Neurobiology*, *320*, 104202. https://doi.org/10.1016/j.resp.2023.104202

Di Fronso, S., Aquino, A., Bondár, R. Z., Montesano, C., Robazza, C., & Bertollo, M. (2020). The influence of core affect on cyclo-ergometer endurance performance: Effects on performance outcomes and perceived exertion. *Journal of Sport and Health Science*, *9*(6), 578–586. https://doi.org/10.1016/j.jshs.2019.12.004

Di Lernia, D., Serino, S., Pezzulo, G., Pedroli, E., Cipresso, P., & Riva, G. (2018). Feel the Time. Time Perception as a Function of Interoceptive Processing. *Frontiers in Human Neuroscience*, *12*, 74. https://doi.org/10.3389/fnhum.2018.00074

Dirlich, G., Vogl, L., Plaschke, M., & Strian, F. (1997). Cardiac field effects on the EEG. *Electroencephalography and Clinical Neurophysiology*, *102*(4), 307–315. https://doi.org/10.1016/S0013-4694(96)96506-2

Edwards, L., Ring, C., McIntyre, D., & Carroll, D. (2001). Modulation of the human nociceptive flexion reflex across the cardiac cycle. *Psychophysiology*, *38*(4), 712–718. https://doi.org/10.1111/1469-8986.3840712

Eidelman-Rothman, M., Ben-Simon, E., Freche, D., Keil, A., Hendler, T., & Levit-Binnun, N. (2019). Sleepless and desynchronized: Impaired inter trial phase coherence of steady-state potentials following sleep deprivation. *NeuroImage*, *202*, 116055. https://doi.org/10.1016/j.neuroimage.2019.116055

Engelen, T., Schuhmann, T., Sack, A. T., & Tallon-Baudry, C. (2025). Cardiac, respiratory, and gastric rhythms independently modulate motor corticospinal excitability in humans. *PLOS Biology*, *23*(11), e3003478. https://doi.org/10.1371/journal.pbio.3003478

F. Wong, K., A. A. Massar, S., Chee, M. W. L., & Lim, J. (2018). Towards an Objective Measure of Mindfulness: Replicating and Extending the Features of the Breath-Counting Task. *Mindfulness*, *9*(5), 1402–1410. https://doi.org/10.1007/s12671-017-0880-1

Faes, L., Marinazzo, D., Stramaglia, S., Jurysta, F., Porta, A., & Giandomenico, N. (2016). Predictability decomposition detects the impairment of brain-heart dynamical networks during sleep disorders and their recovery with treatment. *Philosophical Transactions. Series A, Mathematical, Physical, and Engineering Sciences*, *374*(2067), 20150177. https://doi.org/10.1098/rsta.2015.0177

Faes, L., Nollo, G., Krohova, J., Czippelova, B., Turianikova, Z., & Javorka, M. (2017). Information transfer and information modification to identify the structure of cardiovascular and cardiorespiratory networks. *Annual International Conference of the IEEE Engineering in Medicine and Biology Society. IEEE Engineering in Medicine and Biology Society. Annual International Conference*, *2017*, 1563–1566. https://doi.org/10.1109/EMBC.2017.8037135

Fan, M., Liu, Z., Wei, A., Gao, R., Luan, P., & He, X. (2025). The Relationship Between Schizophrenia and Interoceptive Accuracy and Sensitivity: A Systematic Review and Meta-Analysis. *Neuropsychiatric Disease and Treatment*, *Volume 21*, 2307–2319. https://doi.org/10.2147/NDT.S545022

Farb, N. A. S., Segal, Z. V., & Anderson, A. K. (2013). Attentional Modulation of Primary Interoceptive and Exteroceptive Cortices. *Cerebral Cortex*, *23*(1), 114–126. https://doi.org/10.1093/cercor/bhr385

Farb, N. A. S., Zuo, Z., & Price, C. J. (2023). Interoceptive Awareness of the Breath Preserves Attention and Language Networks amidst Widespread Cortical Deactivation: A Within-Participant Neuroimaging Study. *Eneuro*, *10*(6), ENEURO.0088-23.2023. https://doi.org/10.1523/ENEURO.0088-23.2023

Faul, F., Erdfelder, E., Buchner, A., & Lang, A.-G. (2009). Statistical power analyses using G*Power 3.1: Tests for correlation and regression analyses. *Behavior Research Methods*, *41*(4), 1149–1160. https://doi.org/10.3758/BRM.41.4.1149

Feldman, H., & Friston, K. J. (2010). Attention, Uncertainty, and Free-Energy. *Frontiers in Human Neuroscience*, *4*. https://doi.org/10.3389/fnhum.2010.00215

Feldman, J. L. (1986). Neurophysiology of Breathing in Mammals. In R. Terjung (A c. Di), *Comprehensive Physiology* (1ª ed., pp. 463–524). Wiley. https://doi.org/10.1002/cphy.cp010409

Feldman, J. L., & Del Negro, C. A. (2006). Looking for inspiration: New perspectives on respiratory rhythm. *Nature Reviews Neuroscience*, *7*(3), 232–241. https://doi.org/10.1038/nrn1871

Fields, E. C., & Kuperberg, G. R. (2020). Having your cake and eating it too: Flexibility and power with mass univariate statistics for ERP data. *Psychophysiology*, *57*(2), e13468. https://doi.org/10.1111/psyp.13468

Fittipaldi, S., Abrevaya, S., Fuente, A. de la, Pascariello, G. O., Hesse, E., Birba, A., Salamone, P., Hildebrandt, M., Martí, S. A., Pautassi, R. M., Huepe, D., Martorell, M. M., Yoris, A., Roca, M., García, A. M., Sedeño, L., & Ibáñez, A. (2020). A multidimensional and multi-feature framework for cardiac interoception. *NeuroImage*, *212*, 116677. https://doi.org/10.1016/j.neuroimage.2020.116677

Flexman, J. E., Demaree, R. G., & Simpson, D. D. (1974). Respiratory phase and visual signal detection. *Perception & Psychophysics*, *16*(2), 337–339. https://doi.org/10.3758/BF03203952

Fló, E., Belloli, L., Cabana, Á., Ruyant-Belabbas, A., Jodaitis, L., Valente, M., Rohaut, B., Naccache, L., Rosanova, M., Comanducci, A., Andrillon, T., & Sitt, J. (2024). Predicting

attentional focus: Heartbeat-evoked responses and brain dynamics during interoceptive and exteroceptive processing. *PNAS Nexus*, *3*(12), pgae531. https://doi.org/10.1093/pnasnexus/pgae531

Flynn, D. M., & Clemens, W. J. (1988). On the Validity of Heartbeat Tracking Tasks. *Psychophysiology*, *25*(1), 92–96. https://doi.org/10.1111/j.1469-8986.1988.tb00965.x

Fontanini, A., & Bower, J. M. (2006). Slow-waves in the olfactory system: An olfactory perspective on cortical rhythms. *Trends in Neurosciences*, *29*(8), 429–437. https://doi.org/10.1016/j.tins.2006.06.013

Forkmann, T., Scherer, A., Meessen, J., Michal, M., Schächinger, H., Vögele, C., & Schulz, A. (2016). Making sense of what you sense: Disentangling interoceptive awareness, sensibility and accuracy. *International Journal of Psychophysiology*, *109*, 71–80. https://doi.org/10.1016/j.ijpsycho.2016.09.019

Fox, S. M., Naughton, J. P., & Haskell, W. L. (1971). Physical activity and the prevention of coronary heart disease. *Annals of Clinical Research*, *3*(6), 404–432.

Foxe, J. J., & Snyder, A. C. (2011). The Role of Alpha-Band Brain Oscillations as a Sensory Suppression Mechanism during Selective Attention. *Frontiers in Psychology*, *2*. https://doi.org/10.3389/fpsyg.2011.00154

Friston, K. J. (2019). Waves of prediction. *PLOS Biology*, *17*(10), e3000426. https://doi.org/10.1371/journal.pbio.3000426

Friston, K. J., Bastos, A. M., Pinotsis, D., & Litvak, V. (2015). LFP and oscillations—What do they tell us? *Current Opinion in Neurobiology*, *31*, 1–6. https://doi.org/10.1016/j.conb.2014.05.004

Gallego, J., Perruchet, P., & Camus, J. (1991). Assessing Attentional Control of Breathing by Reaction Time. *Psychophysiology*, *28*(2), 217–224. https://doi.org/10.1111/j.1469-8986.1991.tb00413.x

Gallucci, M. (2019). *GAMLj: General analyses for linear models. [Jamovi module]* [Software]. https://gamlj.github.io/

García-Cordero, I., Esteves, S., Mikulan, E. P., Hesse, E., Baglivo, F. H., Silva, W., García, M. D. C., Vaucheret, E., Ciraolo, C., García, H. S., Adolfi, F., Pietto, M., Herrera, E., Legaz, A., Manes, F., García, A. M., Sigman, M., Bekinschtein, T. A., Ibáñez, A., & Sedeño, L. (2017). Attention, in and Out: Scalp-Level and Intracranial EEG Correlates of Interoception and Exteroception. *Frontiers in Neuroscience*, *11*, 411. https://doi.org/10.3389/fnins.2017.00411

Garfinkel, S. N., & Critchley, H. D. (2016). Threat and the Body: How the Heart Supports Fear Processing. *Trends in Cognitive Sciences*, *20*(1), 34–46. https://doi.org/10.1016/j.tics.2015.10.005

Garfinkel, S. N., Manassei, M. F., Hamilton-Fletcher, G., In Den Bosch, Y., Critchley, H. D., & Engels, M. (2016). Interoceptive dimensions across cardiac and respiratory axes. *Philosophical Transactions of the Royal Society B: Biological Sciences*, *371*(1708), 20160014. https://doi.org/10.1098/rstb.2016.0014

Garfinkel, S. N., Minati, L., Gray, M. A., Seth, A. K., Dolan, R. J., & Critchley, H. D. (2014). Fear from the Heart: Sensitivity to Fear Stimuli Depends on Individual Heartbeats. *The Journal of Neuroscience*, *34*(19), 6573–6582. https://doi.org/10.1523/JNEUROSCI.3507-13.2014

Garfinkel, S. N., Seth, A. K., Barrett, A. B., Suzuki, K., & Critchley, H. D. (2015). Knowing your own heart: Distinguishing interoceptive accuracy from interoceptive awareness. *Biological Psychology*, *104*, 65–74. https://doi.org/10.1016/j.biopsycho.2014.11.004

Giovannini, C., Giromini, L., Bonalume, L., Tagini, A., Lang, M., & Amadei, G. (2014). The Italian Five Facet Mindfulness Questionnaire: A Contribution to its Validity and Reliability. *Journal of Psychopathology and Behavioral Assessment*, *36*(3), 415–423. https://doi.org/10.1007/s10862-013-9403-0

Goheen, J., Wolman, A., Angeletti, L. L., Wolff, A., Anderson, J. A. E., & Northoff, G. (2024). Dynamic mechanisms that couple the brain and breathing to the external environment. *Communications Biology*, *7*(1), 938. https://doi.org/10.1038/s42003-024-06642-3

Gonzalez Campo, C., Salamone, P. C., Rodríguez-Arriagada, N., Richter, F., Herrera, E., Bruno, D., Pagani Cassara, F., Sinay, V., García, A. M., Ibáñez, A., & Sedeño, L. (2020). Fatigue in multiple sclerosis is associated with multimodal interoceptive abnormalities. *Multiple Sclerosis (Houndmills, Basingstoke, England)*, *26*(14), 1845–1853. https://doi.org/10.1177/1352458519888881

Grabauskaitė, A., Baranauskas, M., & Griškova-Bulanova, I. (2017). Interoception and gender: What aspects should we pay attention to? *Consciousness and Cognition*, *48*, 129–137. https://doi.org/10.1016/j.concog.2016.11.002

Gray, M. A., Taggart, P., Sutton, P. M., Groves, D., Holdright, D. R., Bradbury, D., Brull, D., & Critchley, H. D. (2007). A cortical potential reflecting cardiac function. *Proceedings of the National Academy of Sciences*, *104*(16), 6818–6823. https://doi.org/10.1073/pnas.0609509104

Green, D. M., & Swets, J. A. (1966). *Signal Detection Theory and Psychophysics*. John Wiley.

Greenhouse-Tucknott, A., Butterworth, J. B., Wrightson, J. G., Smeeton, N. J., Critchley, H. D., Dekerle, J., & Harrison, N. A. (2022). Toward the unity of pathological and exertional fatigue: A predictive processing model. *Cognitive, Affective & Behavioral Neuroscience*, *22*(2), 215–228. https://doi.org/10.3758/s13415-021-00958-x

Groppe, D. M., Urbach, T. P., & Kutas, M. (2011a). Mass univariate analysis of event-related brain potentials/fields I: A critical tutorial review. *Psychophysiology*, *48*(12), 1711–1725. https://doi.org/10.1111/j.1469-8986.2011.01273.x

Groppe, D. M., Urbach, T. P., & Kutas, M. (2011b). Mass univariate analysis of event-related brain potentials/fields II: Simulation studies. *Psychophysiology*, *48*(12), 1726–1737. https://doi.org/10.1111/j.1469-8986.2011.01272.x

Grossi, E., Groth, N., Mosconi, P., Cerutti, R., Pace, F., Compare, A., & Apolone, G. (2006). Development and validation of the short version of the Psychological General Well-Being Index (PGWB-S). *Health and Quality of Life Outcomes*, *4*(1), 88. https://doi.org/10.1186/1477-7525-4-88

Grund, M., Al, E., Pabst, M., Dabbagh, A., Stephani, T., Nierhaus, T., Gaebler, M., & Villringer, A. (2022). Respiration, Heartbeat, and Conscious Tactile Perception. *The Journal of Neuroscience*, *42*(4), 643–656. https://doi.org/10.1523/JNEUROSCI.0592-21.2021

Hari, R., Karhu, J., Hämäläinen, M., Knuutila, J., Salonen, O., Sams, M., & Vilkman, V. (1993). Functional organization of the human first and second somatosensory cortices: A neuromagnetic study. *The European Journal of Neuroscience*, *5*(6), 724–734. https://doi.org/10.1111/j.1460-9568.1993.tb00536.x

Harrison, O. K., Köchli, L., Marino, S., Luechinger, R., Hennel, F., Brand, K., Hess, A. J., Frässle, S., Iglesias, S., Vinckier, F., Petzschner, F. H., Harrison, S. J., & Stephan, K. E. (2021). Interoception of breathing and its relationship with anxiety. *Neuron*, *109*(24), 4080-4093.e8. https://doi.org/10.1016/j.neuron.2021.09.045

Hart, N., McGowan, J., Minati, L., & Critchley, H. D. (2013). Emotional Regulation and Bodily Sensation: Interoceptive Awareness Is Intact in Borderline Personality Disorder. *Journal of Personality Disorders*, *27*(4), 506–518. https://doi.org/10.1521/pedi_2012_26_049

Harting, C., Hehemann, L., Stetza, L., & Kayser, C. (2025). Respiration shapes response speed and accuracy with a systematic time lag. *Proceedings of the Royal Society B: Biological Sciences*, *292*(2044), 20242566. https://doi.org/10.1098/rspb.2024.2566

Haut, B., Nonclercq, A., Buess, A., Rabineau, J., Rigaut, C., & Sobac, B. (2021). Comprehensive Analysis of Heat and Water Exchanges in the Human Lungs. *Frontiers in Physiology*, *12*, 649497. https://doi.org/10.3389/fphys.2021.649497

Helliwell, A. M., Sweetman, E. C., Stockwell, P. A., Edgar, C. D., Chatterjee, A., & Tate, W. P. (2020). Changes in DNA methylation profiles of myalgic encephalomyelitis/chronic fatigue syndrome patients reflect systemic dysfunctions. *Clinical Epigenetics*, *12*(1), 167. https://doi.org/10.1186/s13148-020-00960-z

Herrero, J. L., Khuvis, S., Yeagle, E., Cerf, M., & Mehta, A. D. (2018). Breathing above the brain stem: Volitional control and attentional modulation in humans. *Journal of Neurophysiology*, *119*(1), 145–159. https://doi.org/10.1152/jn.00551.2017

Hess, A. J., Von Werder, D., Harrison, O. K., Heinzle, J., & Stephan, K. E. (2024). Refining the Allostatic Self-Efficacy Theory of Fatigue and Depression Using Causal Inference. *Entropy*, *26*(12), 1127. https://doi.org/10.3390/e26121127

Hickman, L., Seyedsalehi, A., Cook, J. L., Bird, G., & Murphy, J. (2020). The relationship between heartbeat counting and heartbeat discrimination: A meta-analysis. *Biological Psychology*, *156*, 107949. https://doi.org/10.1016/j.biopsycho.2020.107949

Hölzel, B. K., Lazar, S. W., Gard, T., Schuman-Olivier, Z., Vago, D. R., & Ott, U. (2011). How Does Mindfulness Meditation Work? Proposing Mechanisms of Action From a Conceptual and Neural Perspective. *Perspectives on Psychological Science*, *6*(6), 537–559. https://doi.org/10.1177/1745691611419671

Huber, J. E., Chandrasekaran, B., & Wolstencroft, J. J. (2005). Changes to respiratory mechanisms during speech as a result of different cues to increase loudness. *Journal of Applied Physiology*, *98*(6), 2177–2184. https://doi.org/10.1152/japplphysiol.01239.2004

Huijbers, W., Pennartz, C. M. A., Beldzik, E., Domagalik, A., Vinck, M., Hofman, W. F., Cabeza, R., & Daselaar, S. M. (2014). Respiration phase-locks to fast stimulus presentations: Implications for the interpretation of posterior midline “deactivations”. *Human Brain Mapping*, *35*(9), 4932–4943. https://doi.org/10.1002/hbm.22523

Hunt, K. J., & Hurni, C. C. (2019). Robust control of heart rate for cycle ergometer exercise. *Medical & Biological Engineering & Computing*, *57*(11), 2471–2482. https://doi.org/10.1007/s11517-019-02034-6

Hyvarinen, A. (1999). Fast and robust fixed-point algorithms for independent component analysis. *IEEE Transactions on Neural Networks*, *10*(3), 626–634. https://doi.org/10.1109/72.761722

Iwabe, T., Ozaki, I., & Hashizume, A. (2014). The respiratory cycle modulates brain potentials, sympathetic activity, and subjective pain sensation induced by noxious stimulation. *Neuroscience Research*, *84*, 47–59. https://doi.org/10.1016/j.neures.2014.03.003

Jensen, O., & Mazaheri, A. (2010). Shaping Functional Architecture by Oscillatory Alpha Activity: Gating by Inhibition. *Frontiers in Human Neuroscience*, *4*. https://doi.org/10.3389/fnhum.2010.00186

Jiang, H., He, B., Guo, X., Wang, X., Guo, M., Wang, Z., Xue, T., Li, H., Xu, T., Ye, S., Suma, D., Tong, S., & Cui, D. (2020). Brain–Heart Interactions Underlying Traditional Tibetan Buddhist Meditation. *Cerebral Cortex*, bhz095. https://doi.org/10.1093/cercor/bhz095

Johannknecht, M., & Kayser, C. (2022). The influence of the respiratory cycle on reaction times in sensory-cognitive paradigms. *Scientific Reports*, *12*(1), 2586. https://doi.org/10.1038/s41598-022-06364-8

Judah, M. R., Shurkova, E. Y., Hager, N. M., White, E. J., Taylor, D. L., & Grant, D. M. (2018). The relationship between social anxiety and heartbeat evoked potential amplitude. *Biological Psychology*, *139*, 1–7. https://doi.org/10.1016/j.biopsycho.2018.09.013

Junghöfer, M., Elbert, T., Tucker, D. M., & Rockstroh, B. (2000). Statistical control of artifacts in dense array EEG/MEG studies. *Psychophysiology*, *37*(4), 523–532. https://doi.org/10.1111/1469-8986.3740523

Kanai, R., Komura, Y., Shipp, S., & Friston, K. (2015). Cerebral hierarchies: Predictive processing, precision and the pulvinar. *Philosophical Transactions of the Royal Society B: Biological Sciences*, *370*(1668), 20140169. https://doi.org/10.1098/rstb.2014.0169

Karjalainen, S., Kujala, J., & Parviainen, T. (2025). Neural activity is modulated by spontaneous and volitionally controlled breathing. *Biological Psychology*, *197*, 109026. https://doi.org/10.1016/j.biopsycho.2025.109026

Karunarathne, L. J. U., Amarasiri, W. A. D. L., & Fernando, A. D. A. (2023). Respiratory function in healthy long-term meditators: A cross-sectional comparative study. *Heliyon*, *9*(8), e18585. https://doi.org/10.1016/j.heliyon.2023.e18585

Katkin, E. S., Morell, M. A., Goldband, S., Bernstein, G. L., & Wise, J. A. (1982). Individual Differences in Heartbeat Discrimination. *Psychophysiology*, *19*(2), 160–166. https://doi.org/10.1111/j.1469-8986.1982.tb02538.x

Kato, Y., Takei, Y., Umeda, S., Mimura, M., & Fukuda, M. (2020). Alterations of Heartbeat Evoked Magnetic Fields Induced by Sounds of Disgust. *Frontiers in Psychiatry*, *11*, 683. https://doi.org/10.3389/fpsyt.2020.00683

Kern, M., Aertsen, A., Schulze-Bonhage, A., & Ball, T. (2013). Heart cycle-related effects on event-related potentials, spectral power changes, and connectivity patterns in the human ECoG. *NeuroImage*, *81*, 178–190. https://doi.org/10.1016/j.neuroimage.2013.05.042

Khadir, A., Ghamsari, S. S., Badri, S., & Beigzadeh, B. (2024). Discriminating orientation information with phase consistency in alpha and low-gamma frequency bands: An EEG study. *Scientific Reports*, *14*(1), 12007. https://doi.org/10.1038/s41598-024-62934-y

Khalsa, S. S., Adolphs, R., Cameron, O. G., Critchley, H. D., Davenport, P. W., Feinstein, J. S., Feusner, J. D., Garfinkel, S. N., Lane, R. D., Mehling, W. E., Meuret, A. E., Nemeroff, C. B., Oppenheimer, S., Petzschner, F. H., Pollatos, O., Rhudy, J. L., Schramm, L. P., Simmons, W. K., Stein, M. B., … Interoception Summit 2016 participants. (2018). Interoception and Mental Health: A Roadmap. *Biological Psychiatry. Cognitive Neuroscience and Neuroimaging*, *3*(6), 501–513. https://doi.org/10.1016/j.bpsc.2017.12.004

Khalsa, S. S., Berner, L. A., & Anderson, L. M. (2022). Gastrointestinal Interoception in Eating Disorders: Charting a New Path. *Current Psychiatry Reports*, *24*(1), 47–60. https://doi.org/10.1007/s11920-022-01318-3

Khalsa, S. S., & Lapidus, R. C. (2016). Can Interoception Improve the Pragmatic Search for Biomarkers in Psychiatry? *Frontiers in Psychiatry*, *7*. https://doi.org/10.3389/fpsyt.2016.00121

Khalsa, S. S., Rudrauf, D., Damasio, A. R., Davidson, R. J., Lutz, A., & Tranel, D. (2008). Interoceptive awareness in experienced meditators. *Psychophysiology*, *45*(4), 671–677. https://doi.org/10.1111/j.1469-8986.2008.00666.x

Khalsa, S. S., Rudrauf, D., Feinstein, J. S., & Tranel, D. (2009). The pathways of interoceptive awareness. *Nature Neuroscience*, *12*(12), 1494–1496. https://doi.org/10.1038/nn.2411

Khalsa, S. S., Rudrauf, D., Hassanpour, M. S., Davidson, R. J., & Tranel, D. (2020). The practice of meditation is not associated with improved interoceptive awareness of the heartbeat. *Psychophysiology*, *57*(2), e13479. https://doi.org/10.1111/psyp.13479

Khalsa, S. S., Rudrauf, D., & Tranel, D. (2009). Interoceptive awareness declines with age. *Psychophysiology*, *46*(6), 1130–1136. https://doi.org/10.1111/j.1469-8986.2009.00859.x

Kim, J., & Jeong, B. (2019). Heartbeat Induces a Cortical Theta-Synchronized Network in the Resting State. *Eneuro*, *6*(4), ENEURO.0200-19.2019. https://doi.org/10.1523/ENEURO.0200-19.2019

Kim, J., Park, H.-D., Kim, K. W., Shin, D. W., Lim, S., Kwon, H., Kim, M.-Y., Kim, K., & Jeong, B. (2019). Sad faces increase the heartbeat-associated interoceptive information flow within the salience network: A MEG study. *Scientific Reports*, *9*(1), 430. https://doi.org/10.1038/s41598-018-36498-7

Kleckner, I. R., Wormwood, J. B., Simmons, W. K., Barrett, L. F., & Quigley, K. S. (2015). Methodological recommendations for a heartbeat detection-based measure of interoceptive sensitivity. *Psychophysiology*, *52*(11), 1432–1440. https://doi.org/10.1111/psyp.12503

Kliegl. (2010). Experimental effects and individual differences in linear mixed models: Estimating the relationship between spatial, object, and attraction effects in visual attention. *Frontiers in Psychology*. https://doi.org/10.3389/fpsyg.2010.00238

Klimesch, W., Sauseng, P., & Hanslmayr, S. (2007). EEG alpha oscillations: The inhibition–timing hypothesis. *Brain Research Reviews*, *53*(1), 63–88. https://doi.org/10.1016/j.brainresrev.2006.06.003

Kluger, D. S., Balestrieri, E., Busch, N. A., & Gross, J. (2021). Respiration aligns perception with neural excitability. *eLife*, *10*, e70907. https://doi.org/10.7554/eLife.70907

Kluger, D. S., Forster, C., Abbasi, O., Chalas, N., Villringer, A., & Gross, J. (2023). Modulatory dynamics of periodic and aperiodic activity in respiration-brain coupling. *Nature Communications*, *14*(1), 4699. https://doi.org/10.1038/s41467-023-40250-9

Kluger, D. S., & Gross, J. (2020). Depth and phase of respiration modulate cortico-muscular communication. *NeuroImage*, *222*, 117272. https://doi.org/10.1016/j.neuroimage.2020.117272

Kluger, D. S., & Gross, J. (2021). Respiration modulates oscillatory neural network activity at rest. *PLOS Biology*, *19*(11), e3001457. https://doi.org/10.1371/journal.pbio.3001457

Koreki, A., Goeta, D., Ricciardi, L., Eilon, T., Chen, J., Critchley, H. D., Garfinkel, S. N., Edwards, M., & Yogarajah, M. (2022). The relationship between interoception and agency and its modulation by heartbeats: An exploratory study. *Scientific Reports*, *12*(1), 13624. https://doi.org/10.1038/s41598-022-16569-6

Körmendi, J., Ferentzi, E., & Köteles, F. (2021). Expectation predicts performance in the mental heartbeat tracking task. *Biological Psychology*, *164*, 108170. https://doi.org/10.1016/j.biopsycho.2021.108170

Körmendi, J., Ferentzi, E., & Köteles, F. (2022). A heartbeat away from a valid tracking task. An empirical comparison of the mental and the motor tracking task. *Biological Psychology*, *171*, 108328. https://doi.org/10.1016/j.biopsycho.2022.108328

Kritzman, L., Eidelman-Rothman, M., Keil, A., Freche, D., Sheppes, G., & Levit-Binnun, N. (2022). Steady-state visual evoked potentials differentiate between internally and externally directed attention. *NeuroImage*, *254*, 119133. https://doi.org/10.1016/j.neuroimage.2022.119133

Krohn, F., Novello, M., Van Der Giessen, R. S., De Zeeuw, C. I., Pel, J. J., & Bosman, L. W. (2023). The integrated brain network that controls respiration. *eLife*, *12*, e83654. https://doi.org/10.7554/eLife.83654

Kubin, L., Alheid, G. F., Zuperku, E. J., & McCrimmon, D. R. (2006). Central pathways of pulmonary and lower airway vagal afferents. *Journal of Applied Physiology*, *101*(2), 618–627. https://doi.org/10.1152/japplphysiol.00252.2006

Kuehn, E., Mueller, K., Lohmann, G., & Schuetz-Bosbach, S. (2016). Interoceptive awareness changes the posterior insula functional connectivity profile. *Brain Structure and Function*, *221*(3), 1555–1571. https://doi.org/10.1007/s00429-015-0989-8

Kumral, D., Al, E., Cesnaite, E., Kornej, J., Sander, C., Hensch, T., Zeynalova, S., Tautenhahn, S., Hagendorf, A., Laufs, U., Wachter, R., Nikulin, V., & Villringer, A. (2022). Attenuation of the Heartbeat-Evoked Potential in Patients With Atrial Fibrillation. *JACC: Clinical Electrophysiology*, *8*(10), 1219–1230. https://doi.org/10.1016/j.jacep.2022.06.019

Landler, L., Ruxton, G. D., & Malkemper, E. P. (2018). Circular data in biology: Advice for effectively implementing statistical procedures. *Behavioral Ecology and Sociobiology*, *72*(8), 128. https://doi.org/10.1007/s00265-018-2538-y

Larsson, D. E. O., Esposito, G., Critchley, H. D., Dienes, Z., & Garfinkel, S. N. (2021). Sensitivity to changes in rate of heartbeats as a measure of interoceptive ability. *Journal of Neurophysiology*, *126*(5), 1799–1813. https://doi.org/10.1152/jn.00059.2021

Lavalley, C. A., Hakimi, N., Taylor, S., Kuplicki, R., Forthman, K. L., Stewart, J. L., Paulus, M. P., Khalsa, S. S., & Smith, R. (2024). Transdiagnostic failure to adapt interoceptive precision estimates across affective, substance use, and eating disorders: A replication and extension of previous results. *Biological Psychology*, *191*, 108825. https://doi.org/10.1016/j.biopsycho.2024.108825

Lechinger, J., Heib, D. P. J., Gruber, W., Schabus, M., & Klimesch, W. (2015). Heartbeat-related EEG amplitude and phase modulations from wakefulness to deep sleep: Interactions with sleep spindles and slow oscillations. *Psychophysiology*, *52*(11), 1441–1450. https://doi.org/10.1111/psyp.12508

Lee, W., Kim, E., Park, J., Eo, J., Jeong, B., & Park, H.-J. (2024). Heartbeat-related spectral perturbation of electroencephalogram reflects dynamic interoceptive attention states in the trial-by-trial classification analysis. *NeuroImage*, *299*, 120797. https://doi.org/10.1016/j.neuroimage.2024.120797

Leganes-Fonteneau, M., Bates, M. E., Muzumdar, N., Pawlak, A., Islam, S., Vaschillo, E., & Buckman, J. F. (2021). Cardiovascular mechanisms of interoceptive awareness: Effects of resonance breathing. *International Journal of Psychophysiology*, *169*, 71–87. https://doi.org/10.1016/j.ijpsycho.2021.09.003

Leupin, V., & Britz, J. (2024). Interoceptive signals shape the earliest markers and neural pathway to awareness at the visual threshold. *Proceedings of the National Academy of Sciences*, *121*(37), e2311953121. https://doi.org/10.1073/pnas.2311953121

Levinson, D. B., Stoll, E. L., Kindy, S. D., Merry, H. L., & Davidson, R. J. (2014). A mind you can count on: Validating breath counting as a behavioral measure of mindfulness. *Frontiers in Psychology*, *5*. https://doi.org/10.3389/fpsyg.2014.01202

Lewis, G. F., Furman, S. A., McCool, M. F., & Porges, S. W. (2012). Statistical strategies to quantify respiratory sinus arrhythmia: Are commonly used metrics equivalent? *Biological Psychology*, *89*(2), 349–364. https://doi.org/10.1016/j.biopsycho.2011.11.009

Liuzzi, P., Cassioli, T., Secci, S., Hakiki, B., Scarpino, M., Burali, R., Di Palma, A., Toci, T., Grippo, A., Cecchi, F., Frosini, A., & Mannini, A. (2024). A neurophysiological profiling of

the heartbeat-evoked potential in severe acquired brain injuries: A focus on unconsciousness. *European Journal of Neuroscience*, *60*(3), 4201–4216. https://doi.org/10.1111/ejn.16394

Loescher, M., Haggard, P., & Tallon-Baudry, C. (2025). Interoception vs. Exteroception: Cardiac interoception competes with tactile perception, yet also facilitates self-relevance encoding. *Proceedings of the National Academy of Sciences*, *122*(49), e2516229122. https://doi.org/10.1073/pnas.2516229122

Lopez-Calderon, J., & Luck, S. J. (2014). ERPLAB: An open-source toolbox for the analysis of event-related potentials. *Frontiers in Human Neuroscience*, *8*. https://doi.org/10.3389/fnhum.2014.00213

Lopez-Martin, G., Caparco, A., Van Steenoven, C., Leganes-Fonteneau, M., & Galvez-Pol, A. (2026). Interoceptive rhythms and perceptual experience: Mechanisms, contexts, and strategies for real-world research. *NeuroImage*, *325*, 121650. https://doi.org/10.1016/j.neuroimage.2025.121650

Lopour, B. A., Tavassoli, A., Fried, I., & Ringach, D. L. (2013). Coding of Information in the Phase of Local Field Potentials within Human Medial Temporal Lobe. *Neuron*, *79*(3), 594–606. https://doi.org/10.1016/j.neuron.2013.06.001

Luft, C. D. B., & Bhattacharya, J. (2015). Aroused with heart: Modulation of heartbeat evoked potential by arousal induction and its oscillatory correlates. *Scientific Reports*, *5*(1), 15717. https://doi.org/10.1038/srep15717

Lutz, A. P. C., Schulz, A., Voderholzer, U., Koch, S., Van Dyck, Z., & Vögele, C. (2019). Enhanced cortical processing of cardio-afferent signals in anorexia nervosa. *Clinical Neurophysiology*, *130*(9), 1620–1627. https://doi.org/10.1016/j.clinph.2019.06.009

Lyyra, P., & Parviainen, T. (2018). Behavioral Inhibition Underlies the Link Between Interoceptive Sensitivity and Anxiety-Related Temperamental Traits. *Frontiers in Psychology*, *9*, 1026. https://doi.org/10.3389/fpsyg.2018.01026

MacKinnon, S., Gevirtz, R., McCraty, R., & Brown, M. (2013). Utilizing Heartbeat Evoked Potentials to Identify Cardiac Regulation of Vagal Afferents During Emotion and Resonant Breathing. *Applied Psychophysiology and Biofeedback*, *38*(4), 241–255. https://doi.org/10.1007/s10484-013-9226-5

Mai, S., Wong, C. K., Georgiou, E., & Pollatos, O. (2018). Interoception is associated with heartbeat-evoked brain potentials (HEPs) in adolescents. *Biological Psychology*, *137*, 24–33. https://doi.org/10.1016/j.biopsycho.2018.06.007

Makowski, D., Sperduti, M., Blondé, P., Nicolas, S., & Piolino, P. (2020). The heart of cognitive control: Cardiac phase modulates processing speed and inhibition. *Psychophysiology*, *57*(3), e13490. https://doi.org/10.1111/psyp.13490

Malik, M., Bigger, J. T., Camm, A. J., Kleiger, R. E., Malliani, A., Moss, A. J., & Schwartz, P. J. (1996). Heart rate variability: Standards of measurement, physiological interpretation, and clinical use. *European Heart Journal*, *17*(3), 354–381. https://doi.org/10.1093/oxfordjournals.eurheartj.a014868

Mannocci, A., Di Thiene, D., Del Cimmuto, A., Masala, D., Boccia, A., & De Vito, E. (2010). International Physical Activity Questionnaire: Validation and assessment in an Italian sample. *Italian Journal of Public Health*, *7*(4). https://doi.org/10.2427/5694

Martin, S. L., Kerr, K. L., Bartley, E. J., Kuhn, B. L., Palit, S., Terry, E. L., DelVentura, J. L., & Rhudy, J. L. (2012). Respiration-Induced Hypoalgesia: Exploration of Potential Mechanisms. *The Journal of Pain*, *13*(8), 755–763. https://doi.org/10.1016/j.jpain.2012.05.001

Mather, M., Clewett, D., Sakaki, M., & Harley, C. W. (2016). Norepinephrine ignites local hotspots of neuronal excitation: How arousal amplifies selectivity in perception and memory. *Behavioral and Brain Sciences*, *39*, e200. https://doi.org/10.1017/S0140525X15000667

Mehling, W. E., Price, C., Daubenmier, J. J., Acree, M., Bartmess, E., & Stewart, A. (2012). The Multidimensional Assessment of Interoceptive Awareness (MAIA). *PLoS ONE*, *7*(11), e48230. https://doi.org/10.1371/journal.pone.0048230

Melloni, M., Sedeño, L., Couto, B., Reynoso, M., Gelormini, C., Favaloro, R., Canales-Johnson, A., Sigman, M., Manes, F., & Ibanez, A. (2013). Preliminary evidence about the effects of meditation on interoceptive sensitivity and social cognition. *Behavioral and Brain Functions*, *9*(1), 47. https://doi.org/10.1186/1744-9081-9-47

Mercader, J. M., Fernández-Aranda, F., Gratacòs, M., Aguera, Z., Forcano, L., Ribasés, M., Villarejo, C., & Estivill, X. (2010). Correlation of BDNF blood levels with interoceptive awareness and maturity fears in anorexia and bulimia nervosa patients. *Journal of Neural Transmission*, *117*(4), 505–512. https://doi.org/10.1007/s00702-010-0377-8

Michal, M., Reuchlein, B., Adler, J., Reiner, I., Beutel, M. E., Vögele, C., Schächinger, H., & Schulz, A. (2014). Striking Discrepancy of Anomalous Body Experiences with Normal Interoceptive Accuracy in Depersonalization-Derealization Disorder. *PLoS ONE*, *9*(2), e89823. https://doi.org/10.1371/journal.pone.0089823

Mizuhara, K., Li, L., & Nittono, H. (2024). Auditory mismatch negativity is larger during exhalation than inhalation. *Medicine*, *103*(48), e40683. https://doi.org/10.1097/MD.0000000000040683

Mizuhara, K., Li, L., & Nittono, H. (2025). Effects of cardiac and respiratory phases on auditory evoked potentials. *International Journal of Psychophysiology*, *209*, 112521. https://doi.org/10.1016/j.ijpsycho.2025.112521

Mizuhara, K., & Nittono, H. (2022). Visual discrimination accuracy does not differ between nasal inhalation and exhalation when stimuli are voluntarily aligned to breathing phase. *International Journal of Psychophysiology*, *173*, 1–8. https://doi.org/10.1016/j.ijpsycho.2021.12.009

Mizuhara, K., & Nittono, H. (2023). Effects of respiratory phases on the processing of emotional and non-emotional visual stimuli. *Psychophysiology*, *60*(6), e14261. https://doi.org/10.1111/psyp.14261

Molle, L., & Coste, A. (2022). The respiratory modulation of interoception. *Journal of Neurophysiology*, *127*(4), 896–899. https://doi.org/10.1152/jn.00027.2022

Molle, L., Coste, A., Benoit, C.-E., Derosiere, G., Janaqi, S., Perrey, S., & Dupeyron, A. (2023). Inhalation boosts perceptual awareness and decision speed. *Journal of Neurophysiology*, *130*(3), 516–523. https://doi.org/10.1152/jn.00492.2022

Montoya, P., Schandry, R., & Müller, A. (1993). Heartbeat evoked potentials (HEP): Topography and influence of cardiac awareness and focus of attention. *Electroencephalography and Clinical Neurophysiology/Evoked Potentials Section*, *88*(3), 163–172. https://doi.org/10.1016/0168-5597(93)90001-6

Muñoz-Ortiz, J., Muñoz-Ortiz, E., López-Meraz, M. L., Beltran-Parrazal, L., & Morgado-Valle, C. (2019). El complejo pre-Bötzinger: Generación y modulación del ritmo respiratorio. *Neurología*, *34*(7), 461–468. https://doi.org/10.1016/j.nrl.2016.05.011

Murphy, J., Brewer, R., Catmur, C., & Bird, G. (2017). Interoception and psychopathology: A developmental neuroscience perspective. *Developmental Cognitive Neuroscience*, *23*, 45–56. https://doi.org/10.1016/j.dcn.2016.12.006

Murphy, J., Brewer, R., Hobson, H., Catmur, C., & Bird, G. (2018). Is alexithymia characterised by impaired interoception? Further evidence, the importance of control variables, and the problems with the Heartbeat Counting Task. *Biological Psychology*, *136*, 189–197. https://doi.org/10.1016/j.biopsycho.2018.05.010

Mylius, M., Guendelman, S., Iliopoulos, F., Gallese, V., & Kaltwasser, L. (2023). *The Impact of Meditation on Body Awareness: Prestimulus Alpha Activity Modulates Response Bias in a Somatosensory Signal Detection Task*. https://doi.org/10.22541/au.169445202.28516536/v2

Nakamura, N. H., Fukunaga, M., & Oku, Y. (2018). Respiratory modulation of cognitive performance during the retrieval process. *PLOS ONE*, *13*(9), e0204021. https://doi.org/10.1371/journal.pone.0204021

Nakamura, N. H., Oku, Y., & Fukunaga, M. (2024). "Brain–breath" interactions: Respiration-timing–dependent impact on functional brain networks and beyond. *Reviews in the Neurosciences*, *35*(2), 165–182. https://doi.org/10.1515/revneuro-2023-0062

Neri, B., Callara, A. L., Vanello, N., Menicucci, D., Zaccaro, A., Piarulli, A., Laurino, M., Norbu, N., Kechok, J., Sherab, N., & Gemignani, A. (2024). Report from a Tibetan Monastery: EEG neural correlates of concentrative and analytical meditation. *Frontiers in Psychology*, *15*, 1348317. https://doi.org/10.3389/fpsyg.2024.1348317

Neuhuber, W. L., & Berthoud, H.-R. (2022). Functional anatomy of the vagus system: How does the polyvagal theory comply? *Biological Psychology*, *174*, 108425. https://doi.org/10.1016/j.biopsycho.2022.108425

Nikolova, N., Harrison, O., Toohey, S., Brændholt, M., Legrand, N., Correa, C., Vejlø, M., Jensen, M. S., Fardo, F., & Allen, M. (2022). The respiratory resistance sensitivity task: An automated method for quantifying respiratory interoception and metacognition. *Biological Psychology*, *170*, 108325. https://doi.org/10.1016/j.biopsycho.2022.108325

Noble, D. J., & Hochman, S. (2019). Hypothesis: Pulmonary Afferent Activity Patterns During Slow, Deep Breathing Contribute to the Neural Induction of Physiological Relaxation. *Frontiers in Physiology*, *10*, 1176. https://doi.org/10.3389/fphys.2019.01176

Nociti, V., Santoro, M., Quaranta, D., Losavio, F. A., De Fino, C., Giordano, R., Palomba, N. P., Rossini, P. M., Guerini, F. R., Clerici, M., Caputo, D., & Mirabella, M. (2019). Correction: BDNF rs6265 polymorphism methylation in Multiple Sclerosis: A possible marker of disease progression. *PloS One*, *14*(2), e0212906. https://doi.org/10.1371/journal.pone.0212906

Noda, T., Amemiya, T., Shiramatsu, T. I., & Takahashi, H. (2017). Stimulus Phase Locking of Cortical Oscillations for Rhythmic Tone Sequences in Rats. *Frontiers in Neural Circuits*, *11*. https://doi.org/10.3389/fncir.2017.00002

Nolte, G., Bai, O., Wheaton, L., Mari, Z., Vorbach, S., & Hallett, M. (2004). Identifying true brain interaction from EEG data using the imaginary part of coherency. *Clinical Neurophysiology*, *115*(10), 2292–2307. https://doi.org/10.1016/j.clinph.2004.04.029

Oostenveld, R., Fries, P., Maris, E., & Schoffelen, J.-M. (2011). FieldTrip: Open source software for advanced analysis of MEG, EEG, and invasive electrophysiological data. *Computational Intelligence and Neuroscience*, *2011*, 156869. https://doi.org/10.1155/2011/156869

Oostenveld, R., & Praamstra, P. (2001). The five percent electrode system for high-resolution EEG and ERP measurements. *Clinical Neurophysiology: Official Journal of the International Federation of Clinical Neurophysiology*, *112*(4), 713–719. https://doi.org/10.1016/s1388-2457(00)00527-7

Ørtenblad, N., Westerblad, H., & Nielsen, J. (2013). Muscle glycogen stores and fatigue. *The Journal of Physiology*, *591*(18), 4405–4413. https://doi.org/10.1113/jphysiol.2013.251629

Ottonello, M., Pellicciari, L., Giordano, A., & Foti, C. (2016). Rasch analysis of the Fatigue Severity Scale in Italian subjects with multiple sclerosis. *Journal of Rehabilitation Medicine*, *48*(7), 597–603. https://doi.org/10.2340/16501977-2116

Ozturk, O. C., McFadyen, J., & Azevedo, R. T. (2025). Cardiac Signals Facilitate the Breakthrough to Awareness of Emotional Stimuli. *Psychophysiology*, *62*(10), e70168. https://doi.org/10.1111/psyp.70168

Palmer, B. F., & Clegg, D. J. (2023). Respiratory Acidosis and Respiratory Alkalosis: Core Curriculum 2023. *American Journal of Kidney Diseases*, *82*(3), 347–359. https://doi.org/10.1053/j.ajkd.2023.02.004

Pan, J., & Tompkins, W. J. (1985). A Real-Time QRS Detection Algorithm. *IEEE Transactions on Biomedical Engineering*, *BME-32*(3), 230–236. https://doi.org/10.1109/TBME.1985.325532

Park, H.-D., Barnoud, C., Trang, H., Kannape, O. A., Schaller, K., & Blanke, O. (2020). Breathing is coupled with voluntary action and the cortical readiness potential. *Nature Communications*, *11*(1), 289. https://doi.org/10.1038/s41467-019-13967-9

Park, H.-D., Bernasconi, F., Bello-Ruiz, J., Pfeiffer, C., Salomon, R., & Blanke, O. (2016). Transient Modulations of Neural Responses to Heartbeats Covary with Bodily Self-Consciousness. *Journal of Neuroscience*, *36*(32), 8453–8460. https://doi.org/10.1523/JNEUROSCI.0311-16.2016

Park, H.-D., Bernasconi, F., Salomon, R., Tallon-Baudry, C., Spinelli, L., Seeck, M., Schaller, K., & Blanke, O. (2018). Neural Sources and Underlying Mechanisms of Neural Responses to

Heartbeats, and their Role in Bodily Self-consciousness: An Intracranial EEG Study. *Cerebral Cortex*, *28*(7), 2351–2364. https://doi.org/10.1093/cercor/bhx136

Park, H.-D., & Blanke, O. (2019). Heartbeat-evoked cortical responses: Underlying mechanisms, functional roles, and methodological considerations. *NeuroImage*, *197*, 502–511. https://doi.org/10.1016/j.neuroimage.2019.04.081

Park, H.-D., Piton, T., Kannape, O. A., Duncan, N. W., Lee, K.-Y., Lane, T. J., & Blanke, O. (2022). Breathing is coupled with voluntary initiation of mental imagery. *NeuroImage*, *264*, 119685. https://doi.org/10.1016/j.neuroimage.2022.119685

Parrotta, E., Bach, P., Perrucci, M. G., Costantini, M., & Ferri, F. (2024). Heart is deceitful above all things: Threat expectancy induces the illusory perception of increased heartrate. *Cognition*, *245*, 105719. https://doi.org/10.1016/j.cognition.2024.105719

Pasciucco, M. R., Bubbico, F., Nunziata, S., Iuliano, S., Ruggiero, G., Perrucci, M. G., Croce, P., Costantini, M., & Ferri, F. (2026). Interoceptive predictors of daily functioning in aging and their interaction with exteroceptive bodily representations. *Frontiers in Psychology*, *17*, 1689759. https://doi.org/10.3389/fpsyg.2026.1689759

Pasciucco, M. R., Perrucci, M. G., Croce, P., Kalckert, A., Costantini, M., & Ferri, F. (2025). Predictive role of exteroceptive and interoceptive bodily dimensions to schizotypal personality traits. *Scientific Reports*, *15*(1), 7909. https://doi.org/10.1038/s41598-025-89951-9

Paulus, M. P. (2013). THE BREATHING CONUNDRUM-INTEROCEPTIVE SENSITIVITY AND ANXIETY: Review: The Breathing Conundrum. *Depression and Anxiety*, *30*(4), 315–320. https://doi.org/10.1002/da.22076

Perakakis, P. (2019). *HEPLAB: A Matlab graphical interface for the preprocessing of the heartbeat-evoked potential* (Versione v1.0.0) [Software]. Zenodo. https://doi.org/10.5281/ZENODO.2649943

Perl, O., Ravia, A., Rubinson, M., Eisen, A., Soroka, T., Mor, N., Secundo, L., & Sobel, N. (2019). Human non-olfactory cognition phase-locked with inhalation. *Nature Human Behaviour*, *3*(5), 501–512. https://doi.org/10.1038/s41562-019-0556-z

Petzschner, F. H., Weber, L. A., Wellstein, K. V., Paolini, G., Do, C. T., & Stephan, K. E. (2019). Focus of attention modulates the heartbeat evoked potential. *NeuroImage*, *186*, 595–606. https://doi.org/10.1016/j.neuroimage.2018.11.037

Phillips, G. C., Jones, G. E., Rieger, E. J., & Snell, J. B. (1999). Effects of the presentation of false heart-rate feedback on the performance of two common heartbeat-detection tasks. *Psychophysiology*, *36*(4), 504–510. https://doi.org/10.1017/S0048577299980071

Poli, A., Maremmani, A. G. I., Chiorri, C., Mazzoni, G.-P., Orrù, G., Kolacz, J., Porges, S. W., Conversano, C., Gemignani, A., & Miccoli, M. (2021). Item Reduction, Psychometric and Biometric Properties of the Italian Version of the Body Perception Questionnaire—Short Form (BPQ-SF): The BPQ-22. *International Journal of Environmental Research and Public Health*, *18*(7), 3835. https://doi.org/10.3390/ijerph18073835

Pollatos, O., Herbert, B. M., Mai, S., & Kammer, T. (2016). Changes in interoceptive processes following brain stimulation. *Philosophical Transactions of the Royal Society B: Biological Sciences*, *371*(1708), 20160016. https://doi.org/10.1098/rstb.2016.0016

Pollatos, O., Kirsch, W., & Schandry, R. (2005). Brain structures involved in interoceptive awareness and cardioafferent signal processing: A dipole source localization study. *Human Brain Mapping*, *26*(1), 54–64. https://doi.org/10.1002/hbm.20121

Pollatos, O., & Schandry, R. (2004). Accuracy of heartbeat perception is reflected in the amplitude of the heartbeat-evoked brain potential. *Psychophysiology*, *41*(3), 476–482. https://doi.org/10.1111/1469-8986.2004.00170.x

Pollatos, O., Schandry, R., Auer, D. P., & Kaufmann, C. (2007). Brain structures mediating cardiovascular arousal and interoceptive awareness. *Brain Research*, *1141*, 178–187. https://doi.org/10.1016/j.brainres.2007.01.026

Pollatos, O., Traut-Mattausch, E., & Schandry, R. (2009). Differential effects of anxiety and depression on interoceptive accuracy. *Depression and Anxiety*, *26*(2), 167–173. https://doi.org/10.1002/da.20504

Porciello, G., Monti, A., & Aglioti, S. M. (2018). How the stomach and the brain work together at rest. *eLife*, *7*, e37009. https://doi.org/10.7554/eLife.37009

Power, J. D., Lynch, C. J., Dubin, M. J., Silver, B. M., Martin, A., & Jones, R. M. (2020). Characteristics of respiratory measures in young adults scanned at rest, including systematic changes and "missed" deep breaths. *NeuroImage*, *204*, 116234. https://doi.org/10.1016/j.neuroimage.2019.116234

Pultsina, K., Karjalainen, S., & Parviainen, T. (2025). *Oscillatory markers of interoceptive attention: Beta suppression as a neural signature of heartbeat processing*. Neuroscience. https://doi.org/10.1101/2025.06.24.660939

Rae, C. L., Ahmad, A., Larsson, D. E. O., Silva, M., Praag, C. D. G. V., Garfinkel, S. N., & Critchley, H. D. (2020). Impact of cardiac interoception cues and confidence on voluntary decisions to make or withhold action in an intentional inhibition task. *Scientific Reports*, *10*(1), 4184. https://doi.org/10.1038/s41598-020-60405-8

Raichle, M. E., MacLeod, A. M., Snyder, A. Z., Powers, W. J., Gusnard, D. A., & Shulman, G. L. (2001). A default mode of brain function. *Proceedings of the National Academy of Sciences*, *98*(2), 676–682. https://doi.org/10.1073/pnas.98.2.676

Rebollo, I., Devauchelle, A.-D., Béranger, B., & Tallon-Baudry, C. (2018). Stomach-brain synchrony reveals a novel, delayed-connectivity resting-state network in humans. *eLife*, *7*, e33321. https://doi.org/10.7554/eLife.33321

Ring, C., & Brener, J. (1996). Influence of beliefs about heart rate and actual heart rate on heartbeat counting. *Psychophysiology*, *33*(5), 541–546. https://doi.org/10.1111/j.1469-8986.1996.tb02430.x

Ring, C., Brener, J., Knapp, K., & Mailloux, J. (2015). Effects of heartbeat feedback on beliefs about heart rate and heartbeat counting: A cautionary tale about interoceptive awareness. *Biological Psychology*, *104*, 193–198. https://doi.org/10.1016/j.biopsycho.2014.12.010

Robinson, E., Foote, G., Smith, J., Higgs, S., & Jones, A. (2021). Interoception and obesity: A systematic review and meta-analysis of the relationship between interoception and BMI. *International Journal of Obesity*, *45*(12), 2515–2526. https://doi.org/10.1038/s41366-021-00950-y

Rominger, C., Fink, A., Perchtold-Stefan, C. M., Schlögl, L., & Schwerdtfeger, A. R. (2025). The Interoceptive Brain: Confidence Ratings and Accuracy Scores are Independently and Differently Associated With Task-Related Alpha Power During the Heartbeat Tracking Task. *Psychophysiology*, *62*(4), e70051. https://doi.org/10.1111/psyp.70051

Rominger, C., Graßmann, T. M., Weber, B., & Schwerdtfeger, A. R. (2021). Does contingent biofeedback improve cardiac interoception? A preregistered replication of Meyerholz, Irzinger, Withöft, Gerlach, and Pohl (2019) using the heartbeat discrimination task in a randomised control trial. *PLOS ONE*, *16*(3), e0248246. https://doi.org/10.1371/journal.pone.0248246

Rubinov, M., & Sporns, O. (2010). Complex network measures of brain connectivity: Uses and interpretations. *NeuroImage*, *52*(3), 1059–1069. https://doi.org/10.1016/j.neuroimage.2009.10.003

Saltafossi, M., Zaccaro, A., Kluger, D. S., Perrucci, M. G., Ferri, F., & Costantini, M. (2025). Respiration Facilitates Behavior During Multisensory Integration. *Psychophysiology*, *62*(9), e70145. https://doi.org/10.1111/psyp.70145

Saltafossi, M., Zaccaro, A., Perrucci, M. G., Ferri, F., & Costantini, M. (2023). The impact of cardiac phases on multisensory integration. *Biological Psychology*, *182*, 108642. https://doi.org/10.1016/j.biopsycho.2023.108642

Sandler, C. X., Wyller, V. B. B., Moss-Morris, R., Buchwald, D., Crawley, E., Hautvast, J., Katz, B. Z., Knoop, H., Little, P., Taylor, R., Wensaas, K.-A., & Lloyd, A. R. (2021). Long COVID and Post-infective Fatigue Syndrome: A Review. *Open Forum Infectious Diseases*, *8*(10), ofab440. https://doi.org/10.1093/ofid/ofab440

Sandoval, S. J., Suh, Y.-S., Lee, K.-Y., & Park, H.-D. (2025). *The respiratory phase causally modulates the readiness potential amplitude*. Neuroscience. https://doi.org/10.1101/2025.07.27.666697

Savitzky, Abraham., & Golay, M. J. E. (1964). Smoothing and Differentiation of Data by Simplified Least Squares Procedures. *Analytical Chemistry*, *36*(8), 1627–1639. https://doi.org/10.1021/ac60214a047

Schaefer, M., Hrysanidis, C., Lundström, J. N., & Arshamian, A. (2024). Phase-locked breathing does not affect episodic visual recognition memory but does shape its corresponding ERPs. *Psychophysiology*, *61*(4), e14493. https://doi.org/10.1111/psyp.14493

Schandry, R. (1981). Heart Beat Perception and Emotional Experience. *Psychophysiology*, *18*(4), 483–488. https://doi.org/10.1111/j.1469-8986.1981.tb02486.x

Schandry, R., & Montoya, P. (1996). Event-related brain potentials and the processing of cardiac activity. *Biological Psychology*, *42*(1–2), 75–85. https://doi.org/10.1016/0301-0511(95)05147-3

Schandry, R., Sparrer, B., & Weitkunat, R. (1986). From the heart to the brain: A study of heartbeat contingent scalp potentials. *International Journal of Neuroscience*, *30*(4), 261–275. https://doi.org/10.3109/00207458608985677

Schroeder, C. E., Wilson, D. A., Radman, T., Scharfman, H., & Lakatos, P. (2010). Dynamics of Active Sensing and perceptual selection. *Current Opinion in Neurobiology*, *20*(2), 172–176. https://doi.org/10.1016/j.conb.2010.02.010

Schulz, A., Back, S. N., Schaan, V. K., Bertsch, K., & Vögele, C. (2021). On the construct validity of interoceptive accuracy based on heartbeat counting: Cardiovascular determinants of absolute and tilt-induced change scores. *Biological Psychology*, *164*, 108168. https://doi.org/10.1016/j.biopsycho.2021.108168

Schulz, A., Ferreira de Sá, D. S., Dierolf, A. M., Lutz, A., van Dyck, Z., Vögele, C., & Schächinger, H. (2015). Short-term food deprivation increases amplitudes of heartbeat-evoked potentials. *Psychophysiology*, *52*(5), 695–703. https://doi.org/10.1111/psyp.12388

Schulz, A., Lass-Hennemann, J., Sütterlin, S., Schächinger, H., & Vögele, C. (2013). Cold pressor stress induces opposite effects on cardioceptive accuracy dependent on assessment paradigm. *Biological Psychology*, *93*(1), 167–174. https://doi.org/10.1016/j.biopsycho.2013.01.007

Schulz, A., Stammet, P., Dierolf, A. M., Vögele, C., Beyenburg, S., Werer, C., & Devaux, Y. (2018). Late heartbeat-evoked potentials are associated with survival after cardiac arrest. *Resuscitation*, *126*, 7–13. https://doi.org/10.1016/j.resuscitation.2018.02.009

Sel, A., Azevedo, R. T., & Tsakiris, M. (2016). Heartfelt Self: Cardio-Visual Integration Affects Self-Face Recognition and Interoceptive Cortical Processing. *Cerebral Cortex*, cercor;bhw296v1. https://doi.org/10.1093/cercor/bhw296

Serikov, V. B., & Fleming, N. W. (2001). Pulmonary and bronchial circulations: Contributions to heat and water exchange in isolated lungs. *Journal of Applied Physiology*, *91*(5), 1977–1985. https://doi.org/10.1152/jappl.2001.91.5.1977

Seth, A. K. (2013). Interoceptive inference, emotion, and the embodied self. *Trends in Cognitive Sciences*, *17*(11), 565–573. https://doi.org/10.1016/j.tics.2013.09.007

Seth, A. K., & Friston, K. J. (2016). Active interoceptive inference and the emotional brain. *Philosophical Transactions of the Royal Society B: Biological Sciences*, *371*(1708), 20160007. https://doi.org/10.1098/rstb.2016.0007

Sherman, M. T., Kanai, R., Seth, A. K., & VanRullen, R. (2016). Rhythmic Influence of Top–Down Perceptual Priors in the Phase of Prestimulus Occipital Alpha Oscillations. *Journal of Cognitive Neuroscience*, *28*(9), 1318–1330. https://doi.org/10.1162/jocn_a_00973

Sihn, D., & Kim, S.-P. (2022). Brain Infraslow Activity Correlates With Arousal Levels. *Frontiers in Neuroscience*, *16*, 765585. https://doi.org/10.3389/fnins.2022.765585

Simor, P., Bogdány, T., Bódizs, R., & Perakakis, P. (2021). Cortical monitoring of cardiac activity during rapid eye movement sleep: The heartbeat evoked potential in phasic and tonic rapid-eye-movement microstates. *SLEEP*, *44*(9), zsab100. https://doi.org/10.1093/sleep/zsab100

Simor, P., Lilla, R. Z., Szalárdy, O., Jordán, Z., Halász, L., Erőss, L., Fabó, D., & Bódizs, R. (2025). Heartbeat-related activity in the anterior thalamus differs between phasic and tonic REM sleep. *The Journal of Physiology*, *603*(9), 2839–2855. https://doi.org/10.1113/JP287802

Skora, L. I., Livermore, J. J. A., & Roelofs, K. (2022). The functional role of cardiac activity in perception and action. *Neuroscience & Biobehavioral Reviews*, *137*, 104655. https://doi.org/10.1016/j.neubiorev.2022.104655

Smith, J. C., Ellenberger, H. H., Ballanyi, K., Richter, D. W., & Feldman, J. L. (1991). Pre-Bötzinger Complex: A Brainstem Region that May Generate Respiratory Rhythm in Mammals. *Science*, *254*(5032), 726–729. https://doi.org/10.1126/science.1683005

Smith, R., Feinstein, J. S., Kuplicki, R., Forthman, K. L., Stewart, J. L., Paulus, M. P., Tulsa 1000 Investigators, Aupperle, R. L., Bodurka, J., Savitz, J. B., Victor, T. A., & Khalsa, S. S. (2021). Perceptual insensitivity to the modulation of interoceptive signals in depression, anxiety, and substance use disorders. *Scientific Reports*, *11*(1), 2108. https://doi.org/10.1038/s41598-021-81307-3

Smith, R., Kuplicki, R., Feinstein, J., Forthman, K. L., Stewart, J. L., Paulus, M. P., Tulsa 1000 investigators, & Khalsa, S. S. (2020). A Bayesian computational model reveals a failure to adapt interoceptive precision estimates across depression, anxiety, eating, and substance use disorders. *PLOS Computational Biology*, *16*(12), e1008484. https://doi.org/10.1371/journal.pcbi.1008484

Smith, R., Thayer, J. F., Khalsa, S. S., & Lane, R. D. (2017). The hierarchical basis of neurovisceral integration. *Neuroscience & Biobehavioral Reviews*, *75*, 274–296. https://doi.org/10.1016/j.neubiorev.2017.02.003

Sokol-Hessner, P., Hartley, C. A., Hamilton, J. R., & Phelps, E. A. (2015). Interoceptive ability predicts aversion to losses. *Cognition and Emotion*, *29*(4), 695–701. https://doi.org/10.1080/02699931.2014.925426

Stephan, K. E., Manjaly, Z. M., Mathys, C. D., Weber, L. A. E., Paliwal, S., Gard, T., Tittgemeyer, M., Fleming, S. M., Haker, H., Seth, A. K., & Petzschner, F. H. (2016). Allostatic Self-efficacy: A Metacognitive Theory of Dyshomeostasis-Induced Fatigue and Depression. *Frontiers in Human Neuroscience*, *10*. https://doi.org/10.3389/fnhum.2016.00550

Stephens, M. A. (1969). Multi-sample tests for the Fisher distribution for directions. *Biometrika*, *56*(1), 169–181. https://doi.org/10.1093/biomet/56.1.169

Stetza, L., Hehemann, L., & Kayser, C. (2025). Evidence That Respiratory Phase May Modulate Task-Related Neural Representations of Visual Stimuli. *The Journal of Neuroscience*, *45*(21), e2236242025. https://doi.org/10.1523/JNEUROSCI.2236-24.2025

Still, A. W., & White, A. P. (1981). The approximate randomization test as an alternative to the *F* test in analysis of variance. *British Journal of Mathematical and Statistical Psychology*, *34*(2), 243–252. https://doi.org/10.1111/j.2044-8317.1981.tb00634.x

Stoupi, N. A., Weijs, M. L., Imbach, L., & Lenggenhager, B. (2024). Heartbeat-evoked potentials following voluntary hyperventilation in epilepsy patients: Respiratory influences on cardiac interoception. *Frontiers in Neuroscience*, *18*, 1391437. https://doi.org/10.3389/fnins.2024.1391437

Streeter, C. C., Gerbarg, P. L., Saper, R. B., Ciraulo, D. A., & Brown, R. P. (2012). Effects of yoga on the autonomic nervous system, gamma-aminobutyric-acid, and allostasis in epilepsy, depression, and post-traumatic stress disorder. *Medical Hypotheses*, *78*(5), 571–579. https://doi.org/10.1016/j.mehy.2012.01.021

Studenova, A., Forster, C., Engemann, D. A., Hensch, T., Sanders, C., Mauche, N., Hegerl, U., Loffler, M., Villringer, A., & Nikulin, V. (2023). Event-related modulation of alpha rhythm explains the auditory P300-evoked response in EEG. *eLife*, *12*, RP88367. https://doi.org/10.7554/eLife.88367

Suksasilp, C., & Garfinkel, S. N. (2022). Towards a comprehensive assessment of interoception in a multi-dimensional framework. *Biological Psychology*, *168*, 108262. https://doi.org/10.1016/j.biopsycho.2022.108262

Tamburro, G., Di Fronso, S., Robazza, C., Bertollo, M., & Comani, S. (2020). Modulation of Brain Functional Connectivity and Efficiency During an Endurance Cycling Task: A Source-Level EEG and Graph Theory Approach. *Frontiers in Human Neuroscience*, *14*, 243. https://doi.org/10.3389/fnhum.2020.00243

Tan, Y., Van Den Bergh, O., Qiu, J., & Von Leupoldt, A. (2019). The Impact of Unpredictability on Dyspnea Perception, Anxiety and Interoceptive Error Processing. *Frontiers in Physiology*, *10*, 535. https://doi.org/10.3389/fphys.2019.00535

Tanaka, Y., Terasawa, Y., & Umeda, S. (2021). Effects of interoceptive accuracy in autonomic responses to external stimuli based on cardiac rhythm. *PLOS ONE*, *16*(8), e0256914. https://doi.org/10.1371/journal.pone.0256914

Tang, Y.-Y., Hölzel, B. K., & Posner, M. I. (2015). The neuroscience of mindfulness meditation. *Nature Reviews Neuroscience*, *16*(4), 213–225. https://doi.org/10.1038/nrn3916

Tarvainen, M. P., Niskanen, J.-P., Lipponen, J. A., Ranta-aho, P. O., & Karjalainen, P. A. (2014). Kubios HRV – Heart rate variability analysis software. *Computer Methods and Programs in Biomedicine*, *113*(1), 210–220. https://doi.org/10.1016/j.cmpb.2013.07.024

Terhaar, J., Viola, F. C., Bär, K.-J., & Debener, S. (2012). Heartbeat evoked potentials mirror altered body perception in depressed patients. *Clinical Neurophysiology*, *123*(10), 1950–1957. https://doi.org/10.1016/j.clinph.2012.02.086

Thut, G., & Miniussi, C. (2009). New insights into rhythmic brain activity from TMS-EEG studies. *Trends in Cognitive Sciences*, *13*(4), 182–189. https://doi.org/10.1016/j.tics.2009.01.004

Thut, G., Miniussi, C., & Gross, J. (2012). The functional importance of rhythmic activity in the brain. *Current Biology: CB*, *22*(16), R658-663. https://doi.org/10.1016/j.cub.2012.06.061

Tong, J. Y., & Sataloff, R. T. (2022). Respiratory Function and Voice: The Role for Airflow Measures. *Journal of Voice*, *36*(4), 542–553. https://doi.org/10.1016/j.jvoice.2020.07.019

Tort, A. B. L., Brankačk, J., & Draguhn, A. (2018). Respiration-Entrained Brain Rhythms Are Global but Often Overlooked. *Trends in Neurosciences*, *41*(4), 186–197. https://doi.org/10.1016/j.tins.2018.01.007

Tort, A. B. L., Laplagne, D. A., Draguhn, A., & Gonzalez, J. (2025). Global coordination of brain activity by the breathing cycle. *Nature Reviews Neuroscience*. https://doi.org/10.1038/s41583-025-00920-7

Treves, I. (2020). *Uncovering the Heartbeat Evoked Potential using stereoEEG recordings in insular cortex: A pilot study.* Unpublished. https://doi.org/10.13140/RG.2.2.27006.61761

Treves, I. N., Tello, L. Y., Davidson, R. J., & Goldberg, S. B. (2019). The relationship between mindfulness and objective measures of body awareness: A meta-analysis. *Scientific Reports*, *9*(1), 17386. https://doi.org/10.1038/s41598-019-53978-6

Tsakiris, M., & Critchley, H. (2016). Interoception beyond homeostasis: Affect, cognition and mental health. *Philosophical Transactions of the Royal Society B: Biological Sciences*, *371*(1708), 20160002. https://doi.org/10.1098/rstb.2016.0002

Tsakiris, M., Tajadura-Jiménez, A., & Costantini, M. (2011). Just a heartbeat away from one's body: Interoceptive sensitivity predicts malleability of body-representations. *Proceedings. Biological Sciences*, *278*(1717), 2470–2476. https://doi.org/10.1098/rspb.2010.2547

Tsuchimochi, T., Kanayama, N., Kimura, K., Miki, M., & Hara, M. (2024). Exploring the Enhancement of Heartbeat Awareness through Heartbeat Visualization Using VR Technology. *ICAT-EGVE 2024 - International Conference on Artificial Reality and Telexistence and Eurographics Symposium on Virtual Environments - Posters and Demos*. https://doi.org/10.2312/EGVE.20241410

Tsutsumi, T., Okamoto, Y., Kubota-Takano, N., Wakatsuki, D., Suzuki, H., Sezaki, K., Iwasawa, K., & Nakajima, T. (2014). Time–frequency analysis of the QRS complex in patients with ischemic cardiomyopathy and myocardial infarction. *IJC Heart & Vessels*, *4*, 177–187. https://doi.org/10.1016/j.ijchv.2014.04.008

Ueno, D., Matsuoka, T., Kato, Y., Ayani, N., Maeda, S., Takeda, M., & Narumoto, J. (2020). Individual Differences in Interoceptive Accuracy Are Correlated With Salience Network Connectivity in Older Adults. *Frontiers in Aging Neuroscience*, *12*, 592002. https://doi.org/10.3389/fnagi.2020.592002

Vaitl, D. (1996). Interoception. *Biological Psychology*, *42*(1–2), 1–27. https://doi.org/10.1016/0301-0511(95)05144-9

Van Den Boogert, F., Klein, K., Spaan, P., Sizoo, B., Bouman, Y. H. A., Hoogendijk, W. J. G., & Roza, S. J. (2022). Sensory processing difficulties in psychiatric disorders: A meta-analysis. *Journal of Psychiatric Research*, *151*, 173–180. https://doi.org/10.1016/j.jpsychires.2022.04.020

Van Diepen, R. M., Foxe, J. J., & Mazaheri, A. (2019). The functional role of alpha-band activity in attentional processing: The current zeitgeist and future outlook. *Current Opinion in Psychology*, *29*, 229–238. https://doi.org/10.1016/j.copsyc.2019.03.015

Van Diest, I., Bradley, M. M., Guerra, P., Van Den Bergh, O., & Lang, P. J. (2009). Fear-conditioned respiration and its association to cardiac reactivity. *Biological Psychology*, *80*(2), 212–217. https://doi.org/10.1016/j.biopsycho.2008.09.006

Vangeel, E. B., Kempke, S., Bakusic, J., Godderis, L., Luyten, P., Van Heddegem, L., Compernolle, V., Persoons, P., Lambrechts, D., Izzi, B., Freson, K., & Claes, S. (2018). Glucocorticoid receptor DNA methylation and childhood trauma in chronic fatigue syndrome patients. *Journal of Psychosomatic Research*, *104*, 55–60. https://doi.org/10.1016/j.jpsychores.2017.11.011

Verdejo-Garcia, A., Clark, L., & Dunn, B. D. (2012). The role of interoception in addiction: A critical review. *Neuroscience & Biobehavioral Reviews*, *36*(8), 1857–1869. https://doi.org/10.1016/j.neubiorev.2012.05.007

Verdonk, C., Trousselard, M., Di Bernardi Luft, C., Medani, T., Billaud, J., Ramdani, C., Canini, F., Claverie, D., Jaumard-Hakoun, A., & Vialatte, F. (2021). The heartbeat evoked potential does not support strong interoceptive sensibility in trait mindfulness. *Psychophysiology*, *58*(10), e13891. https://doi.org/10.1111/psyp.13891

Villena-González, M., Moënne-Loccoz, C., Lagos, R. A., Alliende, L. M., Billeke, P., Aboitiz, F., López, V., & Cosmelli, D. (2017). Attending to the heart is associated with posterior alpha band increase and a reduction in sensitivity to concurrent visual stimuli. *Psychophysiology*, *54*(10), 1483–1497. https://doi.org/10.1111/psyp.12894

Wanigatunga, A. A., Simonsick, E. M., Zipunnikov, V., Spira, A. P., Studenski, S., Ferrucci, L., & Schrack, J. A. (2018). Perceived Fatigability and Objective Physical Activity in Mid- to Late-Life. *The Journals of Gerontology. Series A, Biological Sciences and Medical Sciences*, *73*(5), 630–635. https://doi.org/10.1093/gerona/glx181

Waselius, T., Wikgren, J., Penttonen, M., & Nokia, M. S. (2019). Breathe out and learn: Expiration-contingent stimulus presentation facilitates associative learning in trace eyeblink conditioning. *Psychophysiology*, *56*(9), e13387. https://doi.org/10.1111/psyp.13387

Watson, G. S., & Williams, E. J. (1956). On the Construction of Significance Tests on the Circle and the Sphere. *Biometrika*, *43*(3/4), 344. https://doi.org/10.2307/2332913

Weitkunat, R., & Schandry, R. (1990). Motivation and heartbeat evoked potentials. *Journal of Psychophysiology*, *4*, 33–40.

Weng, H. Y., Feldman, J. L., Leggio, L., Napadow, V., Park, J., & Price, C. J. (2021). Interventions and Manipulations of Interoception. *Trends in Neurosciences*, *44*(1), 52–62. https://doi.org/10.1016/j.tins.2020.09.010

Wessely, S., Chalder, T., Hirsch, S., Wallace, P., & Wright, D. (1996). Psychological symptoms, somatic symptoms, and psychiatric disorder in chronic fatigue and chronic fatigue syndrome: A prospective study in the primary care setting. *American Journal of Psychiatry*, *153*(8), 1050–1059. https://doi.org/10.1176/ajp.153.8.1050

Whitehead, W. E., Drescher, V. M., Heiman, P., & Blackwell, B. (1977). Relation of heart rate control to heartbeat perception. *Biofeedback and Self-Regulation*, *2*(4), 317–392.

Wickens, T. D. (2001). *Elementary Signal Detection Theory*. Oxford University Press. https://doi.org/10.1093/acprof:oso/9780195092509.001.0001

Wiebking, C., De Greck, M., Duncan, N. W., Tempelmann, C., Bajbouj, M., & Northoff, G. (2015). Interoception in insula subregions as a possible state marker for depression—An exploratory

fMRI study investigating healthy, depressed and remitted participants. *Frontiers in Behavioral Neuroscience*, *9*. https://doi.org/10.3389/fnbeh.2015.00082

Wiens, S., Mezzacappa, E. S., & Katkin, E. S. (2000). Heartbeat detection and the experience of emotions. *Cognition & Emotion*, *14*(3), 417–427. https://doi.org/10.1080/026999300378905

Wiens, S., & Palmer, S. N. (2001). Quadratic trend analysis and heartbeat detection. *Biological Psychology*, *58*(2), 159–175. https://doi.org/10.1016/s0301-0511(01)00110-7

Willem, C., Gandolphe, M.-C., Roussel, M., Verkindt, H., Pattou, F., & Nandrino, J.-L. (2019). Difficulties in emotion regulation and deficits in interoceptive awareness in moderate and severe obesity. *Eating and Weight Disorders - Studies on Anorexia, Bulimia and Obesity*, *24*(4), 633–644. https://doi.org/10.1007/s40519-019-00738-0

Wilson, C. (2020). Concern coronavirus may trigger post-viral fatigue syndromes. *New Scientist (1971)*, *246*(3278), 10–11. https://doi.org/10.1016/S0262-4079(20)30746-6

Winkler, A. M., Ridgway, G. R., Webster, M. A., Smith, S. M., & Nichols, T. E. (2014). Permutation inference for the general linear model. *NeuroImage*, *92*, 381–397. https://doi.org/10.1016/j.neuroimage.2014.01.060

Xia, M., Wang, J., & He, Y. (2013). BrainNet Viewer: A Network Visualization Tool for Human Brain Connectomics. *PLoS ONE*, *8*(7), e68910. https://doi.org/10.1371/journal.pone.0068910

Yates, A. J., Jones, K. E., Marie, G. V., & Hogben, J. H. (1985). Detection of the Heartbeat and Events in the Cardiac Cycle. *Psychophysiology*, *22*(5), 561–567. https://doi.org/10.1111/j.1469-8986.1985.tb01651.x

Yoris, A., García, A. M., Traiber, L., Santamaría-García, H., Martorell, M., Alifano, F., Kichic, R., Moser, J. S., Cetkovich, M., Manes, F., Ibáñez, A., & Sedeño, L. (2017). The inner world of overactive monitoring: Neural markers of interoception in obsessive–compulsive disorder. *Psychological Medicine*, *47*(11), 1957–1970. https://doi.org/10.1017/S0033291717000368

Yu, J. (2021). A historical perspective of pulmonary rapidly adapting receptors. *Respiratory Physiology & Neurobiology*, *287*, 103595. https://doi.org/10.1016/j.resp.2020.103595

Zaccaro, A., della Penna, F., Mussini, E., Parrotta, E., Perrucci, M. G., Costantini, M., & Ferri, F. (2024). Attention to cardiac sensations enhances the heartbeat-evoked potential during exhalation. *iScience*, *27*(4), 109586. https://doi.org/10.1016/j.isci.2024.109586

Zaccaro, A., Perrucci, M. G., Parrotta, E., Costantini, M., & Ferri, F. (2022). Brain-heart interactions are modulated across the respiratory cycle via interoceptive attention. *NeuroImage*, *262*, 119548. https://doi.org/10.1016/j.neuroimage.2022.119548

Zaccaro, A., Piarulli, A., Laurino, M., Garbella, E., Menicucci, D., Neri, B., & Gemignani, A. (2018). How Breath-Control Can Change Your Life: A Systematic Review on Psycho-Physiological Correlates of Slow Breathing. *Frontiers in Human Neuroscience*, *12*, 353. https://doi.org/10.3389/fnhum.2018.00353

Zamariola, G., Maurage, P., Luminet, O., & Corneille, O. (2018). Interoceptive accuracy scores from the heartbeat counting task are problematic: Evidence from simple bivariate

correlations. *Biological Psychology*, *137*, 12–17. https://doi.org/10.1016/j.biopsycho.2018.06.006

Zareian, B., Maboudi, K., Daliri, M. R., Abrishami Moghaddam, H., Treue, S., & Esghaei, M. (2020). Attention strengthens across-trial pre-stimulus phase coherence in visual cortex, enhancing stimulus processing. *Scientific Reports*, *10*(1), 4837. https://doi.org/10.1038/s41598-020-61359-7

Zelano, C., Jiang, H., Zhou, G., Arora, N., Schuele, S., Rosenow, J., & Gottfried, J. A. (2016). Nasal Respiration Entrains Human Limbic Oscillations and Modulates Cognitive Function. *The Journal of Neuroscience*, *36*(49), 12448–12467. https://doi.org/10.1523/JNEUROSCI.2586-16.2016

Zoccal, D. B., Furuya, W. I., Bassi, M., Colombari, D. S. A., & Colombari, E. (2014). The nucleus of the solitary tract and the coordination of respiratory and sympathetic activities. *Frontiers in Physiology*, *5*. https://doi.org/10.3389/fphys.2014.00238

# Appendix A

# Supplementary Material for Study 1

## Text S1: Pilot Study

*Methods.* Thirty healthy volunteers (20 females; 1 left-handed; age: 26.2 ± 5.1 years [mean ± SD]) were recruited to complete three blocks of a modified heartbeat discrimination task (HDT), with each block corresponding to a different condition: 3 tones, 2 tones, and 1 tone. Each block contained 50 trials, for a total of 150 trials, with an equal distribution of simultaneous (S+) and non-simultaneous (S-) trials. In the S+ condition, the tone onset was delayed by 250 ms after the participant's R-peak onset, while in the S- condition, the tone onset was delayed by 550 ms after the R-peak onset. After each trial, participants were asked to decide whether they perceived the heartbeat and the tones as simultaneous by pressing a specific key on the computer keyboard, and to rate their confidence on a 4-points Likert scale, ranging from 1 (very unconfident) to 4 (very confident).

The HDT was preceded by an exteroceptive audio-visual familiarization task (AV Familiarization task). In the AV Familiarization task (Betka et al., 2021), participants were required to judge the simultaneity between a flashing dot and a sequence of acoustic signals played through computer speakers. The goal of this task was to familiarize participants with the judgment of simultaneity. There were two conditions: simultaneous (S+) and non-simultaneous (S-). In the S+ condition, the flashing dot and tone were presented without delay, while in the S- condition, the tone delivery onset was delayed by 550 ms after the flashing dot onset. The task consisted of 3 blocks corresponding to three different conditions: 3 tones, 2 tones, and 1 tone. Each block contained 10 trials with an equal distribution of S+ and S- trials, presented in random order. After each trial, participants had to decide whether they perceived the flashing dot and tones as simultaneous or not by pressing a specific key on the computer keyboard. They also rated their confidence on a 4-point Likert scale, ranging from 1 (very unconfident) to 4 (very confident).

Cardiac and respiratory activity were simultaneously recorded using three Ag/AgCl pre-gelled electrodes placed over the left and right clavicles and the right costal margin (ground electrode), along with a respiratory belt placed over the chest (respiratory transducer TSD201, BIOPAC Systems, Inc).

*Results.* The results of the Pilot Study showed that, in the 1-tone block, only 23% of participants achieved a performance with accuracy greater than 0.55 (indicating significantly above chance levels), compared to 47% in the 3-tone block, while in the 2-tone condition 43% of participants achieved an acceptable performance. These results are consistent with those reported by Brener in 1994, in which he compared the use of different numbers of consecutive tones (1, 5, and 10, Brener et al., 1994). According to Brener and colleagues, the presentation of a single tone is insufficient to obtain a reliable measure of cardiac interoceptive accuracy, as only 13% of participants were able to perceive the heartbeat with 1 tone, compared to 47% with 10 tones. Brener suggested that the higher proportion of participants able to perceive the heartbeat with multiple tones is due to the processes of orientation and attention facilitated by the sequence of stimuli. When participants have difficulty perceiving their heartbeat, the sequence of tones provides a temporal window in which they can locate the heartbeat, aiding its perception. The interval between tones likely provides a period that allows participants to anticipate the next heartbeat (Brener et al., 1994). Based on our results and those from previous studies, we decided to proceed with the 3-tones condition. Although there remains a risk that consecutive heartbeats may span multiple respiratory phases, this approach ensures that more than 50% of the heartbeats in each trial (i.e., two out of three) fall within the same respiratory phase, allowing us to categorize the entire trial as occurring either during inhalation or exhalation.

To make sure that the observed effects on event-related respiratory signal in the 3-tone condition were not caused by the presentation of three consecutive stimuli instead of one, as in the exteroceptive condition, we evaluated the event-related respiratory signal in the 1-tone condition of the Pilot Study and compared it to the event-related respiratory signal assessed for the tactile detection task (TDT) (Fig. S1); since only 16 (12 females; age: 27 ± 6.39 years [mean ± SD]) out of 30

participants in the Pilot Study met the inclusion criteria (accuracy above 0.55 and d' > 0) in the 1-tone condition, we reduced the exteroceptive sample to 16 participants (7 females; 1 left-handed; age: 25.25 ± 5.2 years) to ensure a more accurate comparison. However, it is important to note that the number of trials differed consistently between the two conditions (50 trials in the 1-tone condition of the Pilot Study compared to 300 trials in the TDT). The comparison revealed a significant difference between 0 and 1 second after cue onset ($t = 2.21$, $p = 0.01$, $p_{FDR} = 0.04$, $d = 0.14$), indicating that the respiratory modulation is not driven by the number of stimuli, but rather reflects a consistent strategy adopted across conditions.

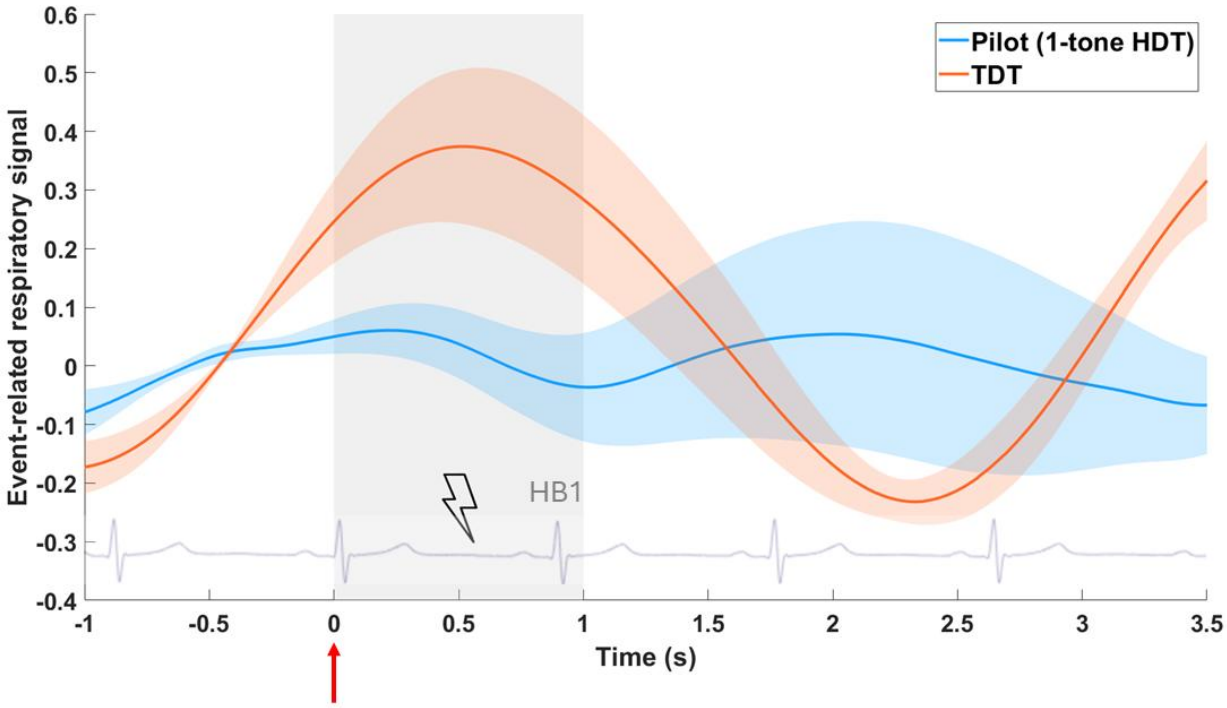



**Figure S1.** Event-related respiratory signal assessed for the 1-tone heartbeat discrimination task (HDT) condition of the Pilot Study and the exteroceptive task (tactile detection task - TDT). The gray area represents the window of statistical significance. The red arrow represents the cue onset in both conditions; lightning symbol represents the onset of the electrical stimulation in the TDT; the overlaid ECG signal represents an example of an S- trial, included to illustrate the temporal dynamics of the trial with the target heartbeat highlighted.

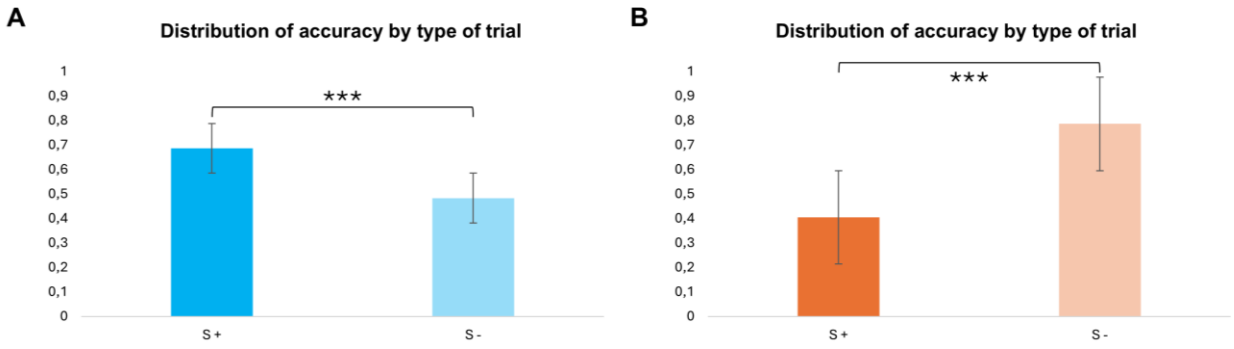



**Figure S2.** Distribution of accuracy by type of trial for **A)** heartbeat discrimination task and **B)** tactile detection task. *** $p < 0.001$.

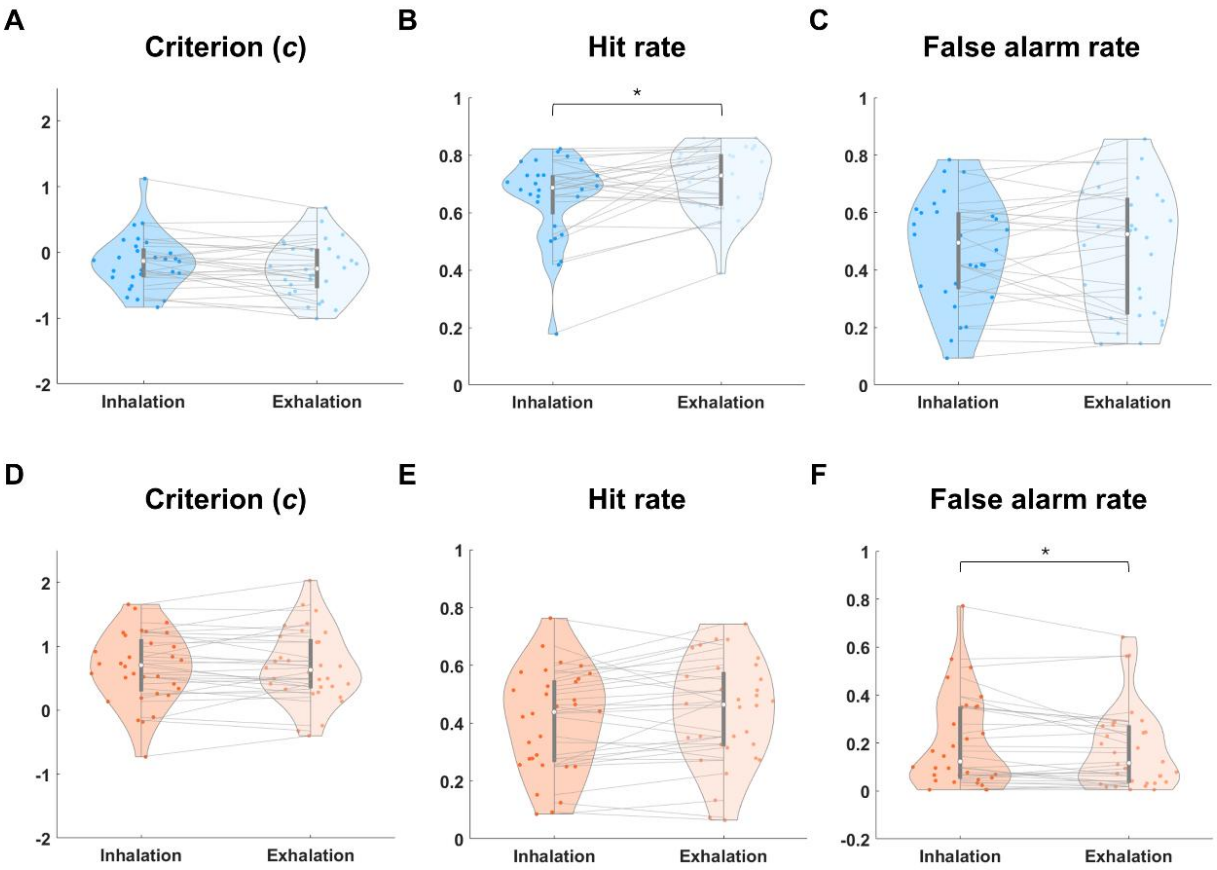



**Figure S3.** A) Criterion, B) hit rate and C) false alarm rate assessed for the heartbeat discrimination task during inhalation and exhalation; D) criterion, E) hit rate and F) false alarm rate assessed for the tactile detection task during inhalation and exhalation. * $p < 0.05$.

| Temporal window | t value | p | p (FDR-corrected) | Effect size (Cohen's d) |
|---|---|---|---|---|
| 0 – 0.5 s | 2.4269 | 0.0076 | 0.0432 | 0.606725 |
| 0.5 – 1 s | 2.2092 | 0.0144 | 0.0432 | 0.5523 |
| 1 – 1.5 s | 1.0912 | 0.1512 | 0.2268 | 0.2728 |
| 1.5 – 2 s | -0.5141 | 0.3333 | 0.3414 | -0.12853 |
| 2 – 2.5 s | -1.2898 | 0.0998 | 0.1996 | -0.32245 |
| 2.5 – 3 s | -0.577 | 0.3415 | 0.3415 | -0.14425 |

**Table S1.** Permutation-based t-test results for event-related respiratory signal differences between the pilot study and the tactile detection task.

| Temporal window | t value | p | p (FDR-corrected) | Effect size (Cohen's d) |
|---|---|---|---|---|
| 0 – 0.5 s | 2.5571 | 0.0044 | 0.0216 | 0.661712 |
| 0.5 – 1 s | 1.7151 | 0.0428 | 0.0856 | 0.443824 |
| 1 – 1.5 s | 0.3932 | 0.3531 | 0.3531 | 0.10175 |
| 1.5 – 2 s | -1.4257 | 0.0806 | 0.1209 | -0.36893 |
| 2 – 2.5 s | -2.3815 | 0.0072 | 0.0216 | -0.61627 |
| 2.5 – 3 s | -0.4596 | 0.3299 | 0.3531 | -0.11893 |

**Table S2.** Permutation-based t-test results for event-related respiratory signal differences between heartbeat discrimination task and tactile detection task.

| Temporal window | t value | p | Effect size (Cohen's d) |
|---|---|---|---|
| 0 – 0.5 s | 0.7965 | 0.2541 | 0.206114 |
| 0.5 – 1 s | 1.1573 | 0.1402 | 0.29948 |
| 1 – 1.5 s | 1.1656 | 0.1322 | 0.301628 |
| 1.5 – 2 s | 0.9678 | 0.1892 | 0.250442 |
| 2 – 2.5 s | 0.4967 | 0.3235 | 0.128533 |
| 2.5 – 3 s | 0.1606 | 0.4447 | 0.041559 |

**Table S3.** Permutation-based t-test results for inter-trial coherence differences between heartbeat discrimination task and tactile detection task.

| Temporal window | t value | p | p (FDR-corrected) | Effect size (Cohen's d) |
|---|---|---|---|---|
| 0 – 0.5 s | 0.0396 | 0.4835 | 0.4835 | 0.007484 |
| 0.5 – 1 s | 0.6853 | 0.2503 | 0.3004 | 0.12951 |
| 1 – 1.5 s | 1.5612 | 0.0632 | 0.0948 | 0.295039 |
| 1.5 – 2 s | 2.3951 | 0.0094 | 0.0188 | 0.452631 |
| 2 – 2.5 s | 2.7682 | 0.0036 | 0.0188 | 0.523141 |
| 2.5 – 3 s | 2.492 | 0.0088 | 0.0188 | 0.470944 |

**Table S4.** Permutation-based t-test results for inter-trial coherence differences between active phase and baseline in the heartbeat discrimination task.

| Temporal window | t value | p | p (FDR-corrected) | Effect size (Cohen's d) |
|---|---|---|---|---|
| 0 – 0.5 s | -0.6637 | 0.2577 | 0.2577 | -0.11733 |
| 0.5 – 1 s | 1.3084 | 0.1042 | 0.125 | 0.231295 |
| 1 – 1.5 s | 4.3872 | 0.0002 | 0.0003 | 0.775555 |
| 1.5 – 2 s | 7.5703 | 0.0002 | 0.0003 | 1.338253 |
| 2 – 2.5 s | 8.239 | 0.0002 | 0.0003 | 1.456463 |
| 2.5 – 3 s | 6.5865 | 0.0002 | 0.0003 | 1.16434 |

**Table S5.** Permutation-based t-test results for inter-trial coherence differences between active phase and baseline in the tactile detection task.

| Temporal window | t value | p | p (FDR-corrected) | Effect size (Cohen's d) |
|---|---|---|---|---|
| 0 – 0.5 s | -0.3186 | 0.3945 | 0.3945 | -0.06021 |
| 0.5 – 1 s | -0.9858 | 0.166 | 0.1992 | -0.1863 |
| 1 – 1.5 s | -1.4697 | 0.0764 | 0.111 | -0.27775 |
| 1.5 – 2 s | -1.6392 | 0.05 | 0.1 | -0.30978 |
| 2 – 2.5 s | -2.09 | 0.019 | 0.057 | -0.39497 |
| 2.5 – 3 s | -2.8054 | 0.0042 | 0.0252 | -0.53017 |

**Table S6.** Permutation-based t-test results for event-related respiratory signal differences between correct and incorrect trials in the heartbeat discrimination task.

| Temporal window | t value | p | Effect size (Cohen's d) |
|---|---|---|---|
| 0 – 0.5 s | 0.9682 | 0.197 | 0.171155 |
| 0.5 – 1 s | 0.1933 | 0.4323 | 0.034171 |
| 1 – 1.5 s | -0.5475 | 0.3079 | -0.09679 |
| 1.5 – 2 s | -0.565 | 0.3029 | -0.09988 |
| 2 – 2.5 s | -0.2676 | 0.4109 | -0.04731 |
| 2.5 – 3 s | 0.7157 | 0.25 | 0.126519 |

**Table S7.** Permutation-based t-test results for event-related respiratory signal differences between correct and incorrect trials in the tactile detection task.

| Temporal window | t value | p | p (FDR-corrected) | Effect size (Cohen's d) |
|---|---|---|---|---|
| 0 – 0.5 s | 0.1176 | 0.4575 | 0.4575 | 0.022224 |
| 0.5 – 1 s | 1.1604 | 0.1344 | 0.1613 | 0.219295 |
| 1 – 1.5 s | 2.3532 | 0.0126 | 0.0189 | 0.444713 |
| 1.5 – 2 s | 3.1484 | 0.0014 | 0.0036 | 0.594992 |
| 2 – 2.5 s | 3.337 | 0.0014 | 0.0036 | 0.630634 |
| 2.5 – 3 s | 3.2093 | 0.0018 | 0.0036 | 0.606501 |

**Table S8.** Permutation-based t-test results for inter-trial coherence differences between correct trials active phase and baseline in the heartbeat discrimination task.

| Temporal window | t value | p | p (FDR-corrected) | Effect size (Cohen's d) |
|---|---|---|---|---|
| 0 – 0.5 s | 0.5198 | 0.3015 | 0.3015 | 0.098233 |
| 0.5 – 1 s | 0.584 | 0.2773 | 0.3015 | 0.110366 |
| 1 – 1.5 s | 0.8777 | 0.2038 | 0.3015 | 0.16587 |
| 1.5 – 2 s | 1.66 | 0.058 | 0.116 | 0.313711 |
| 2 – 2.5 s | 1.9926 | 0.0254 | 0.116 | 0.376566 |
| 2.5 – 3 s | 1.788 | 0.0396 | 0.116 | 0.3379 |

**Table S9.** Permutation-based t-test results for inter-trial coherence differences between incorrect trials active phase and baseline in the heartbeat discrimination task.

| Temporal window | t value | p | p (FDR-corrected) | Effect size (Cohen's d) |
|---|---|---|---|---|
| 0 – 0.5 s | -1.4623 | 0.1332 | 0.1574 | -0.27635 |
| 0.5 – 1 s | -1.243 | 0.1564 | 0.1574 | -0.2349 |
| 1 – 1.5 s | -1.2335 | 0.1574 | 0.1574 | -0.23311 |
| 1.5 – 2 s | -1.5775 | 0.1258 | 0.1574 | -0.29812 |
| 2 – 2.5 s | -2.8467 | 0.0454 | 0.1362 | -0.53798 |
| 2.5 – 3 s | -6.2984 | 0.014 | 0.084 | -1.19029 |

**Table S10.** Permutation-based t-test results for inter-trial coherence differences between correct and incorrect trials in the heartbeat discrimination task.

| Temporal window | t value | p | p (FDR-corrected) | Effect size (Cohen's d) |
|---|---|---|---|---|
| 0 – 0.5 s | -0.4097 | 0.3433 | 0.3433 | -0.07243 |
| 0.5 – 1 s | 1.5752 | 0.065 | 0.078 | 0.278459 |
| 1 – 1.5 s | 4.6354 | 0.0002 | 0.0003 | 0.819431 |
| 1.5 – 2 s | 7.435 | 0.0002 | 0.0003 | 1.314335 |
| 2 – 2.5 s | 7.7452 | 0.0002 | 0.0003 | 1.369171 |
| 2.5 – 3 s | 6.3267 | 0.0002 | 0.0003 | 1.118413 |

**Table S11.** Permutation-based t-test results for inter-trial coherence differences between correct trials active phase and baseline in the tactile detection task.

| Temporal window | t value | p | p (FDR-corrected) | Effect size (Cohen's d) |
|---|---|---|---|---|
| 0 – 0.5 s | -0.7683 | 0.2248 | 0.2248 | -0.13582 |
| 0.5 – 1 s | 0.9305 | 0.1758 | 0.211 | 0.164491 |
| 1 – 1.5 s | 3.5355 | 0.0004 | 0.0006 | 0.624994 |
| 1.5 – 2 s | 5.9421 | 0.0002 | 0.0004 | 1.050425 |
| 2 – 2.5 s | 5.8996 | 0.0002 | 0.0004 | 1.042912 |
| 2.5 – 3 s | 4.4146 | 0.0002 | 0.0004 | 0.780398 |

**Table S12**. Permutation-based t-test results for inter-trial coherence differences between incorrect trials active phase and baseline in the tactile detection task.

| Temporal window | t value | p | Effect size (Cohen's d) |
|---|---|---|---|
| 0 – 0.5 s | -0.1598 | 0.4347 | -0.02825 |
| 0.5 – 1 s | -0.4019 | 0.3511 | -0.07105 |
| 1 – 1.5 s | -0.7406 | 0.2503 | -0.13092 |
| 1.5 – 2 s | -0.3799 | 0.3709 | -0.06716 |
| 2 – 2.5 s | -0.1423 | 0.4475 | -0.02516 |
| 2.5 – 3 s | 0.0583 | 0.4703 | 0.010306 |

**Table S13.** Permutation-based t-test results for inter-trial coherence differences between correct and incorrect trials in the tactile detection task.

| | HDT | | | | TDT | | |
|---|---|---|---|---|---|---|---|
| | **Fixed Factor** | **β** | **t stat** | **p** | **Fixed Factor** | **β** | **t stat** | **p** |
| Model 1 | Intercept | 0.89 | 35.86 | < 0.0001 | Intercept | 0.024 | 1.081 | 0.28 |
| | Condition | -0.2 | -15.9 | < 0.0001 | Condition | 0.38 | 38.63 | < 0.0001 |
| Model 2 | Intercept | 0.89 | 36.01 | < 0.0001 | Intercept | 0.019 | 0.83 | 0.4 |
| | condition | -0.2 | -15.9 | < 0.0001 | condition | 0.38 | 38.63 | < 0.0001 |
| | resp sin | 0.005 | 0.57 | 0.57 | resp sin | 0.0007 | 0.093 | 0.93 |
| | resp cos | -0.026 | -2.81 | 0.005 | resp cos | -0.02 | -2.8 | 0.005 |
| Model 3 | Intercept | 0.89 | 35.8 | < 0.0001 | Intercept | 0.025 | 1.18 | 0.24 |
| | condition | -0.2 | -15.9 | < 0.0001 | condition | 0.38 | 38.5 | < 0.0001 |
| | iHR | -0.001 | -0.74 | 0.46 | iHR | -0.005 | -4.68 | 2.90E-06 |
| Model 4 | Intercept | 0.89 | 36.01 | < 0.0001 | Intercept | 0.02 | 0.82 | 0.41 |
| | condition | -0.2 | -15.9 | < 0.0001 | condition | 0.38 | 38.53 | < 0.0001 |
| | resp sin | 0.005 | 0.57 | 0.57 | resp sin | 0.008 | 1.15 | 0.25 |
| | resp cos | -0.03 | -2.72 | 0.006 | resp cos | -0.025 | -3.37 | 0.0008 |
| | iHR | 1.30E-05 | 0.01 | 0.99 | iHR | -0.005 | -5.18 | 2.22E-07 |
| Model 5 | Intercept | 0.89 | 35.99 | < 0.0001 | Intercept | 0.02 | 0.89 | 0.37 |
| | condition | -0.2 | -15.9 | < 0.0001 | condition | 0.38 | 38.5 | < 0.0001 |
| | resp sin | 0.005 | 0.53 | 0.59 | resp sin | 0.008 | 1.12 | 0.26 |
| | resp cos | -0.026 | -2.7 | 0.0066 | resp cos | -0.02 | -3.24 | 0.001 |
| | iHR | -8.80E-05 | -0.07 | 0.94 | iHR | -0.005 | -4.47 | 7.80E-06 |
| | iHR:sin | 0.002 | 1.2 | 0.23 | iHR:sin | 0.0008 | -0.6 | 0.55 |
| | iHR:cos | -0.0006 | -0.36 | 0.72 | iHR:cos | -0.0017 | 1.15 | 0.25 |

**Table S14.** Summary of the generalized linear mixed model results for the heartbeat discrimination task (HDT; left column) and the tactile detection task (TDT; right column).

| HDT | | | | | TDT | | | | |
|---|---|---|---|---|---|---|---|---|---|
| **Model** | **AIC** | **BIC** | **LR stat** | **p** | **Model** | **AIC** | **BIC** | **LR stat** | **p** |
| 1 | 7621.2 | 7647.7 | | | 1 | 12186 | 12215 | | |
| 2 | 7617.1 | 7656.9 | 8.1244 | 0.017 | 2 | 12182 | 12225 | 7.89 | 0.019 |
| 1 | 7621.2 | 7647.7 | | | 1 | 12186 | 12215 | | |
| 3 | 7622.7 | 7655.8 | 0.54 | 0.46 | 3 | 12166 | 12202 | 21.85 | 2.94E-06 |
| 3 | 7622.7 | 7655.8 | | | 3 | 12166 | 12202 | | |
| 4 | 7619.1 | 7665.5 | 7.58 | 0.023 | 4 | 12157 | 12207 | 12.88 | 0.002 |
| 2 | 7617.1 | 7656.9 | | | 2 | 12182 | 12225 | | |
| 4 | 7619.1 | 7665.5 | 9.35E-05 | 0.99 | 4 | 12157 | 12207 | 26.83 | 2.20E-07 |
| 4 | 7619.1 | 7665.5 | | | 4 | 12157 | 12207 | | |
| 5 | 7621.5 | 7681.2 | 1.54 | 0.46 | 5 | 12160 | 12224 | 1.71 | 0.43 |

**Table S15.** Summary of the likelihood ratios tests results for the heartbeat discrimination task (HDT; left column) and the tactile detection task (TDT; right column).

# Appendix B

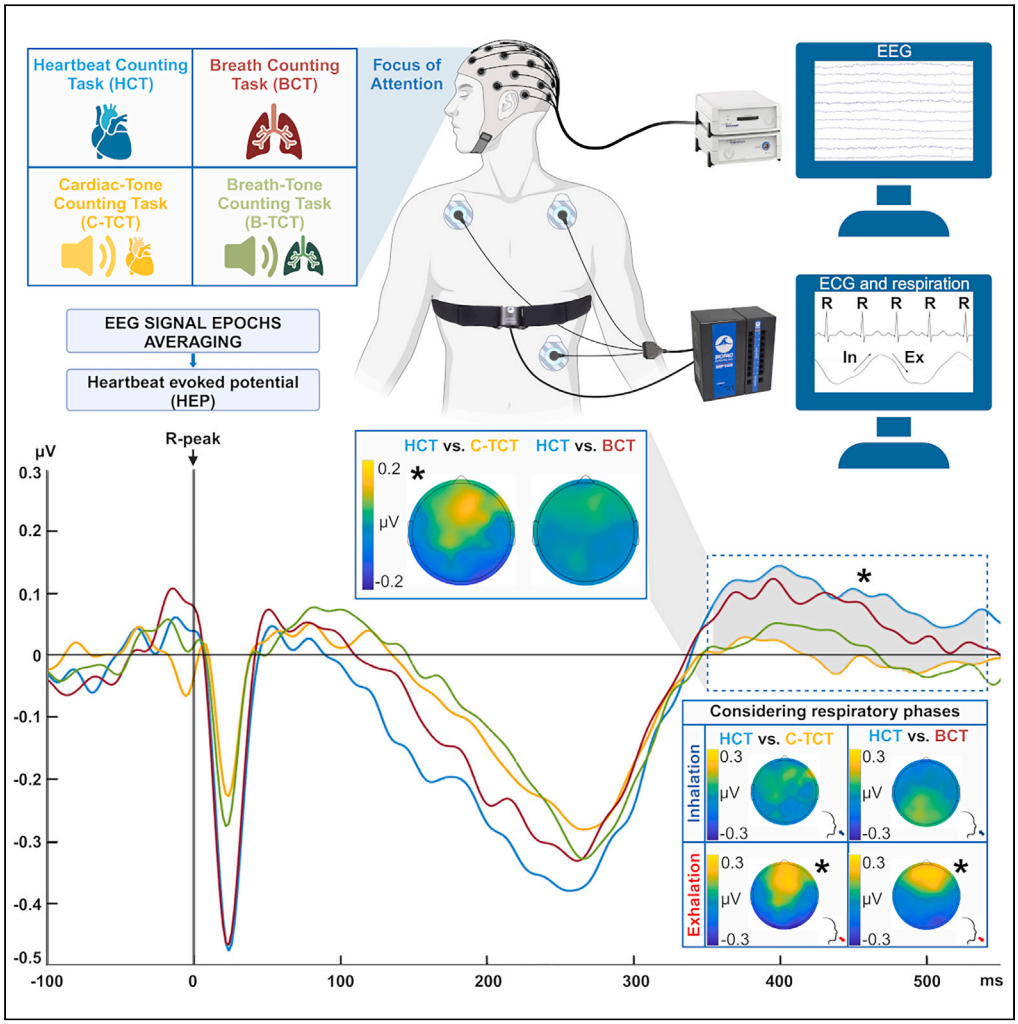
# Published version of Study 2

iScience

CellPress
OPEN ACCESS

Article

# Attention to cardiac sensations enhances the heartbeat-evoked potential during exhalation




Andrea Zaccaro, Francesca della Penna, Elena Mussini, Eleonora Parrotta, Mauro Gianni Perrucci, Marcello Costantini, Francesca Ferri

andrea.zaccaro@unich.it

## Highlights

Late HEP positivity increases during interoceptive tasks

Early HEP negativity increases non-specifically during exhalation

Late HEP increases specifically in the cardiac interoceptive task at exhalation

HEPs recorded at exhalation are linked to mindfulness and interoceptive sensibility

Zaccaro et al., iScience 27, 109586
April 19, 2024 © 2024 The Author(s). Published by Elsevier Inc.
https://doi.org/10.1016/j.isci.2024.109586

iScience

CellPress
OPEN ACCESS

Article

# Attention to cardiac sensations enhances the heartbeat-evoked potential during exhalation

Andrea Zaccaro,[1,4,*] Francesca della Penna,[2] Elena Mussini,[2] Eleonora Parrotta,[2] Mauro Gianni Perrucci,[2,3] Marcello Costantini,[1,3] and Francesca Ferri[2,3]

## SUMMARY

**Respiration and cardiac activity intricately interact through complex physiological mechanisms. The heartbeat-evoked potential (HEP) is an EEG fluctuation reflecting the cortical processing of cardiac signals. We recently found higher HEP amplitude during exhalation than inhalation during a task involving attention to cardiac sensations. This may have been due to reduced cardiac perception during inhalation and heightened perception during exhalation through attentional mechanisms. To investigate relationships between HEP, attention, and respiration, we introduced an experimental setup that included tasks related to cardiac and respiratory interoceptive and exteroceptive attention. Results revealed HEP amplitude increases during the interoceptive tasks over fronto-central electrodes. When respiratory phases were taken into account, HEP increases were primarily driven by heartbeats recorded during exhalation, specifically during the cardiac interoceptive task, while inhalation had minimal impact. These findings emphasize the role of respiration in cardiac interoceptive attention and could have implications for respiratory interventions to fine-tune cardiac interoception.**

## INTRODUCTION

The pulsation of the heart and the flow of respiration are intricately interconnected, together constituting two prominent oscillatory rhythms within the organism and representing major sources of interoceptive information. Cardiac interoceptive information is conveyed via the vagus and glossopharyngeal nerves to the nucleus of the solitary tract and the ventromedial posterior thalamic nucleus.[1–6] Subsequently, it reaches various brain regions including the amygdala, insula, cingulate, and somatosensory cortices. The modulation of EEG activity associated with the heartbeat and typically observed over fronto-central areas reflects this interoceptive information.[7–9] This phenomenon is specifically referred to as the heartbeat-evoked potential (HEP). The HEP is an event-related potential time-locked to the cardiac cycle derived by averaging EEG epochs around simultaneously recorded ECG R-peaks. Originally described by Schandry and colleagues,[10] it has gained interest in the interoception research field,[11,12] where it is considered an electrophysiological signature of the cortical processing of the heartbeat. The physiological pathways underlying HEP generation are still under study, but they are likely associated with mechanoreceptive signals from baroreceptors located in the aortic arch, carotid sinus, and carotid arteries.[13–16]

Cardiac activity is widely intertwined with respiration, another fundamental interoceptive rhythm in the human body.[12,17,18] Given the strong interactions between cardiac function and respiration at the physiological level,[19] we recently investigated the effects of respiratory phases on cardiac interoception in healthy participants. We observed an increase in late HEP amplitude and cardiac interoceptive accuracy during exhalation compared to inhalation while performing the interoceptive condition of the Heartbeat Detection Task (HBD).[20] This task involves focusing attention on the heart and pressing a button in synchrony with it.[21,22] Our interpretation was grounded in the continuous reception of both cardiac and respiratory sensations by the brain through vagal pathways, with the latter predominantly conveyed during inhalation.[23,24] Consequently, heartbeat sensations during inhalation may compete with concurrent respiratory sensations. This competition may decrease during exhalation, resulting in a reduction of respiratory interference. Therefore, during HBD, when cardiac sensations are heightened by attention, increased HEP and interoceptive accuracy may manifest during exhalation.[20]

Despite these findings, some ambiguities remained regarding the relationships between HEP, attention, and respiratory phases. Firstly, while previous studies have compared HEP amplitude between cardiac interoceptive tasks and exteroceptive tasks,[16] there is a lack of research comparing HEP amplitude between cardiac interoceptive tasks and *non-cardiac* interoceptive tasks, which involve focusing on interoceptive sensations unrelated to the heart. As such, HEP augmentation has been associated not only with attention focused toward the heart,

[1]Department of Psychological, Health and Territorial Sciences, "G. d'Annunzio" University of Chieti-Pescara, Chieti, Italy
[2]Department of Neuroscience, Imaging and Clinical Sciences, "G. d'Annunzio" University of Chieti-Pescara, Chieti, Italy
[3]Institute for Advanced Biomedical Technologies, ITAB, "G. d'Annunzio" University of Chieti-Pescara, Chieti, Italy
[4]Lead contact
*Correspondence: andrea.zaccaro@unich.it
https://doi.org/10.1016/j.isci.2024.109586


This is an open access article under the CC BY-NC-ND license (http://creativecommons.org/licenses/by-nc-nd/4.0/).

but also on the bodily self or the self in a broader sense.[25–29] Secondly, in our previous study,[20] confounding factors such as motor activity involved in HBD posed challenges for direct comparison of respiratory phase-related HEP effects between the interoceptive and exteroceptive condition.

Here, we have developed an experimental approach to distinguish the impact of respiratory phases on HEP during different types of interoceptive and exteroceptive attention. We used the Heartbeat Counting Task (HCT) to elicit cardiac interoception while avoiding potential movement-related issues present in HBD. In the first analysis, we compared HEP amplitude between tasks focused on cardiac interoception and exteroception, as well as tasks targeting *non-cardiac* interoception and exteroception, specifically focusing on respiration. Given the established links between HEP and cardiac interoceptive attention,[16] we expected an increase in HEP amplitude during the cardiac interoceptive task (HCT) compared to the exteroceptive task, with no HEP changes during the respiratory interoceptive task. In the second analysis, we explored how attention influenced HEP responses in interaction with respiration, aiming to determine whether putative changes in HEP amplitude during HCT were specific to a given respiratory phase. Given the connections between interoceptive sensibility, trait mindfulness, and HEP activity,[30–32] we also investigated whether they were associated with HEPs recorded during exhalation and inhalation. Based on our previous findings that showed higher late HEPs during exhalation,[20] we predicted a stronger contribution of exhalation in driving the expected HEP amplitude increase during HCT and its associations with interoceptive sensibility and mindfulness. If confirmed, these findings would highlight a previously overlooked role of respiratory phases in modulating cardiac interoception. In addition, recognizing the role of each specific respiratory phase in shaping interoception may provide valuable insights for clinical populations that show altered interoceptive functions, such as major depression or anxiety disorders.[33] For example, specific impairments of cardiac signal processing during exhalation may benefit from the development of respiratory-based interventions to fine-tune cardiac interoception. These findings could potentially refine therapeutic applications, such as mindfulness and slow breathing practices.

## RESULTS

### Overview

After a baseline resting state with eyes open, participants underwent four tasks involving interoceptive and exteroceptive attention (attention focus factor) focused on the cardiac and the respiratory systems (system factor). Tasks included HCT[10,13] and the Breath Counting Task (BCT)[34] as interoceptive tasks, and the Cardiac-Tone Counting Task (C-TCT)[35] and the Breath-Tone Counting Task (B-TCT; adapted from[34]) as exteroceptive tasks.

### Heartbeat-evoked potential activity is related to interoceptive attention

To test whether HEP activity was modulated by attention, we performed a cluster-based permutation test over the whole scalp, with HEP amplitude as the dependent variable and System (cardiac vs. respiratory) and Attention Focus (interoceptive vs. exteroceptive) as within-participant factors (see STAR Methods for details on the interaction and main effects calculation). Included epochs in each task are shown in Table S1. Based on previous research,[4,20,30,36–42] we tested HEP amplitude at each electrode and time point separately in an early (100–350 msec) and a late time window (350–600 msec) after the R-peak.

In the early time window, there was no difference in HEP amplitude between interoceptive and exteroceptive attention (Attention Focus: $t_{31} = -1.312$, $p_{clust} = 0.115$, $d = 0.232$) nor between the cardiac and respiratory system (System: $t_{31} = 0.892$, $p_{clust} = 0.234$, $d = 0.158$). However, there was a significant System by Attention Focus interaction from 242 to 313 msec after the R-peak over the following electrodes: Fp1, AF7, AF3, F3, F1, Fpz, AFz, Fz, FCz, Fp2, AF8, AF4, and F2 ($t_{31} = -4.034$, $p_{clust} = 0.018$, $d = 0.713$, Figure S1A). However, despite the interaction, none of the planned t-tests were significant, showing no HEP difference when comparing the tasks (HCT vs. C-TCT: $t_{31} = -2.376$, $p_{clust} = 0.069$, $d = 0.42$; HCT vs. BCT: $t_{31} = 2.631$, $p_{clust} = 0.067$, $d = 0.465$; BCT vs. B-TCT: $t_{31} = -0.114$, $p_{clust} = 0.434$, $d = 0.02$; and C-TCT vs. B-TCT: $t_{31} = 2.724$, $p_{clust} = 0.312$, $d = 0.485$).

In the late time window, a higher HEP positivity was observed for interoceptive attention over F3, F1, FC1, C3, C1, CP1, CP3, Fpz, AFz, Fz, FCz, Cz, AF4, F6, F2, FC4, and FC2 from 352 to 508 msec after the R-peak (Attention Focus: $t_{31} = 5.039$, $p_{clust} = 0.017$, $d = 0.891$, Figures 1A and S1B). Neither the main effect of the system ($t_{31} = 0.338$, $p_{clust} = 0.738$, $d = 0.06$) nor the System by Attention Focus interaction ($t_{31} = 1.28$, $p_{clust} = 0.872$, $d = 0.227$) were significant. These findings suggest that the impact of attention on late HEP amplitude did not specifically depend on the system being monitored (cardiac vs. respiratory) but was associated with attention directed toward the body. Despite the non-significant interaction, planned t-tests conducted based on previous studies[16] revealed increases in HEP activity only during HCT compared to C-TCT from 352 to 539 msec after the R-peak over F1, FC3, FC1, C1, AFz, Fz, FCz, AF4, F6, F4, F2, FC4, and FC2 ($t_{31} = 4.13$, $p_{clust} = 0.013$, $p_{FDR} = 0.039$, $d = 0.73$, Figures 1B and S1C), but not compared to BCT ($t_{31} = 1.34$, $p_{clust} = 0.19$, $d = 0.273$, Figure 1B). No differences were observed between BCT vs. B-TCT ($t_{31} = 0.627$, $p_{clust} = 0.231$, $d = 0.111$, Figure 1B), nor between C-TCT vs. B-TCT ($t_{31} = -0.683$, $p_{clust} = 0.5$, $d = 0.121$, Figure 1B).

### Heartbeat-evoked potential activity is related to the respiratory phase

To test whether HEP activity was modulated by the respiratory phase, we differentiated HEPs occurring during inhalation and exhalation. We found more epochs during inhalation than exhalation, likely due to higher Heart Rate (HR) during inhalation, resulting in the detection of more R-peaks (Table S2). We first ran a cluster-based permutation t-test comparing HEP amplitude between inhalation and exhalation during the baseline. In the early time window, the analysis showed a positive posterior cluster of higher HEP amplitude during exhalation compared to inhalation from 195 to 328 msec after the R-peak (CP1, CP3, CP5, P1, P3, P5, PO3, CPz, Pz, POz, C4, CP2, CP4, CP6, P2, P4, P6, and PO4)

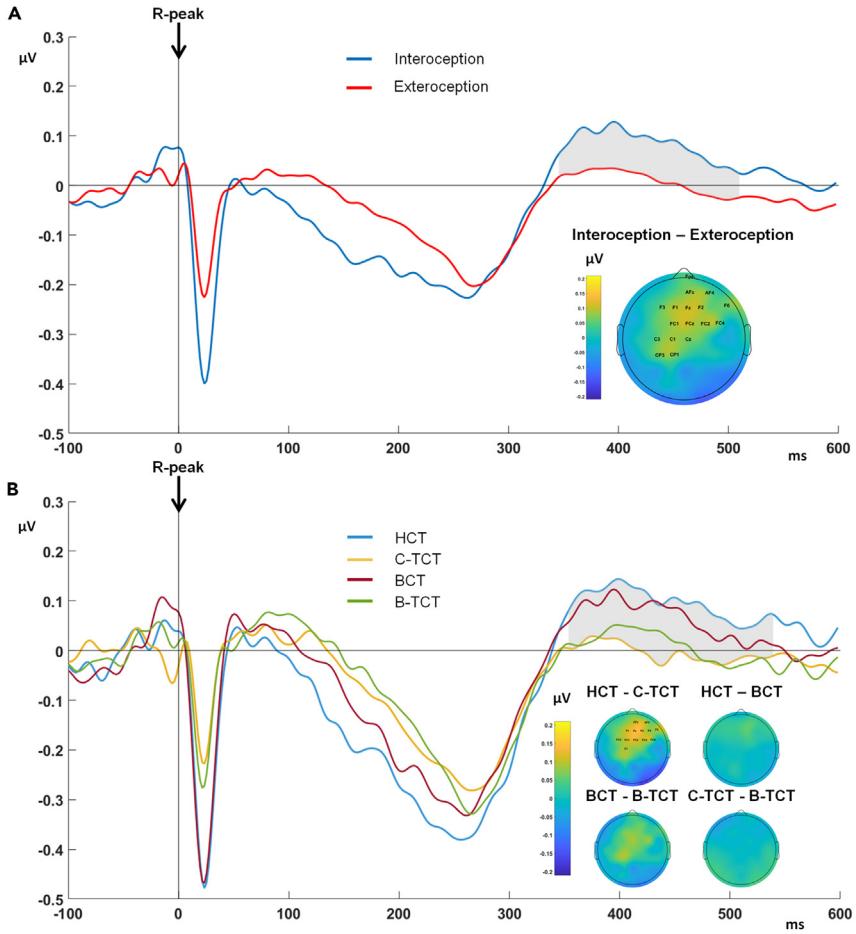



**Figure 1. HEP activity is related to interoceptive attention**

(A) Grand-average HEP pooled for significant electrodes illustrating the main effect of Attention Focus. The shaded area marks significant differences between Interoception (blue) and Exteroception (red). The topographical distribution represents HEP differences between Interoception vs. Exteroception. Labels represent significant electrodes (cluster-based t-test: $t_{31} = 5.039$, $p_{clust} = 0.017$, $d = 0.891$). The scale bar unit of measurement is μV.

(B) Grand-average HEP pooled for significant electrodes during HCT (light blue), C-TCT (orange), BCT (purple), and B-TCT (green). The shaded area marks significant differences between HCT and C-TCT. The topographical distributions represent HEP differences between HCT vs. C-TCT, HCT vs. BCT, BCT vs. B-TCT, and C-TCT vs. B-TCT. Labels represent significant electrodes (cluster-based t-test: $t_{31} = 4.13$, $p_{clust} = 0.013$, $p_{FDR} = 0.039$, $d = 0.73$). The scale bar unit of measurement is μV. Abbreviations: HCT-Heartbeat Counting Task, C-TCT-Cardiac-Tone Counting Task, BCT-Breath Counting Task, B-TCT-Breath-Tone Counting Task.

($t_{27} = 3.9$, $p_{clust} = 0.012$, $d = 0.738$, Figure S2) and a negative frontal cluster from 195 to 336 msec (Fp1, AF7, AF3, F5, F3, F1, FC5, FC3, C3, C5, Fpz, AFz, Fz, FCz, Fp2, AF8, AF4, F6, F4, F2, FC6, FC4, FC2, and C6) ($t_{27} = 3.18$, $p_{clust} = 0.012$, $d = 0.601$, Figure S2). We found no significant differences in the late time window ($t_{27} = 2.7$, $p_{clust} = 0.303$, $d = 0.489$).

We then conducted two cluster-based permutation tests: one for the early and one for the late time window, both focused on the significant fronto-central cluster observed in the previous analysis that did not consider the respiratory phase. In these analyses, HEP amplitude served as the dependent variable, with System (cardiac vs. respiratory), Attention Focus (interoceptive vs. exteroceptive), and respiratory Phase (inhalation vs. exhalation) as within-participant factors. In the early time window, we found a main effect of Phase from 117 to 266 msec after the R-peak over Fp1, AF7, AF3, F5, F3, F1, FC3, FC1, AFz, Fz, FCz, AF8, AF4, F6, F4, F2, and FC4 ($t_{27} = -3.32$, $p_{clust} = 0.007$, $d = 0.627$, Figures 2A and S3A), indicating that HEP negativity was consistently higher during exhalation compared to inhalation across all tasks. There was no main effect of System ($t_{27} = -1.65$, $p_{clust} = 0.054$, $d = 0.311$) or Attention Focus ($t_{27} = -2.71$, $p_{clust} = 0.472$, $d = 0.512$). Moreover, no interactions were significant (System by Attention Focus by Phase: $t_{27} = 0.544$, $p_{clust} = 0.089$, $d = 0.103$; System by Attention Focus: $t_{27} = 1.68$, $p_{clust} = 0.698$, $d = 0.318$; Attention Focus by Phase: $t_{27} = -0.674$, $p_{clust} = 0.55$, $d = 0.127$; System by Phase: $t_{27} = 1.40$, $p_{clust} = 0.098$, $d = 0.265$).

In the late time window, we found no main effect of System ($t_{27} = 0.2$, $p_{clust} = 0.319$, $d = 0.038$), Attention Focus ($t_{27} = 2.057$, $p_{clust} = 0.857$, $d = 0.389$), or Phase ($t_{27} = 0.777$, $p_{clust} = 0.174$, $d = 0.147$) on HEP. Similarly, there were no significant System by Attention Focus ($t_{27} = -1.705$, $p_{clust} = 0.974$, $d = 0.322$), System by Phase ($t_{27} = -0.45$, $p_{clust} = 0.318$, $d = 0.085$), or Attention Focus by Phase interactions ($t_{27} = 1.058$,

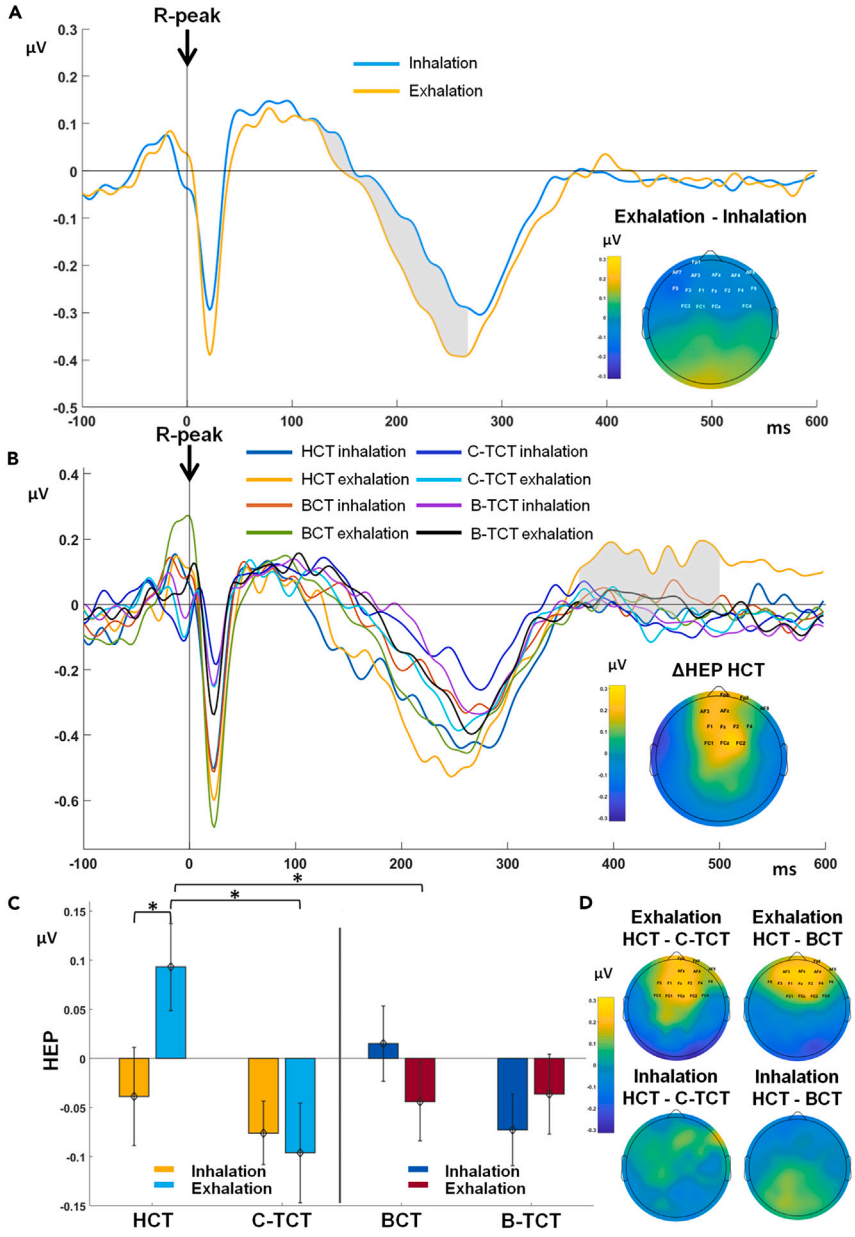



**Figure 2. HEP activity is related to the respiratory phase**

(A) Grand-average HEP pooled for significant electrodes illustrating the main effect of Phase. The shaded area marks significant differences between Exhalation (orange) and Inhalation (light blue). The topographical distribution represents HEP differences between Exhalation vs. Inhalation. Labels represent significant electrodes (cluster-based t-test: $t_{27} = -3.32$, $p_{clust} = 0.007$, d = 0.627). The scale bar unit of measurement is μV.

(B) Grand-average HEP pooled for significant electrodes during different respiratory phases: HCT-inhalation (dark turquoise), HCT-exhalation (orange), BCT-inhalation (brown), BCT-exhalation (green), C-TCT-inhalation (blue), C-TCT-exhalation (light blue), B-TCT-inhalation (purple), B-TCT-exhalation (black). The shaded area marks significant differences between exhalation and inhalation (ΔHEP) during HCT. The topographical distribution represents HEP differences between Exhalation vs. Inhalation during HCT. Labels represent significant electrodes (cluster-based t-test: $t_{27} = 3.8$, $p_{clust} = 0.005$, $p_{FDR} = 0.02$, d = 0.719). The scale bar unit of measurement is μV.

(C) Mean HEP amplitude over significant electrodes across tasks and respiratory phases. Data are presented as mean +/− standard error. Significant planned t-tests are indicated by asterisks (*p < 0.05).

(D) Topographical distributions represent HEP differences during exhalation between HCT vs. C-TCT and HCT vs. BCT, and during inhalation between HCT vs. C-TCT and HCT vs. BCT. Labels represent significant electrodes (Exhalation HCT vs. C-TCT cluster-based t-test: $t_{27} = 3.668$, $p_{clust} = 0.003$, $p_{FDR} = 0.02$, d = 0.693; Exhalation HCT vs. BCT cluster-based t-test: $t_{27} = 3.572$, $p_{clust} = 0.018$, $p_{FDR} = 0.048$, d = 0.675). The scale bar unit of measurement is μV. Abbreviations: HCT-Heartbeat Counting Task, C-TCT-Cardiac-Tone Counting Task, BCT-Breath Counting Task, B-TCT-Breath-Tone Counting Task.

$p_{clust}$ = 0.676, d = 0.199). Crucially, however, the three-way System by Attention Focus by Phase interaction was significant from 430 to 523 msec over Fp1, AF3, F5, F3, F1, FC1, Fpz, AFz, Fz, Fp2, AF8, AF4, F4, F2, FC4, and FC2 ($t_{27}$ = 3.98, $p_{clust}$ = 0.031, d = 0.583, Figure S3B). This interaction was explained by the following planned t-tests, which showed that HEP positivity increased during exhalation compared to inhalation specifically in HCT, from 367 to 500 msec after the R-peak, over AF3, F1, FC1, Fpz, AFz, Fz, FCz, Fp2, AF8, F4, F2, and FC2 ($t_{27}$ = 3.8, $p_{clust}$ = 0.005, $p_{FDR}$ = 0.02, d = 0.719, Figures 2B, 2C, and S3C). In contrast, there were no changes in HEP activity between exhalation and inhalation in BCT ($t_{27}$ = −0.357, $p_{clust}$ = 0.129, d = 0.067), C-TCT ($t_{27}$ = 0.116, $p_{clust}$ = 0.667, d = 0.022), or B-TCT ($t_{27}$ = 1.01, $p_{clust}$ = 0.392, d = 0.192). The ΔHEPs waveforms, defined as the difference between HEPs during exhalation and HEPs during inhalation, are represented for each task in Figure S4. Interestingly, HEPs recorded during exhalation in HCT were higher than those recorded during exhalation in C-TCT from 383 to 508 msec after the R-peak over F3, F1, FC3, FC1, Fpz, AFz, Fz, FCz, Fp2, AF8, AF4, F6, F4, F2, FC4, and FC2 ($t_{27}$ = 3.668, $p_{clust}$ = 0.003, $p_{FDR}$ = 0.02, d = 0.693, Figures 2C, 2D, and S3D), and during exhalation in BCT from 445 to 500 msec over AF3, F5, F3, F1, FC1, AFz, Fz, FCz, Fp2, AF8, AF4, F6, F4, F2, FC4, and FC2 ($t_{27}$ = 3.572, $p_{clust}$ = 0.018, $p_{FDR}$ = 0.048, d = 0.675, Figures 2C, 2D, and S3E). In contrast, there were no changes between HEPs recorded during inhalation in HCT and those recorded during inhalation in C-TCT ($t_{27}$ = 0.428, $p_{clust}$ = 0.654, d = 0.081, Figure 2D) nor BCT ($t_{27}$ = −1.061, $p_{clust}$ = 0.895, d = 0.2, Figure 2D). These results showed higher late HEP positivity during exhalation compared to inhalation specifically for HCT. Importantly, they highlight that the observed increases in HEP amplitude during HCT primarily stem from HEPs recorded during exhalation, with minimal contribution from HEPs recorded during inhalation.

### Heartbeat-evoked potential and cardio-respiratory physiology

We performed control analyses at both the participant and trial levels to assess whether observed changes in HEP amplitude were related to cardio-respiratory physiology[8,43–47] (STAR Methods). Cardio-respiratory features of interest are described in the STAR Methods. We found negligible effects of cardio-respiratory physiology on HEP changes across tasks and respiratory phases (Figures S5–S10; Tables S3–S5).

### Respiratory cycle analyses during the Heartbeat Counting Task

To capture HEP changes across the respiratory cycle during HCT, we employed circular statistics and divided the respiratory cycle into phase bins. We used the interquartile range to categorize HEPs into low and high-amplitude HEPs. The Rayleigh test rejected the uniform distribution for both low (z = 11.282, p < 0.001) and high-amplitude HEPs (z = 3.809, p = 0.021). Low-amplitude HEPs were clustered around the middle phase of inhalation (first and second quadrants; mean angle = 100.45°, Figure 3A), while high-amplitude HEPs were clustered around the early phase of inhalation (first quadrant) and extended to the exhalation phase (third and fourth quadrant), with the mean direction occurring near the transition from exhalation to inhalation (19.99°, Figure 3B). The Watson-Williams test revealed significant differences between low and high-amplitude HEPs ($F_{1,54}$ = 15.665, p < 0.001).

We assessed HEP amplitude changes in HCT across the respiratory cycle using six equally sized bins covering the 0°–360° interval. A one-way repeated measures ANOVA revealed significant HEP amplitude changes across phase bins ($F_{5,135}$ = 3.23, p = 0.009, $\eta$p2 = 0.107). Planned t-tests showed that HEPs detected in the 60°–120° range (middle inhalation) had lower amplitude than those detected in the 240°–300° range (middle exhalation: $t_{27}$ = −2.995, p = 0.006, $p_{FDR}$ = 0.027, d = 0.566) and the 300°–360° range (late exhalation: $t_{27}$ = −2.43, p = 0.022, $p_{FRD}$ = 0.049, d = 0.459). Furthermore, HEPs detected in the 120°–180° range (late inhalation) had lower amplitude than those detected in the 240°–300° range (middle exhalation: $t_{27}$ = −3.063, p = 0.005, $p_{FRD}$ = 0.027, d = 0.578) and the 300°–360° range (late exhalation: $t_{27}$ = −2.731, p = 0.011, $p_{FRD}$ = 0.033, d = 0.516) (Figure 3C). All the other comparisons did not show significant differences.

### Correlation between the heartbeat evoked potential, behavioral and psychometric data

Task accuracy changed across tasks (Table S6). A 2 × 2 repeated measures ANOVA revealed a main effect of System ($F_{1,31}$ = 73.1, p < 0.001, $\eta$p2 = 0.702) and Attention Focus ($F_{1,31}$ = 108.5, p < 0.001, $\eta$p2 = 0.778), with lower accuracy in the cardiac than respiratory condition and in the interoceptive than exteroceptive condition. We also found a significant system by attention focus interaction ($F_{1,31}$ = 110.7, p < 0.001, $\eta$p2 = 0.781). Planned t-tests revealed lower task accuracy in HCT compared to C-TCT ($t_{31}$ = −10.78, p < 0.001, d = 1.91) and BCT ($t_{31}$ = −9.66, p < 0.001, d = 1.71), and lower task accuracy in B-TCT compared to C-TCT ($t_{31}$ = −2.6, p = 0.048, d = 0.365). No differences were observed between BCT and B-TCT ($t_{31}$ = −1.81, p = 0.08, d = 0.32). Correlations with HEP amplitude showed no relationship with HCT accuracy (r = 0.117, p = 0.524) or confidence (r = 0.108, p = 0.558). Similarly, HEPs amplitude during inhalation or exhalation did not correlate with HCT accuracy (inhalation: r = 0.074, p = 0.708; exhalation: r = −0.047, p = 0.812) or confidence (inhalation: r = 0.183, p = 0.352; exhalation: r = −0.086, p = 0.663). The absence of correlation might arise from the inherent limitations of HCT in assessing accuracy.[48–50] In addition, while interoceptive accuracy is related to the conscious perception of heartbeats, HEP changes may also be attributed to unconscious processes.[51]

Given previous associations of HEP activity with specific self-reported interoceptive sensibility and trait mindfulness,[30–32] we examined the correlations between scores obtained on the Trusting and Not-Worrying scales of the Multidimensional Assessment of Interoceptive Awareness (MAIA) and the total score of the Five Facet Mindfulness Questionnaire (FFMQ) with HEP amplitude recorded during inhalation and exhalation during HCT. HEPs recorded during inhalation did not correlate with any of the scales (FFMQ Total Score: r = −0.01, p = 0.963, Figure 4A; MAIA Trusting: r = 0.163, p = 0.437; Figure 4B; MAIA Not-Worrying: r = −0.348, p = 0.088; Figure 4C). In contrast, HEPs recorded during exhalation exhibited a positive correlation with FFMQ total score (r = 0.407, p = 0.044, Figure 4D) and MAIA Trusting scale (r = 0.399, p = 0.048, Figure 4E), but not with MAIA Not-Worrying scale (r = 0.139, p = 0.506, Figure 4F). None of the other MAIA scales correlated with HEP values. These findings suggest that the relationship between HEP amplitude, interoceptive sensibility, and trait mindfulness is related to HEPs recorded during exhalation.

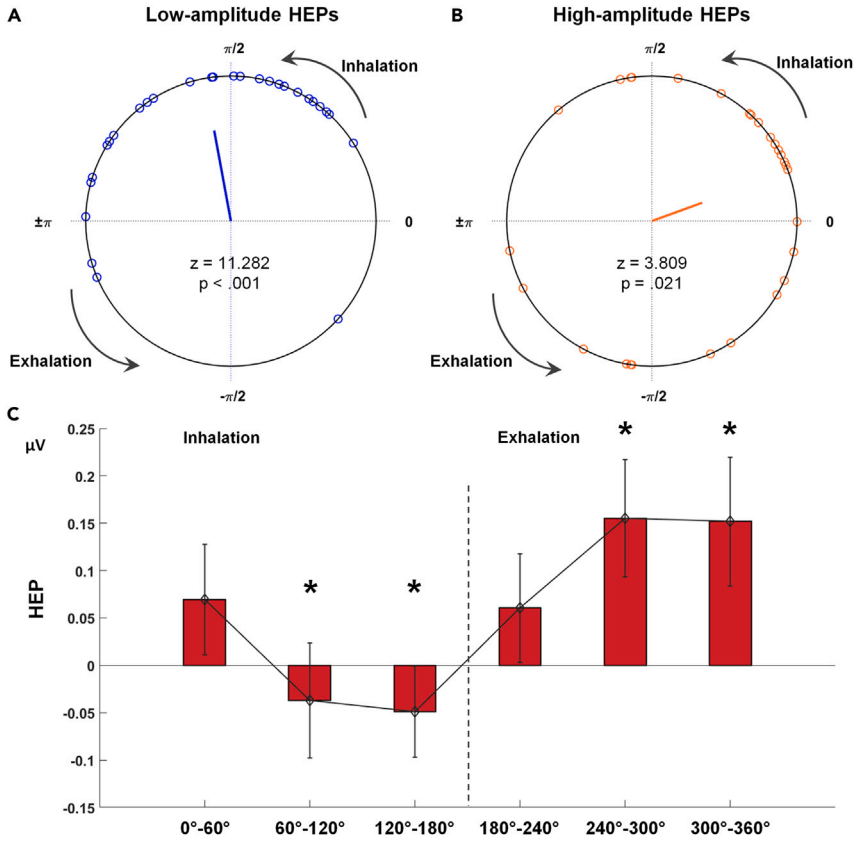



**Figure 3. Respiratory cycle analyses during HCT**

Circular distribution of mean angles (HEPs onsets relative to the respiratory cycle) for (A) low-amplitude HEPs (blue) and (B) high-amplitude HEPs (orange). Zero degree corresponds to inhalation onset. Each dot indicates the mean angle of one participant. Line direction indicates the mean angle across the participants. Arrow length represents the mean resultant length.

(C) The mean amplitude of HEPs as a function of six equally sized bins of the respiratory phase (from 0° to 360°). Data are presented as mean +/− standard error. Significant paired t-tests comparing inhalation and exhalation phase bins are indicated by asterisks (*p < 0.05): 60°–120° vs. 240°–300° ($t_{27} = -2.995$, p = 0.006, $p_{FDR} = 0.027$, d = 0.566); 60°–120° vs. 300°–360° ($t_{27} = -2.43$, p = 0.022, $p_{FRD} = 0.049$, d = 0.459); 120°–180° vs. 240°–300° ($t_{27} = -3.063$, p = 0.005, $p_{FRD} = 0.027$, d = 0.578); 120°–180° vs. 300°–360° ($t_{27} = -2.731$, p = 0.011, $p_{FRD} = 0.033$, d = 0.516).

## DISCUSSION

We assessed HEP activity in healthy volunteers during tasks prompting either interoceptive or exteroceptive attention. Our aim was to investigate HEP and ΔHEP (respiratory phase-related HEP modulations) changes across different interoceptive and exteroceptive attention tasks. The results revealed late HEP amplitude increases during the interoceptive tasks at fronto-central electrodes, while only partially supporting the idea that HEP increases are specifically induced by cardiac interoceptive attention. Additionally, the results suggest that, despite some limitations that may influence its validity in assessing accuracy,[48–50] HCT is a suitable task to elicit cardiac interoceptive attention. Crucially, when respiratory phases were taken into account, a specific modulation of HEP amplitude induced by cardiac interoceptive attention clearly emerged. When comparing the respiratory phase-induced modulations of HEPs between the different tasks (HCT, BCT, C-TCT, and B-TCT), results revealed increased HEP positivity during exhalation compared to inhalation only during the cardiac interoceptive task (HCT). In contrast, no changes in HEP activity were observed between exhalation and inhalation during the other tasks. Circular statistics showed that in HCT low-amplitude HEPs were clustered around the middle part of inhalation and high-amplitude HEPs were concentrated around exhalation and the transition from exhalation to inhalation. We also observed a gradual increase in HEP amplitude throughout the respiratory cycle, peaking at the end of exhalation (240°–360° respiratory phase bins). Importantly, the experimental design allowed a direct comparison of HEP amplitude between inhalation and exhalation among tasks. We found that HEPs recorded during exhalation in HCT showed higher amplitude than HEPs recorded during exhalation in C-TCT and BCT. Notably, no differences were found when comparing HEPs recorded during inhalation in HCT with HEPs recorded during inhalation in C-TCT or BCT. These results extend our previous findings regarding changes in HEP amplitude between respiratory phases.[20] Firstly, they corroborate previous results using HCT in addition to HBD. Secondly, they establish that late HEP modulations related to the respiratory phase are specific to the *cardiac* interoceptive task and do not extend to *non-cardiac* interoceptive tasks (BCT). This also suggests that ΔHEP modulation is a more specific index for cardiac interoceptive attention

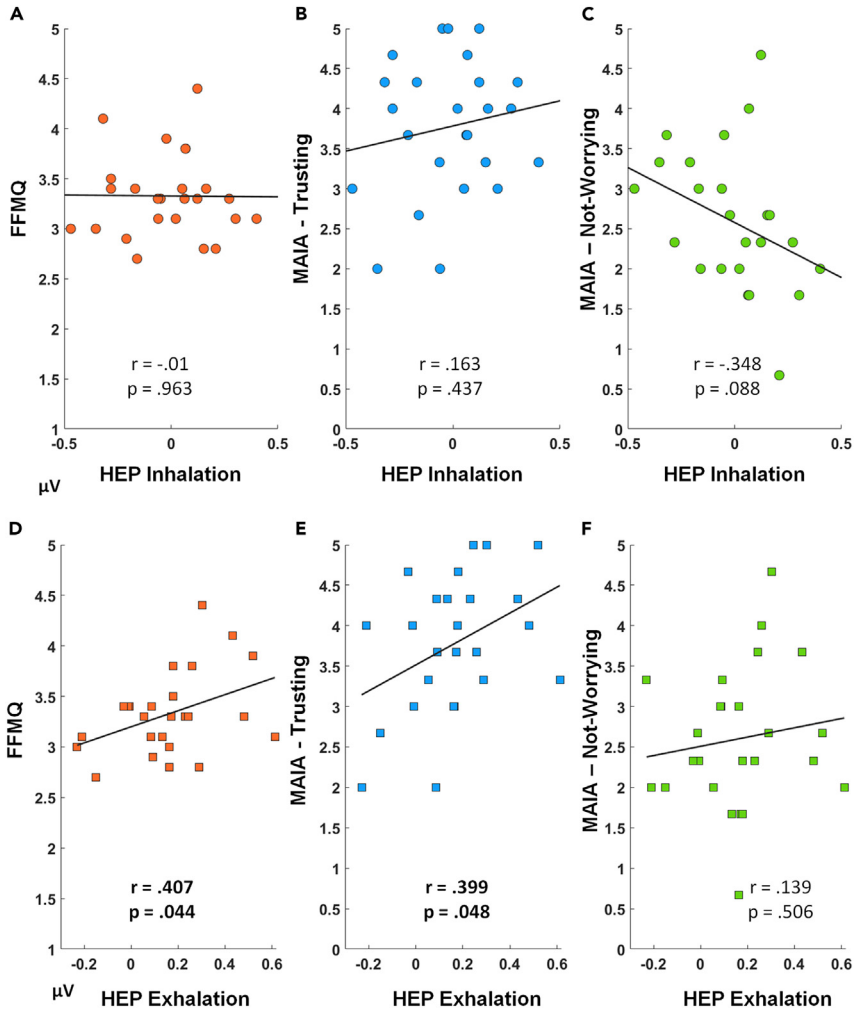



**Figure 4. Correlation between questionnaires and HEPs recorded at inhalation and exhalation**

Scatterplots of the linear relationships (Pearson's correlation) between the FFMQ total score, MAIA Trusting scale, and MAIA Not-Worrying scale and mean HEP amplitude recorded during inhalation (A, B, C) and exhalation (D, E, F).

than HEP amplitude alone, when respiratory phases are not taken into account. Lastly, the results indicate that, during HCT, the brain does not enhance heartbeat sensations during inhalation, but enhances heartbeat sensations exclusively during exhalation.

An additional finding is the association between HEP activity and interoceptive sensibility and trait mindfulness. During HCT, HEP amplitude recorded during exhalation was related to the trusting and not-worrying scales of MAIA and FFMQ total score. In contrast, no association was found between HEP amplitude during inhalation and these indices. This suggests that only HEPs assessed during exhalation are linked to interoceptive sensibility and mindfulness, which are important indicators of well-being and mental health.[33,52–56] These results could explain non-significant findings regarding cardiac interoceptive accuracy changes in mindfulness practitioners (see[57,58] for meta-analyses) that might be attributed to the failure to consider respiratory phases. It is possible that cardiac interoception in experienced meditators is specifically improved during exhalation. These findings may also provide an explanation for previously reported null associations between trait mindfulness and HEP,[32] a link that may be evident only during exhalation. Future studies may shed light on this topic.

We conclude that the increases in HEP amplitude during HCT are driven primarily by HEPs recorded during exhalation, with minimal contribution from HEPs during inhalation. This strengthens our previous interpretation of changes in interoception across the respiratory cycle during HBD[20] and introduces a new perspective on HEP activity that emphasizes the role of exhalation. Our results show that late HEP amplitude increases only when attention is focused on the heart *and* during exhalation. In other words, exhalation may not only serve as a respiratory phase that enhances attention to cardiac interoception compared to inhalation; it may also be a necessary condition for directing attention to heartbeat sensations during cardiac interoceptive tasks. If the first scenario were true, we would also expect to find higher HEP amplitude during inhalation in HCT compared to the other tasks (C-TCT and BCT), which was not observed. Several factors could explain

this phenomenon. A higher-level explanation is in line with a recent hypothesis regarding the role of respiration in interoceptive perception.[59] According to this hypothesis, the brain is constantly engaged in a trade-off between directing attention toward interoceptive or exteroceptive stimuli. Inhalation can hence give priority to external perception by redirecting attention to the environment, while exhalation can optimize interoception by allocating attentional resources to bodily sensations. Imbalance in the allocation of attentional resources toward exteroception during inhalation (e.g., visual,[60] somatosensory;[61] and auditory processing[62]) can disrupt the processing of interoceptive signals, particularly in the case of cardiac sensations, which are notoriously very ambiguous. This is consistent with the observed positive effects of exhalation on *non-exteroceptive* brain functions, such as associative conditioned learning[63,64] and the initiations of voluntary actions[65] and mental imagery of voluntary actions.[66] Alternatively, a peripheral explanation may lie in the connection between respiration and the baroreflex, known as respiratory sinus arrhythmia (RSA).[19] RSA causes faster but weaker heartbeats during inhalation compared to exhalation,[67] potentially resulting in reduced HEP amplitude during inhalation. The non-specific increase observed in the early time window across all tasks, irrespective of attentional focus, could be precisely attributed to this bottom-up mechanism. However, control analyses of late HEP amplitude and cardio-respiratory physiology seem to rule out the substantial contribution of these bottom-up components. Nevertheless, changes in cardiac physiology between respiratory phases do not exclude a concomitant top-down modulation of attention: heartbeats strength reduction during inhalation may enhance exteroceptive attention also due to reduced interference of cardiac signals, while exhalation may facilitate interoceptive attention also due to already increased cardiac sensations.

Regardless of the specific mechanism involved, future studies should differentiate between HEPs recorded between respiratory phases, as exhalation has demonstrated stronger associations with interoceptive attention and sensibility than inhalation. Additionally, the influence of the respiratory phase on cardiac interoception in mental and somatic disorders should be studied. Numerous studies have linked HEP amplitude to clinical conditions such as social anxiety,[68] anorexia nervosa,[69] depression,[70] post-traumatic stress disorder,[71] depersonalization,[72] borderline personality,[73] and chronic pain.[74] However, it is unclear whether these findings reflect an overall change in HEP activity or a change limited to a particular respiratory phase. An interesting exception is the study by Baumert and colleagues,[75] who reported a decrease in HEP amplitude during exhalation compared to inhalation in children with sleep-disordered breathing. Notably, after therapy (adenotonsillectomy), they observed an increase in HEP amplitude during exhalation and no changes during inhalation. This finding is in line with ours, suggesting that the effects of an intervention on cardiac interoception are more easily observed during exhalation. Consequently, the possibility that cardiac interoception in various disorders may be specifically impaired during exhalation may lead to the development of tailored interoceptive interventions to fine-tune cardiac interoception. Mindfulness-based interventions[18,76–78] or slow breathing practices[79,80] could be designed to specifically target this respiratory phase.

In conclusion, our data suggest that respiratory phases play a crucial role in influencing cardiac interoception. It is crucial for future studies to investigate the impact of respiratory phases on other aspects of interoception beyond cardiac sensations. These domains include gastric interoception,[81–83] interoceptive touch,[84–86] and pain perception.[87–90] Recognizing the role of respiration in shaping other interoceptive processes will be critical for developing a comprehensive understanding of reciprocal interactions between the body and the brain.[91–96]

### Limitations of the study

Some limitations of this study deserve consideration. Firstly, HCT performance may have been affected by confounding factors, such as HR estimation and time estimation ability.[48–50] However, it is crucial to note that our primary goal was to elicit cardiac interoceptive attention rather than assess cardiac interoceptive accuracy. Secondly, potential variations in task difficulty across tasks could have impacted HEP amplitude when comparing interoceptive and exteroceptive tasks.[16] Thirdly, the inherent ease of BCT, driven by the salience of respiratory sensations, poses a challenge when comparing it with HCT, characterized by greater ambiguity in cardiac sensations, raising questions about whether BCT qualifies as a true interoceptive task. Nonetheless, the use of BCT was necessary to ensure comparability with HCT, and previous research has suggested that breath counting can indeed elicit interoceptive attention.[34,97,98] Future studies exploring this topic could consider employing alternative tasks, such as the filter detection task,[99] respiratory resistance sensitivity task,[100] respiratory tracking task,[101] or interoceptive/exteroceptive attention task.[102]

## STAR★METHODS

Detailed methods are provided in the online version of this paper and include the following:

- KEY RESOURCES TABLE
- RESOURCE AVAILABILITY
  - Lead contact
  - Materials availability
  - Data and code availability
- EXPERIMENTAL MODEL AND STUDY PARTICIPANT DETAILS
  - Ethics statement
  - Human participants
- METHOD DETAILS
  - Experimental procedure
  - Electrophysiological recording

- ECG data analysis
- Respiratory data analysis
- EEG data analysis
- Task accuracy assessment
- Psychometric questionnaires

- QUANTIFICATION AND STATISTICAL ANALYSIS
  - Heartbeat evoked potential statistical analyses
  - Trial-level cardio-respiratory control analyses
  - Respiratory cycle analyses

## SUPPLEMENTAL INFORMATION

Supplemental information can be found online at https://doi.org/10.1016/j.isci.2024.109586.

## ACKNOWLEDGMENTS

This study was supported by the "Departments of Excellence 2023–2027" initiative of the Italian Ministry of University and Research for the Department of Neuroscience, Imaging and Clinical Sciences (DNISC) of the University of Chieti-Pescara, and by the "Search for Excellence" program, University of Chieti-Pescara, Italy. This study was also funded by the European Union – NextGenerationEU, MUR - Fondo Promozione e Sviluppo – DM 737/2021, INTRIGUE, Interoception and Fatigue: predicting and treating pathological and transient fatigue.

## AUTHOR CONTRIBUTIONS

**Andrea Zaccaro:** conceptualization, methodology, software, validation, formal analysis, investigation, data curation, visualization, writing-original draft, and writing-review and editing. **Francesca della Penna**: investigation, formal analysis, data curation, and writing-review and editing. **Elena Mussini**: software, data curation, and writing-review and editing. **Eleonora Parrotta**: software, data curation, and writing-review and editing. **Mauro Gianni Perrucci**: methodology, software, data curation, resources, and writing-review and editing. **Marcello Costantini**: visualization, supervision, funding acquisition, and writing-review and editing. **Francesca Ferri**: conceptualization, methodology, resources, supervision, project administration, funding acquisition, visualization, and writing-review and editing.

## DECLARATION OF INTERESTS

The authors declare no competing interests.

Received: September 22, 2023
Revised: March 7, 2024
Accepted: March 25, 2024
Published: March 27, 2024

## REFERENCES

1. Craig, A.D. (2003). Interoception: The sense of the physiological condition of the body. Curr. Opin. Neurobiol. *13*, 500–505. https://doi.org/10.1016/S0959-4388(03)00090-4.
2. Critchley, H.D., and Harrison, N.A. (2013). Visceral Influences on Brain and Behavior. Neuron *77*, 624–638. https://doi.org/10.1016/j.neuron.2013.02.008.
3. Garfinkel, S.N., and Critchley, H.D. (2016). Threat and the Body: How the Heart Supports Fear Processing. Trends Cognit. Sci. *20*, 34–46. https://doi.org/10.1016/j.tics.2015.10.005.
4. Gray, M.A., Taggart, P., Sutton, P.M., Groves, D., Holdright, D.R., Bradbury, D., Brull, D., and Critchley, H.D. (2007). A cortical potential reflecting cardiac function. Proc. Natl. Acad. Sci. USA *104*, 6818–6823. https://doi.org/10.1073/pnas.0609509104.
5. Norcliffe-Kaufmann, L. (2019). The Vagus and Glossopharyngeal Nerves in Two Autonomic Disorders. J. Clin. Neurophysiol. *36*, 443–451. https://doi.org/10.1097/WNP.0000000000000604.
6. Silvani, A., Calandra-Buonaura, G., Dampney, R.A.L., and Cortelli, P. (2016). Brain-heart interactions: physiology and clinical implications. Philos. Trans. A Math. Phys. Eng. Sci. *374*, 20150181. https://doi.org/10.1098/rsta.2015.0181.
7. Canales-Johnson, A., Silva, C., Huepe, D., Rivera-Rei, Á., Noreika, V., Garcia, M.D.C., Silva, W., Ciraolo, C., Vaucheret, E., Sedeño, L., et al. (2015). Auditory Feedback Differentially Modulates Behavioral and Neural Markers of Objective and Subjective Performance When Tapping to Your Heartbeat. Cerebr. Cortex *25*, 4490–4503. https://doi.org/10.1093/cercor/bhv076.
8. Kern, M., Aertsen, A., Schulze-Bonhage, A., and Ball, T. (2013). Heart cycle-related effects on event-related potentials, spectral power changes, and connectivity patterns in the human ECoG. Neuroimage *81*, 178–190. https://doi.org/10.1016/j.neuroimage.2013.05.042.
9. Park, H.D., Correia, S., Ducorps, A., and Tallon-Baudry, C. (2014). Spontaneous fluctuations in neural responses to heartbeats predict visual detection. Nat. Neurosci. *17*, 612–618. https://doi.org/10.1038/nn.3671.
10. Schandry, R., Sparrer, B., and Weitkunat, R. (1986). From the heart to the brain: a study of heartbeat contingent scalp potentials. Int. J. Neurosci. *30*, 261–275. https://doi.org/10.3109/00207458608985677.
11. Berntson, G.G., and Khalsa, S.S. (2021). Neural Circuits of Interoception. Trends Neurosci. *44*, 17–28. https://doi.org/10.1016/j.tins.2020.09.011.
12. Chen, W.G., Schloesser, D., Arensdorf, A.M., Simmons, J.M., Cui, C., Valentino, R., Gnadt, J.W., Nielsen, L., Hillaire-Clarke, C.S., Spruance, V., et al. (2021). The Emerging Science of Interoception: Sensing, Integrating, Interpreting, and Regulating Signals within the Self. Trends Neurosci. *44*, 3–16. https://doi.org/10.1016/j.tins.2020.10.007.
13. Pollatos, O., and Schandry, R. (2004). Accuracy of heartbeat perception is reflected in the amplitude of the heartbeat-evoked brain potential. Psychophysiology *41*, 476–482. https://doi.org/10.1111/1469-8986.2004.00170.x.
14. Engelen, T., Solcà, M., and Tallon-Baudry, C. (2023). Interoceptive rhythms in the brain.

Nat. Neurosci. *26*, 1670–1684. https://doi.org/10.1038/s41593-023-01425-1.

15. Park, H.D., and Blanke, O. (2019). Heartbeat-evoked cortical responses: Underlying mechanisms, functional roles, and methodological considerations. Neuroimage *197*, 502–511. https://doi.org/10.1016/j.neuroimage.2019.04.081.
16. Coll, M.P., Hobson, H., Bird, G., and Murphy, J. (2021). Systematic review and meta-analysis of the relationship between the heartbeat-evoked potential and interoception. Neurosci. Biobehav. Rev. *122*, 190–200. https://doi.org/10.1016/j.neubiorev.2020.12.012.
17. Khalsa, S.S., Rudrauf, D., Feinstein, J.S., and Tranel, D. (2009). The pathways of interoceptive awareness. Nat. Neurosci. *12*, 1494–1496. https://doi.org/10.1038/nn.2411.
18. Weng, H.Y., Feldman, J.L., Leggio, L., Napadow, V., Park, J., and Price, C.J. (2021). Interventions and Manipulations of Interoception. Trends Neurosci. *44*, 52–62. https://doi.org/10.1016/j.tins.2020.09.010.
19. Brecher, G.A., and Hubay, C.A. (1955). Pulmonary blood flow and venous return during spontaneous respiration. Circ. Res. *3*, 210–214. https://doi.org/10.1161/01.RES.3.2.210.
20. Zaccaro, A., Perrucci, M.G., Parrotta, E., Costantini, M., and Ferri, F. (2022). Brain-heart interactions are modulated across the respiratory cycle via interoceptive attention. Neuroimage *262*, 119548. https://doi.org/10.1016/j.neuroimage.2022.119548.
21. Fittipaldi, S., Abrevaya, S., Fuente, A.D.L., Pascariello, G.O., Hesse, E., Birba, A., Salamone, P., Hildebrandt, M., Martí, S.A., Pautassi, R.M., et al. (2020). A multidimensional and multi-feature framework for cardiac interoception. Neuroimage *212*, 116677. https://doi.org/10.1016/j.neuroimage.2020.116677.
22. Melloni, M., Sedeño, L., Couto, B., Reynoso, M., Gelormini, C., Favaloro, R., Canales-Johnson, A., Sigman, M., Manes, F., and Ibanez, A. (2013). Preliminary evidence about the effects of meditation on interoceptive sensitivity and social cognition. Behav. Brain Funct. *9*, 47. https://doi.org/10.1186/1744-9081-9-47.
23. Noble, D.J., and Hochman, S. (2019). Hypothesis: Pulmonary Afferent Activity Patterns During Slow, Deep Breathing Contribute to the Neural Induction of Physiological Relaxation. Front. Physiol. *10*, 1176. https://doi.org/10.3389/fphys.2019.01176.
24. Streeter, C.C., Gerbarg, P.L., Saper, R.B., Ciraulo, D.A., and Brown, R.P. (2012). Effects of yoga on the autonomic nervous system, gamma-aminobutyric-acid, and allostasis in epilepsy, depression, and post-traumatic stress disorder. Med. Hypotheses *78*, 571–579. https://doi.org/10.1016/j.mehy.2012.01.021.
25. Babo-Rebelo, M., Wolpert, N., Adam, C., Hasboun, D., and Tallon-Baudry, C. (2016). Is the cardiac monitoring function related to the self in both the default network and right anterior insula? Philos. Trans. R. Soc. Lond. B Biol. Sci. *371*, 20160004. https://doi.org/10.1098/rstb.2016.0004.
26. Babo-Rebelo, M., Richter, C.G., and Tallon-Baudry, C. (2016). Neural responses to heartbeats in the default network encode the self in spontaneous thoughts. J. Neurosci. *36*, 7829–7840. https://doi.org/10.1523/JNEUROSCI.0262-16.2016.
27. Sel, A., Azevedo, R.T., and Tsakiris, M. (2017). Heartfelt Self: Cardio-Visual Integration Affects Self-Face Recognition and Interoceptive Cortical Processing. Cerebr. Cortex *27*, 5144–5155. https://doi.org/10.1093/cercor/bhw296.
28. Park, H.D., Bernasconi, F., Bello-Ruiz, J., Pfeiffer, C., Salomon, R., and Blanke, O. (2016). Transient modulations of neural responses to heartbeats covary with bodily self-consciousness. J. Neurosci. *36*, 8453–8460. https://doi.org/10.1523/JNEUROSCI.0311-16.2016.
29. Park, H.D., Bernasconi, F., Salomon, R., Tallon-Baudry, C., Spinelli, L., Seeck, M., Schaller, K., and Blanke, O. (2018). Neural Sources and Underlying Mechanisms of Neural Responses to Heartbeats, and their Role in Bodily Self-consciousness: An Intracranial EEG Study. Cerebr. Cortex *28*, 2351–2364. https://doi.org/10.1093/cercor/bhx136.
30. Baranauskas, M., Grabauskaitė, A., and Griškova-Bulanova, I. (2017). Brain responses and self-reported indices of interoception: Heartbeat evoked potentials are inversely associated with worrying about body sensations. Physiol. Behav. *180*, 1–7. https://doi.org/10.1016/j.physbeh.2017.07.032.
31. Billeci, L., Faraguna, U., Santarcangelo, E.L., d'Ascanio, P., Varanini, M., and Sebastiani, L. (2021). Heartbeat-evoked cortical potential during sleep and interoceptive sensitivity: A matter of hypnotizability. Brain Sci. *11*, 1089. https://doi.org/10.3390/brainsci11081089.
32. Verdonk, C., Trousselard, M., Di Bernardi Luft, C., Medani, T., Billaud, J.B., Ramdani, C., Canini, F., Claverie, D., Jaumard-Hakoun, A., and Vialatte, F. (2021). The heartbeat evoked potential does not support strong interoceptive sensibility in trait mindfulness. Psychophysiology *58*, e13891. https://doi.org/10.1111/psyp.13891.
33. Bonaz, B., Lane, R.D., Oshinsky, M.L., Kenny, P.J., Sinha, R., Mayer, E.A., and Critchley, H.D. (2021). Diseases, Disorders, and Comorbidities of Interoception. Trends Neurosci. *44*, 39–51. https://doi.org/10.1016/j.tins.2020.09.009.
34. Herrero, J.L., Khuvis, S., Yeagle, E., Cerf, M., and Mehta, A.D. (2018). Breathing above the brain stem: volitional control and attentional modulation in humans. J. Neurophysiol. *119*, 145–159. https://doi.org/10.1152/jn.00551.2017.
35. Wiebking, C., de Greck, M., Duncan, N.W., Tempelmann, C., Bajbouj, M., and Northoff, G. (2015). Interoception in insula subregions as a possible state marker for depression—an exploratory fMRI study investigating healthy, depressed and remitted participants. Front. Behav. Neurosci. *9*, 82. https://doi.org/10.3389/fnbeh.2015.00082.
36. Kumral, D., Al, E., Cesnaite, E., Kornej, J., Sander, C., Hensch, T., Zeynalova, S., Tautenhahn, S., Hagendorf, A., Laufs, U., et al. (2022). Attenuation of the Heartbeat-Evoked Potential in Patients With Atrial Fibrillation. JACC. Clin. Electrophysiol. *8*, 1219–1230. https://doi.org/10.1016/j.jacep.2022.06.019.
37. Petzschner, F.H., Weber, L.A., Wellstein, K.V., Paolini, G., Do, C.T., and Stephan, K.E. (2019). Focus of attention modulates the heartbeat evoked potential. Neuroimage *186*, 595–606. https://doi.org/10.1016/j.neuroimage.2018.11.037.
38. Pollatos, O., Herbert, B.M., Mai, S., and Kammer, T. (2016). Changes in interoceptive processes following brain stimulation. Philos. Trans. R. Soc. Lond. B Biol. Sci. *371*, 20160016. https://doi.org/10.1098/rstb.2016.0016.
39. Schandry, R., and Montoya, P. (1996). Event-related brain potentials and the processing of cardiac activity. Biol. Psychol. *42*, 75–85. https://doi.org/10.1016/0301-0511(95)05147-3.
40. Schulz, A., Stammet, P., Dierolf, A.M., Vögele, C., Beyenburg, S., Werer, C., and Devaux, Y. (2018). Late heartbeat-evoked potentials are associated with survival after cardiac arrest. Resuscitation *126*, 7–13. https://doi.org/10.1016/j.resuscitation.2018.02.009.
41. Simor, P., Bogdány, T., Bódizs, R., and Perakakis, P. (2021). Cortical monitoring of cardiac activity during rapid eye movement sleep: The heartbeat evoked potential in phasic and tonic rapid-eye-movement microstates. Sleep *44*, zsab100. https://doi.org/10.1093/sleep/zsab100.
42. Villena-González, M., Moënne-Loccoz, C., Lagos, R.A., Alliende, L.M., Billeke, P., Aboitiz, F., López, V., and Cosmelli, D. (2017). Attending to the heart is associated with posterior alpha band increase and a reduction in sensitivity to concurrent visual stimuli. Psychophysiology *54*, 1483–1497. https://doi.org/10.1111/psyp.12894.
43. Buot, A., Azzalini, D., Chaumon, M., and Tallon-Baudry, C. (2021). Does stroke volume influence heartbeat evoked responses? Biol. Psychol. *165*, 108165. https://doi.org/10.1016/j.biopsycho.2021.108165.
44. Candia-Rivera, D., Sappia, M.S., Horschig, J.M., Colier, W.N.J.M., and Valenza, G. (2022). Confounding effects of heart rate, breathing rate, and frontal fNIRS on interoception. Sci. Rep. *12*, 20701. https://doi.org/10.1038/s41598-022-25119-z.
45. Dirlich, G., Vogl, L., Plaschke, M., and Strian, F. (1997). Cardiac field effects on the EEG. Electroencephalogr. Clin. Neurophysiol. *102*, 307–315. https://doi.org/10.1016/S0013-4694(96)96506-2.
46. MacKinnon, S., Gevirtz, R., McCraty, R., and Brown, M. (2013). Utilizing heartbeat evoked potentials to identify cardiac regulation of vagal afferents during emotion and resonant breathing. Appl. Psychophysiol. Biofeedback *38*, 241–255. https://doi.org/10.1007/s10484-013-9226-5.
47. Leganes-Fonteneau, M., Bates, M.E., Muzumdar, N., Pawlak, A., Islam, S., Vaschillo, E., and Buckman, J.F. (2021). Cardiovascular mechanisms of interoceptive awareness: Effects of resonance breathing. Int. J. Psychophysiol. *169*, 71–87. https://doi.org/10.1016/j.ijpsycho.2021.09.003.
48. Brener, J., and Ring, C. (2016). Towards a psychophysics of interoceptive processes: The measurement of heartbeat detection. Philos. Trans. R. Soc. Lond. B Biol. Sci. *371*, 20160015. https://doi.org/10.1098/rstb.2016.0015.
49. Desmedt, O., Luminet, O., and Corneille, O. (2018). The heartbeat counting task largely involves non-interoceptive processes: Evidence from both the original and an adapted counting task. Biol. Psychol. *138*,

185–188. https://doi.org/10.1016/j.biopsycho.2018.09.004.
50. Zamariola, G., Maurage, P., Luminet, O., and Corneille, O. (2018). Interoceptive accuracy scores from the heartbeat counting task are problematic: Evidence from simple bivariate correlations. Biol. Psychol. *137*, 12–17. https://doi.org/10.1016/j.biopsycho.2018.06.006.
51. Villena-Gonzalez, M., Rojas-Thomas, F., Morales-Torres, R., and López, V. (2023). Autonomous sensory meridian response is associated with a larger heartbeat-evoked potential amplitude without differences in interoceptive awareness. Psychophysiology *60*, e14277. https://doi.org/10.1111/psyp.14277.
52. Hölzel, B.K., Lazar, S.W., Gard, T., Schuman-Olivier, Z., Vago, D.R., and Ott, U. (2011). How does mindfulness meditation work? Proposing mechanisms of action from a conceptual and neural perspective. Perspect. Psychol. Sci. *6*, 537–559. https://doi.org/10.1177/1745691611419671.
53. Paulus, M.P. (2013). The breathing conundrum - Interoceptive sensitivity and anxiety. Depress. Anxiety *30*, 315–320. https://doi.org/10.1002/da.22076.
54. Tang, Y.Y., Hölzel, B.K., and Posner, M.I. (2015). The neuroscience of mindfulness meditation. Nat. Rev. Neurosci. *16*, 213–225. https://doi.org/10.1038/nrn3916.
55. Tsakiris, M., and Critchley, H. (2016). Interoception beyond homeostasis: Affect, cognition and mental health. Philos. Trans. R. Soc. Lond. B Biol. Sci. *371*, 20160002. https://doi.org/10.1098/rstb.2016.0002.
56. Khalsa, S.S., Adolphs, R., Cameron, O.G., Critchley, H.D., Davenport, P.W., Feinstein, J.S., Feusner, J.D., Garfinkel, S.N., Lane, R.D., Mehling, W.E., et al. (2018). Interoception and Mental Health: A Roadmap. Biol. Psychiatry. Cogn. Neurosci. Neuroimaging *3*, 501–513. https://doi.org/10.1016/j.bpsc.2017.12.004.
57. Khalsa, S.S., Rudrauf, D., Hassanpour, M.S., Davidson, R.J., and Tranel, D. (2020). The practice of meditation is not associated with improved interoceptive awareness of the heartbeat. Psychophysiology *57*, e13479. https://doi.org/10.1111/psyp.13479.
58. Treves, I.N., Tello, L.Y., Davidson, R.J., and Goldberg, S.B. (2019). The relationship between mindfulness and objective measures of body awareness: A meta-analysis. Sci. Rep. *9*, 17386. https://doi.org/10.1038/s41598-019-53978-6.
59. Molle, L., and Coste, A. (2022). The respiratory modulation of interoception. J. Neurophysiol. *127*, 896–899. https://doi.org/10.1152/jn.00027.2022.
60. Kluger, D.S., Balestrieri, E., Busch, N.A., and Gross, J. (2021). Respiration aligns perception with neural excitability. Elife *10*, e70907. https://doi.org/10.7554/eLife.70907.
61. Grund, M., Al, E., Pabst, M., Dabbagh, A., Stephani, T., Nierhaus, T., Gaebler, M., and Villringer, A. (2022). Respiration, Heartbeat, and Conscious Tactile Perception. J. Neurosci. *42*, 643–656. https://doi.org/10.1523/JNEUROSCI.0592-21.2021.
62. Johannknecht, M., and Kayser, C. (2022). The influence of the respiratory cycle on reaction times in sensory-cognitive paradigms. Sci. Rep. *12*, 2586. https://doi.org/10.1038/s41598-022-06364-8.
63. Waselius, T., Wikgren, J., Penttonen, M., and Nokia, M.S. (2019). Breathe out and learn: Expiration-contingent stimulus presentation facilitates associative learning in trace eyeblink conditioning. Psychophysiology *56*, e13387. https://doi.org/10.1111/psyp.13387.
64. Waselius, T., Xu, W., Sparre, J.I., Penttonen, M., and Nokia, M.S. (2022). Cardiac cycle and respiration phase affect responses to the conditioned stimulus in young adults trained in trace eyeblink conditioning. J. Neurophysiol. *127*, 767–775. https://doi.org/10.1152/jn.00298.2021.
65. Park, H.D., Barnoud, C., Trang, H., Kannape, O.A., Schaller, K., and Blanke, O. (2020). Breathing is coupled with voluntary action and the cortical readiness potential. Nat. Commun. *11*, 289. https://doi.org/10.1038/s41467-019-13967-9.
66. Park, H.D., Piton, T., Kannape, O.A., Duncan, N.W., Lee, K.Y., Lane, T.J., and Blanke, O. (2022). Breathing is coupled with voluntary initiation of mental imagery. Neuroimage *264*, 119685. https://doi.org/10.1016/j.neuroimage.2022.119685.
67. Larsson, D.E.O., Esposito, G., Critchley, H.D., Dienes, Z., and Garfinkel, S.N. (2021). Sensitivity to changes in rate of heartbeats as a measure of interoceptive ability. J. Neurophysiol. *126*, 1799–1813. https://doi.org/10.1152/jn.00059.2021.
68. Judah, M.R., Shurkova, E.Y., Hager, N.M., White, E.J., Taylor, D.L., and Grant, D.M. (2018). The relationship between social anxiety and heartbeat evoked potential amplitude. Biol. Psychol. *139*, 1–7. https://doi.org/10.1016/j.biopsycho.2018.09.013.
69. Lutz, A.P.C., Schulz, A., Voderholzer, U., Koch, S., van Dyck, Z., and Vögele, C. (2019). Enhanced cortical processing of cardio-afferent signals in anorexia nervosa. Clin. Neurophysiol. *130*, 1620–1627. https://doi.org/10.1016/j.clinph.2019.06.009.
70. Terhaar, J., Viola, F.C., Bär, K.J., and Debener, S. (2012). Heartbeat evoked potentials mirror altered body perception in depressed patients. Clin. Neurophysiol. *123*, 1950–1957. https://doi.org/10.1016/j.clinph.2012.02.086.
71. Schmitz, M., Müller, L.E., Seitz, K.I., Schulz, A., Steinmann, S., Herpertz, S.C., and Bertsch, K. (2021). Heartbeat evoked potentials in patients with post-traumatic stress disorder: an unaltered neurobiological regulation system? Eur. J. Psychotraumatol. *12*, 1987686. https://doi.org/10.1080/20008198.2021.1987686.
72. Schulz, A., Köster, S., Beutel, M.E., Schächinger, H., Vögele, C., Rost, S., Rauh, M., and Michal, M. (2015). Altered patterns of heartbeat-evoked potentials in depersonalization/derealization disorder: neurophysiological evidence for impaired cortical representation of bodily signals. Psychosom. Med. *77*, 506–516. https://doi.org/10.1097/PSY.0000000000000195.
73. Schmitz, M., Müller, L.E., Schulz, A., Kleindienst, N., Herpertz, S.C., and Bertsch, K. (2020). Heart and brain: Cortical representation of cardiac signals is disturbed in borderline personality disorder, but unaffected by oxytocin administration. J. Affect. Disord. *264*, 24–28. https://doi.org/10.1016/j.jad.2019.11.139.
74. Solcà, M., Park, H.D., Bernasconi, F., and Blanke, O. (2020). Behavioral and neurophysiological evidence for altered interoceptive bodily processing in chronic pain. Neuroimage *217*, 116902. https://doi.org/10.1016/j.neuroimage.2020.116902.
75. Baumert, M., Pamula, Y., Kohler, M., Martin, J., Kennedy, D., Nalivaiko, E., and Immanuel, S.A. (2015). Effect of respiration on heartbeat-evoked potentials during sleep in children with sleep-disordered breathing. Sleep Med. *16*, 665–667. https://doi.org/10.1016/j.sleep.2015.02.528.
76. Farb, N., Daubenmier, J., Price, C.J., Gard, T., Kerr, C., Dunn, B.D., Klein, A.C., Paulus, M.P., and Mehling, W.E. (2015). Interoception, contemplative practice, and health. Front. Psychol. *6*, 763. https://doi.org/10.3389/fpsyg.2015.00763.
77. Gibson, J. (2019). Mindfulness, Interoception, and the Body: A Contemporary Perspective. Front. Psychol. *10*, 2012. https://doi.org/10.3389/fpsyg.2019.02012.
78. Nord, C.L., and Garfinkel, S.N. (2022). Interoceptive pathways to understand and treat mental health conditions. Trends Cognit. Sci. *26*, 499–513. https://doi.org/10.1016/j.tics.2022.03.004.
79. Zaccaro, A., Piarulli, A., Laurino, M., Garbella, E., Menicucci, D., Neri, B., and Gemignani, A. (2018). How Breath-Control Can Change Your Life: A Systematic Review on Psycho-Physiological Correlates of Slow Breathing. Front. Hum. Neurosci. *12*, 353. https://doi.org/10.3389/fnhum.2018.00353.
80. Zaccaro, A., Piarulli, A., Melosini, L., Menicucci, D., and Gemignani, A. (2022). Neural Correlates of Non-ordinary States of Consciousness in Pranayama Practitioners: The Role of Slow Nasal Breathing. Front. Syst. Neurosci. *16*, 803904. https://doi.org/10.3389/fnsys.2022.803904.
81. Rebollo, I., Devauchelle, A.D., Béranger, B., and Tallon-Baudry, C. (2018). Stomach-brain synchrony reveals a novel, delayed-connectivity resting-state network in humans. Elife *7*, e33321. https://doi.org/10.7554/eLife.33321.
82. Porciello, G., Monti, A., and Aglioti, S.M. (2018). How the stomach and the brain work together at rest. Elife *7*, e37009. https://doi.org/10.7554/eLife.33321.
83. Khalsa, S.S., Berner, L.A., and Anderson, L.M. (2022). Gastrointestinal Interoception in Eating Disorders: Charting a New Path. Curr. Psychiatr. Rep. *24*, 47–60. https://doi.org/10.1007/s11920-022-01318-3.
84. Crucianelli, L., Krahé, C., Jenkinson, P.M., and Fotopoulou, A.K. (2018). Interoceptive ingredients of body ownership: Affective touch and cardiac awareness in the rubber hand illusion. Cortex *104*, 180–192. https://doi.org/10.1016/j.cortex.2017.04.018.
85. Crucianelli, L., Enmalm, A., and Ehrsson, H.H. (2022). Interoception as independent cardiac, thermosensory, nociceptive, and affective touch perceptual submodalities. Biol. Psychol. *172*, 108355. https://doi.org/10.1016/j.biopsycho.2022.108355.
86. Di Lernia, D., Cipresso, P., Pedroli, E., and Riva, G. (2018). Toward an embodied medicine: A portable device with programmable interoceptive stimulation for heart rate variability enhancement. Sensors *18*, 2469. https://doi.org/10.3390/s18082469.
87. Arsenault, M., Ladouceur, A., Lehmann, A., Rainville, P., and Piché, M. (2013). Pain modulation induced by respiration: Phase and frequency effects. Neuroscience *252*, 501–511. https://doi.org/10.1016/j.neuroscience.2013.07.048.
88. Iwabe, T., Ozaki, I., and Hashizume, A. (2014). The respiratory cycle modulates

brain potentials, sympathetic activity, and subjective pain sensation induced by noxious stimulation. Neurosci. Res. *84*, 47–59. https://doi.org/10.1016/j.neures.2014.03.003.

89. Martin, S.L., Kerr, K.L., Bartley, E.J., Kuhn, B.L., Palit, S., Terry, E.L., Del Ventura, J.L., and Rhudy, J.L. (2012). Respiration-induced hypoalgesia: exploration of potential mechanisms. J. Pain *13*, 755–763. https://doi.org/10.1016/j.jpain.2012.05.001.
90. Parrotta, E., Bach, P., Perrucci, M.G., Costantini, M., and Ferri, F. (2024). Heart is deceitful above all things: Threat expectancy induces the illusory perception of increased heartrate. Cognition *245*, 105719. https://doi.org/10.1016/j.cognition.2024.105719.
91. Allen, M., Varga, S., and Heck, D.H. (2023). Respiratory rhythms of the predictive mind. Psychol. Rev. *130*, 1066–1080. https://doi.org/10.1037/rev0000391.
92. Boyadzhieva, A., and Kayhan, E. (2021). Keeping the Breath in Mind: Respiration, Neural Oscillations, and the Free Energy Principle. Front. Neurosci. *15*, 647579. https://doi.org/10.3389/fnins.2021.647579.
93. Brændholt, M., Kluger, D.S., Varga, S., Heck, D.H., Gross, J., and Allen, M.G. (2023). Breathing in waves: Understanding Respiratory-Brain Coupling as a Gradient of Predictive Oscillations. Neurosci. Biobehav. Rev. *152*, 105262. https://doi.org/10.1016/j.neubiorev.2023.105262.
94. Corcoran, A.W., Perrykkad, K., Feuerriegel, D., and Robinson, J.E. (2023). Body as First Teacher: The Role of Rhythmic Visceral Dynamics in Early Cognitive Development. Perspect. Psychol. Sci. https://doi.org/10.1177/17456916231185343.
95. Tort, A.B.L., Brankačk, J., and Draguhn, A. (2018). Respiration-Entrained Brain Rhythms Are Global but Often Overlooked. Trends Neurosci. *41*, 186–197. https://doi.org/10.1016/j.tins.2018.01.007.
96. Criscuolo, A., Schwartze, M., and Kotz, S.A. (2022). Cognition through the lens of a body–brain dynamic system. Trends Neurosci. *45*, 667–677. https://doi.org/10.1016/j.tins.2022.06.004.
97. Levinson, D.B., Stoll, E.L., Kindy, S.D., Merry, H.L., and Davidson, R.J. (2014). A mind you can count on: Validating breath counting as a behavioral measure of mindfulness. Front. Psychol. *5*, 1202. https://doi.org/10.3389/fpsyg.2014.01202.
98. F Wong, K., A A Massar, S., Chee, M.W.L., and Lim, J. (2018). Towards an Objective Measure of Mindfulness: Replicating and Extending the Features of the Breath-Counting Task. Mindfulness *9*, 1402–1410. https://doi.org/10.1007/s12671-017-0880-1.
99. Harrison, O.K., Köchli, L., Marino, S., Luechinger, R., Hennel, F., Brand, K., Hess, A.J., Frässle, S., Iglesias, S., Vinckier, F., et al. (2021). Interoception of breathing and its relationship with anxiety. Neuron *109*, 4080–4093.e8. https://doi.org/10.1016/j.neuron.2021.09.045.
100. Nikolova, N., Harrison, O., Toohey, S., Brændholt, M., Legrand, N., Correa, C., Vejlø, M., Jensen, M.S., Fardo, F., and Allen, M. (2022). The respiratory resistance sensitivity task: An automated method for quantifying respiratory interoception and metacognition. Biol. Psychol. *170*, 108325. https://doi.org/10.1016/j.biopsycho.2022.108325.
101. Daubenmier, J., Sze, J., Kerr, C.E., Kemeny, M.E., and Mehling, W. (2013). Follow your breath: Respiratory interoceptive accuracy in experienced meditators. Psychophysiology *50*, 777–789. https://doi.org/10.1111/psyp.12057.
102. Farb, N.A.S., Zuo, Z., and Price, C.J. (2023). Integrative Systems: Interoceptive Awareness of the Breath Preserves Attention and Language Networks amidst Widespread Cortical Deactivation:A Within-Participant Neuroimaging Study. eNeuro *10*, 1–18. https://doi.org/10.1523/ENEURO.0088-23.2023.
103. Delorme, A., and Makeig, S. (2004). EEGLAB: An open source toolbox for analysis of single-trial EEG dynamics including independent component analysis. J. Neurosci. Methods *134*, 9–21. https://doi.org/10.1016/j.jneumeth.2003.10.009.
104. Lopez-Calderon, J., and Luck, S.J. (2014). ERPLAB: An open-source toolbox for the analysis of event-related potentials. Front. Hum. Neurosci. *8*, 213. https://doi.org/10.3389/fnhum.2014.00213.
105. Tarvainen, M.P., Niskanen, J.P., Lipponen, J.A., Ranta-Aho, P.O., and Karjalainen, P.A. (2014). Kubios HRV - Heart rate variability analysis software. Comput. Methods Progr. Biomed. *113*, 210–220. https://doi.org/10.1016/j.cmpb.2013.07.024.
106. Perakakis, P. (2019). HEPLAB: a Matlab graphical interface for the preprocessing of the heartbeat-evoked potential. https://doi.org/10.5281/ZENODO.2649943.
107. Groppe, D.M., Urbach, T.P., and Kutas, M. (2011). Mass univariate analysis of event-related brain potentials/fields I: A critical tutorial review. Psychophysiology *48*, 1711–1725. https://doi.org/10.1111/j.1469-8986.2011.01273.x.
108. Groppe, D.M., Urbach, T.P., and Kutas, M. (2011). Mass univariate analysis of event-related brain potentials/fields II: Simulation studies. Psychophysiology *48*, 1726–1737. https://doi.org/10.1111/j.1469-8986.2011.01272.x.
109. Fields, E.C., and Kuperberg, G.R. (2020). Having your cake and eating it too: Flexibility and power with mass univariate statistics for ERP data. Psychophysiology *57*, e13468. https://doi.org/10.1111/psyp.13468.
110. Bailey, N.W., Biabani, M., Hill, A.T., Miljevic, A., Rogasch, N.C., McQueen, B., Murphy, O.W., and Fitzgerald, P.B. (2023). Introducing RELAX: An automated pre-processing pipeline for cleaning EEG data - Part 1: Algorithm and application to oscillations. Clin. Neurophysiol. *149*, 178–201. https://doi.org/10.1016/j.clinph.2023.01.017.
111. Bailey, N.W., Hill, A.T., Biabani, M., Murphy, O.W., Rogasch, N.C., McQueen, B., Miljevic, A., and Fitzgerald, P.B. (2023). RELAX part 2: A fully automated EEG data cleaning algorithm that is applicable to Event-Related-Potentials. Clin. Neurophysiol. *149*, 202–222. https://doi.org/10.1016/j.clinph.2023.01.018.
112. Faul, F., Erdfelder, E., Buchner, A., and Lang, A.G. (2009). Statistical power analyses using G*Power 3.1: Tests for correlation and regression analyses. Behav. Res. Methods *41*, 1149–1160. https://doi.org/10.3758/BRM.41.4.1149.
113. Raichle, M.E., MacLeod, A.M., Snyder, A.Z., Powers, W.J., Gusnard, D.A., and Shulman, G.L. (2001). A default mode of brain function. Proc. Natl. Acad. Sci. USA *98*, 676–682. https://doi.org/10.1073/pnas.98.2.676.
114. Di Lernia, D., Serino, S., Pezzulo, G., Pedroli, E., Cipresso, P., and Riva, G. (2018). Feel the time. Time perception as a function of interoceptive processing. Front. Hum. Neurosci. *12*, 74. https://doi.org/10.3389/fnhum.2018.00074.
115. Ueno, D., Matsuoka, T., Kato, Y., Ayani, N., Maeda, S., Takeda, M., and Narumoto, J. (2020). Individual Differences in Interoceptive Accuracy Are Correlated With Salience Network Connectivity in Older Adults. Front. Aging Neurosci. *12*, 592002. https://doi.org/10.3389/fnagi.2020.592002.
116. Ardizzi, M., and Ferri, F. (2018). Interoceptive influences on peripersonal space boundary. Cognition *177*, 79–86. https://doi.org/10.1016/j.cognition.2018.04.001.
117. Saltafossi, M., Zaccaro, A., Perrucci, M.G., Ferri, F., and Costantini, M. (2023). The impact of cardiac phases on multisensory integration. Biol. Psychol. *182*, 108642. https://doi.org/10.1016/j.biopsycho.2023.108642.
118. Pan, J., and Tompkins, W.J. (1985). A Real-Time QRS Detection Algorithm. IEEE Trans. Biomed. Eng. *32*, 230–236. https://doi.org/10.1109/TBME.1985.325532.
119. Citi, L., Brown, E.N., and Barbieri, R. (2012). A real-time automated point-process method for the detection and correction of erroneous and ectopic heartbeats. IEEE Trans. Biomed. Eng. *59*, 2828–2837. https://doi.org/10.1109/TBME.2012.2211356.
120. Task Force of the European Society of Cardiology and the North American Society of Pacing and Electrophysiology (1996). Heart rate variability. Standards of measurement, physiological interpretation, and clinical use. Circulation *93*, 1043–1065.
121. Lewis, G.F., Furman, S.A., McCool, M.F., and Porges, S.W. (2012). Statistical strategies to quantify respiratory sinus arrhythmia: Are commonly used metrics equivalent? Biol. Psychol. *89*, 349–364. https://doi.org/10.1016/j.biopsycho.2011.11.009.
122. Power, J.D., Lynch, C.J., Dubin, M.J., Silver, B.M., Martin, A., and Jones, R.M. (2020). Characteristics of respiratory measures in young adults scanned at rest, including systematic changes and "missed" deep breaths. Neuroimage *204*, 116234. https://doi.org/10.1016/j.neuroimage.2019.116234.
123. Savitzky, A., and Golay, M.J.E. (1964). Smoothing and Differentiation of Data by Simplified Least Squares Procedures. Anal. Chem. *36*, 1627–1639. https://doi.org/10.1021/ac60214a047.
124. Al, E., Iliopoulos, F., Forschack, N., Nierhaus, T., Grund, M., Motyka, P., Gaebler, M., Nikulin, V.V., and Villringer, A. (2020). Heart-brain interactions shape somatosensory perception and evoked potentials. Proc. Natl. Acad. Sci. USA *117*, 10575–10584. https://doi.org/10.1073/pnas.1915629117.
125. Al, E., Iliopoulos, F., Nikulin, V.V., and Villringer, A. (2021). Heartbeat and somatosensory perception. Neuroimage *238*, 118247. https://doi.org/10.1016/j.neuroimage.2021.118247.
126. Hyvärinen, A. (1999). Fast and robust fixed-point algorithms for independent component analysis. IEEE Trans. Neural Network. *10*, 626–634. https://doi.org/10.1109/72.761722.
127. Junghöfer, M., Elbert, T., Tucker, D.M., and Rockstroh, B. (2000). Statistical control of

artifacts in dense array EEG/MEG studies. Psychophysiology *37*, 523–532. https://doi.org/10.1017/S0048577200980624.

128. Candia-Rivera, D., Catrambone, V., and Valenza, G. (2021). The role of electroencephalography electrical reference in the assessment of functional brain-heart interplay: From methodology to user guidelines. J. Neurosci. Methods *360*, 109269. https://doi.org/10.1016/j.jneumeth.2021.109269.
129. Alday, P.M. (2019). How much baseline correction do we need in ERP research? Extended GLM model can replace baseline correction while lifting its limits. Psychophysiology *56*, e13451. https://doi.org/10.1111/psyp.13451.
130. Babo-Rebelo, M., Buot, A., and Tallon-Baudry, C. (2019). Neural responses to heartbeats distinguish self from other during imagination. Neuroimage *191*, 10–20. https://doi.org/10.1016/j.neuroimage.2019.02.012.
131. Blankenship, C.M., Hunter, L.L., Keefe, D.H., Feeney, M.P., Brown, D.K., McCune, A., Fitzpatrick, D.F., and Lin, L. (2018). Optimizing Clinical Interpretation of Distortion Product Otoacoustic Emissions in Infants. Ear Hear. *39*, 1075–1090. https://doi.org/10.1097/AUD.0000000000000562.
132. Schandry, R. (1981). Heart Beat Perception and Emotional Experience. Psychophysiology *18*, 483–488. https://doi.org/10.1111/j.1469-8986.1981.tb02486.x.
133. Hart, N., McGowan, J., Minati, L., and Critchley, H.D. (2013). Emotional regulation and bodily sensation: Interoceptive awareness is intact in borderline personality disorder. J. Pers. Disord. *27*, 506–518. https://doi.org/10.1521/pedi_2012_26_049.
134. Garfinkel, S.N., Seth, A.K., Barrett, A.B., Suzuki, K., and Critchley, H.D. (2015). Knowing your own heart: Distinguishing interoceptive accuracy from interoceptive awareness. Biol. Psychol. *104*, 65–74. https://doi.org/10.1016/j.biopsycho.2014.11.004.
135. Baer, R.A., Smith, G.T., Hopkins, J., Krietemeyer, J., and Toney, L. (2006). Using self-report assessment methods to explore facets of mindfulness. Assessment *13*, 27–45. https://doi.org/10.1177/1073191105283504.
136. Giovannini, C., Giromini, L., Bonalume, L., Tagini, A., Lang, M., and Amadei, G. (2014). The Italian five facet mindfulness questionnaire: A contribution to its validity and reliability. J. Psychopathol. Behav. Assess. *36*, 415–423. https://doi.org/10.1007/s10862-013-9403-0.
137. Mehling, W.E., Price, C., Daubenmier, J.J., Acree, M., Bartmess, E., and Stewart, A. (2012). The Multidimensional Assessment of Interoceptive Awareness (MAIA). PLoS One *7*, e48230. https://doi.org/10.1371/journal.pone.0048230.
138. Calì, G., Ambrosini, E., Picconi, L., Mehling, W.E., and Committeri, G. (2015). Investigating the relationship between interoceptive accuracy,interoceptive awareness,and emotional susceptibility. Front. Psychol. *6*, 1202. https://doi.org/10.3389/fpsyg.2015.01202.
139. Still, A.W., and White, A.P. (1981). The approximate randomization test as an alternative to the F test in analysis of variance. Br. J. Math. Stat. Psychol. *34*, 243–252. https://doi.org/10.1111/j.2044-8317.1981.tb00634.x.
140. Anderson, M., and Braak, C.T. (2003). Permutation tests for multi-factorial analysis of variance. J. Stat. Comput. Simulat. *73*, 85–113. https://doi.org/10.1080/00949650215733.
141. Winkler, A.M., Ridgway, G.R., Webster, M.A., Smith, S.M., and Nichols, T.E. (2014). Permutation inference for the general linear model. Neuroimage *92*, 381–397. https://doi.org/10.1016/j.neuroimage.2014.01.060.
142. Kliegl, R., Wei, P., Dambacher, M., Yan, M., and Zhou, X. (2010). Experimental effects and individual differences in linear mixed models: Estimating the relationship between spatial, object, and attraction effects in visual attention. Front. Psychol. *1*, 238. https://doi.org/10.3389/fpsyg.2010.00238.
143. Ambrosini, E., Finotti, G., Azevedo, R.T., Tsakiris, M., and Ferri, F. (2019). Seeing myself through my heart: Cortical processing of a single heartbeat speeds up self-face recognition. Biol. Psychol. *144*, 64–73. https://doi.org/10.1016/j.biopsycho.2019.03.006.
144. Landler, L., Ruxton, G.D., and Malkemper, E.P. (2018). Circular data in biology: advice for effectively implementing statistical procedures. Behav. Ecol. Sociobiol. *72*, 128. https://doi.org/10.1007/s00265-018-2538-y.
145. Berens, P. (2009). CircStat: A MATLAB Toolbox for Circular Statistics. J. Stat. Software *31*, 1–21. https://doi.org/10.18637/jss.v031.i10.
146. Watson, G.S., and Williams, E.J. (1956). On the Construction of Significance Tests on the Circle and the Sphere. Biometrika *43*, 344. https://doi.org/10.2307/2332913.
147. Stephens, M.A. (1969). Multi-Sample Tests for the Fisher Distribution for Directions. Biometrika *56*, 169–181. https://doi.org/10.1093/biomet/56.1.169.
148. Benjamini, Y., and Yekutieli, D. (2001). The Control of the False Discovery Rate in Multiple Testing under Dependency. Ann. Stat. *29*, 1165–1188. https://www.jstor.org/stable/2674075.

# STAR★METHODS

## KEY RESOURCES TABLE

| REAGENT or RESOURCE | SOURCE | IDENTIFIER |
|---|---|---|
| Deposited data | | |
| Zenodo: Analysed ERP data | This paper | https://doi.org/10.5281/zenodo.10829954 |
| Software and algorithms | | |
| MATLAB (R2021a) | MathWorks Inc, Natick, MA, USA | https://it.mathworks.com/products/matlab.html |
| EEGLAB (v2022.1) | Delorme & Makeig, 2004[103] | https://sccn.ucsd.edu/eeglab/index.php |
| ERPLAB (v9.00) | Lopez-Calderon & Luck, 2014[104] | https://erpinfo.org/erplab |
| Kubios HRV Standard (v3.5) | Tarvainen et al., 2014[105] | https://www.kubios.com/ |
| HEPLAB | Perakakis, 2019[106] | https://pandelisperakakis.info/heplab/ |
| Mass Univariate ERP Toolbox | Groppe et al., 2011a, b[107,108] | https://github.com/dmgroppe/Mass_Univariate_ERP_Toolbox |
| Factorial Mass Univariate ERP Toolbox | Fields & Kuperberg, 2020[109] | https://github.com/ericcfields/FMUT |
| Reduction of Electroencephalographic Artifacts toolbox (v1.1.5) | Bailey et al., 2022; Bailey et al., 2022[110,111] | https://github.com/NeilwBailey/RELAX/releases |
| Original Code | This paper | https://doi.org/10.5072/zenodo.37557 Full Changelog: https://github.com/azaccaro90/HEP_attention_respiration_HCT/commits/v1.0 |

## RESOURCE AVAILABILITY

### Lead contact

Further information and requests for resources should be directed to and will be fulfilled by the lead contact, Andrea Zaccaro (andrea.zaccaro@unich.it; a.zaccaro90@gmail.com).

### Materials availability

This study did not generate new unique reagents.

### Data and code availability

- Raw data reported in this paper will be shared by the lead contact upon reasonable request if data privacy can be guaranteed according to the rules of the European General Data Protection Regulation (EU GDPR 2016).
- Analysed ERP data have been deposited at Zenodo and are publicly available. https://doi.org/10.5281/zenodo.10829954.
- Original code used to produce results and statistics has been deposited at GitHub and is publicly available. https://doi.org/10.5072/zenodo.37557. Full Changelog: https://github.com/azaccaro90/HEP_attention_respiration_HCT/commits/v1.0.
- Any additional information required to reanalyse the data reported in this paper is available from the lead contact upon request.

## EXPERIMENTAL MODEL AND STUDY PARTICIPANT DETAILS

### Ethics statement

The Institutional Review Board of Psychology of the Department of Psychological, Health and Territorial Sciences, "G. d'Annunzio" University of Chieti-Pescara, Italy, approved the study (Protocol Number 44_26_07_2021_21016). Participants were blind to the experimental aims. The study was conducted in conformity with the Italian Association of Psychology and the Declaration of Helsinki and its later amendments. All participants read and signed an informed consent.

### Human participants

Thirty-four (19 females; 1 left-handed; age: 27.48 $\pm$ 4.28 years [mean $\pm$ SD]) white healthy volunteers were recruited. The eligibility of each volunteer was confirmed based on self-reported criteria: 1) absence of personal and/or family history of psychiatric, neurological, and somatic disorders; 2) no chronic and/or acute conditions involving the respiratory tracts; 3) no use of substances interacting with the central nervous

system in the previous week; 4) no experience in mindfulness-based meditation and/or breath-control practices. All participants were of normal weight and had normal or corrected-to-normal vision. Sample size was estimated using G*Power 3.1 (v3.1.9.7).[112] Considering a 2x2 factorial design, we estimated a medium effect size of partial eta squared ($\eta$p2) of .06, based on a recent meta-analysis on attentional effects on HEP,[16] which corresponds to a Cohen's f of .25. Significance level was set to alpha = .05, and the power (1 - beta) at .85. The total estimated sample size was 26. We excluded 2 participants from the testing of HEPs, regardless of the respiratory phase, due to noisy EEG (N = 32, 17 females; 1 left-handed; age: 27.57 $\pm$ 4.33 years [mean $\pm$ SD]). Additionally, we excluded 4 participants from the testing of HEP changes among respiratory phases due to noisy respiratory data (N = 28, 13 females; 1 left-handed; age: 27.88 $\pm$ 4.46 years [mean $\pm$ SD]).

## METHOD DETAILS

### Experimental procedure

After a resting-state (baseline), participants performed two interoceptive tasks and two exteroceptive tasks, requiring them to focus their attention inside or outside the body, respectively (Attention Focus factor). During the interoceptive and exteroceptive tasks, participants had to process either cardiac or respiratory signals (System factor). Participants sat comfortably in front of a computer at an optimal distance (around 60 cm) for keyboard use and screen visibility. Room lighting and noise were minimized, and the temperature and humidity were maintained at a comfortable level. Participants received written instructions (see below) presented through E-Prime 3.0 software (Psychology Software Tools, Pittsburgh, PA, USA). Subsequently, the experimenter ensured participants understood the instructions, allowing them to ask questions if any doubts arose. Baseline was always performed first. Participants were seated for 10 minutes in a resting-state condition with eyes open, watching a fixation cross at the centre of a monitor, and letting their mind wander without focusing on anything in particular.[113] Participants were also asked to breathe spontaneously.

The cardiac interoceptive task was HCT.[10,13] Participants were given the following instructions in line with Desmedt et al.[49]: "*In this task, direct your attention to your heart and the associated physical sensations. You are required to sustain your focus on your heart for various durations and count the number of heartbeats you perceive. Begin silently counting when the heart symbol appears on the screen. When the heart symbol disappears, report the number of heartbeats you are sure you felt. Only report the number of heartbeats you are sure about, without trying to estimate your heart rate. During each trial, keep your eyes open, gaze at the screen and avoid moving. Refrain from guiding your responses by checking your pulse in your wrists or neck. Breathe spontaneously and avoid changing your breathing frequency or holding your breath*". HCT consisted of three blocks, each one comprising four randomized trials of the following durations: 25, 35, 45, and 100 seconds,[114–116] for a total of 12 trials. After each trial, participants reported the number of perceived heartbeats and rated their performance (HCT confidence) on a 10-points Likert scale from 0 (very bad) to 9 (excellent). No feedback was provided about their performance. The respiratory interoceptive task was BCT.[34] Participants were given the following instructions: "*In this task, direct your attention to your breath and the associated physical sensations. You are required to sustain your focus on your breath for various durations and count the number of breaths you take. Begin silently counting your breaths when the lungs symbol appears on the screen. When the lungs symbol disappears, report the number of breaths you took. Refrain from changing the rhythm or depth of your breathing, simply stay aware of your breath without making any change*". BCT consisted of five trials of 120 seconds each. After each trial, participants reported the number of performed respiratory cycles, and rated their performance (BCT confidence). They were asked to rate the ease in performing the task without modifying the respiratory rate on a Likert scale from 0 (very difficult) to 9 (very easy). No feedback was provided about their performance. The order of tasks and blocks/trials within each task was randomized.

The exteroceptive tasks mirrored the interoceptive tasks. In C-TCT, participants were presented with digitally constructed heartbeat sounds and instructed to mentally count and report the number of heard heartbeats.[35] C-TCT consisted of three blocks of four randomized trials of different durations (25, 35, 45, and 100 seconds). Heartbeats were presented at an irregular frequency at an average frequency of 60 bpm. After each trial, participants reported the number of heard heartbeats and rated their performance (C-TCT confidence). In B-TCT, participants were presented with audio samples of respiratory sounds (adapted from[34]) comprising inhalation and exhalation sounds at irregular frequencies (mean: 18 breaths per minute). B-TCT consisted of five trials of 120 seconds each. After each trial, participants reported the number of heard respiratory cycles and rated their performance (B-TCT confidence), and the perceived ease in performing the task without modifying the respiratory rate. The order of tasks and blocks/trials within each task was randomized.

The interoceptive and exteroceptive tasks were presented in a counterbalanced order between participants. Before starting the experiment, participants had to perform a brief training session and verbally confirm that they could not feel their heartbeat through the respiratory belt, in case the belt was mounted too tight.[20] To ensure a similar number of epochs, baseline and tasks lasted 10 minutes each. EEG, ECG, and respiratory signals were recorded throughout the entire experiment. The experimental design is depicted in Figure S11. All tasks were administered using the E-Prime 3.0 software (Psychology Software Tools, Pittsburgh, PA, USA).

### Electrophysiological recording

EEG signals were acquired using a 64-channel BrainAmp EEG system (BrainCap MR, BrainVision LLC, Garner, NC, USA). Electrodes were positioned on the scalp following the International 10-20 system. Electrode impedance was kept below 10 k$\Omega$ for all channels. ECG was recorded from three electrodes: two placed over the left costal margin and the right clavicle, and the ground located on the right costal margin (MP160, BIOPAC Systems Inc, Goleta, CA, USA). Three additional electrodes, serving as the backup, were integrated in the EEG recording system via an external Electrode Input Box (BrainProducts GmbH, BrainVision LLC, Gilching, Germany), and were placed over the left and right clavicles, with the ground located on the left costal margin. Breathing activity was recorded via a respiratory belt placed around the chest (respiratory

transducer TSD201, BIOPAC Systems Inc, Goleta, CA, USA). The systems running the BrainAmp EEG, MP160, and TSD201 were connected with the system running the E-Prime 3.0 software and were synchronized with a TriggerStation™ (BRAINTRENDS LTD 2010, Italy). The sampling rate was 2.5 kHz for all signals. Band-pass filtering was applied from .016 to 250 Hz, along with 50-Hz notch filtering. Subsequently, all signals were down-sampled to 512 Hz.

### ECG data analysis

ECG data were processed using custom MATLAB code (R2021a, MathWorks Inc, Natick, MA, USA). ECG signal was high-pass filtered at .1 Hz to remove baseline fluctuations.[117] R-peaks were detected with the Pan-Tompkins algorithm.[118] To measure Heart Rate Variability (HRV), the time series of the distance between consecutive R-peaks (tachogram) was computed and ectopic beats were corrected using a point process model.[119] This procedure corrected very few heartbeats (baseline: range 0-4 heartbeats; HCT: 0-16; BCT: 0-9; C-TCT: 0-11; B-TCT: 0-9). Kubios software (Kubios HRV Standard, v3.5)[105] was used to pre-process the tachogram and extract average HR and frequency-domain HRV features of interest. ECG pre-processing was carried out using Kubios routines. Detrending involved removing the best straight-line fit linear trend from the ECG data. The ECG tachogram was interpolated at 4 Hz. Frequency-domain analysis utilized the Fast Fourier Transform (FFT)-based Welch's periodogram applied to the detrended RR series. In the Welch's periodogram method, the window width was set to 300 seconds, with a default overlap of 50%.[105] We calculated HR (bpm, the average number of heartbeats in one minute), High Frequency (HF: .15-.4 Hz) log power (log ms2/Hz, the log-transformed power of HF band),[120,121] HRV total power (ms2/Hz, the sum of power values in HF, Low Frequency-LF, and Very Low Frequency bands), and Low Frequency/High Frequency ratio (LF/HF).

### Respiratory data analysis

Respiratory data were processed using custom MATLAB scripts (R2021a, MathWorks Inc, Natick, MA, USA). The respiratory signal was first high-pass filtered at .1 Hz to remove baseline wander. Respiratory phases were detected following a validated procedure.[61,122] Outliers (i.e., values exceeding three scaled median absolute deviations from the local median within a moving 1-second window) were linearly interpolated with their neighbouring values. The data were then smoothed with a 1-second-window filter[123] and z-scored. Inhalation and exhalation onsets were identified as the local minima (trough) and the local maxima (peaks). Peaks and troughs were required to be at least 2 seconds apart and the minimum prominence of the interquartile range of the z-scored data was multiplied by a value ranging from .3 to .8, depending on the participant's respiratory trace.[61] A respiratory cycle was defined as the interval from one inhalation onset (referred to as "trough") to the subsequent trough. Respiratory cycles with outlier durations (i.e., different from two times the median) were excluded. Rejected respiratory cycles were 6 $\pm$ 5 [mean $\pm$ SD] for the baseline, 9 $\pm$ 6 for HCT, 4 $\pm$ 3 for BCT, 12 $\pm$ 6 for C-TCT, and 8 $\pm$ 7 for B-TCT. The number of retained artifact-free respiratory cycles in the entire sample was 3997 for the baseline (143 $\pm$ 37 [mean $\pm$ SD]), 3969 for HCT (142 $\pm$ 31), 4053 for BCT (145 $\pm$ 34), 4590 for C-TCT (164 $\pm$ 28), and 4440 for B-TCT (159 $\pm$ 27). Respiratory features of interest were the breathing rate (breaths/min), average inhalation duration (sec), average exhalation duration (sec), and the Inhalation/Exhalation ratio.

### EEG data analysis

EEG data were pre-processed using the EEGLAB toolbox (v2022.1).[103] EEG data were filtered using a Hamming windowed FIR filter from .5 to 45 Hz.[124,125] EEG segments with poor signal quality were manually rejected. Independent Component Analysis (ICA) was applied to remove heartbeat, ocular, and muscle artefacts (FastICA).[126] ECG, respiratory channel, and excessively noisy channels were excluded from ICA decomposition. There were a few noisy channels (less than 5), always peripheral, known not to contribute to HEP generation.[16] Independent Components (ICs) were rejected based on IC time series, scalp map, and power spectrum.[103] Particular attention was given to the Cardiac Field Artifact (CFA), as it highly impacts HEP activity.[16] ICs contaminated by CFA were identified by plotting R-peaks over IC time series. ICs with activations time-locked to ECG R-peak were removed (Figure S12).[20,124,125] To facilitate the visual inspection, the cross-correlation between each IC time course and ECG channel was calculated. Removed ICs ranged from 1 to 6 (3 $\pm$ 1 [mean $\pm$ SD]), while CFA-related ICs ranged from 0 to 3 (1 $\pm$ 1 [mean $\pm$ SD]). After ICA, previously identified noisy channels were interpolated using their neighbours.[127] Pruned EEG signals were then re-referenced to the average ref.[20] as recommended.[128] A depiction of a 10-second comparison of EEG before and after ICA in the same participant is presented in Figure S13.

HEPs were computed using ERPLAB toolbox (v9.00).[104] R-peaks were identified with HEPLAB toolbox.[106] Manual correction of mis-detected peaks was performed[20,125] and EEG was epoched between -100 and 600 msec around each R-peak.[16] To account for potential voltage drifts, a regression baseline correction was employed using the Reduction of Electroencephalographic Artifacts toolbox (RELAX v1.1.5).[110,111] The regression baseline correction method calculates the trial-based average amplitude within the baseline period and regresses out the influence of the baseline period from each time point in the HEP time window. This approach avoids introducing differences from the baseline into the HEP period of interest, contrasting with the subtraction baseline correction method.[129] Epochs followed by an R-peak by less than 600 msec were excluded to avoid overlap between HEP epoch and the following R-peak.[20,130] The number of epochs excluded was generally low (20 $\pm$ 60 [mean $\pm$ SD]). The high SD is attributed to two participants with elevated HR, resulting in a higher number of rejected epochs compared to the average. Epochs were excluded if they exceeded a peak-to-peak threshold of 100 $\mu$V[20,42,131] within a moving window (size: 200 ms; overlap: 50%).[104] The number of rejected epochs exceeding this threshold was very low (4 $\pm$ 10 [mean $\pm$ SD] epochs for the baseline, 4 $\pm$ 11 for HCT, 2 $\pm$ 6 for BCT, 3 $\pm$ 9 for C-TCT, and 3 $\pm$ 10 for B-TCT). Epochs were averaged within participants during each task, resulting in four HEP bins named as follows: HCT, C-TCT, BCT, and B-TCT. HEP epochs were then assigned to inhalation and exhalation based on the

respiratory phase in which the respective R-peak occurred. This resulted in ten HEP bins named as follows: baseline inhalation and exhalation; HCT inhalation and exhalation; C-TCT inhalation and exhalation; BCT inhalation and exhalation; B-TCT inhalation and exhalation.

### Task accuracy assessment

HCT accuracy was calculated following validated procedures[44,132–134] based on the number of counted heartbeats in relation to the heartbeats recorded with ECG. The formula was:

$$\text{HCT accuracy} = 1 - \frac{|(\text{Recorded heartbeats} - \text{Counted heartbeats})|}{\text{Recorded heartbeats}}$$

In the absence of excessive over-reporting, scores range from 0 to 1, where higher scores indicate better accuracy. The accuracy of each trial was then averaged over the 12 HCT trials.[44,133,134] Similarly, C-TCT accuracy was calculated as follows:

$$\text{C - TCT accuracy} = 1 - \frac{|(\text{Presented heartbeats} - \text{Counted heartbeats})|}{\text{Presented heartbeats}}$$

Accuracy for BCT and B-TCT were calculated based on the number of counted respiratory cycles in relation to performed respiratory cycles and presented respiratory sounds, respectively. Within each task, self-reported performance (confidence) was averaged among the trials.

### Psychometric questionnaires

FFMQ[135] (Italian version by[136]) and MAIA[137] (Italian version by[138]) were administered via the Qualtrics online platform (Qualtrics, Provo, UT, USA). In FFMQ, participants were asked to answer to 39 statements on a 5-point Likert scale from 1 (never) to 5 (always). FFMQ measures trait mindfulness, i.e., the tendency to stay aware of perceptions, thoughts, emotions, and actions without distraction, non-judgment, and immediate reaction. We focused on FFMQ total score to correlate HEP amplitude with trait mindfulness.[32] In MAIA, participants were asked to answer to 37 statements on a 6-point Likert scale from 0 (never) to 5 (always). It consists of eight scales assessing facets of interoceptive sensibility. Given previous association with HEP activity,[30,31] we focused on the Trusting and Not-Worrying scales of MAIA. The Trusting scale assesses the experience of the body as safe and trustworthy and the Not-Worrying scale assesses emotional distress for bodily sensations of pain and/or discomfort.

## QUANTIFICATION AND STATISTICAL ANALYSIS

### Heartbeat evoked potential statistical analyses

HEP changes were assessed with the Mass Univariate ERP Toolbox (MUT).[107,108] To test for interaction effects in factorial designs, we followed the procedure included in the Factorial Mass Univariate ERP Toolbox (FMUT).[109] Cluster-based permutation tests were performed with HEP amplitude as dependent variable and System (cardiac vs. respiratory) and Attention Focus (interoceptive vs. exteroceptive) as within-participant factors. The cluster mass tested clusters instead of individual electrodes or time points. Firstly, spatially (neighbouring channels) and temporally (contiguous time points) adjacent points with a p-value below .05 were included into a cluster. A cluster statistic was calculated by summing t-values within each cluster. The null distribution was estimated through Monte Carlo permutations, in which condition labels were randomly shuffled 10000 times and the largest cluster-level statistic for each randomization was entered into the null distribution. Statistical significance was determined by comparing the experimentally observed cluster-level statistics with the randomly-generated null distribution. Clusters exceeding the 1 - alpha percentile of the distribution (two-tails) were significant.[109] The maximum distance for two electrodes to be included into a cluster was 5.44 cm (*chan_hood* = .61). To test for interaction effects, we used the permutation of residuals method.[139–141] For instance, to test the 2x2 interaction (System by Attention Focus) we calculated the difference between the two levels of Attention Focus for each level of System and conducted paired cluster-based permutation t-tests comparing difference values (HCT minus C-TCT vs. BCT minus B-TCT).[108] Planned t-tests were conducted using paired cluster-based permutation t-tests implemented in MUT.[107] Specifically, we planned to compare HCT vs. C-TCT, HCT vs. BCT, BCT vs. B-TCT, and C-TCT vs. B-TCT (number of planned t-tests: 4). Based on previous research,[4,20,30,36–42] we tested HEP amplitude at each electrode and time point separately in an early (100-350 msec) and a late time window (350-600 msec) after the R-peak. We excluded external electrodes (F7, F8, FT7, FT8, T7, T8, TP7, TP8, P7, P8, PO7, PO8, O1, O2, Oz, TP9, and TP10) that are susceptible to noise contamination and contribute less to HEP modulations, in line with a recent meta-analysis.[16] We then investigated HEP differences between inhalation and exhalation across tasks. We conducted a cluster-based permutation tests with HEP as dependent variable, and System (cardiac vs. respiratory), Attention Focus (interoceptive vs. exteroceptive), and Phase (inhalation vs. exhalation) as within-participant factors. The 2x2x2 interaction (System by Attention Focus by Phase) was calculated as with the formula: [(HCT Exhalation – HCT Inhalation) – (C-TCT Exhalation – C-TCT Inhalation)] vs. [(BCT Exhalation – BCT Inhalation) – (B-TCT Exhalation – B-TCT Inhalation)]. The test was performed over the significant time window and electrodes resulting from the previous analysis. Planned t-tests were HCT inhalation vs. HCT exhalation; BCT inhalation vs. BCT exhalation; C-TCT inhalation vs. C-TCT exhalation; B-TCT inhalation vs. B-TCT exhalation; HCT exhalation vs. C-TCT exhalation; HCT exhalation vs. BCT exhalation; HCT inhalation vs. C-TCT inhalation; and HCT inhalation vs. BCT inhalation (number of planned t-tests: 8).

### Trial-level cardio-respiratory control analyses

We controlled for instantaneous HR influences on HEPs between HCT and C-TCT by assessing trial-level data through linear mixed-effects models on 46903 trials clustered around 32 participants.[20,142,143] We also controlled for cardiac influences on HEPs among respiratory phases at the single-trial level during HCT with a linear mixed-effects model on 17406 trials, clustered around 28 participants. Instantaneous HR for each heartbeat was based on the trial-level inter-beat interval. Trial-based ECG amplitude was calculated by averaging ECG voltage in the significant HEP time window. Single-trial HEP activity was calculated by averaging the voltage of the significant channels and time-window of observed HEP effects. Values lying outside three standard deviations from the mean were excluded. Models were implemented with the General Analyses for the Linear Model (GAMLj) module in jamovi (v2.3.21; The jamovi project, 2022), using the Residual Maximum Likelihood (REML) method. The Akaike Information Criterion (AIC) was used to determine the best fitting model. For each parameter of the best fitting model, we reported the estimated coefficient (b), standard error (SE), t-statistic, and p-value. Degrees of freedom were estimated with the Satterthwaite's method.

### Respiratory cycle analyses

Circular statistics were performed to assess HEP activity over the entire respiratory cycle, spanning from one inhalation to the subsequent one. We calculated the angular value of each R-peak using the formula:[124]

$$\text{Angular value} = \left[360 * \frac{(\text{R onset} - \text{previous inhalation onset})}{(\text{subsequent inhalation onset} - \text{previous inhalation onset})}\right]$$

R-peaks angular values ranged from 0° to 360°, with 0° indicating the onset of inhalation. Single-trial angular values were converted to radians (range 0 - 2π) and the corresponding HEP values were derived from electrodes and time window showing significant changes across the respiratory cycle in the binary analysis. Outliers exceeding three standard deviations from the mean were removed. Using the interquartile range method, HEPs were categorized into low (first quartile) and high-amplitude (fourth quartile) HEPs for each participant.[124,125] For each participant, the mean angle direction was calculated for the low and high-amplitude HEPs. At the group level, we tested whether the distribution of low and high-amplitude HEPs deviated from uniform distribution using the Rayleigh test for uniformity[144] as implemented in the Circular Statistics Toolbox.[145] To assess whether the strength of the respiratory phase-locking differed between low and high-amplitude HEPs, we applied the Watson-Williams test.[146,147]

We computed HEPs amplitude based on six equally sized respiration phase bins spanning the 0°-360° interval. A one-way repeated measures ANOVA was conducted to assess changes in HEP amplitude across bins. Planned t-tests were performed between inhalation phase bins (0°-60°, 60°-120°, 120°-180°) and exhalation phase bins (180°-240°, 240°-300°, 300°-360°) (number of planned t-tests: 9).

When appropriate, we used the Benjamini and Yekutieli procedure (FDR),[148] to correct for multiple testing with an FDR threshold of p = .05. Effect sizes were estimated with Cohen's d and partial eta squared ($\eta$p2) indices. Statistical analyses of behavioural and physiological data were conducted using repeated measures ANOVAs. Correlations between behavioural and psychometric data with HEP values were performed using Pearson's correlation. Statistical analyses were conducted in jamovi (v2.3.21; The jamovi project, 2022).

# Appendix C

# Published version of Study 3

NeuroImage 327 (2026) 121711

Contents lists available at ScienceDirect

NeuroImage

journal homepage: www.elsevier.com/locate/ynimg

# Cardio-respiratory interactions in interoceptive perception: The role of heartbeat-modulated cortical oscillations

Andrea Zaccaro [a,*], Francesca della Penna [a], Francesco Bubbico [a], Başak Bayram [a], Eleonora Parrotta [b], Mauro Gianni Perrucci [a,c,d], Marcello Costantini [c,e], Francesca Ferri [a,c]

[a] Department of Neuroscience, Imaging and Clinical Sciences, "G. d'Annunzio" University of Chieti-Pescara, Chieti, Italy
[b] Department of Psychology, University of Rome "La Sapienza", Rome, Italy
[c] Institute for Advanced Biomedical Technologies, "G. d'Annunzio" University of Chieti-Pescara, Chieti, Italy
[d] UdA-TechLab, Research Center, "G. d'Annunzio" University of Chieti-Pescara, Chieti, Italy
[e] Department of Psychology, "G. d'Annunzio" University of Chieti-Pescara, Chieti, Italy

ARTICLE INFO

*Keywords:*
Cardiac interoception
Respiratory phase
Heartbeat-modulated cortical oscillations
Alpha band activity
Interoceptive predictive coding
Heartbeat-evoked potential (HEP)

ABSTRACT

The cardiovascular and respiratory systems are anatomically and functionally integrated, suggesting that breathing continuously influences cardiac interoception. Previously, we demonstrated that the heartbeat-evoked potential (HEP), a neural marker of cardiac signal processing, is modulated by respiration, with enhanced late HEP positivity and increased interoceptive accuracy during exhalation. Here, we reanalysed our previous dataset in the time–frequency domain to investigate heartbeat-modulated cortical oscillations across respiratory phases during rest, cardiac interoception (heartbeat counting), and an exteroceptive control task. During heartbeat counting, exhalation was associated with increased late heartbeat-modulated alpha- and theta-band power and inter-trial coherence over fronto-parietal electrodes, compared with inhalation. Heartbeat-modulated alpha activity was related to HEP amplitude and predicted interoceptive accuracy. Exploratory analyses also indicated enhanced heartbeat-modulated functional connectivity during exhalation. These effects could not be accounted for by cardiac physiology alone and were absent during exteroception. We propose a mechanistic account of cardio-respiratory interactions grounded in interoceptive predictive coding, suggesting that exhalation enhances precision-weighting of cardiac signals by facilitating attentional allocation to interoceptive signals and suppressing task-irrelevant distractions.

## 1. Introduction

Beneath the threshold of awareness, the brain continuously processes signals from the body's internal systems, inferring their states and modulating their activity to maintain vital functions essential for survival and psychophysical health, a process referred to as interoception (Berntson and Khalsa, 2021; Bonaz et al., 2021; Candia-Rivera et al., 2024; Chen et al., 2021; Craig, 2003; Khalsa et al., 2018; Nord and Garfinkel, 2022; Saltafossi, Heck, et al., 2025; Tallon-Baudry, 2023). Among these, the cardiovascular and respiratory systems, anatomically and functionally integrated within the cardio-respiratory system (Eckberg, 2003; Elstad et al., 2018; Parviainen et al., 2022), are regulated by the autonomic nervous system to optimize oxygen uptake and distribution to bodily tissues. This interplay is exemplified by respiratory sinus arrhythmia, a phenomenon in which heart rate fluctuates in synchrony with the phases of respiration (Berntson et al., 1993; Brecher and Hubay, 1955; Yasuma and Hayano, 2004). Furthermore, the two systems share bottom-up interoceptive pathways via the vagus nerve that converge in brain regions such as the insular, somatosensory, and cingulate cortices (Chan et al., 2024; Engelen et al., 2023; Lovelace et al., 2024; Park and Blanke, 2019; Weng et al., 2021). This close connection suggests that respiration continuously modulates the perception of cardiac signals, making it inherently challenging to dissociate the two, a perspective often overlooked in interoception research.

We have previously highlighted such cardio-respiratory interoceptive interactions as reflected in the heartbeat-evoked potential (HEP), an event-related potential time-locked to systole that indicates cortical processing of cardiac signals (Coll et al., 2021; Schandry and Weitkunat, 1986). In two independent samples of healthy individuals, we found

* Corresponding author.
*E-mail address:* andrea.zaccaro@unich.it (A. Zaccaro).

https://doi.org/10.1016/j.neuroimage.2026.121711
Received 22 July 2025; Received in revised form 19 December 2025; Accepted 9 January 2026
Available online 10 January 2026
1053-8119/© 2026 The Authors. Published by Elsevier Inc. This is an open access article under the CC BY-NC-ND license (http://creativecommons.org/licenses/by-nc-nd/4.0/).

increased late HEP positivity (emerging after 300 ms from the R-peak) during exhalation compared to inhalation while participants engaged in two cardiac interoceptive tasks: the heartbeat detection task (HBD; Zaccaro et al., 2022) and the heartbeat counting task (HCT; Zaccaro et al., 2024). In the HBD, greater HEP amplitudes during exhalation compared to inhalation were positively correlated with greater interoceptive accuracy (Zaccaro et al., 2022). In the HCT, late HEP enhancements relative to the C-TCT were predominantly driven by exhalation, with no significant contribution from inhalation (Zaccaro et al., 2024). Notably, these effects were absent while participants engaged in tasks involving attention to external tones (the exteroceptive condition of the HBD and the cardiac-tone counting task, C-TCT) or during respiratory interoception (the breath counting task). Furthermore, these findings could not be explained by differences in respiratory rate, heart rate, or heart rate variability across conditions.

Together, these results supported the hypothesis that exhalation may enhance cardiac interoception compared to inhalation (Molle and Coste, 2022). They were also consistent with evidence that breathing dynamically shapes neural processing in different domains. The respiratory cycle interacts with both resting (Herrero et al., 2018; Kluger et al., 2023; Kluger and Gross, 2021) and task-related brain activity, modulating perceptual (Flexman et al., 1974; Gallego et al., 1991; Goheen et al., 2024; Grund et al., 2022; Harting et al., 2025; Johannknecht and Kayser, 2022; Kluger et al., 2021; Leupin and Britz, 2024; Mizuhara et al., 2024, 2025; Mizuhara and Nittono, 2022; Münch et al., 2019; Saltafossi, Zaccaro, et al., 2025; Stetza et al., 2025), cognitive-emotional (Arshamian et al., 2018; Belli and Fischer, 2024; Brændholt et al., 2025; Huijbers et al., 2014; Molle et al., 2023; Nakamura et al., 2018; Perl et al., 2019; Waselius et al., 2019; 2022; Zelano et al., 2016; Mizuhara and Nittono, 2023; Schaefer et al., 2024), and motor functions (Engelen et al., 2025; Kluger and Gross, 2020; Park et al., 2020; 2022) (see Tort et al., 2025, for an extensive review). However, despite its well-established role in exteroceptive functions, the precise influence of respiration on cardiac interoception remains unclear, particularly due to the strong physiological coupling between heartbeat dynamics and respiratory cycles, which introduces potential confounds and complicates interpretation.

A growing body of evidence suggests that, beyond time-domain HEPs, heartbeat-modulated cortical oscillations in the time-frequency domain may be used as more precise electrophysiological markers of cardiac interoception. A landmark electrocorticography study (Kern et al., 2013) identified heartbeat-modulated power fluctuations over somatosensory areas at rest, predominantly occurring in the low-frequency band (<12 Hz). Similarly, an intracranial EEG (iEEG) study (Park et al., 2018) identified heartbeat-modulated increases in inter-trial coherence (ITC) in the theta band within the insula and frontotemporal regions. These increases were observed both at rest and during a task designed to modulate bodily self-awareness (a full-body illusion paradigm), while no heartbeat-modulated power changes were detected in the same areas. In contrast, an iEEG study by Treves (2020) employing independent component analysis-based denoising reported heartbeat-modulated increases in alpha power but found no changes in ITC. Several EEG studies have investigated heartbeat-modulated changes in power, ITC, and functional connectivity (FC) across a range of conditions, including sleep stages (Lechinger et al., 2015; Simor et al., 2025), states of consciousness (Liuzzi et al., 2024), resting-state (Kim and Jeong, 2019), emotions (Kim et al., 2019; Kato et al., 2020), interoceptive metacognitive awareness (Canales-Johnson et al., 2015), interoceptive-exteroceptive processing (Fló et al., 2024; García-Cordero et al., 2017; Pultsina et al., 2025), Alzheimer's disease (Castellanos et al., 2022), and meditation expertise (Jiang et al., 2020). Recently, Lee et al. (2024) employed a classification approach to highlight the role of heartbeat-related spectral perturbations in the alpha and theta bands in distinguishing interoceptive (heartbeat-focused) from exteroceptive (sound-focused) attentional states. Their results suggest that time-frequency measures may be less susceptible to physiological artifacts, such as the cardiac field artifact.

Taken together, these findings indicate that studying heartbeat-modulated cortical oscillations in the time-frequency domain may help to overcome the limitations of time-domain HEP analysis and may provide deeper insights into the neural mechanisms of cardiac interoception. In this study, we re-analysed our previously collected dataset (Zaccaro et al., 2024) comprising 28 healthy participants. Our investigation focused on heartbeat-modulated activity during the HCT and its exteroceptive control task (C-TCT), separately analysing heartbeats during inhalation and exhalation. Our central hypothesis was that heartbeat-modulated power and ITC would be differentially shaped by respiratory phase and task demands: based on the findings of Lee et al. (2024) and our previous work (Zaccaro et al., 2024), we predicted selective increases in theta (4–8 Hz) and alpha (8–13 Hz) activity during exhalation, emerging in a late post-R-peak window (from 300 ms onward) and specifically during the HCT.

To further investigate the relationship between HEPs and time-frequency measures, we adopted a methodology from a study that reported a negative association between auditory-evoked P300 responses and alpha activity (Studenova et al., 2023). We then applied linear mixed-effects models to assess trial-level relationships between HEP, power, and ITC across respiratory phases, as well as their associations with interoceptive accuracy and cardio-respiratory physiology. Based on prior research identifying alpha power as a marker of interoceptive attention that has been shown to correlate with emotional arousal-related HEP modulations (Luft and Bhattacharya, 2015), interoceptive accuracy (Rominger et al., 2025; Villena-González et al., 2017), and to increase during heartbeat-focused tasks (Crivelli and Balconi, 2025; Kritzman et al., 2022; McCraty et al., 2009; Villena-González et al., 2017), we expected to find positive associations between HEPs, heartbeat-modulated cortical oscillations in the alpha band, and interoceptive accuracy. Finally, we conducted exploratory analyses to evaluate changes in heartbeat-modulated FC and graph theory metrics within the alpha and theta frequency bands, across tasks and respiratory phases. As with power and ITC, we expected to observe increases in heartbeat-modulated FC and graph theory metrics during exhalation compared to inhalation in the HCT. We interpreted our findings within the interoceptive predictive coding framework, examining how respiration shapes predictive processes underlying cardiac interoception and how cardio-respiratory interoceptive interactions may modulate the precision-weighting of cardiac prediction errors.

## 2. Materials and methods

### 2.1. Ethics statement

The study from which the original dataset was derived (Zaccaro et al., 2024) was approved by the Institutional Review Board of the Department of Psychology at the "G. d'Annunzio" University of Chieti-Pescara, Italy (Protocol Number 44_26_07_2021_21016). The study adhered to the ethical guidelines of the Italian Association of Psychology and the Declaration of Helsinki, including its amendments. All participants provided their written informed consent and were unaware of the experimental aims prior to data collection.

### 2.2. Participants

Twenty-eight healthy volunteers (13 female; 1 left-handed; mean age: 27.88 ± 4.46 years) were analysed. Eligibility was determined based on self-reported criteria: (1) no personal or family history of psychiatric, neurological or somatic disorders; (2) no chronic or acute respiratory diseases; (3) no use of central nervous system-affecting substances in the previous week; and (4) no previous experience with mindfulness-based meditation or breath control practices. All participants were of normal weight and had normal or corrected-to-normal vision.

### 2.3. Experimental procedure

As described in Zaccaro et al. (2024), the tasks were administered using the E-Prime 3.0 software (Psychology Software Tools, Pittsburgh, PA, USA). Participants were seated comfortably in front of a computer screen positioned approximately 60 cm away for optimal keyboard use and screen visibility. Room lighting and noise levels were minimised, and the temperature was maintained at a comfortable level. Written instructions were presented before each task. The experimenter then ensured that participants understood the instructions well and invited them to ask questions if necessary. EEG, ECG and respiratory signals were continuously recorded throughout the experiment.

The resting-state condition was recorded first. Participants sat for 10 min resting with their eyes open, looking at a fixation cross in the centre of the screen and allowing their thoughts to wander without focusing on anything in particular. They were also instructed to breathe spontaneously.

The cardiac interoceptive task used was the heartbeat counting task (HCT) (Pollatos et al., 2005; Schandry and Weitkunat, 1986). Participants were given the following instructions, adapted from Desmedt et al. (2018): "*In this task, direct your attention to your heart and the associated physical sensations. You are required to sustain your focus on your heart for various durations and count the number of heartbeats you perceive. Begin silently counting when the heart symbol appears on the screen. When the heart symbol disappears, report the number of heartbeats you are sure you felt. Only report the number of heartbeats you are sure about, without trying to estimate your heart rate. During each trial, keep your eyes open, gaze at the screen and avoid moving. Refrain from guiding your responses by checking your pulse in your wrists or neck. Breathe spontaneously and avoid changing your breathing frequency or holding your breath*". The HCT consisted of three blocks of four randomised trials lasting 25, 35, 45 and 100 s (Ardizzi and Ferri, 2018; Di Lernia et al., 2018; Ueno et al., 2020), for a total of 12 trials. After each trial, participants reported the number of perceived heartbeats and rated their confidence (HCT confidence) on a 10-point Likert scale, ranging from 0 (very poor) to 9 (excellent). They did not receive any feedback on their performance.

The exteroceptive task used was the cardiac-tone counting task (C-TCT). Participants were presented with digitally generated heartbeat sounds and instructed to count and report the number of heartbeats they heard (Wiebking et al., 2015). The C-TCT consisted of three blocks of four randomised trials lasting 25, 35, 45 and 100 s. The heartbeat sounds were presented at irregular intervals, with an average frequency of 60 bpm. After each trial, participants reported the number of heartbeats they heard and rated their confidence (C-TCT confidence). Before starting the experiment, participants completed a short training session and verbally confirmed that they could not perceive their heartbeat through the breathing belt to ensure that it was not too tight.

### 2.4. Electrophysiological recording and pre-processing

Respiratory activity was recorded using a respiratory belt placed around the chest (Respiratory Transducer TSD201, BIOPAC Systems Inc, Goleta, CA, USA). EEG signals were recorded using a 64-channel BrainAmp MR EEG system (BrainCap, BrainVision LLC, Garner, NC, USA) with electrodes positioned according to the International 10–20 system. Electrode impedance was kept below 10 kΩ for all channels. The ECG was recorded using three electrodes: two placed over the left costal margin and the right clavicle, with the ground electrode placed over the right costal margin (MP160, BIOPAC Systems Inc, Goleta, CA, USA). Three additional backup electrodes were integrated into the EEG recording system via an external electrode input box (BrainProducts GmbH, BrainVision LLC, Gilching, Germany) and placed over the left and right clavicles, with the ground at the left costal margin. The BrainAmp MR EEG, MP160 and TSD201 systems were synchronised with the E-Prime 3.0 software using a TriggerStation™ (BRAINTRENDS LTD 2010, Italy). All signals were sampled at 2.5 kHz with a 0.016 to 250 Hz bandpass filter and a 50 Hz notch filter. Signals were then filtered and down-sampled to 256 Hz.

Respiratory data were processed using custom MATLAB scripts (R2021a, MathWorks Inc, Natick, MA, USA). The respiratory signal was high-pass filtered at 0.1 Hz to remove baseline drift. Respiratory phases were detected using a validated method (Grund et al., 2022; Power et al., 2020; Zaccaro et al., 2024). Outliers exceeding three scaled median absolute deviations from the local median within a 1-s moving window were linearly interpolated with the adjacent values. Data were then smoothed with a 1-s window filter (Savitzky and Golay, 1964) and z-scored. Inhalation and exhalation onsets were identified as local minima (troughs) and maxima (peaks), respectively. Peaks and troughs had to be at least 2 s apart, and the minimum prominence of the interquartile range of the z-scored data was multiplied by a factor ranging from 0.3 to 0.8, depending on the participant's respiratory trace (Grund et al., 2022). A breath cycle was defined as the interval between successive inhalations (i.e. from one trough to the next).

EEG data were pre-processed using the EEGLAB toolbox (v2022.1; Delorme and Makeig, 2004). Data were filtered using a Hamming windowed FIR filter between 0.5 and 45 Hz (Al et al., 2020; 2021). EEG segments with poor signal quality were manually rejected. Independent component analysis (ICA) was performed to remove artefacts related to heartbeat, eye and muscle activity (FastICA; Hyvärinen, 1999). The ECG, respiratory channels and excessively noisy channels were excluded from the ICA decomposition. A few noisy channels (<5), typically peripheral and not known to contribute to heartbeat-evoked potential (HEP) generation (Coll et al., 2021), were identified. Independent components (ICs) were rejected based on IC time series, scalp maps, and power spectra (Delorme and Makeig, 2004). Special attention was given to the cardiac field artifact (CFA) and the pulse-related artifact (PA) as they significantly affect HEP activity (Coll et al., 2021). ICs contaminated by CFA and PA were identified by plotting R-peaks over IC time series, and ICs with activation time-locked to the ECG R-peak were removed (Zaccaro et al., 2024). The number of ICs removed ranged from 1 to 6 ($3 \pm 1$ [mean ± SD]), with CFA-related ICs ranging from 0 to 3 ($1 \pm 1$ [mean ± SD]). After ICA, previously identified noisy channels were interpolated using adjacent electrodes (Junghöfer et al., 2000). The cleaned EEG signals were then referenced to the mean reference (Antonacci et al., 2023; Barà et al., 2023; Zaccaro et al., 2024) as recommended (Candia-Rivera et al., 2021). ECG R-peaks were identified using the HEPLAB toolbox (Perakakis, 2019), with manual correction of mis-detected peaks (Al et al., 2021; Zaccaro et al., 2022). EEG data were epoched from −2 to 2 s around each R-peak (Kern et al., 2013). Epochs were averaged within participants for each task and were further classified based on the respiratory phase in which the corresponding R-peak occurred. This resulted in four epoch bins: HCT inhalation and exhalation, and C-TCT inhalation and exhalation. The average number of heartbeats per participant (mean ± SD) was as follows: HCT – inhalation ($315.86 \pm 73.83$) and exhalation ($273.71 \pm 76.48$); C-TCT – inhalation ($334.82 \pm 52.12$) and exhalation ($297.96 \pm 53.01$). At the group level, a greater number of heartbeats was observed during inhalation than exhalation in both tasks, likely reflecting the higher heart rate (HR) during inhalation associated with respiratory sinus arrhythmia. This difference was significant for both HCT (inhalation vs. exhalation: $t_{27} = 3.00$, $p = 0.006$, $d = 0.57$) and C-TCT ($t_{27} = 3.33$, $p = 0.003$, $d = 0.63$).

### 2.5. Heartbeat-modulated cortical oscillations

Heartbeat-modulated cortical oscillations were calculated using the FieldTrip toolbox (version 20231025; Oostenveld et al., 2011) according to established procedures (Park et al., 2018). Time-frequency analysis was performed on the time-series data for each experimental condition. For each trial, we convolved the signal with a complex wavelet constructed by pointwise multiplying the real cosine and imaginary sine components at each frequency with a Hann taper. Both the data and the tapered wavelet were then Fourier transformed, and their element-wise

multiplication in the frequency domain, followed by an inverse Fourier transform, yielded the convolution in the time domain. A sliding window with a Hann taper was used, maintaining a constant number of cycles per time window for all frequencies (4 cycles per time window). Zero padding was applied to round the maximum trial length to the nearest power of 2. Power was then extracted from the resulting complex representation by computing the squared magnitude of the signal. Time-frequency analysis was performed on each EEG channel from 1 Hz to 45 Hz, with a step size of 0.5 Hz, and from −1.5 s to 2 s after the R-peak, with steps of 0.01 s. The mean power value of the pre-R-peak time window (−300 ms to −100 ms) was designated as the baseline and used to normalise the post-R-peak power values in each frequency bin (relative heartbeat-modulated power; Park et al., 2018). This baseline normalisation was intended to prevent smearing of post-R-peak activity into baseline and to mitigate the potential influence of CFA around the ECG P-wave (Park et al., 2018).

To compute heartbeat-modulated inter-trial coherence (ITC), we first normalised the complex Fourier coefficients by their magnitude to focus on the phase information. To derive the average ITC, the resulting phase information was summed and normalised by the number of trials. ITC reflects the consistency of phase across multiple trials at different times and frequencies, with values ranging from 0 to 1, with higher values indicating more consistent phase alignment across trials. Similar to power values, we used the baseline window to normalise ITC values (relative heartbeat-modulated ITC; Park et al., 2018). To remove components reflecting PA and its harmonics, we excluded frequency bands below 4 Hz (Kern et al., 2013; Park et al., 2018).

To extract the heartbeat-modulated functional connectivity (FC), we computed the complex Fourier spectra from 1 Hz to 45 Hz (all settings were the same as for power calculation). Fourier spectra were calculated between −300 and −100 ms before the R-peak (baseline) and between 300 and 600 ms after the R-peak (active period of heartbeat effects; Liuzzi et al., 2024; Zaccaro et al., 2024). The imaginary part of coherency (iCOH) was used as a measure of undirected FC between electrodes in the sensor space, resulting in a connectivity matrix between all pairs of electrodes. The iCOH suppresses spurious coherence due to electromagnetic field propagation, which is indicated by zero-phase synchronisation between sensors (Nolte et al., 2004). We hypothesised that FC would change in the theta (4–8 Hz) and alpha (8–13 Hz) bands, according to previous studies (Fló et al., 2024; Kern et al., 2013; Kim and Jeong, 2019). Correlation matrices were calculated across trials, resulting in a correlation matrix for each participant, task (HCT and C-TCT), cardiac time window (baseline and active), respiratory phase (inhalation and exhalation), and frequency band (alpha and theta). To assess heartbeat-modulated FC, we calculated the ratio of connectivity during the active cardiac time window to that of the baseline cardiac time window (relative heartbeat-modulated FC).

To extract undirected graph theory metrics, we thresholded the iCOH matrices using a proportional threshold that preserves a percentage of the strongest matrix weights (Perl et al., 2019). In graph theory, a network is represented by nodes (each EEG channel) and edges indicating the strength of the connection (the iCOH values for each pair of EEG channels). We used six incremental thresholds ranging from 5 % to 30 % as cutoffs (e.g., a threshold of 5 % means that out of 100 nodes, each node is connected to five other nodes on average) (Perl et al., 2019). All edges that did not reach the threshold were removed. We extracted the following network connectivity measures for each participant, threshold, task, cardiac time window, respiratory phase, and frequency band using the brain connectivity toolbox (Rubinov and Sporns, 2010): i) density: the ratio of current connections to all possible connections, reflecting the overall interconnectivity of the network; ii) clustering coefficient: the ratio of triangles formed around each node, illustrating the degree of dense interconnectivity among neighbouring nodes; iii) global efficiency: a measure of network integration that reflects the network's ability to facilitate long-range information transfer; and iv) local efficiency: a measure of the network's capacity to support short-range information transfer and its resilience to incremental disconnections.

### 2.6. Statistical analyses of heartbeat-modulated cortical oscillations

Changes in heartbeat-modulated cortical oscillations were assessed using the FieldTrip toolbox (v.20231025; Oostenveld et al., 2011). The analysis focused on the cluster mass rather than individual electrodes or time points. Initially, spatial (neighbouring channels) and temporal (adjacent time points) points with a p-value below 0.05 were included in a cluster. A cluster statistic was calculated by summing the t-values within each cluster. The null distribution was estimated by Monte Carlo permutations, with condition labels randomly shuffled 5000 times. The largest cluster-level statistic from each randomisation was included in the null distribution. Statistical significance was determined by comparing the experimentally observed cluster-level statistics with the randomly generated null distribution. Clusters exceeding the $1 - \alpha$ percentile of this distribution (two-tailed) were considered significant. The minimum number of adjacent channels required to form a cluster was set to 2. To test for interaction effects, we used the permutation of residuals method (Anderson and Ter Braak, 2003; Still and White, 1981; Winkler et al., 2014). For instance, to test the 2 × 2 interaction (task × respiratory phase), we calculated the difference between the two levels of phase for each level of task and conducted paired cluster-based permutation *t*-tests comparing difference values (HCT-exhalation minus HCT-inhalation vs. C-TCT-exhalation minus C-TCT-inhalation). Based on Zaccaro et al. (2024), tests were performed at each electrode and time point for the whole late time window (300–600 ms) following the R-peak. We tested each frequency band of interest separately, averaging over their respective frequency bins: theta (4–8 Hz), alpha (8–13 Hz), beta (13–30 Hz), and low-gamma (30–45 Hz). We excluded external electrodes (F7, F8, FT7, FT8, T7, T8, TP7, TP8, P7, P8, PO7, PO8, O1, O2, Oz, TP9, and TP10), which are prone to noise contamination, in line with a recent meta-analysis (Coll et al., 2021). Cluster-based permutation *t*-tests were conducted on the time-frequency data, with heartbeat-modulated power and ITC values as dependent variables. Even in the absence of significant task × phase interactions, we conducted exploratory planned comparisons to specifically test exhalation versus inhalation differences within each task (HCT: exhalation versus inhalation; C-TCT: exhalation versus inhalation), as motivated by our previous findings (Zaccaro et al., 2024). As cluster-based permutation testing intrinsically controls for multiple comparisons across the time × electrode space, we applied an additional Benjamini-Yekutieli false discovery rate (FDR) correction only across the theta and alpha frequency bands, which constituted our a priori hypotheses. Importantly, as respiratory-phase effects were theoretically expected only during interoceptive processing (HCT), FDR correction was restricted to these two planned contrasts (HCT exhalation vs. inhalation for alpha; HCT exhalation vs. inhalation for theta). Analyses in the beta and gamma bands, as well as all comparisons within the C-TCT, were conducted for completeness but were considered exploratory and therefore not corrected for multiple comparisons. An overview of the decision framework for omnibus tests, clustering procedures, and multiple-comparison corrections across all analysis families is provided in Supplementary Table 1.

To examine the interaction effects between tasks and respiratory phases on heartbeat-modulated FC, we applied the same permutation-of-residuals method used for power and ITC. We excluded from the FC analysis the same external electrodes omitted in the power and ITC analyses, as they are particularly susceptible to noise contamination. Relative iCOH values between electrode pairs for each frequency band (theta and alpha) were used as the dependent variable. Planned permutation-based *t*-tests were performed for both the theta and alpha bands, comparing HCT exhalation vs. HCT inhalation, and C-TCT exhalation vs. C-TCT inhalation. Significance was assessed using a single-threshold permutation test for the maximum t-statistics (5000

permutations). Connectivity values showing a significant effect with a p-value $\leq 0.01$ (uncorrected) were used to construct symmetric connectivity matrices for theta and alpha using the BrainNet Viewer toolbox (Xia et al., 2013).

Undirected graph connectivity metrics were analysed using a series of linear mixed-effects models (LMEMs), implemented in jamovi (v2.3.21; GAMLj module; Gallucci, 2019) with restricted maximum likelihood (REML) estimation. Separate models were estimated for the theta and alpha frequency bands. Fixed factors included task (HCT, C-TCT), respiratory phase (inhalation, exhalation), cardiac time window (baseline, active), and threshold (5 %, 10 %, 15 %, 20 %, 25 %, 30 %). Degrees of freedom were estimated using the Satterthwaite method. For each graph-theory metric, the full model included a three-way interaction (task × time × phase), with subject-specific random intercepts and random slopes for the interaction terms. Even in the absence of a significant three-way interaction, we conducted exploratory planned contrasts to probe condition-specific effects that may not be detectable at the omnibus level. Planned pairwise *t*-tests were computed separately for each task and respiratory phase. To control for multiple comparisons, we applied FDR correction across the eight planned contrasts within each frequency band (four contrasts in HCT and four in C-TCT, considered separately for the alpha and theta bands). Specifically, we tested the following comparisons: (i) baseline inhalation versus baseline exhalation, (ii) active inhalation versus active exhalation, (iii) baseline versus active during inhalation, and (iv) baseline versus active during exhalation, each assessed within both the HCT and C-TCT.

### 2.7. Correlational and mixed-effects analyses of heartbeat-modulated EEG activity and interoceptive performance

Based on prior research (Crivelli and Balconi, 2025; Kritzman et al., 2022; Luft and Bhattacharya, 2015; Mccraty et al., 2009; Rominger et al., 2025; Villena-González et al., 2017), we assessed relationships between changes in HEP amplitude across respiratory phases and corresponding differences in heartbeat-modulated alpha power during HCT. Single-trial epochs around each R peak (from −300 to 600 ms) were filtered between 0.5 and 3 Hz (Studenova et al., 2023). To assess the spatial overlap between the distributions of significant heartbeat-modulated alpha power and HEP amplitude changes across respiratory phases, a full-scalp cluster-based permutation *t*-test was performed, using HEP amplitude as the dependent variable, comparing inhalation and exhalation in the late time window (300–600 ms after the R-peak; Zaccaro et al., 2024). HEP amplitude and heartbeat-modulated alpha power values were averaged for each participant, and Δ values between respiratory phases were extracted. Mean values were obtained by averaging across the time windows that previously showed significant power differences between respiratory phases. We computed Spearman's rho and p-values for each channel ($\alpha = 0.05$, two-tailed) by correlating participant-level mean heartbeat-modulated Δalpha power with the corresponding mean ΔHEP values. We applied the FDR correction procedure to control for multiple comparisons across channels. The analysis was repeated for other frequency bands during both HCT and C-TCT, and we also assessed correlations between ΔHEP amplitude and ΔITC, as well as between Δpower and ΔITC across all frequency bands. Finally, we examined correlations between HEP, power, and ITC across all frequency bands during HCT and C-TCT by analysing their absolute values, rather than Δ values. We then computed the instantaneous group-level correlation between Δalpha power and the corresponding ΔHEP values for each time point and frequency bin, yielding a time-frequency representation of Spearman's rho and p-values ($\alpha = 0.05$, two-tailed). The analysis focused on channels that had previously shown a significant participant-level correlation between ΔHEP amplitude and Δalpha power. We compared instantaneous correlations between HCT and C-TCT by applying Fisher's z-normalization to Spearman's rho values averaged across the previously selected channels. Statistical significance at each time point was determined using the cumulative distribution function of the standard normal distribution to evaluate the probability of observing extreme z-differences under the null hypothesis. We applied the FDR correction procedure to control for multiple comparisons across time points.

To examine the relationships between HCT/C-TCT trial-level changes in HEP, heartbeat-modulated power and ITC across respiratory phases, as well as their associations with accuracy and cardiac physiology, we applied multiple LMEMs. For each HCT and C-TCT trial (12 trials per participant per task), we computed the changes across respiratory phases (Δ) in HEP, heartbeat-modulated power, and ITC within the alpha band, along with accuracy and confidence. HCT/C-TCT trial-level Δ values were derived by first extracting the mean values from significant channels and time windows during exhalation and inhalation and then calculating the Δ (exhalation minus inhalation). To account for the influence of cardiac physiology, we also computed ΔHR, which was derived by subtracting the HCT/C-TCT trial-level mean HR during inhalation from that during exhalation.

As an additional control, we modelled instantaneous HR as a covariate in the LMEMs to quantify its contribution to heartbeat-modulated power. Heartbeat-modulated alpha and theta power were computed on a trial-by-trial basis by averaging the significant channels and time points identified in the group-level contrasts. Specifically, we extracted heartbeat-modulated alpha power from the task × respiratory-phase interaction, and heartbeat-modulated alpha and theta power from the exhalation–inhalation contrast during the HCT.

All LMEMs were implemented using the GAMLj module in jamovi (v2.3.21; the jamovi project, 2022; Gallucci, 2019), with REML estimation. For each analysis, we started from a model with the full fixed-effects structure dictated by our experimental design and an initially maximal random-effects structure (random intercepts and slopes). We then simplified the random-effects structure in a stepwise manner by iteratively removing random components that either led to non-convergence or did not improve model fit (as assessed by a reduction of the Akaike information criterion, AIC). The final models retained the full fixed-effects structure and a parsimonious random-effects structure that ensured convergence and adequate fit. The dependent variables were z-scored prior to modelling, and the instantaneous HR covariate was z-scored within participants (clusterwise centering) to preserve within-subject variability. Degrees of freedom were estimated using the Satterthwaite method. For each parameter of the best-fitting model, we reported the estimated coefficient (b), standard error (SE), 95 % confidence intervals, t-statistic, and p-value.

## 3. Results

### 3.1. Main findings

#### 3.1.1. Task- and respiratory phase–dependent changes in heartbeat-modulated power

Following an eyes-open resting-state condition, participants engaged in tasks requiring either cardiac interoceptive (heartbeat counting task - HCT) or exteroceptive (cardiac-tone counting task - C-TCT) attention. We performed a full-scalp cluster-based permutation test using heartbeat-modulated power as the dependent variable and task (HCT vs. C-TCT), respiratory phase (inhalation vs. exhalation), and their interaction as within-participant factors. The test revealed a significant task × phase interaction in the alpha band from 300 to 600 ms over electrodes C4, C6, CP4, and CP6 ($t_{27} = 3.165$, $p_{clust} = 0.037$, $d = 0.598$; Fig. S1A), but no interaction in the theta band ($t_{27} = 1.933$, $p_{clust} = 0.14$, $d = 0.365$). The interaction was explained by planned *t*-test, which showed significantly higher heartbeat-modulated alpha power during HCT from 391 to 600 ms over FCz, FC2, FC4, Cz, C2, C4, C6, CP2, CP4, and CP6 ($t_{27} = 3.049$, $p_{clust} = 0.039$, $p_{FDR} = 0.039$, $d = 0.576$; Fig. 1A) during exhalation compared to inhalation. Despite the absence of a significant task × phase interaction in the theta band, an exploratory planned comparison (see Section 2.6) revealed increased heartbeat-

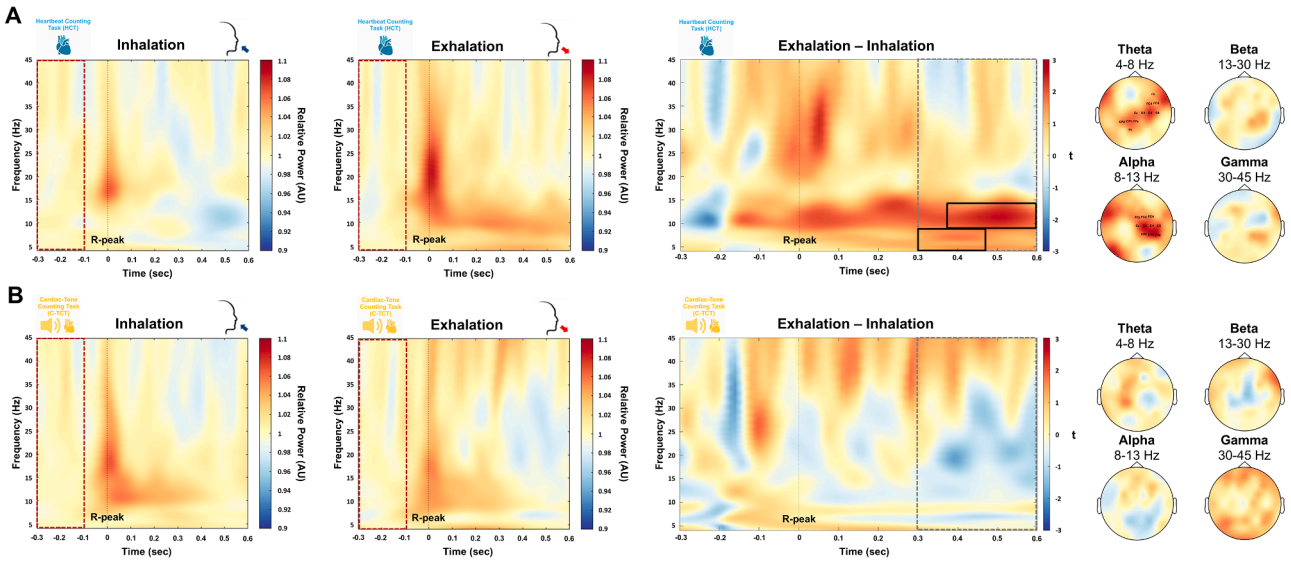



**Fig. 1.** Heartbeat-modulated power changes across respiratory phases and tasks. (A) Grand-averaged heartbeat-modulated power in the heartbeat counting task during inhalation (left), exhalation (middle), and the exhalation-minus-inhalation difference (right). The black rectangle marks significant differences between exhalation and inhalation (cluster-corrected). Topographical distributions illustrate differences, with labels indicating significant electrodes. (B) Grand-averaged heartbeat-modulated power in the cardiac-tone counting task during inhalation (left), exhalation (middle), and the exhalation-minus-inhalation difference (right). The red dotted area represents the baseline window (−300 to −100 ms relative to R-peak onset). The grey dotted area marks the temporal window of interest for statistical analysis (300–600 ms after the R-peak). Abbreviations: AU = arbitrary unit.

modulated theta power during exhalation than inhalation from 300 to 469 ms after the R-peak over F6, FC4, FC6, Cz, C2, C4, C6, CP3, CP1, CPz, CP2, and P1 ($t_{27} = 3.896$, $p_{clust} = 0.039$, $p_{FDR} = 0.039$, $d = 0.736$). No significant interaction was observed in other frequency bands, which were exploratory and are reported for completeness (beta: $t_{27} = 1.714$, $p_{clust} = 0.122$, $d = 0.324$; gamma: $t_{27} = -0.525$, $p_{clust} = 0.276$, $d = 0.099$). No significant differences were found between respiratory phases for beta ($t_{27} = 0.793$, $p_{clust} = 0.343$, $d = 0.149$) or gamma ($t_{27} = -1.375$, $p_{clust} = 0.264$, $d = 0.259$) bands. During C-TCT, we found no change in heartbeat-modulated power between exhalation and inhalation in any of the investigated frequency bands (theta: $t_{27} = 0.261$, $p_{clust} = 1$, $d = 0.049$; alpha: $t_{27} = -0.448$, $p_{clust} = 1$, $d = 0.085$; beta: $t_{27} = -2.661$, $p_{clust} = 0.09$, $d = 0.503$; gamma: $t_{27} = 1.659$, $p_{clust} = 0.052$, $d = 0.314$; Fig. 1B). A subsampling-based sensitivity analysis confirmed that the observed task-by-phase effects were not driven by differences in heartbeat counts across respiratory phases (see Supplementary Material 1). These results suggest that heartbeat-modulated alpha and theta power only increase during exhalation when attention is focused on internal cardiac signals. By contrast, no respiratory phase-dependent modulation emerged during the exteroceptive task. Additional analyses showed that the phase-dependent effects on heartbeat-modulated alpha power were not influenced by gender (see Supplementary Material 2 and Supplementary Fig. 5D).

### 3.1.2. Task- and respiratory phase–dependent changes in heartbeat-modulated inter-trial coherence

We performed a full-scalp cluster-based permutation test using heartbeat-modulated inter-trial coherence (ITC) as the dependent variable and task (HCT vs. C-TCT), respiratory phase (inhalation vs. exhalation), and their interaction as within-participant factors. No significant task × phase interaction was observed for ITC in any of the frequency bands (theta: $t_{27} = 0.129$, $p_{clust} = 0.132$, $d = 0.024$; alpha: $t_{27} = 2.104$, $p_{clust} = 0.072$, $d = 0.398$; beta: $t_{27} = 0.934$, $p_{clust} = 0.432$, $d = 0.177$; gamma: $t_{27} = 2.223$, $p_{clust} = 0.347$, $d = 0.421$; Fig. S1B). We conducted exploratory planned comparisons to specifically test exhalation versus inhalation differences within the HCT in theta and alpha bands (see Section 2.6). We found a significant increase in alpha-band heartbeat-modulated ITC during exhalation compared to inhalation from 422 to 559 ms after the R-peak over C2, C4, CP2, CP4, and CP6 ($t_{27} = 3.238$, $p_{clust} = 0.023$, $p_{FDR} = 0.046$, $d = 0.612$; Fig. 2A), but no changes in the theta band ($t_{27} = 0.229$, $p_{clust} = 1$, $p_{FDR} = 1$, $d = 0.043$). For completeness, we also report a significant increase in gamma band ITC from 441 to 469 ms over C3, C5, CP3, CP5, and P5 ($t_{27} = 3.825$, $p_{clust} = 0.038$, $d = 0.723$). However, this effect was brief (28 ms) and localized over electrodes not typically associated with cardiac interoception (Coll et al., 2021). No significant ITC differences between respiratory phases were found for the other frequency bands (beta: $t_{27} = 0.629$, $p_{clust} = 0.345$, $d = 0.119$). Similarly, no phase-related ITC changes were observed during the C-TCT across all frequency bands (theta: $t_{27} = 0.013$, $p_{clust} = 1$, $d = 0.003$; alpha: $t_{27} = 0.256$, $p_{clust} = 0.186$, $d = 0.048$; beta: $t_{27} = -0.669$, $p_{clust} = 1$, $d = 0.127$; gamma: $t_{27} = 0.324$, $p_{clust} = 0.289$, $d = 0.061$; Fig. 2B). These tests were exploratory and uncorrected for multiple comparisons, and are reported for completeness. A subsampling-based sensitivity analysis confirmed that the observed phase effects were not driven by differences in heartbeat counts across respiratory phases (see Supplementary Material 1). Overall, heartbeat-modulated ITC was selectively shaped by respiratory phase in the alpha range during interoceptive attention, while no corresponding modulation was observed during the exteroceptive task.

### 3.1.3. Heartbeat-modulated oscillations and heartbeat-evoked potentials

We assessed the spatial overlap between the distributions of significant heartbeat-modulated alpha power and heartbeat-evoked potential (HEP) amplitude changes across respiratory phases (Δalpha power and ΔHEP). As previously reported (Zaccaro et al., 2024), significant ΔHEP changes were localized to right centro-frontal electrodes (AFz, F1, Fz, F2, F4, FC1, FCz, FC2, FC4, C1, Cz, C2, and C4) from 360 to 528 ms after the R-peak ($t_{27} = 3.29$, $p_{clust} = 0.016$, $d = 0.621$; Fig. 3A). Although ΔHEP differences occurred in more anterior regions of the scalp compared to the more central Δalpha power differences (same cluster as in Section 3.1.1; Fig. 3B), both distributions converged spatially in fronto-central areas, slightly lateralized to the right hemisphere. To statistically quantify this relationship, we computed Spearman's correlation between participant-level mean heartbeat-modulated Δalpha power with the corresponding mean ΔHEP values within the late significant time window of heartbeat-modulated power effects (390–600

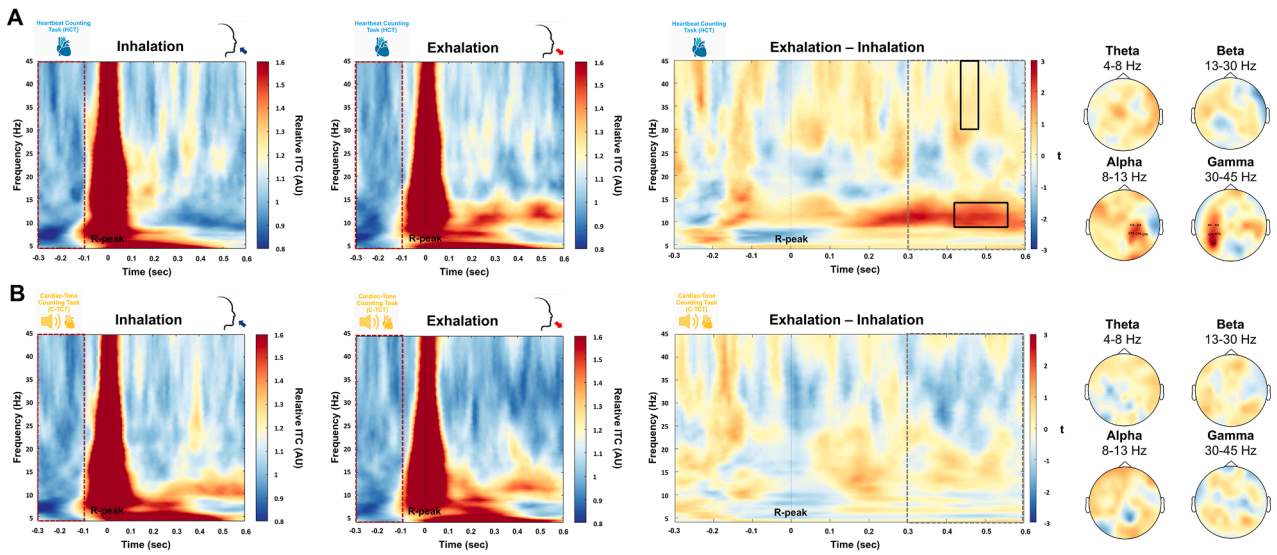



**Fig. 2.** Heartbeat-modulated inter-trial coherence changes across respiratory phases and tasks. (A) Grand-averaged heartbeat-modulated inter-trial coherence in the heartbeat counting task during inhalation (left), exhalation (middle), and the exhalation-minus-inhalation difference (right). The black rectangle marks significant differences between exhalation and inhalation (cluster-corrected). Topographical distributions illustrate differences, with labels indicating significant electrodes. (B) Grand-averaged heartbeat-modulated inter-trial coherence in the cardiac-tone counting task during inhalation (left), exhalation (middle), and the exhalation-minus-inhalation difference (right). The red dotted area represents the baseline window (−300 to −100 ms relative to R-peak onset). The grey dotted area marks the temporal window of interest for statistical analysis (300–600 ms after the R-peak). Abbreviations: ITC = inter-trial coherence, AU = arbitrary unit.

ms after the R-peak). A significant positive correlation was found over frontal electrodes (Fig. 3C), including AFz (rho = 0.519, $p_{FDR}$ = 0.044), AF3 (rho = 0.521, $p_{FDR}$ = 0.044), AF4 (rho = 0.522, $p_{FDR}$ = 0.044), F4 (rho = 0.577, $p_{FDR}$ = 0.038), and Fz (rho = 0.573, $p_{FDR}$ = 0.038). A negative correlation was also observed over channel P6 (rho = −0.512, $p_{FDR}$ = 0.044). When examining correlations between ΔHEP amplitude and heartbeat-modulated Δpower in other frequency bands during both HCT and C-TCT, no significant results were found, confirming that the effects were specific to the alpha band during HCT. Additionally, no significant correlations were observed between ΔHEP amplitude and ΔITC, nor between Δpower and ΔITC across any frequency band in either task (during HCT or C-TCT). Further details on the Spearman's rho values across tasks, frequencies, and electrodes are provided in the supplementary material (Supplementary Table 2). Finally, no correlations were found between HEP, power, or ITC in any frequency band when analysing their absolute values recorded separately for inhalation and exhalation in either task (Supplementary Table 3).

We then computed the instantaneous group-level Spearman's correlation between heartbeat-modulated Δpower and the corresponding ΔHEP values for each time point and frequency band, averaged across the previously identified channels (AFz, AF3, AF4, F4, and Fz), during both the HCT and C-TCT tasks. A significant correlation emerged in the alpha band exclusively during HCT, within a late time window from 422 to 600 ms post-R-peak (Fig. 3D, E, Supplementary Tables 4–5). We compared instantaneous correlations between HCT and C-TCT by applying Fisher's z-transformation to Spearman's rho values averaged across the previously selected channels in the alpha band. This analysis revealed significantly stronger correlations for HCT relative to C-TCT between 512 and 600 ms post-R-peak (Fig. 3F, Supplementary Table 6). Together, these findings indicate that the coupling between ΔHEP amplitude and heartbeat-modulated Δalpha power is selectively enhanced during cardiac interoceptive attention.

### 3.1.4. *Heartbeat-modulated oscillations and task accuracy*

To examine the relationship between HCT trial-level changes in HEP and heartbeat-modulated alpha power and ITC across respiratory phases, as well as their associations with accuracy, we applied multiple linear mixed-effects models (LMEMs). Following previous studies (Fló et al., 2024; Park et al., 2018), we first tested the relationship between changes in heartbeat-modulated alpha power and ITC across respiratory phases and confirmed that no significant relationship was found between the two measures ($b$ = 0.022, SE = 0.056, CI 95 % = [−0.087 0.132], $t$ = 0.399, $p$ = 0.69). Using ΔHEP as the dependent variable, the model revealed a significant interaction between Δalpha power and Δalpha ITC ($b$ = 0.118, SE = 0.056, CI 95 % = [0.008 0.229], $t$ = 2.096, $p$ = 0.037; Fig. 3G), suggesting that Δalpha power moderates the effects of Δalpha ITC on ΔHEP. A simple effects analysis of the interaction indicated a significant relationship between Δalpha ITC and ΔHEP only when Δalpha power was high (mean + 1SD: $b$ = 0.18, SE = 0.079, CI 95 % = [0.026 0.335], $t$ = 2.294, $p$ = 0.023). No main effects were observed for Δalpha power or Δalpha ITC. Notably, no significant effects involving ΔHR were found ($b$ = 0.015, SE = 0.059, CI 95 % = [−0.101 0.132], $t$ = 0.258, $p$ = 0.797). Full details on model selection, parameter estimates, and simple-effects results are provided in Supplementary Tables 7, 8, and 9, respectively.

When we used the HCT trial-level accuracy as the dependent variable, the model revealed a significant three-way interaction between ΔHEP, Δalpha power, and confidence ($b$ = 0.084, SE = 0.032, CI 95 % = [0.021 0.147], $t$ = 2.603, $p$ = 0.009; Fig. 3H), indicating that changes in alpha power and confidence together moderated the effect of ΔHEP on task accuracy. Simple effects analysis showed a significant relationship between ΔHEP and accuracy only when both Δalpha power and confidence were high (mean + 1SD: $b$ = 0.129, SE = 0.052, CI 95 % = [0.028 0.232], $t$ = 2.503, $p$ = 0.013). Additionally, significant main effects were observed for confidence ($b$ = 0.352, SE = 0.077, CI 95 % = [0.202 0.503], $t$ = 4.578, $p$ < 0.001) and Δalpha power ($b$ = −0.064, SE = 0.031, CI 95 % = [−0.126 −0.003], $t$ = −2.041, $p$ = 0.042) on accuracy. No other main effects or significant interactions were found. Notably, no effect of ΔHR on accuracy ($b$ = 0.029, SE = 0.044, CI 95 % = [−0.056 0.115], $t$ = 0.686, $p$ = 0.493) was found (Fig. 3I). Full details on model selection, parameter estimates, and simple-effects results are provided in Supplementary Tables 10, 11, and 12, respectively. A schematic of predictors and interactions during HCT is presented in Supplementary Figures 7A-8A.

Performing an LMEM for C-TCT with ΔHEP as the dependent variable was not feasible due to insufficient random coefficient variance. A

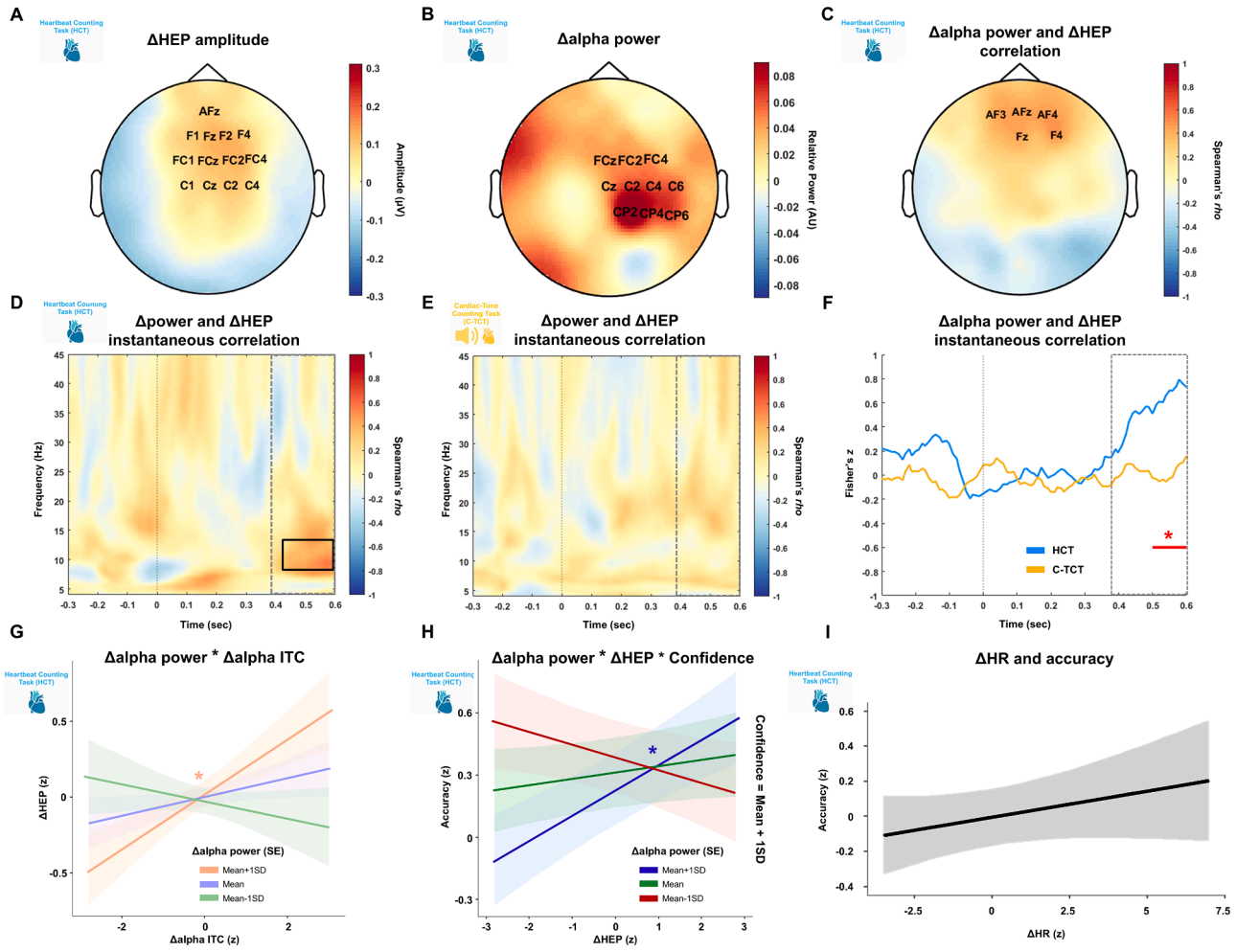



**Fig. 3.** Relationships between heartbeat-modulated cortical oscillations, heartbeat-evoked potentials, and task performance. (A) Topographical distribution of HEP differences between exhalation and inhalation during HCT. (B) Topographical distribution of heartbeat-modulated alpha power differences between exhalation and inhalation during HCT. (C) Topographical distribution of the Spearman correlation between ΔHEP and Δalpha power across channels during HCT. Labels indicate significant electrodes. (D–E) Time–frequency representations of the instantaneous Spearman correlation between Δpower and ΔHEP during HCT (D) and the C-TCT (E). The grey dotted region marks the temporal window of interest for statistical analysis (390–600 ms post R-peak), and the black rectangle indicates significant differences (FDR-corrected). (F) Fisher's z-transformed instantaneous Spearman correlation values (alpha band) comparing HCT and C-TCT. Asterisks indicate significant differences (*$p < 0.05$, FDR-corrected). (G) Linear mixed-effects model showing that the relationship between Δalpha ITC and ΔHEP was moderated by Δalpha power during HCT. Asterisks indicate significant effects (*$p < 0.05$). (H) Linear mixed-effects model demonstrating that the interaction between Δalpha power, ΔHEP, and confidence predicted interoceptive accuracy during HCT. (I) Linear mixed-effects model showing that changes in heart rate (ΔHR) did not predict interoceptive accuracy during HCT. Abbreviations: HEP = heartbeat-evoked potential, ITC = inter-trial coherence, HCT = heartbeat counting task, C-TCT = cardiac-tone counting task, ECG = electrocardiogram, SD = standard deviation, SE = standard error, AU = arbitrary unit.

general linear model revealed no significant interaction between Δalpha power and Δalpha ITC ($b = -0.112$, SE = 0.062, CI 95 % = [−0.233 0.009], $t = -1.815$, $p = 0.071$), nor any main effects for Δalpha power ($b = 0.003$, SE = 0.058, CI 95 % = [−0.111 0.117], $t = 0.046$, $p = 0.964$) or Δalpha ITC ($b = 0.004$, SE = 0.058, CI 95 % = [−0.11 0.118], $t = 0.066$, $p = 0.947$). No role of ΔHR was observed ($b = 0.092$, SE = 0.057, CI 95 % = [−0.021 0.205], $t = 1.6$, $p = 0.111$). Finally, using the trial-level C-TCT accuracy as the dependent variable, the model indicated that only confidence ($b = 0.347$, SE = 0.093, CI 95 % = [0.165 0.528], $t = 3.737$, $p = 0.002$) significantly predicted task accuracy. Again, no role of ΔHR emerged ($b = 0.075$, SE = 0.064, CI 95 % = [−0.052 0.201], $t = 1.59$, $p = 0.251$). Full details on model selection and parameter estimates are provided in Supplementary Tables 13 and 14, respectively. A schematic of predictors and interactions during C-TCT is presented in Supplementary Figures 7B-8B.

Collectively, these results demonstrate selective coupling between HEPs and heartbeat-modulated alpha activity during interoceptive attention, particularly in the late post–R-peak interval. Importantly, these associations occurred exclusively within the alpha band, only during interoceptive attention, and were driven by respiratory phase–dependent differences and not by absolute amplitude changes. This pattern rules out trivial mathematical or preprocessing artifacts and points to a mechanism specific to the task and physiological state. Moreover, when confidence was high, heartbeat-modulated alpha power and HEPs predicted interoceptive accuracy, suggesting that the cortical processing of cardiac signals supports accurate perception of internal cardiac sensations during exhalation. Notably, HR did not explain these effects. Additional analyses on cardiac and respiratory contributions are presented in the following section.

### 3.2. *Control analyses addressing physiological and respiratory confounds*

#### 3.2.1. *Resting-state and task-level comparisons (without respiratory phase)*

To determine whether heartbeat-modulated cortical oscillations varied across respiratory phases during the resting-state, we conducted full-scalp cluster-based permutation tests comparing inhalation to

exhalation. Across all frequency bands, we found no significant differences in heartbeat-modulated power (theta: $t_{27} = 2.085$, $p_{clust} = 0.097$, $d = 0.394$; alpha: $t_{27} = 0.013$, $p_{clust} = 0.989$, $d = 0.003$; beta: $t_{27} = 0.089$, $p_{clust} = 0.929$, $d = 0.017$; gamma: $t_{27} = 2.12$, $p_{clust} = 0.15$, $d = 0.401$; Fig. S2A) or ITC (theta: $t_{27} = -0.915$, $p_{clust} = 0.369$, $d = 0.173$; alpha: $t_{27} = -2.381$, $p_{clust} = 0.096$, $d = 0.45$; beta: $t_{27} = 1.161$, $p_{clust} = 0.178$, $d = 0.219$; gamma: $t_{27} = 1.46$, $p_{clust} = 0.156$, $d = 0.276$; Fig. S2B). Similarly, when not accounting for respiratory phases (i.e., averaging heartbeats occurring during both inhalation and exhalation), we observed no significant differences between HCT and C-TCT in heartbeat-modulated power (theta: $t_{27} = 0.162$, $p_{clust} = 0.872$, $d = 0.031$; alpha: $t_{27} = -0.163$, $p_{clust} = 0.872$, $d = 0.031$; beta: $t_{27} = 0.718$, $p_{clust} = 0.108$, $d = 0.136$; gamma: $t_{27} = 0.129$, $p_{clust} = 0.899$, $d = 0.024$; Fig. S3A) or ITC (theta: $t_{27} = -1.4$, $p_{clust} = 0.174$, $d = 0.264$; alpha: $t_{27} = -2.28$, $p_{clust} = 0.215$, $d = 0.431$; beta: $t_{27} = 1.12$, $p_{clust} = 0.075$, $d = 0.212$; gamma: $t_{27} = 1.7$, $p_{clust} = 0.359$, $d = 0.322$; Fig. S3B). These findings suggest that heartbeat-modulated cortical oscillations are not linked to the respiratory cycles at rest. Furthermore, they suggest that cardiac interoceptive and exteroceptive attention tasks elicit similar changes in heartbeat-modulated power and ITC when respiratory phases are not taken into account.

### 3.2.2. Controlling for heart rate

To examine whether modulation of heartbeat-modulated responses varied as a function of cardiac physiology, we first assessed changes in instantaneous HR across tasks and respiratory phases. The LMEM revealed significant main effects of phase ($b = -0.338$, SE = 0.032, CI 95 % [–0.401 –0.275], $t = -10.45$, $p < 0.001$) and task ($b = 0.153$, SE = 0.051, CI 95 % [0.053 0.253], $t = 3.00$, $p = 0.006$), but no task × phase interaction ($b = 0.031$, SE = 0.032, CI 95 % [–0.032 0.094], $t = 0.96$, $p = 0.348$). Overall, HR was lower during exhalation than inhalation and during interoceptive relative to exteroceptive attention. Full details on model selection and parameter estimates are provided in Supplementary Tables 15 and 16, respectively.

We then quantified the extent to which instantaneous HR accounted for the task × phase modulation of heartbeat-modulated alpha power. The LMEM confirmed a significant task × phase interaction ($b = -0.040$, SE = 0.019, CI 95 % [–0.078 –0.003], $t = -2.11$, $p = 0.035$). No additional main effects or interactions reached significance, including HR ($b = -0.001$, SE = 0.007, CI 95 % [–0.015 0.012], $t = -0.21$, $p = 0.835$), task × HR ($b = -0.024$, SE = 0.014, CI 95 % [–0.050 0.003], $t = -1.75$, $p = 0.080$), phase × HR ($b = 0.005$, SE = 0.013, CI 95 % [–0.021 0.032], $t = 0.40$, $p = 0.691$), or the task × phase × HR interaction ($b = 0.044$, SE = 0.027, CI 95 % [–0.008 0.097], $t = 1.65$, $p = 0.099$). Full details on model selection and parameter estimates are provided in Supplementary Tables 17 and 18, respectively.

Finally, we estimated the contribution of instantaneous HR within the HCT, separately for the alpha and theta frequency bands. For theta power, the LMEM replicated the significant main effect of respiratory phase ($b = 0.027$, SE = 0.01, CI 95 % = [0.007 0.047], $t = 2.645$, $p = 0.008$). In contrast, neither the main effect of instantaneous HR ($b < 0.001$, SE = 0.007, CI 95 % = [−0.014 0.015], $t = 0.083$, $p = 0.934$) nor the phase × HR interaction ($b = -0.009$, SE = 0.015, CI 95 % = [−0.037 0.019], $t = -0.593$, $p = 0.553$) reached significance. For alpha power, the LMEM replicated the significant main effect of respiratory phase ($b = 0.038$, SE = 0.017, CI 95 % = [0.005 0.071], $t = 2.238$, $p = 0.025$). Again, neither the main effect of instantaneous HR ($b = -0.005$, SE = 0.014, CI 95 % = [−0.032 0.022], $t = -0.374$, $p = 0.709$) nor the phase × HR interaction ($b = 0.009$, SE = 0.024, CI 95 % = [−0.039 0.056], $t = 0.35$, $p = 0.726$) were significant. A detailed account of model selection procedures and full parameter estimates for both frequency bands is provided in Supplementary Tables 19–22. Taken together, these analyses show that although HR varies systematically across tasks and respiratory phases, such fluctuations do not account for the observed task × phase modulation of heartbeat-modulated power.

### 3.2.3. Controlling for the cardiac field artifact

We verified that changes in alpha and theta heartbeat-modulated power did not reflect an artificial increase induced by cardiac field artifact (CFA) changes by testing the interaction between tasks and respiratory phases on the time-frequency decomposed ECG signal, time-locked to the R-peak (Daoui et al., 2022; Tsutsumi et al., 2014). This was done using a repeated-measures, FDR-corrected two-tailed *t*-test within the time window and frequency bands where significant effects were observed. We first tested the task × phase interaction from 300 to 600 ms over the time-frequency decomposed averaged ECG signal and found no significant effects in either frequency band (theta: $t_{27} = -1.258$, $p_{FDR} = 0.11$, $d = 0.238$, CI 95 % = [–0.61 0.14]; alpha: $t_{27} = 1.043$, $p_{FDR} = 0.19$, $d = 0.197$, CI 95 % = [–0.18 0.57]; Fig. S4A). We then examined exhalation–inhalation differences in the time–frequency–decomposed averaged ECG signal within the time window corresponding to the significant heartbeat-modulated alpha effects observed during HCT and C-TCT (391–600 ms). Again, no significant effects were detected (HCT: $t_{27} = 0.442$, $p_{FDR} = 0.338$, $d = 0.084$, CI 95 % = [–0.29 0.45], Fig. S4B; C-TCT: $t_{27} = -1.037$, $p_{FDR} = 0.164$, $d = 0.196$, CI 95 % = [−0.57 0.18], Fig. S4C). Together, these null results indicate that the respiratory-phase effects observed in EEG power cannot be attributed to the CFA and instead reflect genuine neural modulation.

### 3.2.4. Breathing adjustments during interoceptive attention

To evaluate whether participants systematically adjusted their breathing during the interoceptive task, we extracted for each HCT trial the average respiratory rate and the inhalation–exhalation ratio (I/E ratio) across the full dataset. LMEMs were used to test within-task changes across trials and to examine whether these respiratory parameters predicted interoceptive accuracy and heartbeat-modulated alpha power and ITC. To avoid overparameterizing models that already included multiple higher-order interactions, respiratory rate and the I/E ratio were evaluated as independent predictors in separate LMEMs. Respiratory rate did not change over the course of the task (omnibus test: $F_{11,297} = 0.92$, $p = 0.52$), whereas the I/E ratio showed a significant modulation across trials (i.e., trial number) ($F_{11,297} = 3.78$, $p < 0.001$), increasing gradually from early to mid-blocks before returning to baseline levels toward the end (see Supplementary Table 23 and Supplementary Figure 5A). We next examined whether respiratory rate and I/E ratio predicted interoceptive accuracy, Δalpha power, or Δalpha ITC. Respiratory rate significantly predicted interoceptive accuracy ($F_{1,297} = 4.16$, $p = 0.042$), such that slower breathing was associated with higher accuracy (Supplementary Figure 5B). No effects of trial number ($F_{11,255} = 0.468$, $p = 0.922$) or trial × respiratory rate interaction emerged ($F_{11,255} = 0.949$, $p = 0.494$). The I/E ratio did not predict accuracy ($F_{1,269} = 0.002$, $p = 0.969$), nor did trial × I/E ratio interaction ($F_{11,258} = 0.974$, $p = 0.471$). For Δalpha power, neither respiratory rate ($F_{1,85} = 1.91$, $p = 0.171$), trial number ($F_{11,258} = 1.15$, $p = 0.326$), nor their interaction ($F_{11,268} = 1.08$, $p = 0.380$) were significant. Likewise, I/E ratio ($F_{1,172} = 0.340$, $p = 0.561$) and its interaction with trial number ($F_{11,272} = 1.172$, $p = 0.307$) did not predict Δalpha power. For Δalpha ITC, neither respiratory rate ($F_{1,74} = 0.075$, $p = 0.785$), trial number ($F_{11,260} = 0.465$, $p = 0.924$), nor their interaction ($F_{11,271} = 0.995$, $p = 0.451$) reached significance. Similarly, neither the main effect of the I/E ratio ($F_{1,21} = 3.612$, $p = 0.071$), nor its interaction with trial number ($F_{11,250} = 1.100$, $p = 0.362$) was significant. These analyses indicate that participants did not systematically slow their breathing over the course of the task, although the I/E ratio showed modest variation across trials. While lower respiratory rate was associated with higher interoceptive accuracy, such respiratory adaptations did not explain or attenuate the primary task- and phase-dependent effects reported in this study.

### 3.2.5. Respiratory bins and phase transitions

To examine whether heartbeat-modulated alpha power varies continuously across the respiratory cycle or shows abrupt changes at

phase transitions, we performed an analysis using a finer-grained representation of respiratory phase. For each breathing cycle in the interoceptive task (HCT), the interval between two consecutive inhalations was divided into four equidistant phase bins (90°), which were subsequently grouped into the following respiratory segments: exhalation-to-inhalation transition (315–45°), inhalation (45–135°), inhalation-to-exhalation transition (135–225°), and exhalation (225–315°). Heartbeat-modulated alpha power was extracted from the significant cluster identified in the exhalation vs. inhalation contrast and averaged across trials for each participant. A repeated-measures ANOVA with phase (four levels) as a within-subject factor replicated the significant main effect of Phase ($F_{3,81} = 3.18$, $p = 0.029$, $\eta^2 p = 0.105$). Post-hoc comparisons indicated that heartbeat-modulated alpha power during inhalation was significantly lower than during the inhalation-to-exhalation transition (mean difference = −0.062, SE = 0.022, $t_{27} = -2.89$, $p = 0.008$) and exhalation (mean difference = −0.070, SE = 0.024, $t_{27} = -2.93$, $p = 0.007$). All remaining comparisons were non-significant (Supplementary Figure 5C). This analysis confirmed that heartbeat-modulated alpha power varies systematically across the respiratory cycle, with a specific reduction during inhalation.

### 3.3. Exploratory analyses of network-level dynamics

#### 3.3.1. Heartbeat-modulated functional connectivity

We conducted an exploratory assessment of heartbeat-modulated functional connectivity (FC) between all pairs of electrodes, estimated for each participant, task, and respiratory phase, separately in the alpha and theta bands. We focused on these frequency bands because they showed significant modulation of heartbeat-modulated power and ITC between respiratory phases. We conducted permutation-based *t*-tests across the entire scalp, using the relative (i.e., active divided by baseline cardiac time window, see Section 2.5) imaginary part of coherency (iCOH) as the dependent variable, with task (HCT vs. C-TCT), respiratory phase (inhalation vs. exhalation) and their interaction as within-participant factors. The analysis revealed a significant task × phase interaction in the theta band over the parieto-occipital cortices, alongside a negative effect in frontal regions (Fig. S6A, Supplementary Table 24). Planned *t*-tests (see Section 2.6) indicated greater theta-band FC during HCT in exhalation compared to inhalation, predominantly lateralized to the right hemisphere, spanning from prefrontal to parieto-occipital areas (Fig. S6B, Supplementary Table 25). During C-TCT, while some theta-band FC increases were observed during exhalation relative to inhalation, these were accompanied by a marked reduction in connectivity in the right hemisphere (Fig. S6C, Supplementary Table 26). In the alpha band, we observed a significant task × phase interaction, which was most pronounced over the right frontal cortices (Fig. S6D, Supplementary Table 27). This effect was driven by a significant increase in FC between right frontal and central regions during exhalation compared to inhalation during HCT (Fig. S6E, Supplementary Table 28). On the other hand, during C-TCT, FC was significantly reduced during exhalation relative to inhalation, particularly over the right frontal and prefrontal regions (Fig. S6F, Supplementary Table 29).

We also ensured that any significant changes in iCOH did not represent an artificial increase in phase synchronisation caused by CFA. Following the procedure outlined in Kim et al. (2019), we tested whether the relative alpha and theta iCOH increased during exhalation compared to inhalation between the ECG and EEG electrodes that showed significant iCOH changes, using permutation-based dependent samples *t*-tests. Comparing relative iCOH between exhalation and inhalation during HCT revealed a significant increase between the ECG and F3 electrode in the theta band ($t_{27} = 1.07$, $p = 0.004$, $d = 0.2$, CI 95 % = [−0.19 0.59]), as well as between the ECG and Fpz electrode in the alpha band ($t_{27} = 1.85$, $p = 0.006$, $d = 0.35$, CI 95 % = [−0.05 0.75]). No significant changes in ECG connectivity were found during C-TCT. These results show that the widespread functional connectivity changes observed between respiratory phases were not attributable to CFA-related connectivity effects. In summary, heartbeat-modulated FC was selectively enhanced during exhalation when attention was directed inward (HCT), particularly in right-lateralized alpha and theta networks, highlighting a task-dependent reconfiguration of large-scale cortical networks.

#### 3.3.2. Heartbeat-modulated graph-theory metrics

To exploratorily assess heartbeat-modulated graph-theory metrics, we estimated a total of eight LMEMs across each frequency band (alpha, theta). Each model included the graph metric as the dependent variable and incorporated task, time, and respiratory phase, as well as their three-way interaction (task × time × phase) as fixed effects. Threshold was included as a fixed factor. All models included participant-specific random intercepts and random slopes for fixed effects (maximal random structure). Models were estimated separately for four graph metrics: density, clustering coefficient, global efficiency, and local efficiency. In the theta frequency band, beyond the expected main effect of the threshold factor, we observed a significant main effect of time (baseline vs. active cardiac time windows) across all four graph theory metrics (density: $b = 0.037$, SE = 0.015, $t = 2.402$, $p = 0.023$; clustering coefficient: $b = 0.039$, SE = 0.014, $t = 2.781$, $p = 0.009$; local efficiency: $b = 0.065$, SE = 0.023, $t = 2.834$, $p = 0.008$; global efficiency: $b = 0.048$, SE = 0.019, $t = 2.504$, $p = 0.019$; Fig. 4A-D, Supplementary Tables 30–33). This suggests that the heartbeat generally reduces connectivity in the theta band. Despite the three-way interaction between task, time, and phase was not significant ($b = 0.041$, SE = 0.062, $t = 0.664$, $p = 0.512$), exploratory planned *t*-tests (see Section 2.6) revealed a significant heartbeat-modulated reduction in network density during inhalation in HCT ($t = -3.566$, $p = 0.001$, $p_{FDR} = 0.010$), resulting in higher density during exhalation compared to inhalation in the active cardiac time window ($t = 2.672$, $p = 0.012$, $p_{FDR} = 0.050$; Fig. 4A, Supplementary Table 34). A similar pattern was observed for the clustering coefficient in HCT, where *t*-tests indicated a heartbeat-modulated reduction during inhalation ($t = -4.01$, $p < 0.001$, $p_{FDR} = 0.003$), leading to higher theta clustering coefficients during exhalation than inhalation in the active cardiac time window ($t = 2.383$, $p = 0.024$, $p_{FDR} = 0.096$; Fig. 4B, Supplementary Table 35), the latter reflecting a trend-level effect following FDR correction. Furthermore, both heartbeat-modulated local and global efficiency significantly decreased during inhalation in HCT (local efficiency: $t = -3.988$, $p < 0.001$, $p_{FDR} = 0.003$, Fig. 4C; global efficiency: $t = -3.793$, $p < 0.001$, $p_{FDR} = 0.005$, Fig. 4D, Supplementary Table 36–37). However, no significant differences were observed between inhalation and exhalation in the active cardiac time window (local efficiency: $t = 1.967$, $p = 0.059$; global efficiency: $t = 1.444$, $p = 0.160$).

In the alpha band, the heartbeat consistently induced a significant increase in alpha connectivity metrics (main effect of time for density: $b = -0.036$, SE = 0.007, $t = -4.72$, $p < 0.001$; clustering coefficient: $b = -0.034$, SE = 0.009, $t = -3.73$, $p < 0.001$; local efficiency: $b = -0.052$, SE = 0.013, $t = -4.11$, $p < 0.001$; global efficiency: $b = -0.041$, SE = 0.009, $t = -4.34$, $p < 0.001$, Supplementary Tables 38–41). Additionally, a significant main effect of task was observed, indicating higher alpha connectivity during HCT compared to C-TCT (density: $b = 0.056$, SE = 0.026, $t = 2.13$, $p = 0.043$; clustering coefficient: $b = 0.061$, SE = 0.029, $t = 2.06$, $p = 0.049$; local efficiency: $b = 0.096$, SE = 0.045, $t = 2.18$, $p = 0.038$; global efficiency: $b = 0.076$, SE = 0.032, $t = 2.35$, $p = 0.026$; as can be inferred from Fig. 4E–H, Supplementary Tables 38–41). Despite the three-way interaction between task, time, and phase was not significant ($b = 0.04$, SE = 0.039, $t = 1.55$, $p = 0.3$), exploratory planned *t*-tests (see Section 2.6) for graph density revealed a significant heartbeat-modulated increase in density during exhalation in HCT ($t = 2.82$, $p = 0.008$, $p_{FDR} = 0.035$), leading to higher alpha density at exhalation compared to inhalation within the active cardiac time window ($t = 2.497$, $p = 0.018$, $p_{FDR} = 0.050$; Fig. 4E, Supplementary Table 42). In contrast, during C-TCT, the heartbeat increased alpha density only during inhalation ($t = 3.188$, $p = 0.003$, $p_{FDR} = 0.028$) and

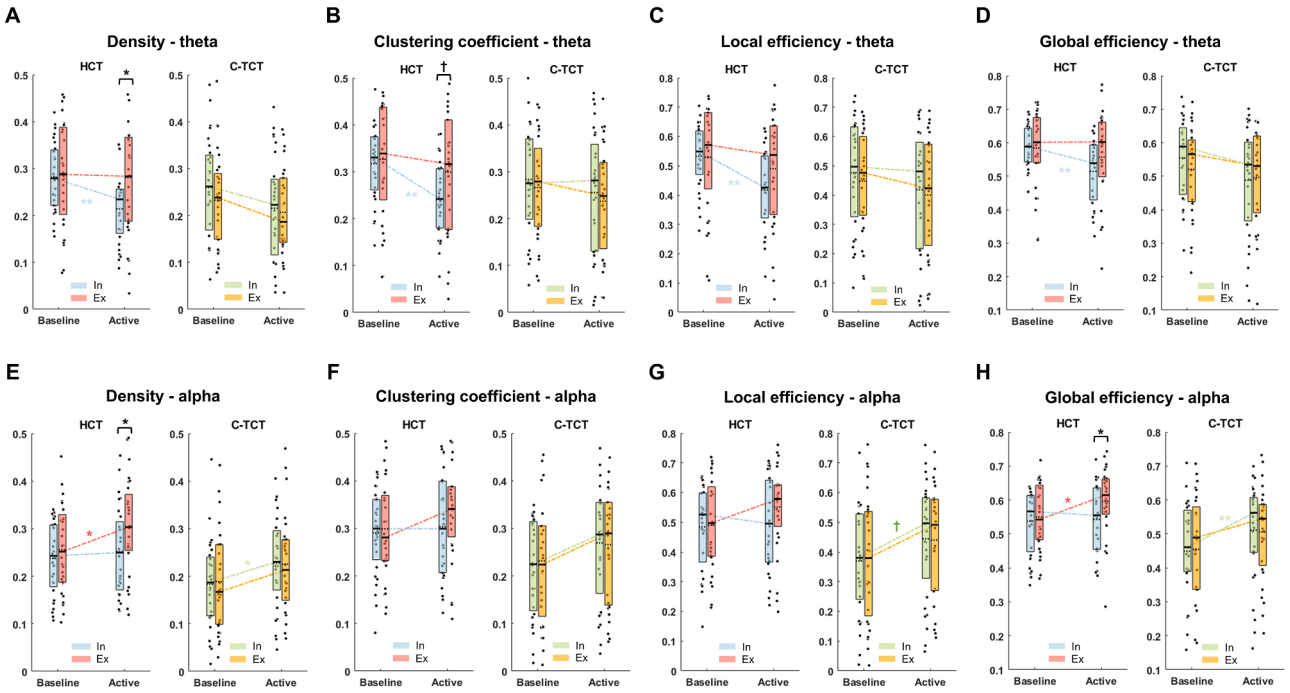



**Fig. 4.** Graph theory metrics across respiratory phases and tasks. Box plots displaying descriptive statistics for graph-theoretic metrics before (baseline) and after (active) the heartbeat during inhalation and exhalation in the heartbeat counting task and the cardiac-tone counting task. (A) Network density in the theta band. (B) Network clustering coefficient in the theta band. (C) Network local efficiency in the theta band. (D) Network global efficiency in the theta band. (E) Network density in the alpha band. (F) Network clustering coefficient in the alpha band. (G) Network local efficiency in the alpha band. (H) Network global efficiency in the alpha band. Significant planned *t*-tests are indicated by asterisks (**$p_{FDR} \leq 0.01$, *$p_{FDR} \leq 0.05$, †$p_{FDR} \leq 0.1$). The y-axis units reflect normalized ratios (arbitrary units). Abbreviations: In = inhalation, Ex = exhalation, HCT = heartbeat counting task, C-TCT = cardiac-tone counting task.

resulted in no significant differences between respiratory phases ($t = -0.132$, $p = 0.896$). For the clustering coefficient, no significant heartbeat-modulated differences between respiratory phases were significant (HCT: $t = 1.615$, $p = 0.117$; C-TCT: $t = -0.214$, $p = 0.832$; Fig. 4F, Supplementary Table 43). For local efficiency, heartbeat-induced increases in the alpha band were observed only during inhalation in C-TCT ($t = 2.871$, $p = 0.007$, $p_{FDR} = 0.056$, Fig. 4G, Supplementary Table 44), reflecting a trend-level effect following FDR correction. Finally, for global efficiency, the heartbeat evoked increased connectivity during exhalation ($t = 2.62$, $p = 0.014$, $p_{FDR} = 0.048$), leading to higher alpha global efficiency at exhalation compared to inhalation in the active cardiac time window during HCT ($t = 2.499$, $p = 0.018$, $p_{FDR} = 0.048$; Fig. 4H, Supplementary Table 45). Conversely, in C-TCT, global efficiency was enhanced by the heartbeat only during inhalation ($t = 3.751$, $p < 0.001$, $p_{FDR} = 0.006$), but no significant differences were found between respiratory phases in the active phase of the cardiac cycle ($t = -0.292$, $p = 0.772$). Overall, these findings revealed that heartbeat-modulated network organization is selectively enhanced during exhalation when attention is directed inward, particularly within theta and alpha frequency bands.

## 4. Discussion

The multilevel connections between the cardiac and respiratory systems suggest that breathing continuously shapes cardiac interoception at both behavioural and neural levels, an aspect that has often been overlooked in interoception research. In previous studies, we found greater late heartbeat-evoked potential (HEP) positivity during exhalation compared to inhalation in healthy participants performing two cardiac interoceptive tasks (Heartbeat detection task - HBD and heartbeat counting task - HCT, Zaccaro et al., 2022; 2024). In the present study, we aimed to extend previous findings to the time-frequency domain by re-analysing our previous dataset and focusing on the interoceptive HCT and the exteroceptive C-TCT (Zaccaro et al., 2024). As hypothesized, and consistent with previous time-domain results, we observed increased late heartbeat-modulated power and inter-trial coherence (ITC) in exhalation compared to inhalation during the HCT. These effects were observed in the alpha and theta frequency bands over right fronto-centro-parietal electrodes. In contrast, no differences were found between exhalation and inhalation during the cardiac-tone counting task (C-TCT). At the participant level, heartbeat-modulated alpha power and HEP changes across respiratory phases (Δalpha power and ΔHEP) were positively correlated over frontal electrodes. This relationship was specific to HCT and was not observed for theta or other frequency bands, nor for ITC changes across respiratory phases (ΔITC). At the HCT-trial level, Δalpha ITC predicted ΔHEP only when Δalpha power was high, whereas ΔHEP predicted interoceptive accuracy only when both Δalpha power and confidence were high. Crucially, these relationships were independent of cardiac physiology and were absent during C-TCT. Overall, these results indicate that when participants focus on their cardiac sensations, the heartbeat elicits higher power and ITC during exhalation compared to inhalation, primarily in the alpha band, which in turn predicts cardiac interoceptive accuracy. The predominance of effects at fronto-centro-parietal electrodes aligns with the canonical topography of the HEP, which reliably shows maximal amplitudes in these regions across studies. This spatial pattern reflects source contributions from insula, cingulate, somatosensory, and medial prefrontal cortices (Coll et al., 2021; Park and Blanke, 2019), and has also emerged in our previous works (Zaccaro et al., 2022; 2024). These findings further indicate that respiratory-phase modulation of cardiac processing is not an automatic physiological consequence of breathing, but a task-dependent phenomenon that emerges only when interoceptive information is behaviourally prioritized.

During HCT, we also exploratively observed a widespread increase in heartbeat-modulated functional connectivity (FC) in the alpha and theta bands during exhalation compared to inhalation, mostly lateralized to the right fronto-central regions. Conversely, during C-TCT, alpha and theta FC in the right hemisphere decreased during exhalation compared

to inhalation. Graph theory analysis further clarified these findings. During HCT, the heartbeat induced a reduction in theta-band graph connectivity during inhalation and increased alpha-band graph connectivity during exhalation. Consequently, both theta-band (density and clustering coefficient) and alpha-band (density and global efficiency) heartbeat-modulated graph connectivity metrics were higher during exhalation than inhalation. No changes were observed in the theta-band graph connectivity during C-TCT, whereas in the alpha band the heartbeat caused some inhalation-related increases that did not result in significant differences between respiratory phases.

To interpret these findings, we outline a model of cardio-respiratory interactions within the framework of interoceptive predictive coding. The predictive coding framework posits that the brain continuously interprets sensory information in light of expectations based on past experience (Clark, 2013; Friston, 2010). When sensory data deviates from predicted outcomes, the brain generates prediction errors. Prediction errors are resolved through either perceptual inference (where prediction errors update prior models) or active inference (where actions modify sensory inputs to match predictions) (Friston et al., 2017; Hohwy, 2012; Palmer et al., 2019; Parr et al., 2018). The selection of either strategy depends on the relative reliability of sensory data versus prior beliefs. This reliability, known as *precision*, determines the weighting assigned to sensory inputs or priors, and its modulation via top-down attention is referred to as *precision-weighting* (Brown and Friston, 2012; Feldman and Friston, 2010; Kanai et al., 2015). The interplay between top-down predictions and bottom-up prediction errors also occurs in the interoceptive domain, where information about bodily states is processed within a hierarchical interoceptive network (Barrett and Simmons, 2015; Ondobaka et al., 2017; Owens et al., 2018; Petzschner et al., 2021; Pezzulo, 2014; Seth, 2013; Seth and Friston, 2016; Smith et al., 2017). According to this framework, cardiac signals during systole are usually predicted and attenuated by the brain and do

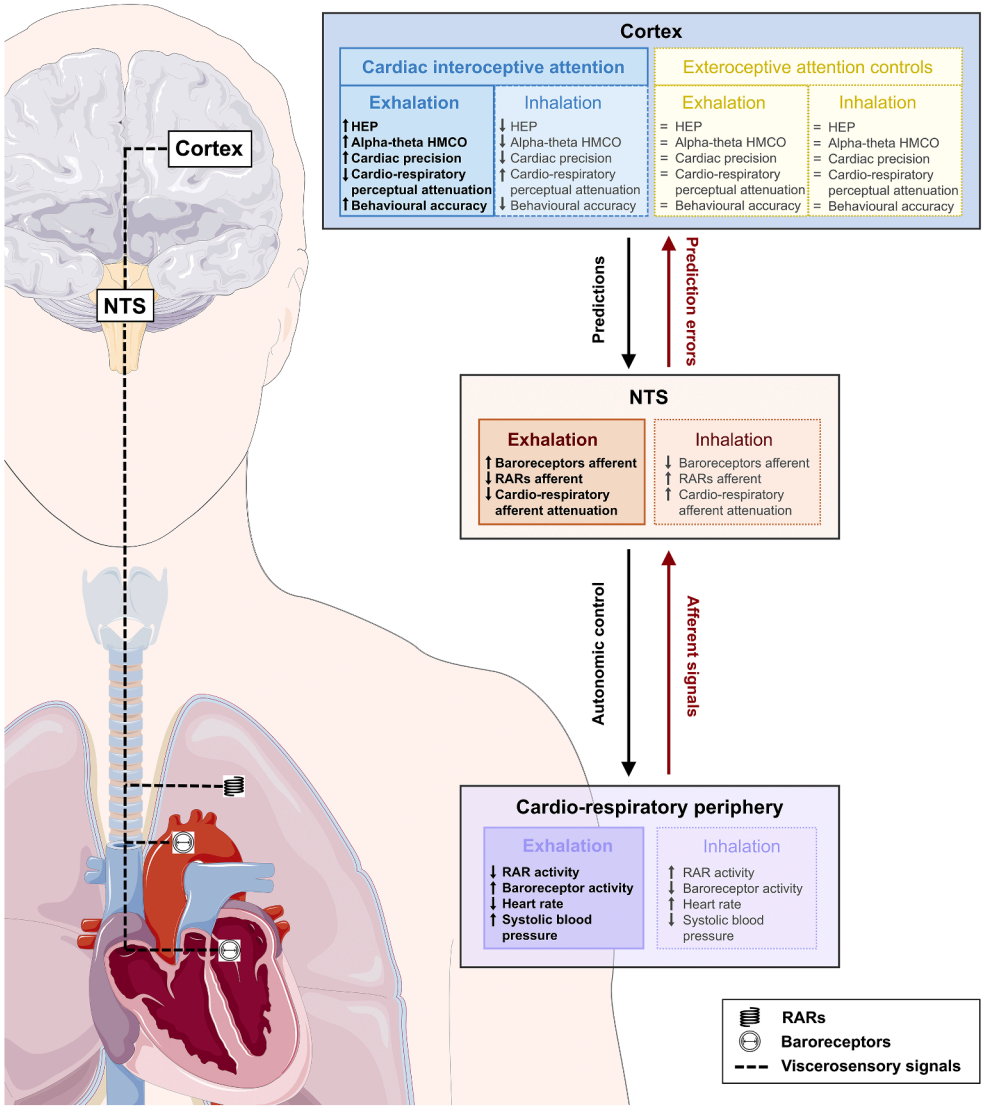



**Fig. 5.** A hierarchical predictive-coding model of cardio–respiratory interactions across respiratory phases. The model depicts cardio–respiratory interactions across three hierarchical levels: the peripheral cardio–respiratory system, the brainstem, and the cortex. At the peripheral level, respiratory phase–dependent changes in baroreceptor and pulmonary RAR activity shape the salience of cardiac signals. These signals are integrated in the brainstem, specifically within the NTS, where phase-dependent gain control may attenuate cardiac signals during inhalation relative to exhalation. At the cortical level, cardiac interoceptive attention enhances the precision of cardiac signals during exhalation, as indexed by HEPs, alpha–theta HMCO, and behavioural accuracy, whereas no comparable modulation is observed during exteroceptive control tasks. Inter-level communication is conceptualized within a predictive-coding framework, with top-down predictions and bottom-up prediction errors operating between adjacent levels. Dashed boxes indicate reduced or absent modulation during exhalation relative to inhalation. Abbreviations: NTS = nucleus of the solitary tract, RARs = rapidly adapting pulmonary receptors, HEP = heartbeat-evoked potential, HMCO = heartbeat-modulated cortical oscillations.

not generate conscious perception (Ainley et al., 2016; Allen, Levy, et al., 2022). Furthermore, cardiac signals are generally inhibitory (Lacey, 1978; Paci et al., 2024; Rau and Elbert, 2001; Saltafossi et al., 2023), so when perceptual sensitivity is required, the brain actively reduces the impact of systole through a parasympathetically driven decrease in heart rate (HR) (Skora et al., 2022). On the contrary, when cardiac interoceptive accuracy is required, the brain increases the precision of cardiac signals through attentional focus, leading to higher cardiac prediction errors, prior updating, and conscious heartbeat perception (Ainley et al., 2016; Petzschner et al., 2019). In this scenario, cardiac interoceptive accuracy is determined by an increase in the precision (saliency) of each heartbeat, rather than by an increase in HR (Leganes-Fonteneau et al., 2021; MacKinnon et al., 2013; Larsson et al., 2021).

The present findings, together with previous studies (Zaccaro et al., 2022; 2024), highlight the role of cardio-respiratory interactions in interoceptive perception, which occur across at least three levels of the interoceptive hierarchy: the peripheral, brainstem, and cortical levels (see Fig. 5 for a graphical representation of the model). At the peripheral level, cardiovascular and respiratory processes are coupled on a cycle-by-cycle basis by the baroreflex (Draghici and Taylor, 2016; Magder, 2018; Shaffer et al., 2014; Shaffer and Venner, 2013). During inhalation, the decrease in thoracic pressure reduces left ventricular filling and stroke volume, leading to a decrease in blood pressure and baroreceptor activity. This initiates the baroreflex, mediated by the nucleus of the solitary tract (NTS) and the nucleus ambiguous, which stabilises blood pressure and cardiac output by increasing the HR when heartbeats are weak. In contrast, higher baroreceptor activity during exhalation leads to the reduction of the sympathetic tone and HR. This interplay creates oscillations in HR between respiratory phases (Ben-Tal et al., 2012; Bernardi et al., 2001; Giardino et al., 2003; Hayano and Yasuma, 2003) and leads to slower but stronger (more salient) cardiac signals during exhalation than inhalation (Larsson et al., 2021). At the brainstem level, cardiac and respiratory afferents are then integrated into the caudal NTS, which receives both aortic and carotid baroreceptors and rapidly adapting pulmonary receptors (RARs) terminations from the vagus and glossopharyngeal nerves (Neuhuber and Berthoud, 2022; Smith et al., 2017; Zoccal et al., 2014). As RARs are mainly activated by lung stretch during inhalation and are relatively silent during exhalation (Del Negro et al., 2018; Krohn et al., 2023; Kubin et al., 2006; Noble and Hochman, 2019), weak cardiac signals are integrated with strong respiratory stimuli during inhalation and, on the other hand, strong cardiac signals are processed with minimal respiratory interference during exhalation. In this context, recent predictive coding models of respiratory interoception (Allen, Varga, et al., 2022; Boyadzhieva and Kayhan, 2021; Braendholt et al., 2023; Corcoran et al., 2018) propose that similar to the heartbeat, the brain generates predictions about the interoceptive consequences of each inhalation, attenuating or "predicting them away" to adaptively optimize perception and action. We propose that in the NTS, as weak cardiac inputs are processed together with strong respiratory inputs, the brain is more likely to attenuate cardiac signals together with respiratory signals during inhalation (see Al et al., 2020, 2021, for a similar interpretation in the somatosensory domain), leading to reduced cardiac interoception during inhalation compared to exhalation (Zaccaro et al., 2022; 2024). Finally, at the highest cortical level, a similar predictive process may also occur, given the topological overlap between cardiac and respiratory signal processing in the cingulate, orbitofrontal/medial prefrontal and somatosensory cortices, amygdala, insula, and precuneus (Engelen et al., 2023; Goheen et al., 2022; Heck et al., 2022; Kluger and Gross, 2021; Park and Blanke, 2019).

We further propose that, at this highest level, reduced cortical excitability during exhalation, particularly in the insula and somatosensory regions, may enhance cardiac interoception, as reflected in increased heartbeat-modulated cortical oscillations in the alpha range. Studies using both periodic and aperiodic MEG/EEG signal analysis have found higher cortical inhibition in the late phase of exhalation and in the transition from exhalation to inhalation (Kluger et al., 2023; Nakamura et al., 2024; Karjalainen et al., 2025). Furthermore, neuroimaging studies have found that interoceptive accuracy is mediated by insula inhibition, suggesting an "addition by subtraction" mechanism for interoceptive attention (Farb et al., 2023; Kuehn et al., 2016; Wiebking et al., 2015). Complementary EEG evidence has shown enhanced alpha power during interoceptive tasks (Crivelli and Balconi, 2025; Kritzman et al., 2022; Mccraty et al., 2009), which correlates with task accuracy (Rominger et al., 2025; Villena-González et al., 2017). This has been interpreted as an active inhibitory mechanism that suppresses the processing of distracting signals (Cooper et al., 2003; Foxe and Snyder, 2011; Jensen and Mazaheri, 2010; Klimesch et al., 2007; Van Diepen et al., 2019; Neri et al., 2024). Additionally, in the context of predictive coding, alpha activity has been linked to the precision-weighting of prediction errors and prior updating (Bastos et al., 2012; Braendholt et al., 2023; Friston, 2019; Friston et al., 2015; Sherman et al., 2016). Therefore, synthesizing this body of literature, our findings of increased heartbeat-modulated alpha power, ITC, and FC during exhalation can be interpreted as neurophysiological signatures of enhanced cardiac interoception. This enhancement likely reflects a state of increased top-down attentional allocation toward interoceptive signals (Molle and Coste, 2022), supported by active inhibition of irrelevant sensory input facilitated by heightened cortical inhibition (particularly in insular and somatosensory regions) during the exhalation phase. Such a configuration may optimize the precision-weighting of cardiac prediction errors, ultimately contributing to improved heartbeat perception and confidence. This interpretation is consistent with the null results observed during the C-TCT: when attention is allocated to an external cue, sensory precision is directed toward exteroceptive stimuli, reducing the salience of cardiac input and abolishing phase-dependent modulations.

As we observed increases in both heartbeat-modulated alpha power and ITC during exhalation, we cannot conclusively determine whether the observed HEP modulations between respiratory phases result from an enhanced phase-reset mechanism. Such modulations would be supported by ITC increases without concurrent power increases (Lopour et al., 2013; Park et al., 2018). We propose that respiration modulates HEP amplitude through increases in both evoked amplitude and phase-reset mechanisms in the alpha band. This interpretation is supported by the moderating effect of heartbeat-modulated power changes on the ITC—HEP relationship: while power and ITC changes across respiratory phases did not correlate (as in Park et al., 2018), ITC increases were positively associated with HEP enhancements only when power increases were also high. This suggests that the two processes (alpha power and ITC increases) stem from distinct yet interactive mechanisms, both essential for cardiac perception. We speculate that positive Δalpha power may serve as an index of interoceptive sensory gating mediated by top-down attention (Crivelli and Balconi, 2025; Kritzman et al., 2022; Molle and Coste, 2022; Rominger et al., 2025; Villena-González et al., 2017), whereas increased Δalpha ITC may reflect increased precision-weighting of cardiac prediction errors (Park et al., 2018; Petzschner et al., 2019).

Several additional questions remain to be answered. First, another key mechanism in cardio-respiratory interoceptive interactions may involve somatosensory and motor pathways (Cameron and Minoshima, 2002; Kern et al., 2013; Khalsa et al., 2009). Since inhalation is an active process driven by motor commands, the brain generates predictions about the sensory consequences of chest expansion to attenuate somatosensory feedback. Because somatosensory and tactile inputs from inhalation overlap with those generated by heartbeats at the level of the somatosensory cortices, the brain may primarily interpret cardiac somatosensory signals as a byproduct of chest expansion (Al et al., 2020; 2021). In contrast, exhalation is largely passive, producing weaker and less precise expected sensory consequences, which may lead to reduced predictive suppression of cardiac-related tactile inputs. Second, the breathing pathway (nasal vs. mouth) may also play a role in

cardio-respiratory interoceptive interactions (Fontanini and Bower, 2006; Tort et al., 2018). Further investigation is needed to determine whether inhalation disrupts cardiac interoception specifically during nasal breathing or whether this effect persists during mouth breathing. Third, directing attention to the heart reduces respiratory rate, likely as a form of respiratory active inference to increase cardiac salience (Candia-Rivera et al., 2022; Zaccaro et al., 2022; 2024). Future studies should investigate the role of voluntary respiratory modulation (in depth, phase, or frequency) in shaping cardiac interoceptive accuracy, emphasizing the contribution of respiratory active inference to cardiac interoceptive attention (Stoupi et al., 2024).

In conclusion, our findings indicate that cardio-respiratory interactions occur at high levels of the interoceptive hierarchy (Smith et al., 2017; Suksasilp and Garfinkel, 2022). We propose that these interactions are fundamental to understanding cardiac interoception, as they provide additional explanatory power for how the central nervous system optimizes the interplay between interoceptive processes. Furthermore, we suggest that such interactions extend beyond the cardiac and respiratory systems and that the predictive coding framework offers valuable insights for their investigation. Finally, we hypothesize that the dynamic interplay between the cardio-respiratory system and the brain has functional significance and may be altered in clinical conditions. This is supported by evidence showing that a respiratory perturbation (breath-holding) enhanced the interoceptive precision assigned to cardiac signals only in healthy individuals, whereas no such effect was observed in individuals with various psychiatric disorders, including depression, anxiety, substance use, and eating disorders (Lavalley et al., 2024; Smith et al., 2020; 2021). Thus, difficulties in adjusting the precision of afferent cardiac signals across respiratory phases during spontaneous breathing may represent a transdiagnostic marker of vulnerability to somatic and mental health disorders.

## Funding

This study was supported by: PRIN 2022 - Interoception and Active Aging (InterActing) - Prot. 2022JS4SY2. PRIN 2022 PNRR Project “Metaphor and epistemic injustice in mental illness: the case of schizophrenia” - CUP D53D23020890001. “Departments of Excellence 2023–2027” initiative of the Italian Ministry of University and Research for the Department of Neuroscience, Imaging and Clinical Sciences (DNISC) of the “G. d'Annunzio” University of Chieti-Pescara.

## Data and code availability statement

The pre-processed EEG data used for all analyses reported in this paper have been deposited on Zenodo and are publicly available (DOI: 10.5281/zenodo.17953246). Trial-level datasets used to fit the linear mixed-effects models reported in this study have also been deposited on Zenodo and are publicly available (DOI: 10.5281/zenodo.17963339). These datasets contain the complete set of trial-by-trial variables from which all statistical models were estimated. The original code used to generate the results and perform the primary analyses is available on Zenodo (DOI: 10.5281/zenodo.17963239). Raw data will be shared by the corresponding author upon reasonable request, provided that data privacy can be ensured in accordance with the European General Data Protection Regulation (EU GDPR 2016). Any additional information required to reanalyse the data reported in this paper is available from the corresponding author upon request.

## CRediT authorship contribution statement

**Andrea Zaccaro:** Writing – review & editing, Writing – original draft, Visualization, Validation, Methodology, Formal analysis, Data curation, Conceptualization. **Francesca della Penna:** Writing – review & editing, Investigation, Formal analysis, Data curation. **Francesco Bubbico:** Writing – review & editing, Software, Data curation. **Başak Bayram:** Writing – review & editing, Software, Data curation. **Eleonora Parrotta:** Writing – review & editing, Software, Data curation. **Mauro Gianni Perrucci:** Writing – review & editing, Software, Resources, Methodology, Data curation. **Marcello Costantini:** Writing – review & editing, Supervision, Funding acquisition. **Francesca Ferri:** Writing – review & editing, Visualization, Supervision, Resources, Project administration, Methodology, Funding acquisition, Conceptualization.

## Declaration of competing interest

The authors declare no competing interests.

## Acknowledgment

We sincerely thank Isabella Pohle-Kaupp for her valuable support in the implementation and interpretation of the linear mixed-effects models.

## Supplementary materials

Supplementary material associated with this article can be found, in the online version, at doi:10.1016/j.neuroimage.2026.121711.

## References

Ainley, V., Apps, M.A.J., Fotopoulou, A., Tsakiris, M., 2016. Bodily precision: a predictive coding account of individual differences in interoceptive accuracy. Philos. Trans. R. Soc. B 371 (1708). https://doi.org/10.1098/rstb.2016.0003.

Al, E., Iliopoulos, F., Forschack, N., Nierhaus, T., Grund, M., Motyka, P., Gaebler, M., Nikulin, V.V., Villringer, A., 2020. Heart-brain interactions shape somatosensory perception and evoked potentials. Proc. Natl. Acad. Sci. U.S.A. 117 (19), 10575–10584. https://doi.org/10.1073/pnas.1915629117.

Al, E., Iliopoulos, F., Nikulin, V.V., Villringer, A., 2021. Heartbeat and somatosensory perception. Neuroimage 238. https://doi.org/10.1016/j.neuroimage.2021.118247.

Allen, M., Levy, A., Parr, T., Friston, K.J., 2022a. In the Body's Eye: the computational anatomy of interoceptive inference. PLoS. Comput. Biol. 18 (9), 1–27. https://doi.org/10.1371/journal.pcbi.1010490.

Allen, M., Varga, S., Heck, D.H., 2022b. Respiratory rhythms of the predictive mind. Psychol. Rev. 130 (4), 1066–1080. https://doi.org/10.1037/rev0000391.

Anderson, M.J., Ter Braak, C.J.F., 2003. Permutation tests for multi-factorial analysis of variance. J. Stat. Comput. Simul. 73 (2), 85–113. https://doi.org/10.1080/00949650215733.

Antonacci, Y., Barà, C., Zaccaro, A., Ferri, F., Pernice, R., Faes, L., 2023. Time-varying information measures: an adaptive estimation of information storage with application to brain-heart interactions. Front. Netw. Physiol. 3. https://doi.org/10.3389/fnetp.2023.1242505.

Ardizzi, M., Ferri, F., 2018. Interoceptive influences on peripersonal space boundary. Cognition 177, 79–86. https://doi.org/10.1016/j.cognition.2018.04.001.

Arshamian, A., Iravani, B., Majid, A., Lundström, J.N., 2018. Respiration modulates olfactory memory consolidation in humans. J. Neurosci. 38 (48), 10286–10294. https://doi.org/10.1523/JNEUROSCI.3360-17.2018.

Barà, C., Zaccaro, A., Antonacci, Y., Dalla Riva, M., Busacca, A., Ferri, F., Faes, L., Pernice, R., 2023. Local and global measures of information storage for the assessment of heartbeat-evoked cortical responses. Biomed. Signal. Process. Control 86. https://doi.org/10.1016/j.bspc.2023.105315.

Barrett, L.F., Simmons, W.K., 2015. Interoceptive predictions in the brain. Nature Rev. Neurosci. 16 (7), 419–429. https://doi.org/10.1038/nrn3950.

Bastos, A.M., Usrey, W.M., Adams, R.A., Mangun, G.R., Fries, P., Friston, K.J., 2012. Canonical microcircuits for predictive coding. Neuron 76 (4), 695–711. https://doi.org/10.1016/j.neuron.2012.10.038.

Belli, F., Fischer, M.H., 2024. Breathing shifts visuo-spatial attention. Cognition 243. https://doi.org/10.1016/j.cognition.2023.105685.

Ben-Tal, A., Shamailov, S.S., Paton, J.F.R., 2012. Evaluating the physiological significance of respiratory sinus arrhythmia: looking beyond ventilation-perfusion efficiency. J. Physiol. 590 (8), 1989–2008. https://doi.org/10.1113/jphysiol.2011.222422.

Bernardi, L., Porta, C., Gabutti, A., Spicuzza, L., Sleight, P., 2001. Modulatory effects of respiration. Auton. Neurosci. 90 (1–2), 47–56. https://doi.org/10.1016/S1566-0702(01)00267-3.

Berntson, G.G., Khalsa, S.S., 2021. Neural circuits of interoception. Trends. Neurosci. 44 (1), 17–28. https://doi.org/10.1016/j.tins.2020.09.011.

Berntson, G.G., Cacioppo, J.T., Quigley, K.S., 1993. Respiratory sinus arrhythmia: autonomic origins, physiological mechanisms, and psychophysiological implications. Psychophysiology 30 (2), 183–196. https://doi.org/10.1111/j.1469-8986.1993.tb01731.x.

Bonaz, B., Lane, R.D., Oshinsky, M.L., Kenny, P.J., Sinha, R., Mayer, E.A., Critchley, H.D., 2021. Diseases, disorders, and comorbidities of interoception. Trends. Neurosci. 44 (1), 39–51. https://doi.org/10.1016/j.tins.2020.09.009.

Boyadzhieva, A., Kayhan, E., 2021. Keeping the breath in mind: respiration, neural oscillations, and the free energy principle. Front. Neurosci. 15. https://doi.org/10.3389/fnins.2021.647579.

Brændholt, M., Nikolova, N., Vejlø, M., Banellis, L., Fardo, F., Kluger, D.S., Allen, M., 2025. The respiratory cycle modulates distinct dynamics of affective and perceptual decision-making. PLoS. Comput. Biol. 21 (5), e1013086. https://doi.org/10.1371/journal.pcbi.1013086.

Braendholt, M., Kluger, D.S., Varga, S., Heck, D.H., Gross, J., Allen, M., 2023. Breathing in waves: understanding Respiratory-brain coupling as a gradient of predictive oscillations. Neurosci. Biobehav. Rev. 152, 105262. https://doi.org/10.1016/j.neubiorev.2023.105262.

Brecher, G.A., Hubay, C.A., 1955. Pulmonary blood flow and venous return during spontaneous respiration. Circ. Res. 3 (2), 210–214. https://doi.org/10.1161/01.RES.3.2.210.

Brown, H.R., Friston, K.J., 2012. Dynamic causal modelling of precision and synaptic gain in visual perception - an EEG study. Neuroimage 63 (1), 223–231. https://doi.org/10.1016/j.neuroimage.2012.06.044.

Cameron, O.G., Minoshima, S., 2002. Regional brain activation due to pharmacologically induced adrenergic interoceptive stimulation in humans. Psychosom. Med. 64 (6), 851–861. https://doi.org/10.1097/01.PSY.0000038939.33335.32.

Canales-Johnson, A., Silva, C., Huepe, D., Rivera-Rei, Á., Noreika, V., Del Carmen Garcia, M., Silva, W., Ciraolo, C., Vaucheret, E., Sedeño, L., Couto, B., Kargieman, L., Baglivo, F., Sigman, M., Chennu, S., Ibáñez, A., Rodríguez, E., Bekinschtein, T.A., 2015. Auditory feedback differentially modulates behavioral and neural markers of objective and subjective performance when tapping to your heartbeat. Cerebral Cortex 25 (11), 4490–4503. https://doi.org/10.1093/cercor/bhv076.

Candia-Rivera, D., Catrambone, V., Valenza, G., 2021. The role of electroencephalography electrical reference in the assessment of functional brain-heart interplay: from methodology to user guidelines. J. Neurosci. Methods 360, 109269. https://doi.org/10.1016/j.jneumeth.2021.109269.

Candia-Rivera, D., Engelen, T., Babo-Rebelo, M., Salamone, P.C., 2024. Interoception, network physiology and the emergence of bodily self-awareness. Neurosci. Biobehav. Rev. 165. https://doi.org/10.1016/j.neubiorev.2024.105864.

Candia-Rivera, D., Sappia, M.S., Horschig, J.M., Colier, W.N.J.M., Valenza, G., 2022. Confounding effects of heart rate, breathing rate, and frontal fNIRS on interoception. Sci. Rep. 12 (1), 1–14. https://doi.org/10.1038/s41598-022-25119-z.

Castellanos, N., Diez, G.G., Pereda, E., López, M.E., Bruña, R., Cuesta, P., Bartolomé, M. G., 2022. Heart evoked brain synchronization predicts progression to Alzheimer' s Journal of Cardiac and pulmonary Heart evoked brain synchronization predicts progression to Alzheimer' s disease. J. Cardiac Pulmonary Rehabil. 5 (4), 1–7. https://doi.org/10.4172/jcpr.1000145.

Chan, P.Y.S., Lee, L.Y., Davenport, P.W., 2024. Neural mechanisms of respiratory interoception. Autonomic Neurosci. 253. https://doi.org/10.1016/j.autneu.2024.103181.

Chen, W.G., Schloesser, D., Arensdorf, A.M., Simmons, J.M., Cui, C., Valentino, R., Gnadt, J.W., Nielsen, L., Hillaire-Clarke, C.S., Spruance, V., Horowitz, T.S., Vallejo, Y.F., Langevin, H.M., 2021. The emerging science of interoception: sensing, integrating, interpreting, and regulating signals within the self. Trends. Neurosci. 44 (1), 3–16. https://doi.org/10.1016/j.tins.2020.10.007.

Clark, A., 2013. Whatever next? Predictive brains, situated agents, and the future of cognitive science. Behav. Brain Sci. 36 (3), 181–204. https://doi.org/10.1017/S0140525x12000477.

Coll, M.P., Hobson, H., Bird, G., Murphy, J., 2021. Systematic review and meta-analysis of the relationship between the heartbeat-evoked potential and interoception. Neurosci. Biobehav. Rev. 122, 190–200. https://doi.org/10.1016/j.neubiorev.2020.12.012.

Cooper, N.R., Croft, R.J., Dominey, S.J.J., Burgess, A.P., Gruzelier, J.H., 2003. Paradox lost? Exploring the role of alpha oscillations during externally vs. internally directed attention and the implications for idling and inhibition hypotheses. Int. J. Psychophysiol. 47 (1), 65–74. https://doi.org/10.1016/s0167-8760(02)00107-1.

Corcoran, A.W., Pezzulo, G., Hohwy, J., 2018. Commentary: respiration-entrained brain rhythms are global but often overlooked. Front. Syst. Neurosci. 12. https://doi.org/10.3389/fnsys.2018.00025.

Craig, A.D., 2003. Interoception: the sense of the physiological condition of the body. Curr. Opin. Neurobiol. 13 (4), 500–505. https://doi.org/10.1016/S0959-4388(03)00090-4.

Crivelli, D., Balconi, M., 2025. Electrophysiological signature of interoceptive attention: a spectral and source localization analysis. Cognit. Affect. Behav. Neurosci. 25 (2), 402–414. https://doi.org/10.3758/s13415-024-01235-3.

Daoui, A., Karmouni, H., Sayyouri, M., Qjidaa, H., 2022. New method for bio - signals zero - watermarking using quaternion shmaliy moments and short-time fourier transform. Multimed. Tools. Appl. 81 (12), 17369–17399. https://doi.org/10.1007/s11042-022-12660-2.

Del Negro, C.A., Funk, G.D., Feldman, J.L., 2018. Breathing matters. Nature Rev. Neurosci. 19 (6), 351–367. https://doi.org/10.1038/s41583-018-0003-6.

Delorme, A., Makeig, S., 2004. EEGLAB: an open source toolbox for analysis of single-trial EEG dynamics including independent component analysis. J. Neurosci. Methods 134 (1), 9–21. https://doi.org/10.1016/j.jneumeth.2003.10.009.

Desmedt, O., Luminet, O., Corneille, O., 2018. The heartbeat counting task largely involves non-interoceptive processes: evidence from both the original and an adapted counting task. Biol. Psychol. 138, 185–188. https://doi.org/10.1016/j.biopsycho.2018.09.004.

Di Lernia, D., Cipresso, P., Pedroli, E., Riva, G., 2018. Toward an embodied medicine: a portable device with programmable interoceptive stimulation for heart rate variability enhancement. Sensors 18 (8). https://doi.org/10.3390/s18082469.

Draghici, A.E., Taylor, J.A., 2016. The physiological basis and measurement of heart rate variability in humans. J. Physiol. Anthropol. 35 (1), 1–8. https://doi.org/10.1186/s40101-016-0113-7.

Elstad, M., O'Callaghan, E.L., Smith, A.J., Ben-Tal, A., Ramchandra, R., 2018. Cardiorespiratory interactions in humans and animals: rhythms for life. Am. J. Physiol. Heart. Circ. Physiol. 315 (1), H6–H17. https://doi.org/10.1152/ajpheart.00701.2017.

Eckberg, D.L., 2003. The human respiratory gate. J. Physiol. 548 (Pt 2), 339–352. https://doi.org/10.1113/jphysiol.2002.037192.

Engelen, T., Schuhmann, T., Sack, A.T., Tallon-Baudry, C., 2025. Cardiac, respiratory, and gastric rhythms independently modulate motor corticospinal excitability in humans. PLoS. Biol. 23 (11), e3003478. https://doi.org/10.1371/journal.pbio.3003478.

Engelen, T., Solcà, M., Tallon-Baudry, C., 2023. Interoceptive rhythms in the brain. Nat. Neurosci. 26 (10), 1670–1684. https://doi.org/10.1038/s41593-023-01425-1.

Farb, N.A.S., Zuo, Z., Price, C.J., 2023. Integrative systems: interoceptive awareness of the breath preserves attention and language networks amidst widespread cortical deactivation: a within-participant neuroimaging study. eNeuro 10 (6), 1–18. https://doi.org/10.1523/ENEURO.0088-23.2023.

Feldman, H., Friston, K.J., 2010. Attention, uncertainty, and free-energy. Front. Hum. Neurosci. 4, 1–23. https://doi.org/10.3389/fnhum.2010.00215.

Flexman, J.E., Demaree, R.G., Simpson, D.D., 1974. Respiratory phase and visual signal detection. Percept. Psychophys. 16 (2), 337–339.

Fló, E., Belloli, L., Cabana, Á., Ruyant-Belabbas, A., Jodaitis, L., Valente, M., Rohaut, B., Naccache, L., Rosanova, M., Comanducci, A., Andrillon, T., Sitt, J., 2024. Predicting attentional focus: heartbeat-evoked responses and brain dynamics during interoceptive and exteroceptive processing. PNAS. Nexus. 3 (12). https://doi.org/10.1093/pnasnexus/pgae531.

Fontanini, A., Bower, J.M., 2006. Slow-waves in the olfactory system: an olfactory perspective on cortical rhythms. Trends. Neurosci. 29 (8), 429–437. https://doi.org/10.1016/j.tins.2006.06.013.

Foxe, J.J., Snyder, A.C., 2011. The role of alpha-band brain oscillations as a sensory suppression mechanism during selective attention. Front. Psychol. 2. https://doi.org/10.3389/fpsyg.2011.00154.

Friston, K., 2010. The free-energy principle: a unified brain theory? Nature Rev. Neurosci. 11 (2), 127–138. https://doi.org/10.1038/nrn2787.

Friston, K., FitzGerald, T., Rigoli, F., Schwartenbeck, P., Pezzulo, G., 2017. Active inference: a process theory. Neural Comput. 29 (1), 1–49. https://doi.org/10.1162/NECO_a_00912.

Friston, K.J., 2019. Waves of prediction. PLoS. Biol. 17 (10). https://doi.org/10.1371/journal.pbio.3000426.

Friston, K.J., Bastos, A.M., Pinotsis, D., Litvak, V., 2015. LFP and oscillations-what do they tell us? Curr. Opin. Neurobiol. 31 (1–6). https://doi.org/10.1016/j.conb.2014.05.004.

Gallego, J., Perruchet, P., Camus, J.F., 1991. Assessing attentional control of breathing by reaction time. Psychophysiology. 28 (2), 217–224. https://doi.org/10.1111/j.1469-8986.1991.tb00413.x.

García-Cordero, I., Esteves, S., Mikulan, E.P., Hesse, E., Baglivo, F.H., Silva, W., García, M., del, C., Vaucheret, E., Ciraolo, C., García, H.S., Adolfi, F., Pietto, M., Herrera, E., Legaz, A., Manes, F., García, A.M., Sigman, M., Bekinschtein, T.A., Ibáñez, A., Sedeño, L., 2017. Attention, in and out: scalp-level and intracranial EEG correlates of interoception and exteroception. Front. Neurosci. 11. https://doi.org/10.3389/fnins.2017.00411.

Giardino, N.D., Glenny, R.W., Borson, S., Chan, L., 2003. Respiratory sinus arrhythmia is associated with efficiency of pulmonary gas exchange in healthy humans. Am. J. Physiol. Heart. Circ. Physiol. 284, 1585–1591. https://doi.org/10.1152/ajpheart.00893.2002.-Respiratory.

Goheen, J., Anderson, J.A.E., Zhang, J., Northoff, G., 2022. From lung to brain-respiration modulates neural and mental activity. Neurosci. Bull. https://doi.org/10.1007/s12264-023-01070-5.

Goheen, J., Wolman, A., Angeletti, L.L., Wolff, A., Anderson, J.A.E., Northoff, G., 2024. Dynamic mechanisms that couple the brain and breathing to the external environment. Commun. Biol. 7 (1). https://doi.org/10.1038/s42003-024-06642-3.

Grund, M., Al, E., Pabst, M., Dabbagh, A., Stephani, T., Villringer, A., 2022. Respiration, heartbeat, and conscious tactile perception. J. Neurosci. 42 (4), 643–656. https://doi.org/10.1523/JNEUROSCI.0592-21.2021.

Harting, C., Hehemann, L., Stetza, L., Kayser, C., 2025. Respiration shapes response speed and accuracy with a systematic time lag. Proc. R. Soc. B, 29220242566. http://doi.org/10.1098/rspb.2024.2566.

Hayano, J., Yasuma, F., 2003. Hypothesis: respiratory sinus arrhythmia is an intrinsic resting function of cardiopulmonary system. Cardiovasc. Res. 58 (1), 1–9. https://doi.org/10.1016/S0008-6363(02)00851-9.

Heck, D.H., Correia, B.L., Fox, M.B., Liu, Y., Allen, M., Varga, S., 2022. Recent insights into respiratory modulation of brain activity offer new perspectives on cognition and emotion. Biol. Psychol. 170. https://doi.org/10.1016/j.biopsycho.2022.108316.

Herrero, J.L., Khuvis, S., Yeagle, E., Cerf, M., Mehta, A.D., 2018. Breathing above the brain stem: volitional control and attentional modulation in humans. J. Neurophysiol. 119 (1), 145–159. https://doi.org/10.1152/jn.00551.2017.

Hohwy, J., 2012. Attention and conscious perception in the hypothesis testing brain. Front. Psychol. 3. https://doi.org/10.3389/fpsyg.2012.00096.

Huijbers, W., Pennartz, C.M.A., Beldzik, E., Domagalik, A., Vinck, M., Hofman, W.F., Cabeza, R., Daselaar, S.M., 2014. Respiration phase-locks to fast stimulus presentations: implications for the interpretation of posterior midline "deactivations. Hum. Brain Mapp. 35 (9), 4932–4943. https://doi.org/10.1002/hbm.22523.

Hyvärinen, A., 1999. Fast and robust fixed-point algorithms for independent component analysis. IEEE Trans. Neural Netw. 10 (3), 626–634. https://doi.org/10.1109/72.761722.

Jensen, O., Mazaheri, A., 2010. Shaping functional architecture by oscillatory alpha activity: gating by inhibition. Front. Hum. Neurosci. 4. https://doi.org/10.3389/fnhum.2010.00186.

Jiang, H., He, B., Guo, X., Wang, X., Guo, M., Wang, Z., Xue, T., Li, H., Xu, T., Ye, S., Suma, D., Tong, S., Cui, D., 2020. Brain-heart interactions underlying traditional Tibetan Buddhist Meditation. Cerebral Cortex 30 (2), 439–450. https://doi.org/10.1093/cercor/bhz095.

Johannknecht, M., Kayser, C., 2022. The influence of the respiratory cycle on reaction times in sensory-cognitive paradigms. Sci. Rep. 12 (1), 1–17. https://doi.org/10.1038/s41598-022-06364-8.

Junghöfer, M., Elbert, T., Tucker, D.M., Rockstroh, B., 2000. Statistical control of artifacts in dense array EEG/MEG studies. Psychophysiology 37 (4), 523–532. https://doi.org/10.1017/S0048577200980624.

Kanai, R., Komura, Y., Shipp, S., Friston, K., 2015. Cerebral hierarchies: predictive processing, precision and the pulvinar. Philos. Trans. R. Soc. B 370 (1668). https://doi.org/10.1098/rstb.2014.0169.

Karjalainen, S., Kujala, J., Parviainen, T., 2025. Neural activity is modulated by spontaneous and volitionally controlled breathing. Biol. Psychol. 197, 109026. https://doi.org/10.1016/j.biopsycho.2025.109026.

Kato, Y., Takei, Y., Umeda, S., Mimura, M., Fukuda, M., 2020. Alterations of heartbeat evoked magnetic fields induced by sounds of disgust. Front. Psychiatry 11, 1–12. https://doi.org/10.3389/fpsyt.2020.00683.

Kern, M., Aertsen, A., Schulze-Bonhage, A., Ball, T., 2013. Heart cycle-related effects on event-related potentials, spectral power changes, and connectivity patterns in the human ECoG. Neuroimage 81, 178–190. https://doi.org/10.1016/j.neuroimage.2013.05.042.

Khalsa, S.S., Adolphs, R., Cameron, O.G., Critchley, H.D., Davenport, P.W., Feinstein, J. S., Feusner, J.D., Garfinkel, S.N., Lane, R.D., Mehling, W.E., Meuret, A.E., Nemeroff, C.B., Oppenheimer, S., Petzschner, F.H., Pollatos, O., Rhudy, J.L., Schramm, L.P., Simmons, W.K., Stein, M.B., Zucker, N., 2018. Interoception and Mental health: a roadmap. Biol. Psychiatry 3 (6), 501–513. https://doi.org/10.1016/j.bpsc.2017.12.004.

Khalsa, S.S., Rudrauf, D., Feinstein, J.S., Tranel, D., 2009. The pathways of interoceptive awareness. Nat. Neurosci. 12 (12), 1494–1496. https://doi.org/10.1038/nn.2411.

Kim, J., Jeong, B., 2019. Heartbeat induces a cortical theta-synchronized network in the resting state. eNeuro 6 (4). https://doi.org/10.1523/ENEURO.0200-19.2019.

Kim, J., Park, H.D., Kim, K.W., Shin, D.W., Lim, S., Kwon, H., Kim, M.Y., Kim, K., Jeong, B., 2019. Sad faces increase the heartbeat-associated interoceptive information flow within the salience network: a MEG study. Sci. Rep. 9 (1), 430. https://doi.org/10.1038/s41598-018-36498-7.

Klimesch, W., Sauseng, P., Hanslmayr, S., 2007. EEG alpha oscillations: the inhibition-timing hypothesis. Brain Res. Rev. 53 (1), 63–88. https://doi.org/10.1016/j.brainresrev.2006.06.003.

Kluger, D.S., Balestrieri, E., Busch, N.A., Gross, J., 2021. Respiration aligns perception with neural excitability. Elife 10. https://doi.org/10.7554/eLife.70907.

Kluger, D.S., Forster, C., Abbasi, O., Chalas, N., Villringer, A., Gross, J., 2023. Modulatory dynamics of periodic and aperiodic activity in respiration-brain coupling. Nat. Commun. 14 (1). https://doi.org/10.1038/s41467-023-40250-9.

Kluger, D.S., Gross, J., 2020. Depth and phase of respiration modulate cortico-muscular communication. Neuroimage 222. https://doi.org/10.1016/j.neuroimage.2020.117272.

Kluger, D.S., Gross, J., 2021. Respiration modulates oscillatory neural network activity at rest. PLoS. Biol. 19 (11). https://doi.org/10.1371/journal.pbio.3001457.

Kritzman, L., Eidelman-Rothman, M., Keil, A., Freche, D., Sheppes, G., Levit-Binnun, N., 2022. Steady-state visual evoked potentials differentiate between internally and externally directed attention. Neuroimage 254, 119133. https://doi.org/10.1016/j.neuroimage.2022.119133.

Krohn, F., Novello, M., van der Giessen, R.S., De Zeeuw, C.I., Pel, J.J.M., Bosman, L.W.J., 2023. The integrated brain network that controls respiration. Elife 12. https://doi.org/10.7554/elife.83654.

Kubin, L., Alheid, G.F., Zuperku, E.J., Mccrimmon, D.R., Kubin, G.F., Alheid, E.J., Zuperku, D.R., Mccrimmon, D.R., 2006. Reflexes from the Lungs and airways Central pathways of pulmonary and lower airway vagal afferents. J. Appl. Physiol. 101, 618–627. https://doi.org/10.1152/japplphysiol.00252.2006.

Kuehn, E., Mueller, K., Lohmann, G., Schuetz-Bosbach, S., 2016. Interoceptive awareness changes the posterior insula functional connectivity profile. Brain Struct. Function 221 (3), 1555–1571. https://doi.org/10.1007/s00429-015-0989-8.

Lacey, B.C., Lacey, J.I., 1978. Two-way communication between the heart and the brain. Significance of time within the cardiac cycle. Am. Psychol. 33 (2), 99–113. https://doi.org/10.1037//0003-066x.33.2.99.

Lavalley, C.A., Hakimi, N., Taylor, S., Kuplicki, R., Forthman, K.L., Stewart, J.L., Paulus, M.P., Khalsa, S.S., Smith, R., 2024. Transdiagnostic failure to adapt interoceptive precision estimates across affective, substance use, and eating disorders: a replication and extension of previous results. Biol. Psychol. 191. https://doi.org/10.1016/j.biopsycho.2024.108825.

Lechinger, J., Heib, D.P.J., Gruber, W., Schabus, M., Klimesch, W., 2015. Heartbeat-related EEG amplitude and phase modulations from wakefulness to deep sleep: interactions with sleep spindles and slow oscillations. Psychophysiology. 52 (11), 1441–1450. https://doi.org/10.1111/psyp.12508.

Lee, W., Kim, E., Park, J., Eo, J., Jeong, B., Park, H.J., 2024. Heartbeat-related spectral perturbation of electroencephalogram reflects dynamic interoceptive attention states in the trial-by-trial classification analysis. Neuroimage 299. https://doi.org/10.1016/j.neuroimage.2024.120797.

Leganes-Fonteneau, M., Bates, M.E., Muzumdar, N., Pawlak, A., Islam, S., Vaschillo, E., Buckman, J.F., 2021. Cardiovascular mechanisms of interoceptive awareness: effects of resonance breathing. Int. J. Psychophysiol. 169, 71–87. https://doi.org/10.1016/j.ijpsycho.2021.09.003.

Leupin, V., Britz, J., 2024. Interoceptive signals shape the earliest markers and neural pathway to awareness at the visual threshold. Proc. Natl. Acad. Sci. U.S.A. 121 (37). https://doi.org/10.1073/pnas.2311953121.

Liuzzi, P., Cassioli, T., Secci, S., Hakiki, B., Scarpino, M., Burali, R., di Palma, A., Toci, T., Grippo, A., Cecchi, F., Frosini, A., Mannini, A., 2024. A neurophysiological profiling of the heartbeat-evoked potential in severe acquired brain injuries: a focus on unconsciousness. Eur. J. Neurosci. 60 (3), 4201–4216. https://doi.org/10.1111/ejn.16394.

Lopour, B.A., Tavassoli, A., Fried, I., Ringach, D.L., 2013. Coding of information in the phase of local field potentials within human medial temporal lobe. Neuron 79 (3), 594–606. https://doi.org/10.1016/j.neuron.2013.06.001.

Lovelace, J.W., Ma, J., Augustine, V., 2024. Defining cardioception: heart-brain crosstalk. Neuron 112 (22), 3671–3674. https://doi.org/10.1016/j.neuron.2024.10.009.

Luft, C.D.B., Bhattacharya, J., 2015. Aroused with heart: modulation of heartbeat evoked potential by arousal induction and its oscillatory correlates. Sci. Rep. 5, 1–11. https://doi.org/10.1038/srep15717.

MacKinnon, S., Gevirtz, R., McCraty, R., Brown, M., 2013. Utilizing heartbeat evoked potentials to identify cardiac regulation of vagal afferents during emotion and resonant breathing. Appl. Psychophysiol. Biofeedback 38 (4), 241–255. https://doi.org/10.1007/s10484-013-9226-5.

Magder, S., 2018. Heart-lung interaction in spontaneous breathing subjects: the basics. Ann. Transl. Med. 6 (18), 348. https://doi.org/10.21037/atm.2018.06.19, 348.

Mccraty, R., Atkinson, M., Tomasino, D., Bradley, R.T., 2009. The coherent heart heart-brain interactions, psychophysiological coherence, and the emergence of system-wide order. Integral Rev. 5 (2), 10–115.

Mizuhara, K., Li, L., Nittono, H., 2025. Effects of cardiac and respiratory phases on auditory evoked potentials. Int. J. Psychophysiol. 209. https://doi.org/10.1016/j.ijpsycho.2025.112521.

Mizuhara, K., Nittono, H., 2022. Visual discrimination accuracy does not differ between nasal inhalation and exhalation when stimuli are voluntarily aligned to breathing phase. Int. J. Psychophysiol. 173, 1–8. https://doi.org/10.1016/j.ijpsycho.2021.12.009.

Mizuhara, K., Li, L., Nittono, H., 2024. Auditory mismatch negativity is larger during exhalation than inhalation. Medicine (Baltimore) 103 (48), e40683. https://doi.org/10.1097/md.0000000000040683.

Mizuhara, K., Nittono, H., 2023. Effects of respiratory phases on the processing of emotional and non-emotional visual stimuli. Psychophysiology. 60 (6), e14261. https://doi.org/10.1111/psyp.14261.

Molle, L., Coste, A., 2022. The respiratory modulation of interoception. J. Neurophysiol. 127 (4), 896–899. https://doi.org/10.1152/jn.00027.2022.

Molle, L., Coste, A., Benoit, C.E., Derosiere, G., Janaqi, S., Perrey, S., Dupeyron, A., 2023. Inhalation boosts perceptual awareness and decision speed. J. Neurophysiol. 130 (3), 516–523. https://doi.org/10.1152/jn.00492.2022.

Münch, E.E., Vögele, C., Van Diest, I., Schulz, A., 2019. Respiratory modulation of intensity ratings and psychomotor response times to acoustic startle stimuli. Neurosci. Lett. 711. https://doi.org/10.1016/j.neulet.2019.134388.

Nakamura, N.H., Fukunaga, M., Oku, Y., 2018. Respiratory modulation of cognitive performance during the retrieval process. PLoS. One 13 (9). https://doi.org/10.1371/journal.pone.0204021.

Nakamura, N.H., Oku, Y., Fukunaga, M., 2024. Brain–breath" interactions: respiration-timing–dependent impact on functional brain networks and beyond. Rev. Neurosci. 35 (2), 165–182. https://doi.org/10.1515/revneuro-2023-0062.

Neri, B., Callara, A.L., Vanello, N., Menicucci, D., Zaccaro, A., Piarulli, A., Laurino, M., Norbu, N., Kechok, J., Sherab, N., Gemignani, A., 2024. Report from a Tibetan Monastery: EEG neural correlates of concentrative and analytical meditation. Front. Psychol. 15, 1348317. https://doi.org/10.3389/fpsyg.2024.1348317.

Neuhuber, W.L., Berthoud, H.R., 2022. Functional anatomy of the vagus system: how does the polyvagal theory comply? Biol. Psychol. 174. https://doi.org/10.1016/j.biopsycho.2022.108425.

Noble, D.J., Hochman, S., 2019. Hypothesis: pulmonary afferent activity patterns during slow, deep breathing contribute to the neural induction of physiological relaxation. Front. Physiol. 10. https://doi.org/10.3389/fphys.2019.01176.

Nolte, G., Bai, O., Wheaton, L., Mari, Z., Vorbach, S., Hallett, M., 2004. Identifying true brain interaction from EEG data using the imaginary part of coherency. Clin. Neurophysiol. 115 (10), 2292–2307. https://doi.org/10.1016/j.clinph.2004.04.029.

Nord, C.L., Garfinkel, S.N., 2022. Interoceptive pathways to understand and treat mental health conditions. Trends Cogn. Sci. (Regul. Ed.) 26 (6), 499–513. https://doi.org/10.1016/j.tics.2022.03.004.

O Larsson, D.E., Esposito, G., Critchley, H.D., Dienes, Z., 2021. Sensitivity to changes in rate of heartbeats as a measure of interoceptive ability. J. Neurophysiol. 126 (5), 1799–1813. https://doi.org/10.1152/jn.00059.2021.

Ondobaka, S., Kilner, J., Friston, K., 2017. The role of interoceptive inference in theory of mind. Brain Cogn. 112, 64–68. https://doi.org/10.1016/j.bandc.2015.08.002.

Oostenveld, R., Fries, P., Maris, E., Schoffelen, J.M., 2011. FieldTrip: open source software for advanced analysis of MEG, EEG, and invasive electrophysiological data. Comput. Intell. Neurosci. 2011. https://doi.org/10.1155/2011/156869.

Owens, A.P., Allen, M., Ondobaka, S., Friston, K.J., 2018. Interoceptive inference: from computational neuroscience to clinic. Neurosci. Biobehav. Rev. 90, 174–183. https://doi.org/10.1016/j.neubiorev.2018.04.017.

Paci, M., Cardellicchio, P., Di Luzio, P., Perrucci, M.G., Ferri, F., Costantini, M., 2024. When the heart inhibits the brain: cardiac phases modulate short-interval

intracortical inhibition. iScience, 109140. https://doi.org/10.1016/j.isci.2024.109140.
Palmer, C.E., Auksztulewicz, R., Ondobaka, S., Kilner, J.M., 2019. Sensorimotor beta power reflects the precision-weighting afforded to sensory prediction errors. Neuroimage 200, 59–71. https://doi.org/10.1016/j.neuroimage.2019.06.034.
Park, H.D., Barnoud, C., Trang, H., Kannape, O.A., Schaller, K., Blanke, O., 2020. Breathing is coupled with voluntary action and the cortical readiness potential. Nat. Commun. 11 (1). https://doi.org/10.1038/s41467-019-13967-9.
Park, H.D., Bernasconi, F., Salomon, R., Tallon-Baudry, C., Spinelli, L., Seeck, M., Schaller, K., Blanke, O., 2018. Neural sources and underlying mechanisms of Neural responses to heartbeats, and their role in bodily self-consciousness: an intracranial EEG study. Cerebral Cortex 28 (7), 2351–2364. https://doi.org/10.1093/cercor/bhx136.
Park, H.D., Blanke, O., 2019. Heartbeat-evoked cortical responses: underlying mechanisms, functional roles, and methodological considerations. Neuroimage 197, 502–511. https://doi.org/10.1016/j.neuroimage.2019.04.081.
Park, H.D., Piton, T., Kannape, O.A., Duncan, N.W., Lee, K.Y., Lane, T.J., Blanke, O., 2022. Breathing is coupled with voluntary initiation of mental imagery. Neuroimage 264, 119685. https://doi.org/10.1016/j.neuroimage.2022.119685.
Parr, T., Benrimoh, D.A., Vincent, P., Friston, K.J., 2018. Precision and false perceptual inference. Front. Integr. Neurosci. 12. https://doi.org/10.3389/fnint.2018.00039.
Parviainen, T., Lyyra, P., Nokia, M.S., 2022. Cardiorespiratory rhythms, brain oscillatory activity and cognition: review of evidence and proposal for significance. Neurosci. Biobehav. Rev. 142, 104908. https://doi.org/10.1016/j.neubiorev.2022.104908.
Perakakis, P. (2019). HEPLAB: a Matlab graphical interface for the preprocessing of the heartbeat-evoked potential. https://doi.org/10.5281/ZENODO.2649943.
Perl, O., Ravia, A., Rubinson, M., Eisen, A., Soroka, T., Mor, N., Secundo, L., Sobel, N., 2019. Human non-olfactory cognition phase-locked with inhalation. Nat. Hum. Behav. 3 (5), 501–512. https://doi.org/10.1038/s41562-019-0556-z.
Petzschner, F.H., Garfinkel, S.N., Paulus, M.P., Koch, C., Khalsa, S.S., 2021. Computational models of interoception and body regulation. Trends. Neurosci. 44 (1), 63–76. https://doi.org/10.1016/j.tins.2020.09.012.
Petzschner, F.H., Weber, L.A., Wellstein, K.V., Paolini, G., Do, C.T., Stephan, K.E., 2019. Focus of attention modulates the heartbeat evoked potential. Neuroimage 186, 595–606. https://doi.org/10.1016/j.neuroimage.2018.11.037.
Pezzulo, G., 2014. Why do you fear the bogeyman? An embodied predictive coding model of perceptual inference. Cognit. Affect. Behav. Neurosci. 14 (3), 902–911. https://doi.org/10.3758/s13415-013-0227-x.
Pollatos, O., Kirsch, W., Schandry, R., 2005. Brain structures involved in interoceptive awareness and cardioafferent signal processing: a dipole source localization study. Hum. Brain Mapp. 26 (1), 54–64. https://doi.org/10.1002/hbm.20121.
Power, J.D., Lynch, C.J., Dubin, M.J., Silver, B.M., Martin, A., Jones, R.M., 2020. Characteristics of respiratory measures in young adults scanned at rest, including systematic changes and "missed" deep breaths. Neuroimage 204. https://doi.org/10.1016/j.neuroimage.2019.116234.
Pultsina, K., Karjalainen, S., Parviainen, T., 2025. Oscillatory markers of interoceptive attention: beta suppression as a neural signature of heartbeat processing. bioRxiv. https://doi.org/10.1101/2025.06.24.660939.
Rau, H., Elbert, T., 2001. Psychophysiology of arterial baroreceptors and the etiology of hypertension. Biol. Psychol. 57 (1–3), 179–201. https://doi.org/10.1016/s0301-0511(01)00094-1.
Rominger, C., Fink, A., Perchtold-Stefan, C.M., Schlögl, L., Schwerdtfeger, A.R., 2025. The interoceptive brain: confidence ratings and accuracy scores are independently and differently associated with task-related alpha power during the heartbeat tracking task. Psychophysiology. 62 (4). https://doi.org/10.1111/psyp.70051.
Rubinov, M., Sporns, O., 2010. Complex network measures of brain connectivity: uses and interpretations. Neuroimage 52 (3), 1059–1069. https://doi.org/10.1016/j.neuroimage.2009.10.003.
Saltafossi, M., Heck, D., Kluger, D.S., Varga, S., 2025a. Common threads: altered interoceptive processes across affective and anxiety disorders. J. Affect. Disord. 369, 244–254. https://doi.org/10.1016/j.jad.2024.09.135.
Saltafossi, M., Zaccaro, A., Kluger, D.S., Perrucci, M.G., Ferri, F., Costantini, M., 2025b. Respiration facilitates behavior during multisensory integration. Psychophysiology. 62 (9), e70145. https://doi.org/10.1111/psyp.70145.
Saltafossi, M., Zaccaro, A., Perrucci, M.G., Ferri, F., Costantini, M., 2023. The impact of cardiac phases on multisensory integration. Biol. Psychol. 182. https://doi.org/10.1016/j.biopsycho.2023.108642.
Savitzky, A., E, M.J., 1964. Smoothing and differentiation of data by simplified least squares procedures. Z. Physiol. Chem. 40 (2). https://pubs.acs.org/sharinguidelines.
Schaefer, M., Hrysanidis, C., Lundstrom, J.N., Arshamian, A., 2024. Phase-locked breathing does not affect episodic visual recognition memory but does shape its corresponding ERPs. Psychophysiology. 61 (4), e14493. https://doi.org/10.1111/psyp.14493.
Schandry, R., Weitkunat, R., 1986. From the heart to the brain: a study of heartbeat contingent scalp potentials. Int. J. Neurosci. 30 (4), 261–275. https://doi.org/10.3109/00207458608985677.
Seth, A.K., 2013. Interoceptive inference, emotion, and the embodied self. Trends Cogn. Sci. (Regul. Ed.) 17 (11), 565–573. https://doi.org/10.1016/j.tics.2013.09.007.
Seth, A.K., Friston, K.J., 2016. Active interoceptive inference and the emotional brain. Philos. Trans. R. Soc. B 371 (1708). https://doi.org/10.1098/rstb.2016.0007.
Shaffer, F., McCraty, R., Zerr, C.L., 2014. A healthy heart is not a metronome: an integrative review of the heart's anatomy and heart rate variability. Front. Psychol. 5, 1–19. https://doi.org/10.3389/fpsyg.2014.01040.
Shaffer, F., Venner, J., 2013. Heart rate variability anatomy and physiology. Biofeedback 41 (1), 13–25. https://doi.org/10.5298/1081-5937-41.1.05.
Sherman, M.T., Kanai, R., Seth, A.K., Van Rullen, R., 2016. Rhythmic influence of top-down perceptual priors in the phase of prestimulus occipital alpha oscillations. J. Cogn. Neurosci. 28 (9), 1318–1330. https://doi.org/10.1162/jocn_a_00973.
Simor, P., Lilla, R.Z., Szalárdy, O., Jordán, Z., Halász, L., Erőss, L., Fabó, D., Bódizs, R., 2025. Heartbeat-related activity in the anterior thalamus differs between phasic and tonic REM sleep. J. Physiol. 603 (9), 2839–2855. https://doi.org/10.1113/JP287802.
Skora, L.I., Livermore, J.J.A., Roelofs, K., 2022. The functional role of cardiac activity in perception and action. Neurosci. Biobehav. Rev. 137. https://doi.org/10.1016/j.neubiorev.2022.104655.
Smith, R., Feinstein, J.S., Kuplicki, R., Forthman, K.L., Stewart, J.L., Paulus, M.P., Aupperle, R.L., Bodurka, J., Savitz, J.B., Victor, T.A., Khalsa, S.S., 2021. Perceptual insensitivity to the modulation of interoceptive signals in depression, anxiety, and substance use disorders. Sci. Rep. 11 (1). https://doi.org/10.1038/s41598-021-81307-3.
Smith, R., Kuplicki, R., Feinstein, J., Forthman, K.L., Stewart, J.L., Paulus, M.P., Khalsa, S.S., 2020. A Bayesian computational model reveals a failure to adapt interoceptive precision estimates across depression, anxiety, eating, and substance use disorders. PLoS. Comput. Biol. 16 (12). https://doi.org/10.1371/journal.pcbi.1008484.
Smith, R., Thayer, J.F., Khalsa, S.S., Lane, R.D., 2017. The hierarchical basis of neurovisceral integration. Neurosci. Biobehav. Rev. 75, 274–296. https://doi.org/10.1016/j.neubiorev.2017.02.003.
Stetza, L., Hehemann, L., Kayser, C., 2025. Evidence that respiratory phase may modulate task-related neural representations of visual stimuli. J. Neurosci. 45 (21), e2236242025. https://doi.org/10.1523/JNEUROSCI.2236-24.2025.
Still, A.W., White, A.P., 1981. The approximate randomization test as an alternative to the F test in analysis of variance. British J. Math. Stat. Psychol. 34 (2), 243–252. https://doi.org/10.1111/j.2044-8317.1981.tb00634.x.
Stoupi, N.A., Weijs, M.L., Imbach, L., Lenggenhager, B., 2024. Heartbeat-evoked potentials following voluntary hyperventilation in epilepsy patients: respiratory influences on cardiac interoception. Front. Neurosci. 18, 1391437. https://doi.org/10.3389/fnins.2024.1391437.
Studenova, A., Forster, C., Engemann, D.A., Hensch, T., Sanders, C., Mauche, N., Hegerl, U., Loffler, M., Villringer, A., Nikulin, V., 2023. Event-related modulation of alpha rhythm explains the auditory P300-evoked response in EEG. Elife 12. https://doi.org/10.7554/eLife.88367.
Suksasilp, C., Garfinkel, S.N., 2022. Towards a comprehensive assessment of interoception in a multi-dimensional framework. Biol. Psychol. 168. https://doi.org/10.1016/j.biopsycho.2022.108262.
Tallon-Baudry, C., 2023. Interoception: probing internal state is inherent to perception and cognition. Neuron 111 (12), 1854–1857. https://doi.org/10.1016/j.neuron.2023.04.019.
Tort, A.B.L., Brankačk, J., Draguhn, A., 2018. Respiration-entrained brain rhythms are global but often overlooked. Trends. Neurosci. 41 (4), 186–197. https://doi.org/10.1016/j.tins.2018.01.007.
Tort, A.B.L., Laplagne, D.A., Draguhn, A., Gonzalez, J., 2025. Global coordination of brain activity by the breathing cycle. Nat. Rev. Neurosci. 26 (6), 333–353. https://doi.org/10.1038/s41583-025-00920-7.
Treves, I.N., & Sciences, C. (2020). Uncovering the heartbeat-evoked potential with insular cortex stereoEEG recordings. https://doi.org/10.13140/RG.2.2.27006.61761.
Tsutsumi, T., Okamoto, Y., Kubota-Takano, N., Wakatsuki, D., Suzuki, H., Sezaki, K., Iwasawa, K., Nakajima, T., 2014. Time-frequency analysis of the QRS complex in patients with ischemic cardiomyopathy and myocardial infarction. IJC Heart Vessels 4 (1), 177–187. https://doi.org/10.1016/j.ijchv.2014.04.008.
Ueno, D., Matsuoka, T., Kato, Y., Ayani, N., Maeda, S., Takeda, M., Narumoto, J., 2020. Individual differences in interoceptive accuracy are correlated with salience network connectivity in older adults. Front. Aging Neurosci. 12, 1–11. https://doi.org/10.3389/fnagi.2020.592002.
Van Diepen, R.M., Foxe, J.J., Mazaheri, A., 2019. The functional role of alpha-band activity in attentional processing: the current zeitgeist and future outlook. Curr. Opin. Psychol. 29, 229–238. https://doi.org/10.1016/j.copsyc.2019.03.015.
Villena-González, M., Moënne-Loccoz, C., Lagos, R.A., Alliende, L.M., Billeke, P., Aboitiz, F., López, V., Cosmelli, D., 2017. Attending to the heart is associated with posterior alpha band increase and a reduction in sensitivity to concurrent visual stimuli. Psychophysiology 54 (10), 1483–1497. https://doi.org/10.1111/psyp.12894.
Waselius, T., Wikgren, J., Penttonen, M., Nokia, M.S., 2019. Breathe out and learn: expiration-contingent stimulus presentation facilitates associative learning in trace eyeblink conditioning. Psychophysiology 56 (9). https://doi.org/10.1111/psyp.13387.
Waselius, T., Xu, W., Sparre, J.I., Penttonen, M., Nokia, M.S., 2022. Cardiac cycle and respiration phase affect responses to the conditioned stimulus in young adults trained in trace eyeblink conditioning. J. Neurophysiol. 127 (3), 767–775. https://doi.org/10.1152/jn.00298.2021.
Weng, H.Y., Feldman, J.L., Leggio, L., Napadow, V., Park, J., Price, C.J., 2021. Interventions and manipulations of interoception. Trends. Neurosci. 44 (1), 52–62. https://doi.org/10.1016/j.tins.2020.09.010.
Wiebking, C., de Greck, M., Duncan, N.W., Tempelmann, C., Bajbouj, M., Northoff, G., 2015. Interoception in insula subregions as a possible state marker for depression—An exploratory fMRI study investigating healthy, depressed and remitted participants. Front. Behav. Neurosci. 9. https://doi.org/10.3389/fnbeh.2015.00082.

Winkler, A.M., Ridgway, G.R., Webster, M.A., Smith, S.M., Nichols, T.E., 2014. Permutation inference for the general linear model. Neuroimage 92, 381–397. https://doi.org/10.1016/j.neuroimage.2014.01.060.

Xia, M., Wang, J., He, Y., 2013. BrainNet Viewer: a network visualization tool for Human Brain connectomics. PLoS One 8 (7). https://doi.org/10.1371/journal.pone.0068910.

Yasuma, F., Hayano, J., 2004. Respiratory sinus arrhythmia: why does the heartbeat synchronize with respiratory rhythm? Chest 125 (2), 683–690. https://doi.org/10.1378/chest.125.2.683.

Zaccaro, A., della Penna, F., Mussini, E., Parrotta, E., Perrucci, M.G., Costantini, M., Ferri, F., 2024. Attention to cardiac sensations enhances the heartbeat-evoked potential during exhalation. iScience 27 (4). https://doi.org/10.1016/j.isci.2024.109586.

Zaccaro, A., Perrucci, M.G., Parrotta, E., Costantini, M., Ferri, F., 2022. Brain-heart interactions are modulated across the respiratory cycle via interoceptive attention. Neuroimage 262, 119548. https://doi.org/10.1016/j.neuroimage.2022.119548.

Zelano, C., Jiang, H., Zhou, G., Arora, N., Schuele, S., Rosenow, J., Gottfried, J.A., 2016. Nasal respiration entrains human limbic oscillations and modulates cognitive function. J. Neurosci. 36 (49), 12448–12467. https://doi.org/10.1523/JNEUROSCI.2586-16.2016.

Zoccal, D.B., Furuya, W.I., Bassi, M., Colombari, D.S.A., Colombari, E., 2014. The nucleus of the solitary tract and the coordination of respiratory and sympathetic activities. Front. Physiol. 5. https://doi.org/10.3389/fphys.2014.00238.